

© 2025 IWA Publishing

This is an Open Access book distributed under the terms of the Creative Commons Attribution-Non Commercial-No Derivatives Licence (CC BY-NC-ND 4.0), which permits copying and redistribution in the original format for non-commercial purposes, provided the original work is properly cited. (http://creativecommons.org/licenses/by-nc-nd/4.0/). This does not affect the rights licensed or assigned from any third party in this book.

This title was made available Open Access through a partnership with Knowledge Unlatched.

IWA Publishing would like to thank all the libraries for pledging to support the transition of this title to Open Access through the 2025 KU Partner Package program.



Knowledge Unlatched





Computational Techniques for Modelling and Simulating Adsorption Processes for (Waste)Water Treatment

Anshul Yadav and Pawan Labhasetwar

IWA PUBLISHING

Computational Techniques for Modelling and Simulating Adsorption Processes for (Waste)Water Treatment

Computational Techniques for Modelling and Simulating Adsorption Processes for (Waste)Water Treatment

Anshul Yadav and
Pawan Labhasetwar

IWA PUBLISHING

Published by **IWA Publishing**
Unit 104–105, Export Building
1 Clove Crescent
London E14 2BA, UK
Telephone: +44 (0)20 7654 5500
Fax: +44 (0)20 7654 5555
Email: publications@iwap.co.uk
Web: www.iwaponline.com

First published 2026
© 2026 IWA Publishing

Apart from any fair dealing for the purposes of research or private study, or criticism or review, as permitted under the UK Copyright, Designs and Patents Act (1998), no part of this publication may be reproduced, stored or transmitted in any form or by any means, without the prior permission in writing of the publisher, or, in the case of photographic reproduction, in accordance with the terms of licenses issued by the Copyright Licensing Agency in the UK, or in accordance with the terms of licenses issued by the appropriate reproduction rights organization outside the UK. Enquiries concerning reproduction outside the terms stated here should be sent to IWA Publishing at the address printed above.

The publisher makes no representation, express or implied, with regard to the accuracy of the information contained in this book and cannot accept any legal responsibility or liability for errors or omissions that may be made.

Disclaimer
The information provided and the opinions given in this publication are not necessarily those of IWA and should not be acted upon without independent consideration and professional advice. IWA and the Editors and Authors will not accept responsibility for any loss or damage suffered by any person acting or refraining from acting upon any material contained in this publication.

British Library Cataloguing in Publication Data
A CIP catalogue record for this book is available from the British Library

ISBN: 9781789063936 (paperback)
ISBN: 9781789063943 (eBook)
ISBN: 9781789063950 (ePub)

Doi: 10.2166/9781789063943

This eBook was made Open Access in February 2026.

© 2026 IWA Publishing
This is an Open Access book distributed under the terms of the Creative Commons Attribution Licence (CC BY-NC-ND 4.0), which permits copying and redistribution for non-commercial purposes with no derivatives, provided the original work is properly cited (https://creativecommons.org/licenses/by-nc-nd/4.0/). This does not affect the rights licensed or assigned from any third party in this book.



Contents

Foreword xi
Preface xiii
Disclaimer xv
Acknowledgements xvii

Chapter 1
(Waste)water treatment ***1***
1.1 Introduction 1
1.2 Water Pollution: Sources, Types, and Effects 2
1.2.1 Sources of water pollution 2
1.2.2 Types of water pollution 4
1.2.3 Effects of water pollution 5
1.3 Major Pollutants in Water 6
1.3.1 Heavy metal ions 8
1.3.2 Nitrates/Nitrites 9
1.3.3 Geogenic contaminants 10
1.3.4 Pharmaceuticals and personal care products 13
1.3.5 Pesticides and herbicides 14
1.3.6 Dyes 15
1.3.7 Microbial contaminants 16
1.4 Techniques for (Waste)Water Treatment 17
1.4.1 Physical methods 17
1.4.2 Chemical methods 19
1.4.3 Biological methods 20
1.5 Stages in (Waste)Water Treatment Processes 21
1.5.1 Preliminary treatment 21
1.5.2 Primary treatment 23
1.5.3 Secondary treatment 23
1.5.4 Tertiary treatment 24
1.6 Summary 24

Chapter 2
Adsorption process for wastewater treatment ***27***
2.1 Introduction 27
2.2 Adsorption Process 28
2.3 Factors Affecting the Adsorption Process. 29
2.3.1 Contact time 29
2.3.2 pH 30
2.3.3 Initial contaminant concentration. 30
2.3.4 Adsorbent dose. 30
2.3.5 Temperature 30
2.3.6 Presence of other ions 30
2.3.7 Adsorbent characteristics 30
2.4 Characterisation of Adsorbents 32
2.4.1 Chemical characterisation 33
2.4.2 Physical characterisation 34
2.4.3 Thermal characterisation 35
2.5 Classification of the Adsorption Process 35
2.5.1 Type of interactions 36
2.5.2 Mode of operation 37
2.6 Empirical Adsorption Process Models 38
2.6.1 Adsorption isotherms 39
2.6.2 Adsorption kinetics 40
2.6.3 Adsorption thermodynamics 45
2.7 Computational Modelling, Simulation, and Optimisation of the Adsorption Process. 48
2.8 Summary. 50

Chapter 3
Computational techniques for simulation and optimisation of adsorption processes ***53***
3.1 Introduction 53
3.2 Hierarchical Modelling of Adsorption Processes 55
3.2.1 Molecular-level modelling. 58
3.2.2 Mesoscale and macroscale modelling 58
3.3 Overview of Computational Methods 58
3.3.1 Density functional theory calculations 58
3.3.2 Molecular dynamics and grand canonical Monte Carlo simulations 60
3.3.3 Quantitative structure–property relationship analysis 61
3.3.4 Artificial intelligence and machine learning 61
3.3.5 Process simulation and optimisation. 63
3.4 Challenges in Using Computational Tools in the Adsorption Process. . . . 64
3.4.1 Learning and reproducibility challenges. 65
3.4.2 Data challenges 65
3.4.3 Benchmarking and validating challenges 66

3.4.4 Result comparison challenges . . . 66
3.4.5 Explainability challenges . . . 66
3.5 Recent Advances in Computational Tools . . . 67
3.6 Summary . . . 68

Chapter 4
Density functional theory calculations for the adsorption process . . . 71
4.1 Introduction . . . 71
4.2 History and Early Developments . . . 72
4.3 Density Functional Theory . . . 73
4.3.1 Exchange-correlation energy . . . 74
4.3.2 Spin polarisation . . . 74
4.3.3 Dispersion corrections . . . 75
4.3.4 Hybrid functionals . . . 75
4.4 Density Functional Theory Calculation for Adsorption Interactions . . 75
4.4.1 Adsorption energy . . . 75
4.4.2 Distance between two atoms . . . 77
4.4.3 Frontier molecular orbitals . . . 77
4.4.4 Mulliken and natural charges . . . 78
4.4.5 Reactivity descriptors . . . 78
4.4.6 Recovery time . . . 79
4.4.7 Distortion energy . . . 79
4.4.8 Charge density difference . . . 80
4.4.9 Spin density . . . 80
4.4.10 Density of states . . . 80
4.4.11 Geometry optimisation . . . 80
4.5 Software Packages for Density Functional Theory Computations 82
4.6 Case Studies . . . 84
4.6.1 Case study I: Adsorption of pesticides on boron nitride nanosheets . . . 84
4.6.2 Structural properties . . . 84
4.6.3 Case study II: Adsorption of pharmaceutical and personal care products on graphene, boron nitride, and boron carbon nitride nanosheets . . . 88
4.7 Summary . . . 93

Chapter 5
Molecular dynamics and grand canonical Monte Carlo simulations of adsorption processes . . . 95
5.1 Introduction . . . 95
5.2 History and Early Developments . . . 96
5.3 Fundamentals of Molecular Simulations . . . 97
5.3.1 Statistical mechanics and ensembles . . . 99
5.3.2 Molecular dynamics: theory and algorithms . . . 101
5.3.3 Monte Carlo and grand canonical Monte Carlo methods 104

5.4 Interatomic Potentials and Force Fields . . . 107
5.4.1 Bonded interactions: bonds, angles, torsions . . . 108
5.4.2 Non-bonded interactions: van der Waals and electrostatics . . . 109
5.4.3 Long-range treatments: Ewald summation and particle mesh Ewald . . . 109
5.4.4 Specialised force fields for adsorption systems . . . 110
5.5 Modelling Adsorbents and Fluids . . . 110
5.5.1 Structural models of adsorbents . . . 110
5.5.2 Water and solvent models . . . 111
5.6 Simulation Workflows and Analyses . . . 113
5.6.1 Molecular dynamics workflows . . . 113
5.6.2 Grand canonical Monte Carlo workflows . . . 115
5.7 Advanced Simulation Techniques: Hybrid Molecular Dynamics–Grand Canonical Monte Carlo Approaches . . . 117
5.8 Software Packages for Molecular Dynamics and Grand Canonical Monte Carlo Simulations . . . 118
5.9 Case Studies . . . 120
5.9.1 Case study I . . . 120
5.9.2 Case study II . . . 127
5.10 Summary . . . 130

Chapter 6
***Quantitative structure–property relationship analysis of adsorption processes* . . . 133**
6.1 Introduction . . . 133
6.2 History and Early Developments . . . 134
6.3 Quantitative Structure–Property Relationship Analysis . . . 135
6.3.1 Basic concepts . . . 136
6.3.2 Principles underpinning quantitative structure–property relationship . . . 137
6.3.3 Molecular descriptors . . . 137
6.4 Model Development Workflow and Best Practices for Quantitative Structure–Property Relationship Modelling . . . 140
6.4.1 OECD principles . . . 140
6.4.2 Data considerations . . . 142
6.4.3 Descriptor selection . . . 143
6.4.4 Validation methods . . . 143
6.4.5 Multitask modelling . . . 144
6.4.6 Applicability domain and predictive reliability . . . 145
6.4.7 Interpretability . . . 145
6.5 Quantitative Structure–Property Relationship Modelling of Adsorption Processes . . . 146
6.5.1 Adsorbent and adsorbate specifics . . . 147
6.5.2 Types of molecular descriptors in adsorption studies . . . 147

6.5.3 Steps in developing quantitative structure–property relationship for adsorption . . . 148
6.6 Advanced Modelling Approaches . . . 150
6.6.1 Hybrid and consensus models . . . 150
6.6.2 Machine learning across adsorbent classes . . . 151
6.6.3 Defect and stability considerations . . . 152
6.7 Software Packages for Quantitative Structure–Property Relationship Analysis . . . 153
6.8 Summary . . . 154

Chapter 7
***Artificial intelligence and machine learning in adsorption processes* . . . 157**
7.1 Introduction . . . 157
7.2 History and the Early Developments . . . 158
7.3 Artificial Intelligence and Machine Learning Algorithms . . . 159
7.3.1 Supervised learning . . . 160
7.3.2 Unsupervised learning . . . 170
7.3.3 Reinforcement learning . . . 172
7.3.4 Hybrid artificial intelligence techniques . . . 174
7.3.5 Search and optimisation algorithms . . . 174
7.3.6 Fuzzy logic . . . 179
7.4 Selecting an Artificial Intelligence/Machine Learning Model for Adsorption . . . 181
7.4.1 Identifying the type of problem . . . 182
7.4.2 Constructing the dataset: Top-down vs. bottom-up . . . 182
7.4.3 Selecting input features and target outputs . . . 182
7.4.4 Matching the model to the dataset . . . 183
7.4.5 Evaluating model performance . . . 183
7.4.6 Practical guidelines for implementation . . . 183
7.5 Software Packages for Artificial Intelligence/Machine Learning Simulations . . . 185
7.6 Case Study . . . 186
7.6.1 Data exploration . . . 186
7.6.2 Random Forest model . . . 188
7.6.3 k-Nearest neighbour neural network . . . 190
7.6.4 Decision tree . . . 191
7.6.5 Support vector machine . . . 193
7.6.6 Comparative insights . . . 194
7.7 Summary . . . 196

Chapter 8
***Adsorption process simulation and optimisation* . . . 199**
8.1 Introduction . . . 199
8.2 History and Early Developments . . . 200
8.3 Process Simulation of the Adsorption Process . . . 202

8.3.1 Stages of computational fluid dynamics modelling 203
8.3.2 Post-processing. 203
8.3.3 Solution algorithms in computational fluid dynamics. 204
8.3.4 Discretisation methods 206
8.3.5 Meshing. 207
8.4 Governing Equations. 209
8.4.1 Continuity equation (mass conservation) 210
8.4.2 Initial and boundary conditions. 212
8.5 Optimisation of the Adsorption Process. 214
8.5.1 Classical method 215
8.5.2 Response surface methodology 216
8.5.3 Artificial neural network for process optimisation 222
8.6 Software Packages for Process Simulation and Optimisation 229
8.7 Case Studies 230
8.7.1 Case study I: Computational fluid dynamics 230
8.7.2 Case study II: Artificial neural networks for optimisation . . . 234
8.7.3 Case study III: Response surface methodology 241
8.8 Summary. 249

References 251

Foreword

Water is probably the most important inheritance of our planet. For me, it has been central to my academic and personal journey. Yet, clean water is a luxury for many. This situation is largely because the human race has missed *responsibility* in its urge for *development*. Restoring balance would need us to reimagine, understand and manage water, with its vital interconnections to every aspect of the planet and its inhabitants.

This book, *Computational Techniques for Modelling and Simulating Adsorption Processes for (Waste)Water Treatment*, is built on that vision. Written by Anshul Yadav and Pawan Labhasetwar, it brings together two vital streams of modern science: the classical principles of adsorption and the powerful world of computational modelling. It presents adsorption not as a static process but as a dynamic interplay of molecules, surfaces, and forces – something that can now be visualized, simulated, and improved with remarkable precision.

Adsorption has long been a workhorse for removing contaminants. With density functional theory, molecular dynamics, and artificial intelligence, we can now understand adsorption in greater detail. The authors have carefully structured their work to guide readers from the fundamentals to advanced simulation methods, and they have done so with an emphasis on clarity, reproducibility, and real-world applicability.

As someone deeply engaged with sustainable water solutions, I find this integration of computation and environmental science deeply inspiring. The sentences that molecules help us write can be structured with detailed understanding. This effort accelerates the discovery of materials for enhanced adsorption, the optimization of processing conditions, and can predict treatment performance before an experiment is conducted. The science presented is rigorous, predictive, and compassionate in its purpose.

The work of Yadav and Labhasetwar reflects a new generation of researchers who see sustainability not as a constraint but as an opportunity for innovation. Their approach exemplifies the spirit of collaboration across disciplines, where chemistry, computation, and environmental engineering converge to address

one of humanity's greatest challenges. In fact, sustainability must be relooked at from multiple angles with the ever-pervading impact of artificial intelligence.

I am sure that this book will inspire young researchers to explore this exciting frontier — to view clean water not only as a global need but also as a beautiful problem in science waiting to be solved. The tools and ideas presented here will undoubtedly influence the next decade of adsorption science and beyond.

Dr Thalappil Pradeep
Institute Professor
Indian Institute of Technology Madras

Preface

Water pollution remains one of the most pressing environmental issues impacting human health, ecosystem stability, and global water availability. With rapid urbanisation, industrial growth, and agricultural expansion, the demand for clean water resources continues to rise, making efficient and sustainable (waste)water treatment techniques essential. In this context, adsorption has emerged as a promising approach for purifying (waste)water due to its simplicity, cost-effectiveness, and adaptability for removing a wide range of contaminants. However, optimising adsorption processes for practical application is a complex challenge requiring an in-depth understanding of chemical interactions, thermodynamics, process dynamics, and robust computational tools for modelling and simulation.

This book, *Computational Techniques for Modelling and Simulating Adsorption Processes for (Waste)Water Treatment,* offers a comprehensive exploration of adsorption as a (waste)water treatment technique, from fundamental principles to advanced computational methods. It seeks to bridge the gap between theoretical concepts and practical applications, providing researchers, engineers, and students with a systematic approach to understanding, modelling, and optimising adsorption processes. With advancements in computational power and software, there is a tremendous opportunity to harness computer-aided tools in designing effective adsorption systems for water treatment.

In Chapter 1, the book begins by presenting an overview of (waste)water treatment, offering a context for the significance of adsorption in environmental remediation. Chapter 2 delves into the adsorption process, introducing the readers to fundamental adsorption isotherms, kinetics, and thermodynamics, establishing a foundation for understanding the adsorption process. Chapter 3 introduces different hierarchical and computational modelling techniques. Chapters 4 through 8 focus on computational tools and techniques that simulate and optimise adsorption processes for (waste)water treatment. Each subsequent chapter focuses on a specific computational method, with in-depth discussions on density functional theory in Chapter 4, molecular dynamics simulations and

grand canonical Monte Carlo methods in Chapter 5, quantitative structure–property relationships in Chapter 6, and artificial intelligence/machine learning techniques in Chapter 7. These chapters offer insights into each approach's theoretical underpinnings, critical methodologies, and practical considerations, highlighting their relevance and limitations for adsorption modelling in (waste)water treatment. Chapter 8 explores computational fluid dynamics as a powerful tool to simulate complex fluid interactions in adsorption processes and addresses optimisation techniques for adsorption processes, comparing classical optimisation methods, response surface methodologies, and artificial neural networks to identify optimal adsorption conditions and process parameters.

Throughout the book, case studies illustrate practical applications of each computational technique, grounding the theoretical concepts in real-world scenarios and showcasing how these methods have been successfully applied in recent research. We hope this book will inspire further research and innovation in computational adsorption modelling, supporting the development of sustainable solutions to the global water crisis.

Disclaimer

This book is a comprehensive compilation of current knowledge and techniques related to computational modelling and simulation of adsorption processes for (waste)water treatment. The content has been created using a wide array of publicly available data and resources in the field. Wherever specific data, theories, or research findings are included, appropriate references are cited to ensure credit is given to original sources and to allow readers to trace the origins of these ideas. The design principles and criteria presented in this book are formulated based on the authors' experience, extensive review of the available literature, and consultations with experts and practitioners specialising in adsorbent-based water and wastewater treatment systems.

While the authors have endeavoured to provide an accurate, up-to-date, and thorough account of the subject, the information contained within is based on data that may not be exhaustive or universally applicable due to national and regional variations in adsorption processes and water treatment standards. Furthermore, the rapidly advancing nature of this field means that certain data or methods used in this book may evolve as new findings emerge. Although the authors have made every effort to ensure the adequacy and correctness of the information, human errors and omissions are possible. This work relies on the latest available research and industry practices, but some data from recent years was also incorporated when it provided relevant context.

The concepts and designs discussed here are meant to serve as a guide, not as absolute or universally applicable solutions. While the principles are based on rigorous research and professional experience, they are not guaranteed to succeed under all circumstances due to the scientific complexities involved, as well as variations in adsorbent properties, contaminant characteristics, and regional requirements for water and wastewater treatment. Any resemblance between the information contained in this book and other available literature is purely coincidental, as care was taken to compile original insights into the modelling and simulation of adsorption systems.

This book is intended to be used as a resource for academic and research purposes. Readers are advised to consult with professionals and conduct

thorough testing before implementing any design principles or computational techniques outlined here. The authors accept no liability for any outcomes resulting from the application of the principles in this book, particularly where untested or novel adsorbent materials and treatment conditions are involved.

Ultimately, the information presented here should be viewed as a contribution to ongoing discourse and development in the field of water and wastewater treatment. The authors sincerely hope that this book will aid researchers and practitioners in advancing safe, effective, and innovative solutions to water quality challenges worldwide.

Acknowledgements

As we tread through and look around, water pollution is omnipresent. Water treatment has been practised since time immemorial, as evidenced by Sanskrit literature dating back to 2000 BC. People then knew sand and gravel filtration, and straining, and that boiling/heating water could treat it. Hence, writing a book on a topic as old as water treatment, which evolved over 4000 years, is complex. The book is complete now, and we look back to acknowledge the inputs and efforts of many without whom this task seemed herculean. The completion of this book, *Computational Techniques for Modelling and Simulating Adsorption Processes for (Waste)Water Treatment* would not have been possible without the guidance, encouragement, and support of many individuals and organisations. We are deeply grateful to everyone who contributed their time, expertise, and resources to this endeavour.

First and foremost, we would like to express our sincere gratitude to the researchers, scientists, and industry professionals whose work laid the foundation for the topics covered in this book. Their pioneering contributions to adsorption, computational modelling, and wastewater treatment were invaluable sources of inspiration and knowledge. We wish to thank the Council of Scientific and Industrial Research (CSIR), which supported us in writing this book through our institutes, CSIR-Central Salt and Marine Chemicals Research Institute, Bhavnagar (CSIR-CSMCRI) and CSIR-National Environmental Engineering Research Institute, Nagpur (CSIR-NEERI). We gained knowledge and experience in these institutes, which helped us put our thoughts through as a book. The CSIR-CSMCRI PRIS number for this manuscript is 73/2024. We also acknowledge the motivation received from the Indian Institute of Technology Madras (IIT Madras) and the Indian Institute of Technology Roorkee (IIT Roorkee) to complete an academic task by receiving tangible and intangible inputs and support.

A book on such a topic cannot be completed without the help and input from many people. We thank Mark Hammond, Andrew Peart and other International Water Association staff for accepting our proposal to write the book. We are also grateful to Katharine Allenby for her help during the

editing and proofreading stages. We also thank our colleagues from CSIR-CSMCRI, Bhavnagar, CSIR-NEERI, Nagpur, IIT Madras, and IIT Roorkee for directly and indirectly compiling this book. We are incredibly thankful to the practitioners and experts in water and wastewater treatment who shared their real-world experiences, helping us shape practical approaches and design strategies discussed in the text.

Padma Shri Prof. T. Pradeep, IIT Madras, kindly consented to write a Foreword, which added value to the book. We also thank anonymous reviewers who kindly reviewed our book proposals, which improved the book's contents.

Further, we also thank our family members Mrs Swati Gupta (wife of Anshul Yadav), Mr Ram Karan and Mrs Anupama Yadav (parents of Anshul Yadav), Dr Suvarna Labhasetwar (wife of Pawan Labhasetwar), Dr Prabhakar and Mrs Sunita Labhasetwar (parents of Pawan Labhasetwar) and Dr Nitin Labhasetwar (brother of Pawan Labhasetwar) for keeping our morale high during the writing of this book.

We extend our heartfelt thanks to everyone who contributed in large and small ways. This book is a testament to the collective efforts of a community committed to advancing sustainable solutions for water treatment.

doi: 10.2166/9781789063943 _0001

Chapter 1
(Waste)water treatment

1.1 INTRODUCTION

Water plays a fundamental role in sustaining the Earth's ecosystems and is an essential interconnecting element among them. Water is critical for sustainability, socio-economic development, and human survival. However, access to safe and potable drinking water remains a critical challenge in numerous regions globally. The escalating global population and intensified economic activities have driven a surge in water demand across diverse sectors, including domestic use, industry, agriculture, recreation, and power generation. Competing demand among these sectors makes the provisioning of drinking water complex. The widening water supply–demand gap is further exacerbated by challenges such as groundwater depletion due to overexploitation, low surface water storage capacity, erratic rainfall due to climate change, poor quality of drinking water sources, and so on.

The rapid decline in water quality stems primarily from the discharge of untreated or partially treated (waste)water and other anthropogenic activities. The synthetic materials (or chemicals) released from anthropogenic activities and matter released in the environment due to natural events such as earthquakes, volcanic eruptions, floods, leaching from parent rocks, and so on, are the most common causes of contaminated freshwater sources (Akhtar *et al.*, 2021). This alarming trend has garnered global attention, prompting urgent action to address water quality deterioration. Rising population, urbanisation, industrialisation, and climate change have increased freshwater demand, further exacerbating the water crisis. Due to the current water crisis, many options to identify alternate water sources and treat polluted sources to meet water quality criteria for various usages are being explored to strengthen supply-side measures.

© 2026 IWAP. This is an Open Access book chapter distributed under the terms of the Creative Commons Attribution Licence (CC BY-NC-ND 4.0) which permits copying and redistribution for non-commercial purposes with no derivatives, provided the work is properly cited (https://creativecommons.org/licenses/by-nc-nd/4.0/). The chapter is from the book *Computational Techniques for Modelling and Simulating Adsorption Processes for (Waste)Water Treatment*, A. Yadav and P. Labhasetwar (Authors).

Managing water pollution is a critical focus of contemporary research, with wastewater treatment and reuse emerging as key strategies to address water scarcity. Figure 1.1 illustrates the global water cycle and the interplay between human activities, pollution sources, and treatment processes. Treatment and reuse of (waste)water, notably sewage, is increasingly being practised to meet current water demand, and the trend will continue. Reusing (waste)water necessitates treatment and implementing adequate (waste)water treatment systems. To avoid adverse impacts, particularly on human health, a minimum treatment is essential to reuse (waste)water, even for non-potable purposes. Several physical, chemical, and biological techniques have been developed and modified for (waste)water treatment.

This chapter provides a comprehensive understanding of (waste)water treatment processes, the sources and types of water pollution, and the effects of contaminants on ecosystems and human health. The chapter outlines the significant sources of water pollution, including point, non-point, and transboundary sources, and highlights the types of pollution impacting water quality, such as surface water pollution. It also covers various pollutants—from heavy metals and nitrates to pharmaceuticals and pesticides—and their potential effects. Furthermore, the chapter introduces vital techniques for (waste)water treatment, including physical, chemical, and biological methods. These insights aim to enhance understanding of effective methods for managing water quality, controlling pollutants, and promoting sustainable treatment practices.

1.2 WATER POLLUTION: SOURCES, TYPES, AND EFFECTS

Water pollution occurs when harmful substances, such as chemicals or microorganisms, exceed tolerable concentrations, impairing water quality and rendering it unsafe for human use or environmental health. The increased concentration of harmful substances (often chemicals or microorganisms) beyond a tolerable limit contaminates rivers, lakes, oceans, aquifers, or other water sources. Such contaminants degrade the water quality and render it unsafe for humans and/or the environment. Polluted water adversely affects all the lifeforms that rely directly or indirectly on that source. Water pollution's effects can be felt in the short or long term. A schematic showing sources, types, effects, and treatment methods for water pollution is shown in Figure 1.2.

1.2.1 Sources of water pollution

Sources of water pollution can be divided into three main categories: (i) point-source, (ii) nonpoint-source, and (iii) transboundary source of water pollution (Ahmad et al., 2019). These sources of pollution are discussed subsequently.

1.2.1.1 Point source

Point source pollution emanates from a single, identifiable outlet, such as industrial discharges or sewage treatment plant effluents. In other words, if the contaminant originates only from a single outlet, the source is referred to as a point source. Discharging untreated wastewater from an industrial operation or disposing of partially treated sewage from the outlet of a treatment plant

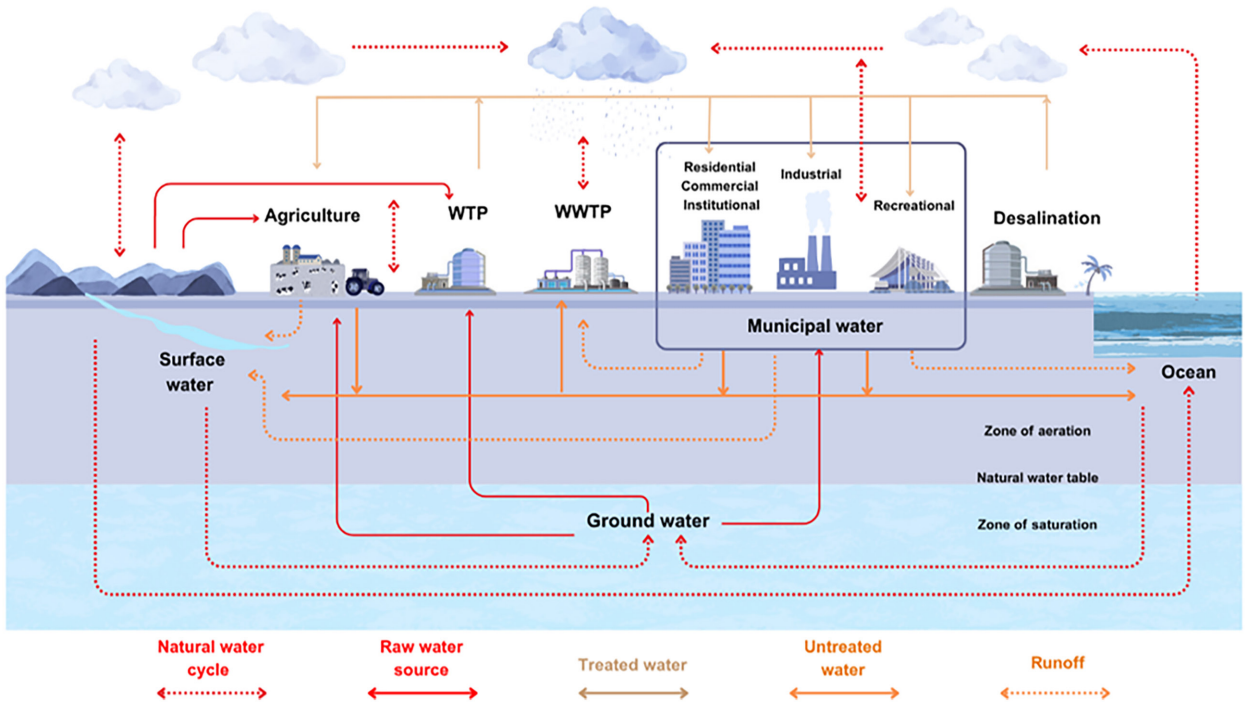


Figure 1.1 Interconnection of the natural water cycle, pollution sources, and (waste)water treatment processes.

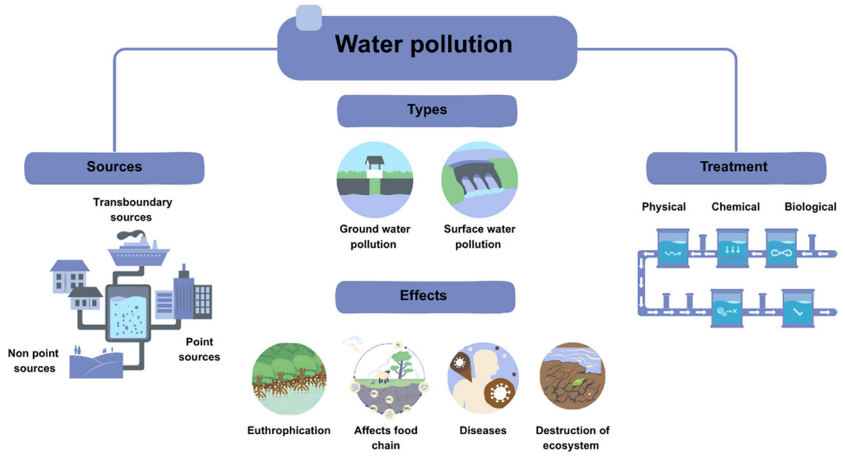


Figure 1.2 Water pollution: types, sources, effects, and treatment methods.

are some examples of point sources responsible for water pollution. Despite originating from a single source, pollutants can disperse over long distances, influenced by pollutant stability, concentration, and the recipient water body's flow and quality, impacting distant water bodies. As a result, the contaminants can adversely affect the quality of the recipient water bodies, which are far from the pollution source.

1.2.1.2 Non-point source

Non-point source pollution arises from diffuse sources, such as agricultural runoff, storm-driven debris, or widespread domestic waste dumping. One of the primary contributors to water pollution is non-point sources. However, controlling the contamination caused by non-point sources is extremely difficult.

1.2.1.3 Transboundary source

Transboundary pollution occurs when contaminated water crosses geopolitical boundaries, affecting downstream regions. Water contamination in a particular region can affect the water sources far away. If the contaminated water from one region comes in contact with the freshwater sources from another region, the water quality of the latter deteriorates. Such contamination arising due to the slow, downriver creep of wastewater discharge is due to transboundary pollution. Oceanic chemical spills from multinational activities also constitute transboundary pollution. This type of pollution underscores the need for international cooperation in water management.

1.2.2 Types of water pollution

Water pollution has significantly threatened water availability, rendering sources useless unless appropriately treated. Introducing synthetic chemicals

and untreated (waste)water from industrial and domestic sources has intensified this problem. In addition to geogenic contaminants, which need to be tackled to make water potable, anthropogenic sources constitute a significant challenge from treatment considerations (Chaudhry and Malik, 2017).

1.2.2.1 Groundwater pollution

Groundwater, a critical freshwater resource, is vulnerable to contamination by invisible pollutants, such as fertilisers, pesticides, industrial effluents, heavy metals, and geogenic contaminants like arsenic and fluoride. Although the groundwater is safe from large-size debris or contaminants, invisible contaminants such as fertilisers, pesticides, effluents generated from industrial discharge, and heavy metals can render the groundwater without treatment unsafe for human needs (Pradhan *et al.*, 2023). In addition, geogenic contaminants such as arsenic, fluoride, and so on, due to natural rocks/alluvium, through which water percolates, also contribute to contamination. These contaminants infiltrate groundwater through soil percolation or recharge, rendering it unsafe without treatment. Polluted groundwater reserves can be unsafe for a few years or even decades, depending on the extent of contamination and surrounding environmental factors. Preventing groundwater contamination is a tedious task and can be impossible at times. Moreover, the cost factor associated with such processes makes them even more challenging to implement.

1.2.2.2 Surface water pollution

Ponds, lakes, rivers, and oceans make up the surface water. However, the quantity of freshwater reserves on the surface is relatively low. More than 60% of the water supply for household activities comes from these limited surface freshwater sources (Carrard *et al.*, 2019). Nevertheless, a significant pool of that water is in peril. However, over half of the rivers and one-third of the lakes are heavily contaminated and unsuitable for swimming, drinking, or fishing (UNEP, 2021). Pollution caused by excessive nutrients (such as phosphates and nitrates) is one of the leading issues and has raised serious concerns. Surface water pollution may occur naturally (floods or tsunamis that pick up fertilisers, pesticides, debris, and other contaminants), accidentally (oil spills and agricultural runoff), or intentionally (industries dumping waste directly into waterways) (Brusseau et al., 2019).

1.2.3 Effects of water pollution

The concentration, toxicity, and stability of the pollutant are the key factors that determine the effects of a particular pollutant. Besides this, the location of the freshwater source is also an important determining factor. Urban and industrial areas typically exhibit higher pollution levels. In general, water sources in urban areas and areas close to industries are likely to be highly polluted. Polluted water poses significant risks to human health and aquatic ecosystems, with toxic chemicals penetrating aquatic organisms and entering food chains. In some cases, it can be fatal to life forms (WHO, 2022).

Apart from the organic molecules, metals like lead, cadmium, arsenic, and mercury enter the food chain through marine animals (like fish) that humans

consume and continue to travel up the food chain (Briffa *et al.*, 2020). Heavy metals generally reduce aquatic animals' life span and directly affect their reproductive ability. Pathogens from faecal contamination cause waterborne diseases like cholera, typhoid, and hepatitis, with outbreaks common in regions with poor water quality (WHO, 2023). It is a common observation that regions with highly polluted water sources often face the outbreak of various infectious diseases. The disease-causing pathogens are responsible for such outbreaks and originate from these polluted water bodies. The polluted water is a suitable environment and medium for growing various disease-causing bacteria. Typhoid, cholera, giardiasis, and so on, are common diseases in regions with extreme water pollution.

An abundance of nutrients promotes plant and algae growth when water pollution causes an algal bloom in a lake or marine environment. Lack of oxygen, or eutrophication, suffocates organisms and may lead to 'dead zones', or regions of lifeless water. These harmful algal blooms occasionally release neurotoxins that are lethal to wildlife, such as whales and turtles, in the sea.

Marine debris, including plastics and fishing gear, poses physical threats to aquatic species, causing entanglement or ingestion. Soda cans and plastic bags are ubiquitous in surface water sources. These substances travel from small freshwater sources to rivers and eventually to oceans. Low-grade plastics, polymeric materials, and metal cans turn the water bodies into 'trash soups' and float on the water surface, forming garbage patches. Other types of debris, such as discarded fishing gear, can cause harm to more than 200 aquatic species (Nelms *et al.*, 2021).

Chemicals like dioxins disrupt reproduction and promote cancer, bioaccumulating through food chains. Bioaccumulation of dioxin in chicken, meat, and fish is a channel through which it enters the human body. Such chemicals travel to the upper side of the food chain and eventually enter the human body, affecting health. Consequently, water pollution will seriously affect the entire food chain (Committee on the Implications of Dioxin in the Food Supply, 2003).

Ocean acidification, driven by increased CO_2 absorption, reduces carbonate availability, impairing shell formation in marine organisms like corals (Doney *et al.*, 2020). Acidification leads to decreased carbonate levels in the water, which may lead to difficulty surviving for several organisms. Several susceptible marine life forms, such as corals and shells, are vulnerable. The acidification of oceans affects the process of shell production in these life forms, thereby making their survival difficult. Moreover, these pollutants affect the nervous systems of clownfish, sharks, and several other species, resulting in an imbalance in their biological processes and behaviour.

1.3 MAJOR POLLUTANTS IN WATER

Pollutants have different characteristics, and each has a distinct toxicological profile. These pollutants do not always change the water's colour, meaning they are often invisible. These pollutants may harm people and biota, even at concentrations as low as nanograms. Major pollutants, their sources, and their health effects are depicted in Figure 1.3.

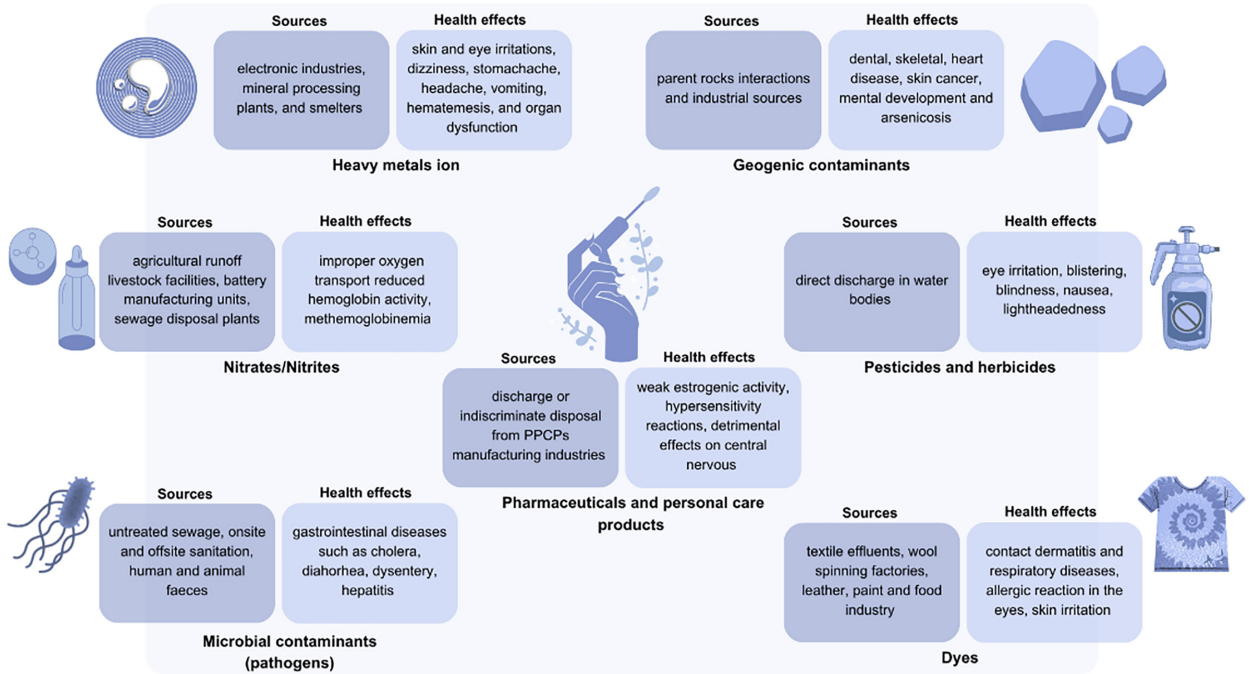


Figure 1.3 Major water pollutants: sources and health effects.

1.3.1 Heavy metal ions

Heavy metals are metallic elements known for their high density and potential toxicity at elevated concentrations. There is a rapid increase in the concentration of heavy metals in freshwater sources, and therefore, it has become a significant concern. The heavy metals may be found in surface and groundwater via anthropogenic sources from industrial and agricultural activities, apart from geogenic sources (Madhav & Singh, 2021). Table 1.1 lists various heavy metals, their sources, permissible levels, and health effects if they are in excess amounts.

Table 1.1 Sources, adverse health effects, and permissible levels of heavy metals in water (WHO, 2022).

Element	Sources	Adverse Health Effects	Permissible Level (mg L^{-1})
Arsenic (As)	Geogenic, chemical wastes, pesticides, mining by-products	Skin lesions, cancer, cardiovascular effects, neurotoxicity	0.01
Cadmium (Cd)	Industrial discharge, metal plating, Ni-Cd batteries, mining waste	Kidney damage, bone demineralisation, cardiovascular diseases	0.003
Chromium (Cr^{6+})	Tanning industries, metal plating, industrial effluents	Respiratory problems, allergic reactions, carcinogenicity	0.05
Copper (Cu)	Corrosion of pipes, mining, and metal industries	Liver and kidney damage, gastrointestinal distress	2.0
Lead (Pb)	Lead pipes, plumbing, battery manufacturing, and mining	Neurotoxicity, developmental delays in children, and kidney damage	0.01
Manganese (Mn)	Mining waste, steel industries, glass and leather processing	Neurological effects, cognitive deficits	0.08
Mercury (Hg)	Industrial waste, mercury-based pesticides, and volcanic activity	Toxic to nervous, digestive, and immune systems; affects lungs, kidneys, skin, and eyes	0.006
Molybdenum (Mo)	Natural deposits, industrial runoff	Joint pain, fatigue, headache, and appetite loss	0.07
Nickel (Ni)	Plumbing, industrial activities, and weathering of rocks	Allergic dermatitis, cardiovascular and kidney diseases, and lung fibrosis	0.07
Zinc (Zn)	Galvanised pipes, industrial waste, metal plating	Gastrointestinal distress interferes with copper metabolism	3.0

It is crucial to monitor and regulate the levels of heavy metals in the environment to prevent adverse health effects, despite their essential roles in biological processes in trace amounts. In plants, excess concentrations of these heavy metals can affect the photosynthetic pathway and hamper chlorophyll production. Besides affecting photosynthesis rates, heavy metals can also negatively impact reproduction as they decrease the viability of pollen and seeds (Madhav & Singh, 2021). Iron, copper, zinc, manganese, and cobalt are essential for living organisms, but are required in minimal quantities for the smooth functioning of various biochemical processes. However, their presence in the body beyond a permissible level damages the cell membrane and affects human enzyme actions. Non-essential heavy metals, even if present in small amounts, can cause severe damage to the functioning of the human body. Excess exposure to heavy metals by humans results in skin and eye irritations, stomach ache, headache, vomiting, hematemesis, dizziness, and organ dysfunction (necrosis, cirrhosis, etc.) (WHO, 2022).

Several spectroscopic techniques can be employed to detect the presence of heavy metals and their concentration, such as inductively coupled plasma-optical emission spectrometry (ICP-OES), atomic absorption spectroscopy (AAS) and inductively coupled plasma mass spectrometry (ICP-MS). These techniques are highly sensitive and can detect trace quantities of metals in water. As the permissible levels/guideline values/standards for the heavy metals are extremely low, that is, of the order of mg L^{-1} or even μg L^{-1} in some cases, these techniques become essential (WHO, 2022).

1.3.2 Nitrates/Nitrites

Nitrogen is an essential element required for the proper functioning of ecosystems and living organisms. Through the nitrogen cycle, various essential processes in nature take place. During the nitrogen cycle, several intermediate species are formed that are stable. Among these, nitrate (NO_3^-) and nitrite (NO_2^-) are the common species, both negatively charged oxygenated nitrogen compounds. Nitrates are usually present in low water concentrations (0–18 mg L^{-1}) (Alfaifi *et al.*, 2020; Fallahzadeh *et al.*, 2019). However, the concentrations can increase due to contamination mainly because of anthropogenic activities, agricultural runoffs, industrial (waste)water discharge, and refuse dump runoffs. The point sources responsible for releasing these species (nitrate and nitrite) in groundwater include livestock facilities, battery manufacturing units, and sewage disposal plants. In contrast, the non-point sources may include croplands with fertiliser applications, lawns, gardens, and natural sources.

Excess nitrates cause infant methaemoglobinemia ('blue baby syndrome') and threaten aquatic ecosystems. If present in large amounts in water bodies, nitrate (NO_3^-) and nitrite (NO_2^-) can threaten aquatic life.

According to WHO guidelines, the permissible values for nitrate and nitrite in drinking water are 50 and 3 mg L^{-1}, respectively (WHO, 2022). According to ISO guidelines, the detection limits for these species range from 0.01 to 1 mg L^{-1} (ISO, 1986, 1988).

Spectrometric techniques are generally employed to detect the presence of nitrates or nitrites in freshwater or drinking water. Molecular absorption

spectrometry can detect these species in water, with a detection limit ranging from 0.005–0.01 mg L^{-1} (ISO, 1984). Similarly, continuous-flow spectrometry with a limit of detection ranging from 0.05–5 mg L^{-1} for nitrate and 1 to 100 mg L^{-1} for nitrite ion can be employed (ISO, 1996). Determination of nitrates and nitrites can also be done using liquid chromatography (up to 0.1 mg L^{-1} for nitrate and 0.05 mg L^{-1} for nitrite) (ISO, 1992).

1.3.3 Geogenic contaminants

Geogenic contamination refers to pollutants that arise from geological sources and occur through the interactions between groundwater and aquifer rocks, which can lead to releasing these contaminants into the water (Wang *et al.*, 2021). Nonetheless, when the concentration of a particular substance becomes high enough to pose a threat to biological life, it is recognised as a geogenic contaminant. In nature, it is typical to encounter geogenic contaminants like salinity, arsenic, fluoride, and iron. Geogenic contaminants include nitrates, phosphates, heavy metals, and trace metals, which may also originate from human activities such as domestic waste disposal, septic tank systems, industrial effluents, and agricultural operations. Groundwater salinity challenges are most pronounced in coastal regions and are subsequently observed in arid and semiarid areas.

Arsenic is abundant in natural environments, including the Earth's crust, rock, soil, water, and air. Its concentration varies in continental crust, igneous rock, and sedimentary rock. Arsenic transport and distribution are complex, continuously cycling through air, soil, and water. It is introduced during weathering, leaching, and runoff and can also be introduced from anthropogenic sources. In groundwater, it is present as arsenate (AsV) and arsenite (AsIII), with inter-conversion occurring through oxidation–reduction. Arsenic compounds are introduced through geological and human activities, and small amounts enter soil and water through biological sources rich in arsenic (CGWB, 2014). Humans highly absorb arsenic, but excessive exposure can cause severe health issues. Common effects include respiratory distress, gastrointestinal issues, anaemia, leucopenia, neural injury, and skin disorders. Long-term exposure can lead to hyperkeratosis, warts, and hyperpigmentation in the face, neck, and back. Inhalation of inorganic arsenic increases the risk of lung and skin cancer.

Salinity is the amount of dissolved particles and ions in water. It is usually expressed as total dissolved solids (TDS) – that is milligrams dissolved solids per litre of water, but use of chloride content (mg L^{-1}) or the electrical conductivity (EC, in $\mu S\ cm^{-1}$) is also widespread in expressing salinity. The main contributors to water are chloride (Cl^-), sodium (Na^+), nitrate (NO_3^-), calcium (Ca^{2+}), magnesium (Mg^{2+}), bicarbonate (HCO_3^-), and sulfate (SO_4^{2-}) (CGWB, 2014). Groundwater, containing naturally occurring salts from dissolving rocks and organic material, can be high in salinity due to overdraft in coastal areas, allowing seawater to intrude on aquifers. High salt concentrations can harm crops, plant growth, water quality, and industrial equipment. Chloride concentrations can make water unfit for human consumption and industrial use, but health issues have not been critically observed.

Selenium is a metalloid element found in ores of metals like iron, lead, silver, and copper. It is not poisonous but has highly toxic compounds.

Selenium combines with hydrogen, forming hydrogen selenide, H_2Se, and forms selenides with most metals. Selenate does not form complexes and is easily leached from soil to groundwater. Selenium mobility depends on various factors, including temperature, moisture, concentrations of water-soluble selenium, climate, organic matter content, and microbial activity. Agriculture increases selenium content in soil and surface water, as selenium is brought along in irrigation drainage water. Selenium can accumulate in organisms' tissues and pass through the food chain, leading to reproductive failure and congenital disabilities. In northwestern India, selenium toxicity has been observed in snow-white chlorosis in wheat and sugar cane plants and chronic selenosis in animals and humans. Animals experience loss of body condition, hair loss, necrosis of the tail tip, reluctance to move, stiff gait, overgrowth of the hoof, cracks, and abnormalities in horn growth. In humans, exposure to selenium occurs through food or water, with symptoms like finger-toe nail and hair loss, progressive health deterioration, nausea, headache, tooth decay, and brittleness.

Chromium, the 21st most abundant element in the Earth's crust, is found in the environment due to erosion and volcanic eruptions. It exists in trivalent and hexavalent oxidation states, with Cr(VI) being more mobile and toxic than Cr(III). The equilibrium concentration of Cr in natural water is small compared to the Cr(VI) concentration. Chromium is converted to less mobile Cr(III) by a reduction reaction. Water-insoluble chromium compounds and metals are not considered a health hazard, but their toxicity and carcinogenic properties have been known for a long time. Acute oral toxicity ranges between 1.5 and 3.3 mg kg^{-1}.

Fluorine, the lightest halogen group element and most electronegative, forms fluoride (F^-) in solution and forms strong solute complexes with many cations. Common fluoride minerals include fluorite (CaF_2), apatite ($Ca_5(Cl,F,OH)(PO_4)_3$), and amphiboles like hornblende and micas. Fluoride can form strong complexes with aluminium, beryllium, ferric ions, and mixed fluoride–hydroxide complexes with boron. Fluoride can be associated with silica in acid solutions, but is rarely stable in natural water. High fluoride concentrations are more likely in water with low calcium concentrations. Fluoride adsorption in groundwater is predominantly geogenic, with enrichment mainly through leaching and weathering of fluoride-bearing minerals. Fluoride can also be an anthropogenic source, such as phosphatic fertiliser, cow dung, and urban waste. Fluorosis is a health issue caused by high fluoride concentrations in groundwater. It can be dental, skeletal, or non-skeletal. Dental fluorosis is characterised by the loss of lustre and shine of dental enamel, affecting inner and outer surfaces. Skeletal fluorosis is caused by excessive fluoride deposits in the skeleton, affecting both young children and adults. Non-skeletal fluorosis affects skeletal muscles, erythrocytes, the gastrointestinal system, ligaments, or a combination. Fluorosis is irreversible, and no treatment exists to treat it. Prolonged exposure to high fluoride concentrations can lead to severe pain, restricted movements, and crippling deformities.

Iron, the second most abundant metallic element in the Earth's outer crust, is present in water in small concentrations due to its chemical behaviour

and solubility in water. The solubility of iron in groundwater depends on the amount of oxygen and pH in the water system. Iron can occur in two forms: Fe^{2+} and Fe^{3+}. Iron dissolves readily when dissolved oxygen levels are low, particularly in acidic groundwater. When aquifers contain organic matter, the oxygen is depleted, causing iron to dissolve as Fe^{2+}. Dissolved iron reacts with atmospheric oxygen when pumped to the surface, forming rust-coloured iron minerals. High iron levels can make water taste astringent and stain utensils, laundry, and equipment. Iron plays a crucial role in human nutrition, forming the protein haemoglobin and being involved in cellular metabolism and enzymes. Excessive iron consumption can lead to iron overload, resulting from gene mutations. Untreated iron overload can lead to haemochromatosis.

Manganese, the 12th most abundant element in the biosphere, is found as iron in only about 1/5th of the Earth's crust. Its chemistry is similar to iron's, as both metals participate in redox processes in weathering environments. Manganese levels in groundwater vary depending on the types of minerals in the aquifer. It is not an essential constituent of common silicate rock minerals but can substitute for iron, magnesium, or calcium in silicate structures. Manganese can form mixed-valence oxides and has three possible valence states in such environments. It is a significant constituent of basalt, dolomite, and limestone and is more commonly found in deeper wells and coal mining regions. Manganese mobility in soil is sensitive to soil conditions, with solubility controlled by redox potential and soil pH. Manganese availability and solubility are generally low at high pH and organic matter content, while its availability is high in acid soils with low organic matter content. Manganese is easily concentrated in the brain, causing an irreversible neurological syndrome similar to Parkinson's disease. High doses of manganese affect DNA replication, mutations in microorganisms and mammalian cells, and can cause DNA damage and chromosome aberrations.

Uranium, found in the Earth's crust at an average concentration of 0.0003%, is a radiological hazard with low radiotoxicity. However, its chemical toxicity is not ignored, with only dissolved uranium being chemically toxic. Complex formation, hydrolytic processes, and redox properties influence uranium's chemical behaviour in aqueous solutions. It also depends on the sorption of minerals and colloids in naturally occurring waters. Uranyl ions (UO_2^{2+}) are the most prevalent form in aqueous medium, forming compounds like carbonate, chloride, and sulfate. In ancient times, uranium produced yellow glazes in ceramics. Water with low uranium levels is usually safe to drink, but it is not likely to accumulate in groundwater. Uranium present in fish and vegetables is eliminated quickly through urine and faeces. Uranium concentrations are higher in phosphate-rich soil but do not exceed normal ranges for uncontaminated soil. Plants absorb uranium through their roots, and a large amount of uranium intake may damage the kidneys and cause cancer. The provisional WHO guideline for drinking water is 15 $\mu g\ L^{-1}$.

Radon is produced by the radioactive decay of radium-226, found in various rocks such as uranium ores, phosphate rock, shales, and igneous and metamorphic rocks. Groundwater has a higher radon concentration than surface water due to continuous production. Radon is sparingly soluble

in water but more soluble than the lighter noble gases. Its occurrence and groundwater distribution vary among rock types and within the same geologic formation. De-ionisation of water reduces radon concentration, which is inversely correlated with the water sample pH. An internationally prescribed radioactivity exposure limit is one mSv/year. Radon presents dual exposure pathways for individuals through drinking water and inhaling air containing radon released from groundwater. The primary adverse health effect associated with chronic exposure to radon is lung cancer, but other harmful respiratory effects include emphysema, pulmonary fibrosis, chronic interstitial pneumonia, silicosis, and respiratory lesions. Radon also has the potential to generate genotoxic effects, such as a higher incidence of chromosomal aberrations.

Strontium is a soft, silver-yellow metal with three allotropic crystalline forms, similar to calcium and barium. It naturally occurs in combination with other elements and compounds due to its extreme reactivity to air. The most significant strontium minerals are celestite and strontianite. Strontium compounds can be water-soluble, with seawater containing 8 mg L^{-1} and river water containing 50 μg L^{-1}. It is primarily dissolved in water as Sr^{2+} or $SrOH^{+}$. The human body contains approximately 4.6 mg kg^{-1} strontium, which is absorbed due to its similar chemistry to calcium. A daily intake of 0.8–5 mg is harmless, but radioactive strontium intake is mainly based on its carcinogenic and mutagenic mechanisms, cell division problems, and increased infant mortality.

Table 1.2 shows the commonly accepted drinking water quality guidelines for geogenic contaminants.

1.3.4 Pharmaceuticals and personal care products

Pharmaceutical and personal care products (PPCPs) are an emerging class of pollutants currently being investigated for their potential hazards. These products from PPCPs manufacturing units enter water bodies by direct discharge or indiscriminate disposal. Common PPCPs, such as analgesics, antibiotics, parabens, anti-inflammatories, painkillers, and so on, have been identified as emerging pollutants. PPCPs also enter the environmental domains through human or animal excrement. Conventional treatment methods are ineffective in decreasing the water pollution caused by these micro-pollutants.

PPCPs can harm animals and humans due to their intrinsic physicochemical properties, even at low dosages. They can be absorbed by the animal and human tissues (especially the liver and kidneys) by interfering with metabolism and inhibiting hormone receptors (WHO, 2022). It can also lead to the development of antibiotic-resistant pathogens in the human body, leaving humans at high risk of complex health complications. Furthermore, some other medical issues, such as weak estrogenic activity, hypersensitivity reactions, and inhibition of the enzyme responsible for the activity of the central nervous system, have also been reported (Chakraborty *et al.*, 2023).

Recent improvements in analytical apparatus and methodologies have made it possible to identify compounds in groundwater and (waste)water at extremely low concentrations (between ng L^{-1} and g L^{-1}). Reverse-phase high-performance liquid chromatography (HPLC), gas–liquid chromatography with electrolytic conductivity detection, gas chromatography-electron capture

Table 1.2. Commonly accepted drinking water quality guidelines for geogenic contaminants (CGWB, 2014), (WHO, 2022), (BIS, 2012).

Constituent	Drinking Water Standards (mg L^{-1})			Undesirable Effect When Present Beyond Acceptable Limit in Drinking Water
	BIS (2012)		WHO (2022)	
	Acceptable Limit	*Permissible Limit in the Absence of an Alternate Source*	*Guideline Values*	
Arsenic (As)	0.01	0.05	0.01	Skin lesions, cancer, cardiovascular effects
Fluoride (F^-)	1.0	1.5	1.5	Dental and skeletal fluorosis
Iron (Fe)	0.3	1.0	–	Taste, discolouration, and staining of laundry and plumbing
Manganese (Mn)	0.1	0.3	0.08	Neurotoxicity, staining, taste and odour issues
Nitrate (NO_3^-)	45	No relaxation	50	Methaemoglobinemia ('blue baby syndrome')
Selenium (Se)	0.01	No relaxation	0.04	Hair loss, nail brittleness, nervous system abnormalities
Lead (Pb)	0.01	No relaxation	0.01	Neurotoxicity, developmental effects in children
Chromium (Cr^{6+})	0.05	0.05	0.05	Skin irritation, carcinogenic effects
Cadmium (Cd)	0.003	No relaxation	0.003	Kidney damage, bone demineralisation
Copper (Cu)	0.05	1.5	2.0	Gastrointestinal irritation, liver and kidney damage
Total Hardness (as $CaCO_3$)	300	600	–	Scaling in pipes, reduced soap efficiency
pH	6.5–8.5	6.5–9.2	6.5–8.5	Corrosion, taste alteration

detector (GC-ECD) after liquid–liquid extraction, UV detection, HPLC with UV absorbance detection, gas chromatography-mass spectrometry (GC-MS), and so on, can be used to detect and determine the presence of PPCPs in water.

1.3.5 Pesticides and herbicides

Pesticides and herbicides pollution of water bodies results from agricultural and urban runoff, or sometimes leaching through the soil. The pesticides include

fungicides, herbicides, nematicides, insecticides, and soil fumigants. These compounds are employed in agriculture to increase crop yield and quality while lowering expenses. Since agriculture has become more intensive during the past few decades, a greater variety of agricultural contaminants, including pesticides, fertilisers, trace elements, and salts, are found in freshwater. An increasing quantity of pesticides is used in agriculture to protect crops from pests, weeds, and illnesses. The agroecosystem is severely threatened because up to 80% of applied pesticides injure non-target plants and remain in the environment as pesticide residue.

Children and newborns are more sensitive to pesticide/herbicide toxicity than adults. Pesticides have the potential to have both short-term effects on health and long-term adverse effects that may appear months or years after exposure. Consumption of pesticides and herbicides may lead to severe health effects, which include eye irritation, blistering, blindness, nausea, lightheadedness, diarrhoea, and so on (Choudri *et al.*, 2020).

Reverse-phase HPLC, gas–liquid chromatography with conductivity detection, GC-ECD after liquid–liquid extraction, UV detection, HPLC with UV absorbance detection, and GC-MS can trace and evaluate pesticides and herbicides in water.

1.3.6 Dyes

Dyes are water-soluble compounds that are employed in the textile, food processing, pharmaceutical, and paper dyeing industries for different purposes, which include the colouring of fibre and cloth colouring, biological and biochemical stains, foods and cosmetics, colour photography, electronics and lasers, solar cells, display panels, pigments in modern paints, printer inks, and leather products (Nachiyar *et al.*, 2023). Because of their high molecular weight and complicated structure, they are stable under high temperatures. Textile dyes that do not bind to the fabric in the textile industry during the dyeing process are released into water bodies.

The presence of dyes in water significantly affects aquatic life, plants, and humans. They prevent sunlight from entering the water body and reduce dissolved oxygen, thus upsetting the biological activity of aquatic life and the photosynthesis process of aquatic plants such as algae (Al-Tohamy *et al.*, 2020). Humans can be exposed to dye toxicity by consuming vegetables and fish that bioaccumulate the dye. Once a toxic or carcinogenic dye enters the human body via the skin, it can induce harmful toxicological effects in human cells, causing DNA damage or diseases such as cancer. Dyes can cause allergies such as contact dermatitis and respiratory diseases, allergic reactions in the eyes, skin irritation, and irritation to mucous membranes and the upper respiratory tract. The dye is cytotoxic, genotoxic, carcinogenic and mutagenic.

HPLC, typically paired with other analytical instruments like diode array detection (DAD) and fluorescence detection (FD), as well as a mass spectrometer (MS), is a very sensitive approach for the identification of organic dyes. Except for indigo, fluorescence distorts the Raman spectra, making it challenging to identify organic dyes using Raman spectroscopy. The surface-enhanced Raman

spectroscopy (SERS) approach has been widely employed to investigate organic dyes in textiles, paints, and glazes to get around the fluorescence effect.

1.3.7 Microbial contaminants

Microorganisms, called microbes, are tiny living entities crucial in sustaining life on our planet. These organisms inhabit diverse environments, including aquatic systems, terrestrial soils, atmospheric conditions, flora, geological formations, and fauna, as well as extreme habitats such as geothermal springs and the icy regions of Antarctica. Microbial contamination in water is one of the most serious threats to human health across several parts of the globe (Kristanti *et al.*, 2022) (Figure 1.4). Consuming microbial-contaminated (pathogenic microorganisms) water leads to many diseases, including diarrhoea, cholera, typhoid, paratyphoid, hepatitis A, and dermatitis. Moreover, such contamination can lead to various chronic health issues. Given the significant health threats associated with microbial contamination of water, even from a solitary consumption of such water, microbial quality assessment is deemed the foremost water quality evaluation. This is particularly relevant compared to chemical contaminants, which are more likely to result in long-term health complications.

Several analytical techniques have been used to detect microbes in the water. The Bacterial culturing method is one of the most used techniques. However, there are other techniques like enzyme-linked immunosorbent assay (ELISA), chromatography (which requires high technicality), capillary electrophoresis (CE), and so on.

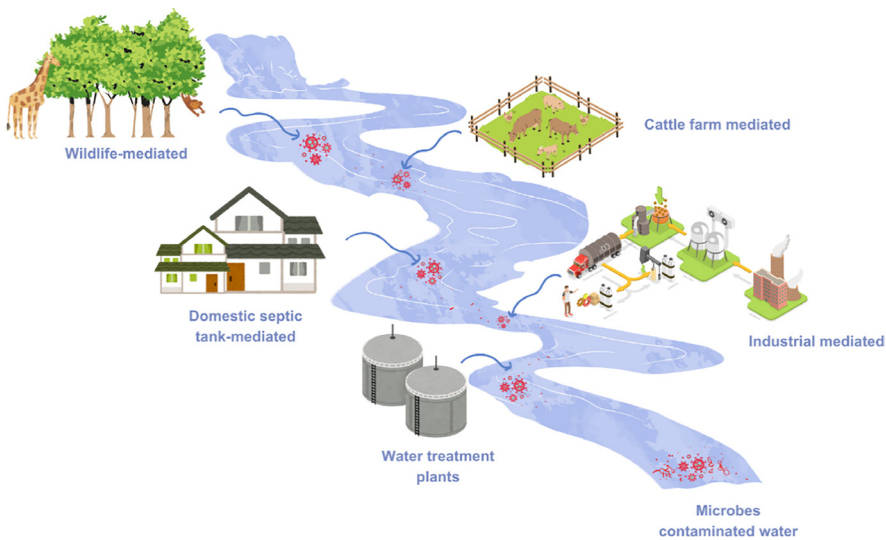


Figure 1.4 Microbial contamination of water from different sources.

1.4 TECHNIQUES FOR (WASTE)WATER TREATMENT

Water and wastewater treatment theoretically differ even in application and extent of treatment technologies, primarily due to source or inlet water characteristics. Conventional treatment, designed for protected sources with natural pollutants, is often inadequate for heavily contaminated water, necessitating advanced techniques. Conventional water treatment can also treat/remove contaminants from anthropogenic sources, albeit to a small extent. These conventional water treatment units include aeration, coagulation, flocculation, sedimentation, filtration, and disinfection, and they are used to supply water to the community. However, due to the continuous degradation of water sources, conventional water treatment plants no longer remain a viable option to provide potable water in some settings. In such settings, which have highly contaminated water sources, many options in terms of water treatment units are being used in addition to conventional water treatment units. These additional water treatment units are similar to those primarily used in wastewater treatment plants. However, exclusive water and wastewater treatment units are included separately, whereas mutually inclusive treatment units are presented only once in subsequent sections.

The techniques reported for wastewater treatment in the literature typically include physical, chemical, and biological processes considered effective for wastewater treatment in many ways (Crini and Lichtfouse, 2019), as shown in Figure 1.5. Their selection depends on factors like the concentration of various contaminants, wastewater characteristics, cost of the process, or the intended post-treatment applications. The distinctive features of each treatment process can be beneficial in one way but restricted in another.

1.4.1 Physical methods

Physical (waste)water treatment is the initial phase in treating industrial and sanitary effluents (sewage), enhancing the efficiency of subsequent steps and safeguarding chemical and biological treatment equipment (Bahuguna *et al.*,

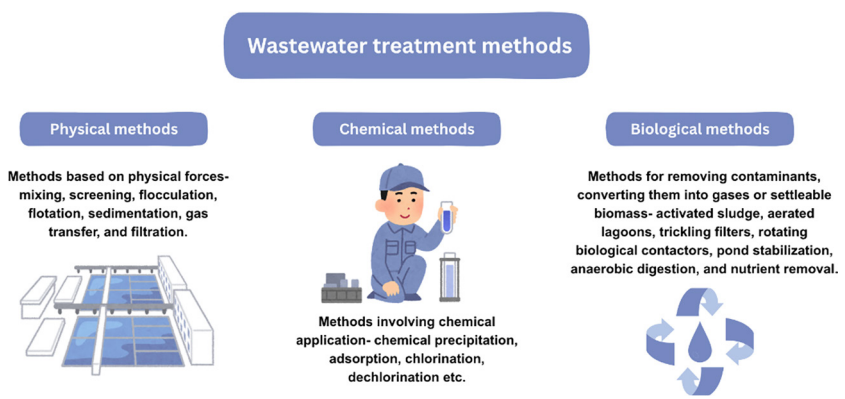


Figure 1.5 Schematic showing different wastewater treatment methods.

2021). The choice of equipment and processes is influenced by the effluent type and desired water quality, considering factors such as colour, biochemical and chemical oxygen content, electrical conductivity, and alkalinity. Various parameters, including pollutant type, (waste)water composition, desired treated water quality, chemical costs, operating expenses, and waste collection costs, play a pivotal role in determining the most suitable and cost-effective (waste) water treatment method.

These methods are effective for dyes, minerals, and suspended particles but require high energy and maintenance. They are suitable for almost all pollutants like dyes, mineral ions, suspended particles, and so on. Contrary to this, they require high energy, maintenance, and operation costs.

Screening

Screening is the first unit operation used at (waste)water treatment plants. To prevent damage and blockages in downstream equipment, piping, and appurtenances, it is necessary to address the presence of paper, plastics, and metals. A combination of coarse and fine screens is commonly employed in modern (waste)water treatment plants. Coarse screens have precise openings ranging from 6 to 150 mm, while fine screens have openings less than 6 mm. Micro screens with openings less than 0.5 mm are also utilised. Utilising these screening devices is vital in ensuring the reliability and effectiveness of the treatment process.

Grit removal

Grit, which ranges in size from 140 to 300 μm or more, constitutes a blend of organic and inorganic materials found in the influent of wastewater treatment plants, encompassing various solid components like eggshells, bone chips, seeds, coffee grounds (organic), and sand, gravel, and cinder (inorganic), introduced into the (waste)water from diverse sources, including domestic waste. Grit in (waste)water treatment processes can result in equipment damage, abrasion, and clogs in (waste)water treatment plants, the extent of which depends on its composition and quantity. Grit removal is crucial in separate and combined sewer systems and (waste)water treatment plants. The primary source of grit in collection systems stems from surface water runoff in impervious areas, particularly during the initial stages of a storm. Additionally, significant contributions of grit to collection systems are attributed to industrial activities and construction endeavours. Grit removal typically entails the application of sedimentation technologies before the primary treatment, and the separated grit is commonly disposed of in landfills.

Sedimentation

Sedimentation, a process where particles suspended in water settle out due to gravity, leads to the formation of sediment or sludge. This method provides various advantages, including reduced chemical usage, lower costs, and minimised water quality variation while simplifying subsequent processes. In (waste)water treatment, a sedimentation tank eliminates particles from the water, with the accumulated solids or sludge settling at the tank's bottom and

being periodically removed. Coagulants are often introduced into the water before sedimentation to aid the settling process. Following sedimentation, additional treatment steps are commonly implemented. The continued settling and consolidation of sediment into a dense layer is termed consolidation. The utilisation of mechanical means to aid in the thickening of sediment or sludge is referred to as thickening.

Skimming

The specialised skimmer is crucial in segregating liquids from a distinct liquid medium, particularly oil and suspended particles. Its primary function is to remove oil and suspended solids from water within the confines of a (waste) water treatment plant. A skimming tank is the designated container where the accumulation of scum is facilitated through the introduction of air via diffusion in the wastewater. These tanks are specifically employed to eliminate grease and fatty oils from the sewage. Air diffusers are strategically installed at the tank's base to aid in this process.

1.4.2 Chemical methods

Chemical methods are simple, rapid, and efficient processes and have multiple approaches concerning oxidants (Gupta *et al.*, 2012). A range of chemical treatment processes is available, among which chemical neutralisation, adsorption, precipitation, disinfection, and ion exchange are the most frequently employed. While these processes exhibit distinct methodologies, they are united by a commonality: they influence the substance by modifying external conditions.

1.4.2.1 Neutralisation

Chemical neutralisation plays a crucial role in the treatment of (waste)water, effectively eliminating pollutants and lowering acidity levels. Adding acidic or alkaline agents is employed to maintain the pH of (waste)water at approximately 7 (6.5–9). When the water lacks acidity, an appropriate acid is incorporated to adjust the pH accordingly. Similarly, if the water's alkalinity is inadequate, a base is introduced to attain the necessary pH balance.

1.4.2.2 Adsorption

Adsorption is crucial in (waste)water treatment as an efficient and cost-effective method for removing a wide range of dissolved pollutants, especially at low concentrations. It is particularly effective for treating industrial effluents and municipal (waste)water containing persistent organic compounds, dyes, heavy metals, and emerging contaminants such as pharmaceuticals and personal care products. The process involves the transfer of contaminants from the aqueous phase onto the surface of a solid material, allowing for targeted removal without altering the overall composition of the water. Adsorption is often used as a tertiary or polishing treatment step to meet stringent discharge standards or enable water reuse. Its operational simplicity, adaptability to various (waste)water types, and integration with other treatment technologies make adsorption valuable in modern (waste)water treatment systems.

1.4.2.3 Precipitation

The process of chemical precipitation entails the application of an acid or alkali to eliminate dissolved inorganic substances from (waste)water. This process can be facilitated by adjusting the temperature or adding certain chemicals. The precipitate formed can then be separated using the flotation or sedimentation process.

1.4.2.4 Disinfection

Disinfection generally involves a chemical treatment method (exceptions such as UV disinfection also exist) wherein (waste)water undergoes treatment to neutralise pathogens, including viruses, microbes, and protozoa. The main objective of this process is to safeguard the microbial quality of the (waste) water.

1.4.2.5 Ion exchange

The ion exchange process involves removing unwanted dissolved ions from (waste)water through a chemical reaction that replaces these ions with more favourable alternatives. The fundamental aim of the chemical treatment process is softening. This process is characterised as a reversible reaction involving replacing one charged ion with another with a similar charge.

1.4.2.6 Advanced oxidation

Advanced oxidation is a chemical reaction characterised by loss of electrons from atoms or groups of atoms. Advanced oxidation may involve electrochemical, photo-electrochemical, UV-assisted Fenton, and ozonation. Electrochemical oxidation is an effective method that employs the electrochemical generation of hydroxyl radicals to degrade pollutants, whereas photo-electrochemical oxidation employs photocatalysts to generate reactive species like hydroxyl radicals and superoxide ions to degrade pollutants. UV-assisted Fenton oxidation uses UV or sunlight irradiation for radical formation. The ozonation process employs an electric discharge field or ultraviolet radiation for radical formation during the degradation of pollutants. Generally, catalysts and pH play an essential role in the oxidation process.

1.4.3 Biological methods

The biological methods for the complete degradation of (waste)water have benefits such as being eco-friendly, cost-competitive, producing less sludge, giving non-hazardous metabolites or complete mineralisation, and requiring less water (higher concentration or less dilution requirement) compared with the physical/oxidation method (Sathya *et al.*, 2023). The biological treatment is a simple and economically attractive technique. Still, it is a slow process, has low biodegradability, and requires an optimally favourable environment and proper maintenance of microorganisms. The methods for the biological treatment of (waste)water are primarily categorised into two distinct types: aerobic or anaerobic techniques.

1.4.3.1 Aerobic treatment techniques

Aerobic treatment techniques represent effective biological processes that utilise oxygen to eliminate organic pollutants from (waste)water. Beyond the commonly employed activated sludge process, various other aerobic methods exist, including trickling filters, aerated lagoons, and oxidation ponds. Trickling filters, often percolating filters, are designed to remove substances such as ammonia following primary treatment. Aerated lagoons facilitate the mechanical introduction of oxygen to enhance biological oxidation, resulting in effluent that can be reused after additional treatment of the settled sludge. Oxidation ponds depend on the collaborative action of bacteria, algae, and other organisms to decompose organic materials; however, they necessitate substantial land areas and are most effective for small, rural communities. Collectively, these methods provide various effective solutions for aerobic (waste)water treatment. Moving-bed biofilm reactor (MBBR), membrane bioreactor (MBR), sequencing batch reactors (SBRs), and so on, are a few more examples of aerobic wastewater treatment techniques.

1.4.3.2 Anaerobic treatment represents

Anaerobic treatment represents a biological methodology for managing high-strength (waste)water, utilising microorganisms that function without oxygen. This process is proficient in diminishing organic solids by 40–60% and results in the generation of biogas, primarily composed of methane (CH_4) and carbon dioxide (CO_2) (Singh *et al.*, 2014). Compared to aerobic treatment, anaerobic methods produce significantly less sludge and are frequently implemented to stabilise sludge within (waste)water treatment facilities. Despite its slower pace and multi-stage nature, the anaerobic treatment effectively prepares (waste) water for subsequent processing, offering benefits such as reduced biomass production and enhanced biogas output, which can facilitate energy recovery while simultaneously stabilising the (waste)water.

1.5 STAGES IN (WASTE)WATER TREATMENT PROCESSES

When treating (waste)water, the optimal treatment technique should be selected to meet the decontamination goals (as established by legislation). Solids such as colloids, organic matter, nutrients, and soluble pollutants are removed from (waste)water using a mix of physical, chemical, and/or biological processes. (A few of these techniques have already been mentioned in earlier subsections.) Hence, a (waste)water treatment plant treats water through a series of physical, chemical, and biological processes until it becomes fit to be discharged into the environment or reused/recycled. A (waste)water treatment typically entails sequential processes (Seow *et al.*, 2016), as shown in Figure 1.6.

1.5.1 Preliminary treatment

Preliminary treatment represents the initial phase of (waste)water treatment, aimed at preparing the water for further purification (Riffat and Husnain, 2022). Pre-treatment separates heavy sediments from suspended materials, such as dead animals, loose branches, paper, rags, and inorganic solids. In this process,

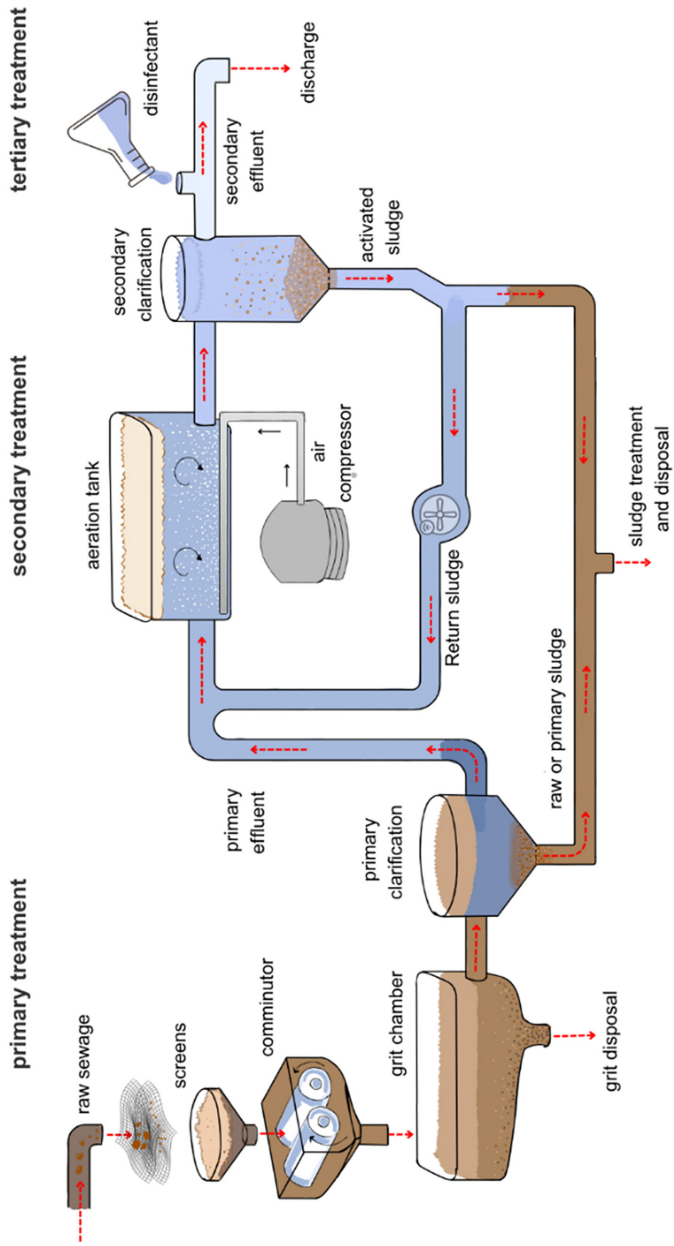


Figure 1.6 Stages in (waste)water treatment process.

(waste)water is also cleaned of oils, grease, and so on, which aids in reducing the biological and chemical oxygen demand of the (waste)water by 15–30%. Filtration, scum tanks, crushers, flotation machines, screen and filter tanks are a few of the equipment used in pre-treatment. As described earlier, a screen is utilised to eliminate large suspended particles. Large suspended materials are crushed in the grinder. Filter tanks with skimmers and floating units remove grease and oil. This is done to prevent them from damaging the equipment used in the next steps of water treatment. The materials removed during screening and grit removal are generally taken to a landfill and disposed of properly.

1.5.2 Primary treatment

The initial stage, known as primary treatment, is crucial in (waste)water treatment (Riffat and Husnain, 2022). In the initial treatment, organic and inorganic particles are removed using the physical treatments of sedimentation and flotation. The primary treatment removes 5–50% of the biochemical and chemical oxygen demand, 50–70% of the total suspended solids, and 65% of the oil and grease (Singh, 2017). Primary precipitation eliminates organic nitrogen, phosphorus, and heavy metals bound to solids while retaining colloidal and dissolved components. A circular or rectangular basin with a depth of 3–5 m and a hydraulic residence time of 2–3 h can serve as the primary settling tank. A central sump is filled with the settled solids (primary sludge) and pumped to a sludge treatment facility. Using mechanical techniques or water jetting, foam can be removed from the tank's surface and taken to a sludge treatment facility.

The chemical-enhanced primary treatment has also been used to hasten the process, in which the desired chemicals (metal salts and/or polymers in organic polyelectrolytes) are used (Shewa & Dagnew, 2020). The primary objective of such a process is to remove the organic carbon and nutrients while concentrating these substances in the generated sludge. This sludge can be viewed as a valuable resource for enhancing energy recovery. The primary treatment ensures that the water returned to the environment is safe for all living organisms, including wildlife, vegetation, and humans, if not reused/recycled.

1.5.3 Secondary treatment

The primary clarifier contains 60–80% of the elemental unstable organic matter initially present in the (waste)water (Riffat and Husnain, 2022). Additional processing is required to remove the colloidal organic matter that passes the initial clarifier. Organic matter undergoes oxidation or nitrification during secondary or biological (waste)water treatment, changing its characteristics and transforming into stable species. The secondary treatment of (waste)water can be done in various ways. Filtration, trickling filter, membrane bioreactor, sequencing batch reactor, moving-bed biofilm reactor, and activated sludge are broad categories that include these techniques. The secondary (waste)water treatment process involves biological methods that focus on lowering organic matter levels in (waste)water before it is directed to a disposal field for final treatment and integration into the soil, if not reused/recycled. The wastewater

generated through secondary treatment is of markedly higher quality than that obtained from a septic tank.

1.5.4 Tertiary treatment

When specific (waste)water constituents that the secondary treatment units cannot separate need to be eliminated, tertiary treatment is used before reusing, recycling, or releasing into the environment (Riffat and Husnain, 2022). Implementing tertiary treatment technologies can be viewed as advancing conventional secondary biological treatment, designed to enhance the stabilisation of oxygen-demanding materials in (waste)water and effectively eliminate nitrogen and phosphorus. The final cleaning step enhances the quality of the wastewater. Inorganic chemicals and compounds, including phosphorus and nitrogen, are removed throughout the treatment.

Generally, chlorination is commonly utilised as a disinfection strategy in the tertiary treatment stage during (waste)water treatment. Chlorine, recognised for its strong oxidising properties, engages with organic materials; however, it can also produce harmful chlorinated by-products that adversely affect human health and environmental integrity. Apart from chlorination, some common tertiary treatment methods are electrolytic precipitation, membrane technology, electrochemical processes, ion exchange, photocatalytic degradation, adsorption and thermal evaporation. However, the choice of technology is influenced by multiple factors. Primarily, the composition of the (waste)water and the volume requiring treatment must be assessed, which is primarily dictated by its source – urban, industrial, or agricultural. Additionally, treated reclaimed water must adhere to specific regulations based on its intended use, such as irrigation, groundwater replenishment, or potable water supply. The main aim of this treatment is to achieve good-quality wastewater that complies with disposal regulations.

1.6 SUMMARY

The proper functioning of the Earth's ecosystems is dependent on water. While the quantity of water available on the Earth is finite owing to the hydrological cycle, stress factors such as population growth, urbanisation, rising aspirations, and, more importantly, climate change are affecting water's spatial and temporal availability across the globe. Competing water demand for irrigation, industries, and domestic purposes made water management extremely complex. Discharging untreated (waste)water exacerbates water quality decline, necessitating advanced treatment and reuse strategies. Numerous contaminants, particularly chemicals, are being added to (waste)water, making it difficult to detect these chemicals. Pathogens contribute significantly to waterborne diseases and are becoming more robust and resistant to available disinfection techniques. In this complex water scenario, reusing treated (waste) water is an inevitable solution to meet ever-growing water demand. Various treatment processes are developed and implemented to treat (waste)water for reuse, varying in type and scale. However, these treatment processes primarily

rely on physical, chemical, and biological methods for removing contaminants, particularly organics in (waste)water.

This chapter provides a detailed overview of (waste)water treatment, exploring water pollution's fundamental causes and impacts and examining both conventional and advanced treatment methods. Beginning with an introduction to water pollution, the chapter identifies significant sources and types of pollution and discusses the consequences of various pollutants, including heavy metals, nitrates, and organic compounds. It categorises pollutants, including heavy metals, nitrates, PPCPs, and microbes, and evaluates physical, chemical, and biological treatment methods across preliminary, primary, secondary, and tertiary stages. Finally, the chapter outlines the stages of the wastewater treatment process, including preliminary, primary, secondary, and tertiary treatment. Effective (waste)water management is critical for sustainable water resources and environmental protection.

doi: 10.2166/9781789063943 _0027

Chapter 2

Adsorption process for wastewater treatment

2.1 INTRODUCTION

Numerous techniques for treating and reusing water are already in vogue. The most popular and well-known techniques are ion exchange, reverse osmosis, electrodialysis, adsorption, and electrolysis. The techniques, except adsorption, are expensive, costing between 10 and 450 USD per million litres of treated water. Depending on water quality, adsorption treatment costs 10–200 USD per million litres (Ali & Gupta, 2006). Besides the cost-effectiveness, simplicity, low energy requirements, short process time, broad applicability, flexibility, and ease of control are the factors that make adsorption a promising process for water treatment. Moreover, the process offers an advantage over other techniques as it removes soluble and insoluble contaminants and microbiological contaminants. Moreover, the removal efficiency of this process is as high as 90–99%. The following elements determine how economically and technically viable an adsorption process is:

- type of adsorbent,
- water characteristics (quality),
- pollutants to be removed,
- process configuration,
- efficiency,
- variety of solvents as adsorbents,
- recovery of the adsorbent and the adsorbate,
- regeneration, and
- waste (spent adsorbent) disposal

To separate and retain trace levels of contaminants of concern, such as organic materials in wastewater streams, adsorption separation is crucial. Adsorption is typically the first option when the contaminant level of the water is very low because of solid separation and utilisation capabilities. The mass transfer between a solution phase and a solid phase containing the target molecules (contaminants)

© 2026 IWAP. This is an Open Access book chapter distributed under the terms of the Creative Commons Attribution Licence (CC BY-NC-ND 4.0) which permits copying and redistribution for non-commercial purposes with no derivatives, provided the work is properly cited (https://creativecommons.org/licenses/by-nc-nd/4.0/). The chapter is from the book *Computational Techniques for Modelling and Simulating Adsorption Processes for (Waste)Water Treatment*, A. Yadav and P. Labhasetwar (Authors).

is the foundation of the adsorption separation technique. The porous structure of the adsorbent in the solid phase increases the separation (treatment) effectiveness.

The efficiency of the adsorption processes is governed by temperature and the nature of the adsorbate and adsorbent. Some other controllable factors are also involved in determining the adsorption process efficiency, including pH, pollutant concentration, contact time, and adsorbent particle size. It is crucial to emphasise that adsorption is an effective treatment process for contaminants between ng L^{-1} and mg L^{-1} (Dotto & McKay, 2020).

The chapter examines the adsorption process as a critical technique for wastewater treatment, highlighting its fundamental principles, influencing factors, and practical applications. This chapter explains the adsorption mechanism and the variables that impact its effectiveness. Additionally, it provides insights into various characterisation techniques for adsorbents (chemical, physical, and thermal) and explores classifications of the adsorption process based on interactions and operation modes. Through a discussion on adsorption models – including isotherms, kinetics, and thermodynamics – and computational simulations, this chapter seeks to present a comprehensive understanding of the adsorption process to improve wastewater treatment efficiency and pollutant removal.

2.2 ADSORPTION PROCESS

The adsorption process treats (waste)water in which a molecule or ion from a liquid or gaseous bulk phase adheres to a solid surface (Faust and Aly, 2013). The adsorption process is a surface phenomenon in which the adsorbate comes and adheres to the adsorbent surface; the adsorbate should not enter the interior of the adsorbent. Adsorption of the adsorbate over the adsorbent surface is a result of the fact that the surface particles of the adsorbent have asymmetrical or residual attractive forces that are not in the same condition as the bulk adsorbent's particles, which have all the forces balanced together. Adsorption is a temperature-dependent surface phenomenon that increases the concentration of a particular component (known as 'adsorbate') on a solid or liquid medium (known as 'adsorbent'). Adsorption can also take place at the interface between the two phases. The adsorption process has three parts (Figure 2.1). Adsorbate first undergoes external mass transfer from the bulk solution to the adsorbent's surface, diffuses internally to the absorption sites, and finally undergoes actual adsorption.

Generally, the adsorption process is classified into two broad categories, that is, chemical and physical adsorption (Alaqarbeh, 2021). This classification depends upon the adherence of the adsorbate to the adsorbent surface. Chemical adsorption is also called chemisorption, in which the adsorbate molecules adhere to the adsorbent surface due to covalent bonds. In physical adsorption, the adsorbate molecules adhere to the adsorbent surface due to weak forces like electrostatic attraction and van der Waals forces. The physical adsorption process is also referred to as physisorption. Chemisorption is slower than physisorption and typically results in the formation of a monolayer on the surface of the adsorbent, whereas physisorption typically results in the formation of a multilayer.

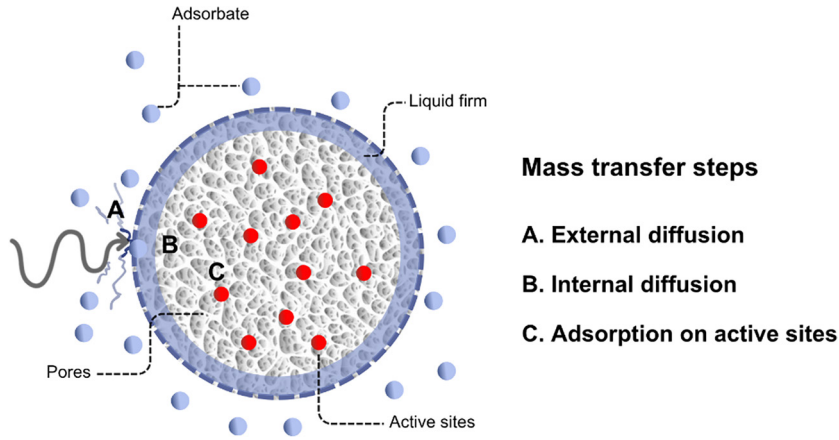


Figure 2.1 Adsorption mass transfer steps.

2.3 FACTORS AFFECTING THE ADSORPTION PROCESS

The performance of the adsorption process is affected by several parameters, as shown in Figure 2.2. These parameters are described below (Ottewill, 2012).

2.3.1 Contact time

The adsorption process is significantly influenced by contact time. Process effectiveness and adsorption rate can both be impacted by contact time. At the beginning of the process, the rate of adsorption is usually rapid because numerous active sites are available on the adsorbent surface. As time progresses, these sites gradually become occupied, and the adsorption rate slows down until equilibrium is reached. Beyond the equilibrium time, no significant increase in

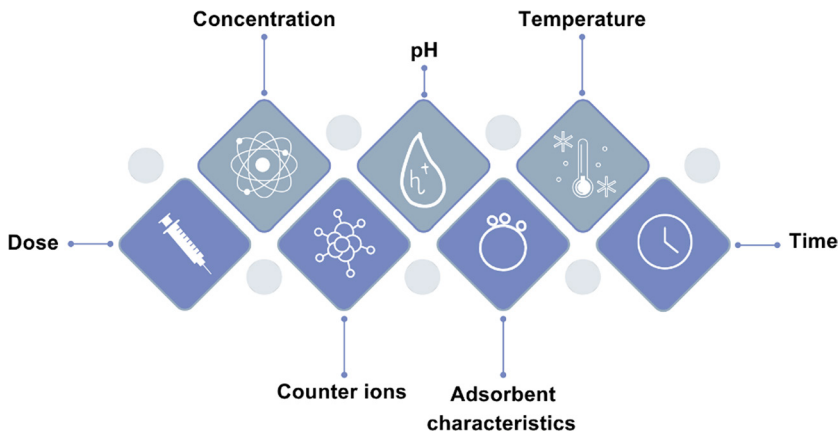


Figure 2.2 Factors affecting the adsorption process.

adsorption occurs, as all available sites are saturated or the driving force for mass transfer diminishes.

2.3.2 pH

One variable that impacts the adsorbent's ability to adsorb contaminants throughout the (waste)water treatment process is pH. The degree of ionisation of the adsorbent molecules is determined by a change in pH and the surface characteristics of the adsorbent.

2.3.3 Initial contaminant concentration

The initial contaminant concentration plays a crucial role in determining the adsorption performance of an adsorbent material. Generally, at lower concentrations, the available active sites on the adsorbent surface are sufficient to capture most of the contaminant molecules. However, as the contaminant concentration increases, these sites become occupied more rapidly, leading to saturation. Beyond this point, no additional contaminants can be adsorbed, resulting in a decrease in adsorption efficiency.

2.3.4 Adsorbent dose

The adsorption dosage, a critical factor, substantially impacts the extent of the adsorption process. The adsorbate removal efficiency typically increases with increasing volumes of adsorbent material because there are more accessible adsorption sites on the surface that have been adsorbed. The effect of the adsorbent dosage can alter a material's capacity to adsorb, and even a minute amount of adsorption indicates the material's economic importance.

2.3.5 Temperature

The thermodynamic parameters are utilised in conjunction with the temperature to characterise the adsorption process, and so on. Whether the process is exothermic or endothermic, spontaneity and chance affect the appropriate temperature. DG^0, DH^0, and DS^0, which stand for changes in Gibbs free energy, enthalpy, and entropy respectively are significant thermodynamic parameters. Positive DG^0 values indicate spontaneous adsorption processes. A positive DS^0 number, on the other hand, implies that the process is endothermic.

2.3.6 Presence of other ions

Coexisting ions in the solution significantly influence removal efficiency in adsorption processes, resulting in competitive adsorption on the adsorbent surface. A wide variety of additional ions coexist in water, in addition to heavy metal ions and colour molecules, and the concentration of these ions impacts adsorbate (pollutant) absorption. The presence of Na^+, K^+, Ca^{2+}, Mg^{2+}, Cl^-, NO^{3-}, and SO_4^{2-} ions in the solution can reduce the adsorption capacity of heavy metal ions.

2.3.7 Adsorbent characteristics

As the adsorbent's surface area increases, adsorption rises due to the availability of more adsorbent sites and a larger surface area. Distinct

framework structures result in different adsorbent properties such as acid strength, molecule size adsorbed, different compounds' adsorption/desorption rate, capacity, and stability. Therefore, these characteristics specify the adsorbent's selectivity to a particular molecule and interactions between the adsorbent and adsorbate. The second adsorbent feature is capacity, which is the amount of the desired component that is adsorbed from the feed when the adsorbent is exposed to the feed. An adsorbent's capacity is expressed as the weight or volume of the required component, and it can adsorb per volume or weight of the adsorbent. Having capacity values as high as physically possible is preferred. The pulse test tool is used to assess selectivity and capacity.

In recent years, numerous studies have been conducted on using various materials for (waste)water treatment. The synthesis of new adsorbents with excellent adsorption properties for water pollutants is an ongoing area of research. Chemical composition, structure, and surface chemistry are essential parameters for determining the performance of adsorbents in wastewater and water treatment. However, adsorbents' physical and chemical characteristics can be tuned for particular applications using the right synthesis strategies.

The selection, development, and characterisation of adsorbent materials are essential in designing the (waste)water treatment adsorption process. A suitable adsorbent for water treatment needs the following characteristics:

- **Accessibility and low cost:** Since the adsorbent material contributes to 70% of operational costs interchangeably, considerable quantities must be conveniently synthesised and easily transported to the treatment plants.
- **Chemical stability:** Because the absorbent's effectiveness may be affected by the chemical characteristics of different water matrices (pH, ionic strength, conductivity), the adsorbents must be chemically stable. Additionally, the adsorbent must be mechanically stable because continuous water treatment must be done in columns to prevent high-pressure drops and preferred paths.
- **Good physicochemical and textural properties:** The adsorbent should have a large surface area, a large pore volume, and functional groups that can interact with pollutants on the surface. These essential characteristics have influenced the following three criteria.

(1) **High adsorption capacity:** Adsorbents must be highly effective at adsorbing contaminants per unit weight of material.
(2) **High efficiency:** Ensure that a high percentage of contaminants is removed from the water and transported to the adsorbent.
(3) **Fast kinetics:** High adsorbed concentrations should be released fast due to the adsorbent properties. Because of the short time required for complete treatment, the treatment plant's size and ensuing capital cost are affected.

Naturally, producing an adsorbent with all the properties mentioned above is challenging. Numerous studies have been done to develop various adsorbents for water treatment. Carbonaceous materials such as charcoal, biochar, activated carbon, and nanomaterials have been developed for adsorption-based

water treatment. Chitin and chitosan-derived products are different classes of water absorbents. Biosorbents and agricultural waste are also subjects of great interest. Geopolymers, zeolites, and layered double hydroxides are examples of inorganic-based materials in different classes. Metal-organic frameworks (MOFs) were created to remove pollutants from water. Silica-based materials are also employed as adsorbents for the purification of water. Most of these adsorbent materials have extensive literature on preparation and cutting-edge characterisation techniques. In general, it can be said that a variety of well-developed and characterised materials exist that are appropriate for use as adsorbents in water treatment. However, there is no question that the continuous development of new adsorbent materials is required to achieve all the above properties, leading to more effective adsorption processes for water treatment.

2.4 CHARACTERISATION OF ADSORBENTS

The development and advancement of adsorbent materials is an essential area of research due to the relevance of adsorption processes for several applications in (waste)water treatment. A thorough characterisation is needed when a new adsorbent material is developed to understand its performance in the desired process and support its application and properties. Depending on the type of adsorbent material to be studied and the instruments at hand, multiple techniques can be used to collect a variety of physical and chemical characteristics (Pellenz *et al.*, 2023; Tran *et al.*, 2017). These techniques permit the identification of the morphology, elemental composition, functional groups, structure, topography, magnetic properties, and size, among other physical properties of the adsorbent (Figure 2.3).

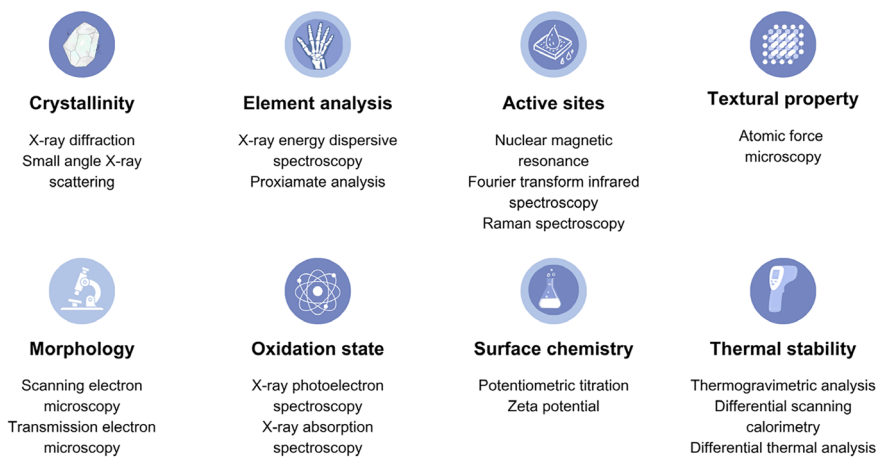


Figure 2.3 Important properties of adsorbents and their quantification techniques.

2.4.1 Chemical characterisation

Adsorbents can be chemically characterised using several methods that offer pertinent details on the chemical compositions in terms of their identification, location, and quantification. The functional groups present in adsorbents directly influence the adsorption mechanisms. This includes hydrogen bonding, complexation, coordination/chelation, electrostatic, hydrophobic, and π–π stacking interactions, which can be determined using chemical characterisation. This section discusses the chemical characterisation methods used for adsorbent materials.

2.4.1.1 Ultra-violet–vis spectroscopy

To identify and quantify the presence and concentration of specific chemicals or functional groups in the sample, UV–vis spectroscopy (also known as spectrophotometry) is employed. UV–vis spectroscopy is also employed as a supporting instrument when addressing the effectiveness and mechanisms of adsorption.

2.4.1.2 Fourier-transform infrared spectroscopy

Different functional groups in the adsorbent are identified using Fourier-transform infrared spectroscopy (FTIR). An adsorbent's surface functional groups offer interaction sites for the attachment of the target adsorbates.

2.4.1.3 Raman spectroscopy

Raman spectroscopy (RS) and surface-enhanced Raman scattering (SERS) are used to identify the chemical and structural information of the adsorbent. This information includes identifying its lattice structure and assessing compounds present in the sample through the unique Raman fingerprint of its molecular bonds.

2.4.1.4 X-ray photoelectron spectroscopy

X-ray photoelectron spectroscopy (XPS) is used to identify atoms and functional groups present on the surface of a solid adsorbent. It also characterises the adsorbent's chemical composition, evaluating the synthesis and functionalisation processes. This technique is also proper for the characterisation of an adsorbent post-adsorption.

2.4.1.5 X-ray absorption scattering

X-ray absorption scattering analysis can be applied to study the adsorption mechanism of metals onto adsorbents since they can provide information on the oxidation state and coordination geometry of a metal in the adsorbent, coordination number, distance of a metal atom from neighbouring atoms, coordination type, and bond length.

2.4.1.6 Energy-dispersive X-ray spectroscopy

Energy-dispersive X-ray (EDX) spectroscopy is widely applied for elemental identification and compositional mapping of an adsorbent. It is also possible to map the distribution of the adsorbent's chemical compositions along its

surface using EDX in conjunction with SEM or TEM. Moreover, these analyses assist in studying the distribution of the elements and functional groups on the surface of the adsorbent, as well as how the adsorbate is dispersed after adsorption. This is also helpful for identifying potential interactions between the adsorbent's functional groups and the adsorbate.

2.4.1.7 Ultimate analysis

The ultimate analysis measures the weight% of carbon, hydrogen, nitrogen, and sulfur in a wide range of organic and inorganic adsorbents, solid and liquid.

2.4.1.8 Zeta potential

In adsorption processes, the zeta potential is employed to investigate the surface charge of adsorbents and their possible interactions with the adsorbates. Since electrostatic interactions and complexation reactions between the adsorbent and adsorbate can favour or hinder the adsorption of charged molecules, such as metals and ionic forms of organic compounds, knowledge of the adsorbent charge is significant.

2.4.1.9 Solid-state nuclear magnetic resonance

The atomic-level structure of adsorbent material and the molecular-level interaction between the adsorbate and the adsorbent can be examined with solid-state nuclear magnetic resonance (ss NMR).

2.4.2 Physical characterisation

Adsorbent materials should be examined to study their structure, topography, morphology, magnetic properties, and size, among other physical characteristics. This section discusses the physical characterisation methods used in adsorbent materials.

2.4.2.1 X-ray diffraction

The crystal characteristics of adsorbent materials are commonly investigated using X-ray diffraction (XRD), which evaluates the atomic arrangement, crystal size, lattice parameters, and defects. Chemical modifications frequently alter the structure of the material, which can be seen in changes to the peak's intensity, breadth, and angle, as well as in the appearance of new XRD peaks.

2.4.2.2 Scanning electron microscopy/field emission scanning electron microscopy

Scanning electron microscopy (SEM) and field emission SEM (FESEM) offer details on the adsorbent material morphology, topographic characteristics, crystal structure and orientation, compositional variation, phase distribution, and the location of imperfections.

2.4.2.3 Transmission electron microscopy

Transmission electron microscopy (TEM) examines adsorbents' chemical and electrical structure and identifies imperfections like vacancies and dislocations. However, it may also reveal individual particles' size, shape, and approximate

thickness. Scanning transmission electron microscopy (STEM), a form of TEM, is used to study how high-density elements are distributed on the surface of the adsorbent.

2.4.2.4 Atomic force microscopy

An adsorbent topography is evaluated using atomic force microscopy (AFM), which produces three-dimensional images with atomic resolution. Sheet-like and membrane adsorbents' height variation and sheet thickness can be assessed with an AFM.

2.4.2.5 Surface area and porosimetry

Brunauer–Emmett–Teller studies are performed for porous adsorbent materials to determine the specific surface area, pore volume, particle size, porosity, surface energy, uniformity, area, and pore-size distribution.

2.4.2.6 Value stream mapping

Value stream mapping (VSM) is a method that reveals details about an adsorbent magnetisation. VSM can be used to assess the feasibility of magnetic composites of adsorbents for magnetic separation when dispersed in a liquid environment. Currently, magnetic separation is more frequently used to separate catalysts, but it might also be used to separate adsorbents that resemble powder.

2.4.2.7 Dynamic light scattering

Dynamic light scattering (DLS) is used to characterise adsorbents by determining the size distribution of nanomaterials and the information related to synthesising the adsorbents or materials. DLS can also be employed to examine particle aggregation and homogeneity, and it provides options for separating the material from the medium.

2.4.3 Thermal characterisation

The physical properties of adsorbents are assessed as a function of temperature in thermal analysis, which can be accomplished by employing various techniques. Thermogravimetry (TG), differential thermal analysis (DTA), differential scanning calorimetry (DSC), temperature-programmed reduction/oxidation (TPR/TPO), and other analytical techniques that base their evaluation on physical property as a function of temperature, which includes TG, DTA, and TPR/TPO.

2.5 CLASSIFICATION OF THE ADSORPTION PROCESS

The adsorbent performance exhibited a non-linear relationship with several operating parameters, which include fluid properties such as pH and temperature, contaminant properties such as concentrations, charges on contaminants, and so on. The adsorbent performance also depends upon the presence of competitive ions. The properties of adsorbents are known to determine adsorption mechanisms, including ion exchange, electrostatic interactions, surface deposition, chemical reactions, or combinations thereof.

2.5.1 Type of interactions

Depending on how strongly the adsorbate interacts with the adsorbent, the adsorption process is usually called a chemisorption or physisorption process (Ottewill, 2012) (Figure 2.4).

2.5.1.1 Physical adsorption or physisorption

In physical adsorption, weak electrostatic interactions such as London dispersion forces, dipole–dipole forces, and Van der Waals interactions are involved between the adsorbent and the adsorbates (contaminants). When Van der Waals interaction is present in adsorption, the process is also referred to as a reversible adsorption process because of the weak Van der Waals interaction force. Physical adsorption is reversible, has a low enthalpy, and occurs at temperatures much below the adsorbate's boiling point. In this instance, multilayer adsorption is feasible since the adsorption energy is as low as 5–40 kJ mol^{-1}. The distinction between physisorption and chemisorption should be understood as a generic behaviour rather than a dogma.

2.5.1.2 Chemical adsorption or chemisorption

If there is an exchange of electrons between the adsorbent and the adsorbate, it is chemical adsorption or chemisorption. In this case, the adsorption is accompanied by electron transfer. It has a high energy of 40–800 kJ mol^{-1}, so it is challenging to desorb, and it is irreversible and flows only as a single layer. In chemisorption, interactions can occur mainly through ionic or covalent bonds, either by electron sharing or electron transfer. In chemisorption, a single adsorbate layer is formed on the adsorbent, while in physisorption, multiple adsorbate layers are formed on the adsorbent. High enthalpy, irreversible chemisorption happens at all temperatures.

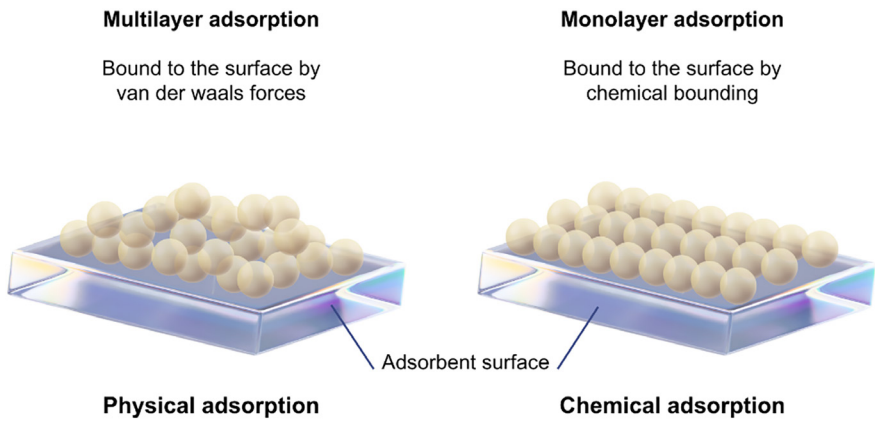


Figure 2.4 Chemical and physical adsorption.

2.5.2 Mode of operation

Batch and column techniques can be used in the laboratory to develop and optimise adsorption parameters (Ottewill, 2012). A large column implements the adsorption technology on pilot and commercial plants.

2.5.2.1 Batch adsorption

The primary technique mentioned in the literature on water treatment is batch adsorption (batch adsorbent), as shown in Figure 2.5. The adsorbent is placed in a tank of contaminated water in this operation. The mixture is stirred up until equilibrium is reached. After that, decantation, filtering, or centrifugation separates the solid from the liquid. At the laboratory scale, it is beneficial to maximise adsorption factors. However, it is inefficient for handling large volumes of water because it requires a large physical surface area and additional plant work to separate solids and liquids.

2.5.2.2 Continuous fixed-bed adsorption

A significant application for broad-based treatment, fixed-bed mode, as shown in Figure 2.6, is convincingly supported in the literature. The contaminated water is directly pumped into an adsorbent-containing column during this process. The process is repeated until the column is saturated at the intake and outflow with the same pollutant concentrations. Throughout the process, contaminant concentration at the column output is monitored. These data can be used to create breakthrough curves, which prolong the adsorption process. It is possible to assess factors like bed height and flow rate using this method of operation. Fixed-bed operations do not need extra separation processes because they can manage enormous volumes of water in a small physical space. On the other hand, interactions between fluids and particles are not always efficient. This mode of operation is subject to hydrodynamic limitations such as preferential path formation and high-pressure drop.

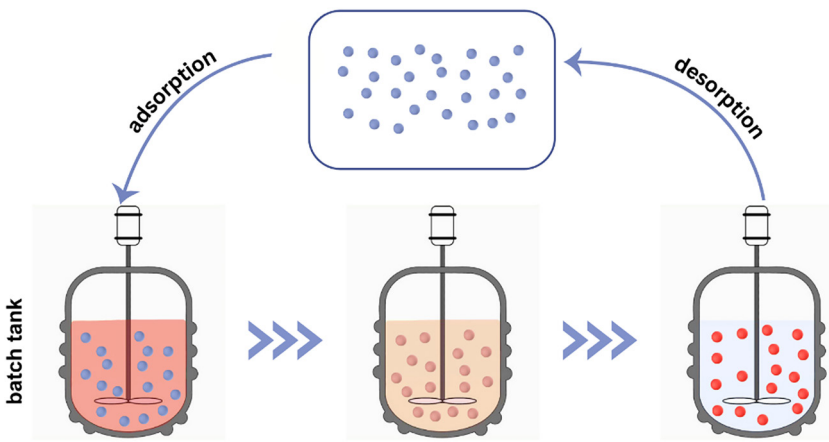


Figure 2.5 Batch adsorption process.

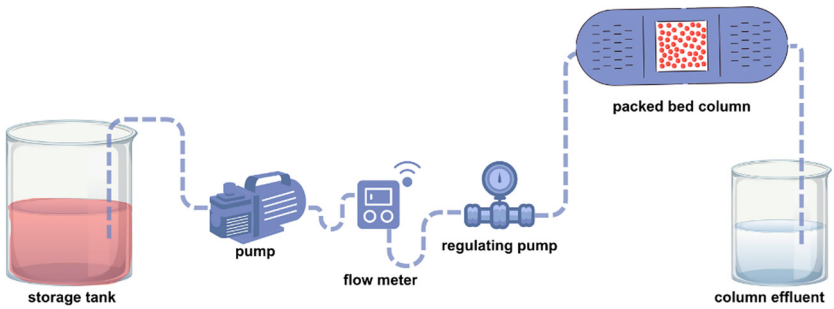


Figure 2.6 Fixed-bed adsorption process.

Discontinuous adsorbents are extensively documented in the literature regarding adsorption regimes, and they should be used at the laboratory scale to optimise experimental adsorption settings. On the other hand, fixed-bed operations have undergone more research regarding their design and efficacy than batch adsorption at the laboratory scale. Water treatment techniques can be scaled up commercially using fixed-bed operation. The primary challenge is to create and develop new modes of operation that enable more effective fluid particle communication and straightforward phase separation. We gain from treating fewer physical surfaces, less downtime, greater throughput, lower costs, and other advantages. Expanded bed, fluidised bed, funnel bed, simulated moving bed, continuous stirred tank reactor, and multi-batch adsorption reactor studies are recommended as possible alternatives.

In the laboratory, batch and column methods can be performed to develop and optimise adsorption parameters. Large columns are used to implement the adsorption technology at both pilot and industrial scales.

Both batch and continuous adsorption techniques offer several benefits in (waste)water treatment. Batch reactors can assess adsorption rates, maximum capacity, and thermodynamic parameters. They also include the analysis of adsorbent(s) and their interactions with the contaminants and other counter ions. Packed-bed columns are appropriate for large-scale water treatment applications where considerable volumes of liquids can be handled quickly. A compact column adsorption test is necessary to determine pertinent scaling factors, including breakthrough and saturation periods, bed adsorption capacity, and mass transfer parameters. This process configuration enables us to ascertain the adsorbent's maximal performance and the ideal dynamic business scenario.

2.6 EMPIRICAL ADSORPTION PROCESS MODELS

Adsorption models are non-linear and multivariate, primarily used to analyse multi-component systems (e.g., groundwater, industrial wastewater, and wastewater). Modelling of adsorption processes refers to designing, operating, optimising, and controlling water treatment technologies for practical

applications. The three types of adsorption models are theoretical, semi-empirical, and empirical. They could be intricate systems of algebraic and differential equations or straightforward analytical formulas that consider mass transport events. As a result, modelling adsorption data is a challenging mathematical problem requiring non-linear data regression techniques to identify model parameters with suitable error functions and in-depth statistical analysis to assess model performance. Depending on the model's complexity, several computational techniques are frequently required when connecting adsorption data. For instance, partial differential equations are solved numerically using mass transfer models. The adsorption model should have the appropriate mathematical complexity, provide an acceptable level of accuracy in correlating and evaluating adsorption performance under various operating conditions, and provide a reliable assessment of process performance without extensive experimental data. The model should help assess how operating variables affect adsorption effectiveness. The chosen model must balance mathematical complexity and accuracy to explain the process.

It should be emphasised that depending on the adsorption system under investigation and operational conditions, the quantitative performance of the adsorption model cannot be specified *a priori*, and data analysis may be constrained. In reality, no single model can describe all adsorbent/adsorbent systems. Hence, it is necessary to test various adsorption models to find the best one for each case. The relative benefits and drawbacks of the now available models have not yet been sufficiently studied, especially when analysing adsorption processes for removing essential water contaminants in multi-component systems. Due to antagonistic, synergistic, and non-interactive effects, multi-component adsorption systems pose difficulties for existing models, as was previously highlighted. For instance, the synergistic adsorption promoted by dye molecules and competing adsorption among metal species make the simultaneous removal of heavy metals and acid dyes challenging. Existing models might not be able to replicate and forecast the performance of adsorbents in various operating settings for these combinations. Reliable adsorption models are needed to evaluate multi-component systems containing a variety of organic and inorganic contaminants that should be typical of groundwater, wastewater, and industrial effluent.

Empirical correlations are frequently utilised in adsorption processes for ion/molecular separations to forecast separations and link process variables to separation effectiveness. These empirical models can be highly accurate and can be applied to adsorption kinetics and isotherms. The modelling of the adsorption process for (waste)water treatment is thoroughly researched in the literature. In general, isotherms, thermodynamics, and kinetics, all covered in the next section, are studied to interpret a specific adsorption process.

2.6.1 Adsorption isotherms

The isothermal curves link the amounts of contaminants retained in the water in thermodynamic equilibrium and the amounts that have been adsorbed in the adsorbent. The processes by which pollutants interact with adsorbents are also described by adsorption isotherm models, which consider both equilibrium

data and adsorption characteristics. According to the isothermal shape of adsorbate–adsorbate pairs, adsorption isotherms can be classified into six types by the IUPAC (International Union of Pure and Applied Chemistry), as presented in Table 2.1 (Al-Ghouti & Da'ana, 2020).

The primary requirement is that the data and isotherm function fit together accurately. The reduced chi-square statistics are used to evaluate the quality of the fit and can be obtained by dividing the variance of the fit by the average variance of the data. Second, the isotherm function should be accurate in terms of thermodynamics. Three requirements must be satisfied: the slope must be positive for all concentrations, the isotherm must be linear when the concentration hits zero, and a finite capacity must be at the maximum concentration.

Isotherm models, their linear and non-linear equations, and the parameters to plot the equation are summarised in Table 2.2 (Al-Ghouti & Da'ana, 2020).

2.6.2 Adsorption kinetics

Kinetic studies are crucial for adsorption to be effective in water treatment. In the case of discontinuous systems, the kinetic curves can be represented as plots of adsorption capacity vs time or pollutant concentration over time. When a bed is fixed, the representation can be either dimensionally free pollutant concentration at the column outlet over time or dimensionally free pollutant concentration at the column outlet across the bed's volume. Numerous empirical and semi-empirical models can be used to represent the kinetics of adsorption. While some models assume that diffusion is the rate-limiting phase in the adsorption process, others are predicated on the idea that absorption is the rate-limiting process. Clarification of the adsorption mechanism is thus made possible by adapting the models.

The pseudo-first-order (PFO) and pseudo-second-order (PSO) models were initially presented and have since been widely used for characterising the adsorption kinetics in colloid systems. However, there have not been many proposed adsorption mechanisms to back up the usage of these models. These models are, in theory, mathematically equivalent to the standard models based on first- and second-order reaction kinetics. The word 'pseudo' stands for a lack of reference to the kinetics of homogeneous reactions in the models.

2.6.2.1 Pseudo-first-order models

In 1898, Lagergren first proposed the PFO model. Eq. (2.1) describes the PFO model's differential form (Lagergren, 1898):

$$\frac{dq_t}{dt} = k_1\left(q_e - q_t\right) \tag{2.1}$$

On integrating Eq. (2.1) for the boundary conditions ($q_0 = 0$), it gives the following results:

$$q_t = q_\infty\left(1 - e^{-k_1 t}\right) \tag{2.2}$$

Table 2.1 Categorisation of adsorption isotherms. (Al-Ghouti & Da'ana, 2020).

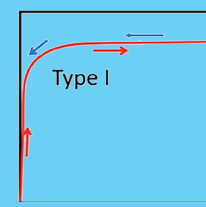
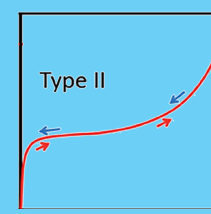
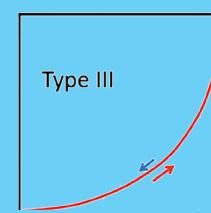
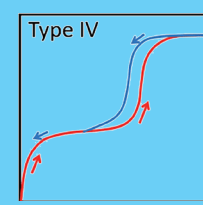
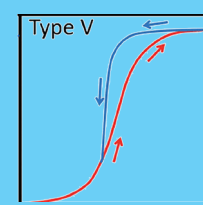
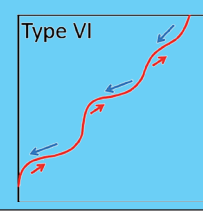
Isotherm Type	Description	Sample Graph (Adsorbed Volume vs Relative Pressure)
Type I isotherms (convex upward)	A horizontal plateau represents high pressure of adsorbate.	
Type II isotherms	Adsorption on materials with mesoporous monolayers at low pressure and materials with mesoporous multilayers at high pressure.	
Type III isotherms (concave upward)	Adsorbate–adsorbate interaction is larger than the adsorbate–sorbent interaction.	
Type IV isotherms	Adsorption behaviour of particular mesoporous adsorbents demonstrates pore condensation and hysteresis between desorption and adsorption branches.	
Type V isotherms	Represents phase change in mesopores.	
Type VI isotherms	Isotherm displays progressive multilayer adsorption at low temperatures.	

Table 2.2 Illustration of the linear forms, non-linear forms and plots of various isotherm models. (Al-Ghouti & Da'ana, 2020).

Isotherm Model	Linear Form	Non-linear Form	References
Henry	$q_e = kC_e$		Thomas (1944)
Langmuir	$\frac{C_e}{q_e} = Q_o - \frac{q_e}{bC_e}$	$q_e = \frac{Q_o b C_e}{1 + bC_e}$	Langmuir (1918)
Freundlich	$\log q_e = \log K_F + \frac{1}{n}\log C_e$	$q_e = K_F \ln C_e$	Freundlich (1909)
Dubinin–Radushkevich	$\ln q_e = q_s - K\varepsilon^2$	$q_e = q_{se} - K\varepsilon^2$	Dubinin and Radushkevich (1973)
Temkin	$q_e = \frac{RT}{b_T}\ln A_T + \left(\frac{RT}{b_T}\right)\ln C_e$	$q_e = \frac{RT}{b_T}\ln A_T C_e$	Tempkin *et al.* (1940)
Flory–Huggins	$\log\left(\frac{\theta}{C_o}\right) = \log K_{FH} + n_{FH}\log(1-\theta)$	$\frac{\theta}{C_o} = K_{FH}(1-\theta)^{n_{FH}}$	Flory (1942), Huggins (1941)
Hill	$\log\left(\frac{q_e}{q_{SH} - q_e}\right) = n_H \log C_e - \log K_D$	$q_e = \left(\frac{q_{SH} C_e^{nH}}{K_D + C_e^{nH}}\right)$	Hill (1952)
Halsey	$\ln q_e = \left(\frac{1}{n_H}\right)\ln K_H - \left(\frac{1}{n_H}\right)\ln C_e$	$q_e = e^{\left[\frac{\ln K_H - \ln C_e}{n_H}\right]}$	Halsey (1948)
Jovanovich	$\ln q_e = \ln q_{\max} - K_J C_e$	$q_e = q_{\max}\left(1 - e^{K_J C_e}\right)$	Jovanović (1969)
BET	$\frac{C_e}{q_e(C_s - C_e)} = \frac{1}{q_m C_{\text{BET}}} + \frac{(C_{\text{BET}} - 1)C_s}{q_m C_{\text{BET}} C_e}$	$q_e = \frac{q_e C_{\text{BET}} C_e}{C_s - C_e[1 + (C_{\text{BET}} - 1)C_e/C_s]}$	Brunauer *et al.* (1938)
Redlich–Peterson	$\ln\left(\frac{K_R C_e}{q_e} - 1\right) = g\ln C_e + \ln a_R$	$q_e = \frac{K_R C_e}{1 + a_R C_e^g}$	Redlich and Peterson (1959)
Toth	$\ln\left(\frac{q_e}{K_T}\right) = \ln C_e - \frac{1}{t}\ln(a_T + C_e)$	$q_e = \frac{K_T C_e}{(a_T + C_e)^{\frac{1}{t}}}$	Tóth (1981)
Sips	$\beta S \ln Ce = \ -\ln KSqe + \ln aS$	$q_e = \frac{K_S C_e^{\beta} S}{1 + a_S C_e^{\beta} S}$	Sips (1948, 1950)
Weber–Van Vliet	Weber–Van Vliet in a non-linear model only	$C_e = P_1 q_e^{P_2 q_e^{P_3 + P_4}}$	van Vliet *et al.* (1980)
Marczewski–Jaroniec	–	$q_e = q_{MMJ}\left(\frac{(K_{MJ}C_e)^{nMJ}}{1 + (K_{MJ}C_e)^{nMJ}}\right)^{\frac{M_{MJ}}{n_{MJ}}}$	Marczewski and Jaroniec (1983)
Fritz–Schluder	$\frac{C_e}{q_e} = \frac{1}{k_s q_{\text{MFS}}} + \frac{1}{q_{\text{MFS}}} C_e^{\alpha}$	$q_e = \frac{1_m F S_s K_1 C_e^{\alpha_{FS}}}{1 + K_2 C_e^{\beta_{FS}}}$	Fritz and Schluender (1974)

The linear form of the PFO model is given below.

$$\ln(q_e - q_t) = \ln q_e - k_1 t \tag{2.3}$$

To fit the kinetics data and get the parameters q_e and k_1, Eq. (2.3) is typically employed by plotting $\ln(q_e - q_t)$ vs. t. However, the linearisation process may cause inaccurate estimations of the parameters.

PFO theory meets three of the requirements shown in Figure 2.7. The first is that C_0 has a high value. The adsorption process remains in its early stages, which is the second factor. The third is that the adsorbent material has limited active sites.

2.6.2.2 Pseudo-second-order models

The PSO model (Eq. (2.4)) was first applied to model the adsorption of lead onto peat (Ho *et al.*, 1996). The PSO model was then widely used to explain the adsorption processes. The adsorption experimental data and rate constants are generally predicted and calculated using the PSO model.

$$\frac{dq_t}{dt} = k_1 (q_e - q_t)^2 \tag{2.4}$$

The integrated PSO model is described as follows:

$$q_t = \frac{q_e^2 k_2 t}{1 + q_e k_2 t} \tag{2.5}$$

The linearisation of the PSO model changes the weight of q_t and introduces propagated errors, which leads to inaccurate calculations of the model parameters.

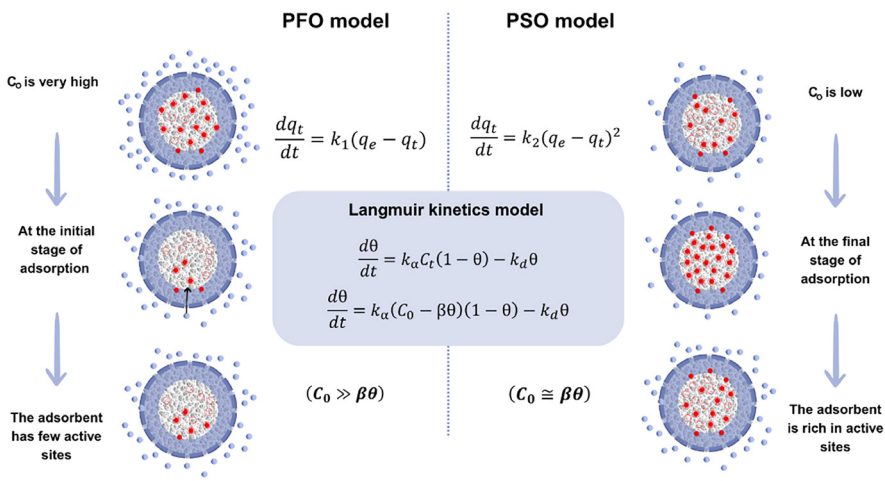


Figure 2.7 Physical meanings of the pseudo-first-order and pseudo-second-order models (Wang & Guo, 2020).

Table 2.3 Adsorption kinetic models (Wang & Guo, 2020).

Model	Linear Form	Non-linear Form	References
PFO model	$\ln(q_e - q_t) = \ln q_e - k_1 t$	$q_t = q_\infty\left(1 - e^{-k_1 t}\right)$	Lagergreen (1907)
PSO model	$\frac{t}{q_t} = \frac{1}{q_e^2 k_2} + \frac{t}{q_e}$	$q_t = \frac{q_e^2 k_2 t}{1 + q_e k_2 t}$	Ho *et al.* (1996)
Mixed order model	$\frac{dq_t}{dt} = k'_1(q_e - q_t) + k'_2[q_e - q_t]^2$	–	Guo and Wang (2019)
Ritchie's equation	$\frac{\partial\theta}{\partial t} = \alpha[1-\theta]^n$	$q_t = q_e(1 - e^{-\partial t});\ (n=1)$ $q_t = q_e - \frac{q_e[1+(n-1)\partial t]1}{1-n}(n \neq 1)$	Ritchie (1977)
PNO model	$\frac{\partial q_t}{dt} = k_n[q_e - q_t]^n$	$q_t = q_e\left(1 - \frac{1}{\left(1+(n-1)q_e^{n-1}k_n t^{\frac{1}{n-1}}\right)}\right);(n \neq 1)$	Ozer (2007)
Elovic model	$q_t = \frac{1}{\beta}\ln(\alpha\beta) + \frac{1}{\beta}\ln(t)$	$q_t = \frac{1}{b}\ln(1+abt)$	Elovich and Larionov (1962)
Boyd's external diffusion equation	$\ln\left(1 - \frac{q_t}{q_\infty}\right) = -Rt + A$	$q_t = q_\infty(1 - e^{-Rt})$	Boyd *et al.* (1947)
EMT model	$\frac{\partial q_t}{\partial t} = \frac{k_s}{\rho}(C_t - C_{et}) = k_{ext}(C_t - C_{et})$	$q_t = \frac{q_{\max}K_L C_{et}}{1 + K_L C_{et}}$	Hines and Maddox (1985), Ruthven (1984)
Boyd's intraparticle – diffusion model		$\mathrm{Byt} = 2\pi - \frac{\pi^2 F}{3} - 2\pi\left(1 - \frac{\pi\frac{q_t}{q_e}}{3}\right)^{1/2} \quad \left(0 \leq \frac{q_t}{q_e} \leq 0.85\right)$ $\mathrm{Byt} = -\ln\left(\frac{\pi^2}{6}\right)\left(1 - \frac{q_t}{q_e}\right) \quad \left(0.86 \leq \frac{q_t}{q_e} \leq 1\right)$	Boyd *et al.* (1947)
IMT model	$\frac{\partial q_t}{\partial t} = k_{\mathrm{int}}(q_{et} - q_t)$	–	Glueckauf and Coates (1947), Yang (1997)

The PSO hypothesis satisfies three conditions, as presented in Figure 2.7. The first one is that the value of C_0 is low. The second one is at the final stage of the adsorption process. The third one is that the adsorbent material is abundant with active sites.

Several adsorption kinetic models are summarised in Table 2.3.

2.6.3 Adsorption thermodynamics

According to the second law of thermodynamics, the adsorption of substances (contaminants) on solids takes place to reduce the free surface energy of the solid. The energy of forming a chemical bond on a solid's surface can be depicted using the Lennard–Jones potential energy curve (Lenhard *et al.*, 2024). Therefore, Lennard–Jones potential can be used to explain the energetic phenomenon occurring during an adsorption or desorption process. Figure 2.8 represents the molecule's energy as a function of the distance (z) from the mass centre of the molecule to the surface. The well results from the balance of two forces: van der Waals attraction and repulsion between the electron clouds at the surface and that of the sorbed molecule. When a molecule reaches the well, it is trapped or, in other words, 'adsorbed' by this potential energy until it has sufficient energy to desorb. Thus, lowering the molecule's energy makes it easier for the molecule to fall and stick in the chemisorption well. Two types of wells are presented on the curve: chemisorption and physisorption wells. The physisorption well is located after the chemisorption one (i.e., when the distance is considerable) because the bonds formed are short-ranged and stronger in the case of chemisorption.

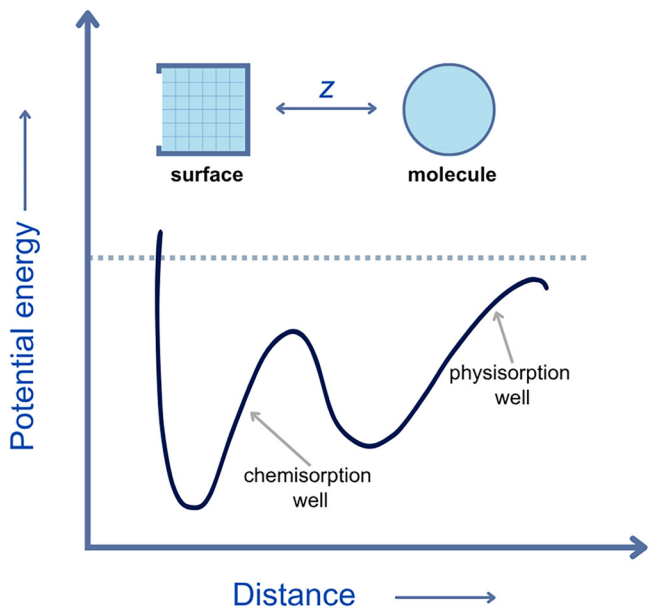


Figure 2.8 Lennard–Jones diagrams: potential energy versus distance.

From the thermodynamic point of view, any system tries to reduce its energy to reach the lowest values of Gibbs energy (G). Adsorption is the process that occurs in an isolated system at a constant temperature. Therefore, for such a system, the Gibbs free energy is given by the following relation:

$$\mathrm{DG} = \mathrm{DH} - \mathrm{TDS} \tag{2.6}$$

where DG, DH and DS are, respectively, the changes in Gibbs energy, enthalpy and entropy during the adsorption process.

Thermodynamic parameters are crucial to confirm the spontaneity and viability of the adsorption process. They offer the knowledge required to create an adsorption process. Thermodynamic characteristics of adsorption processes can be quickly evaluated because the adsorption process is temperature-dependent. Adsorption experiments' thermodynamic considerations are required to determine the spontaneity and viability of such processes. Therefore, thermodynamic parameters such as Gibbs free energy change (ΔG_0), enthalpy change (ΔH_0), entropy change (ΔS_0), isosteric heat of adsorption (ΔH_X), adsorption potential (A), number of jumps (n), probability of sticking (S^*), adsorption density, and activation energy (E_a) are calculated using experimental data of adsorption processes.

One uses the Gibbs free energy of change to evaluate the spontaneity and viability of adsorption processes. A process is confirmed as spontaneous when the ΔG^0 value is negative and non-spontaneous when the ΔG^0 value is positive. The fundamental Gibbs equation relates to the equilibrium constant and the change in free energy during an adsorption process.

$$\Delta G^0 = -RT \ln K_C \tag{2.7}$$

where R = universal gas constant, T = temperature, K_C = equilibrium constant. The above equation determines how temperature changes affect the equilibrium constant.

When the system does not perform more work, the energy transferred as heat at constant pressure is known as the change in enthalpy (ΔH°). A calorimeter typically determines the enthalpy change by tracking temperature changes under constant pressure. The Van 't Hoff equation is typically used to calculate the enthalpy change in adsorption investigations, which offers insight into the nature and mechanism of the adsorption process.

$$\log K_C = \frac{\Delta S^\circ}{2.303R} - \frac{\Delta H^\circ}{2.303RT} \tag{2.8}$$

$$K_C\left(\text{Distribution coefficient}\right) = \frac{C_a}{C_e} \tag{2.9}$$

where C_a = amount of adsorbate adsorbed at equilibrium, C_e = equilibrium concentration of adsorbate in solution.

ΔH° indicates the nature of the absorption process, that is, an exothermic and an endothermic adsorption process. For example, when ΔH° value is positive, the process is endothermic and vice versa.

Van 't Hoff equation can also assess the entropy change during adsorption. The positive value of ΔS indicates the increase in randomness at the solid/liquid interface, an affinity of the adsorbent towards the adsorbate, and some structural alterations in the adsorbent and adsorbate.

The isosteric heat of adsorption, determined at a constant amount of adsorbate adsorbed, is the ratio of the smallest change in adsorbate enthalpy to the smallest change in quantity adsorbed at constant temperature and pressure. The Clausius–Clapeyron equation is usually used to calculate this number, essential for defining adsorption processes.

$$\frac{d\left(\ln C_e\right)}{dT} = -\frac{\Delta H_x}{RT^2} \tag{2.10}$$

Isosteric heat of adsorption

$$n = \frac{1}{(1-\theta)\theta} \tag{2.11}$$

The faster the adsorption process, the smaller the hopping number (n), which can be used to characterise how quickly an adsorption process occurs.

The adsorption potential theory was first proposed by Polanyi in 1914 to describe the physical adsorption of gases on solids. Adsorption potential is the chemical potential that emerges as an adsorbate molecule moves from solution to the surface of an adsorbent during an adsorption process. This parameter can gauge an adsorbent's molecular adsorption capacity at a specific temperature. The adsorption potential can be calculated using the following expression (A):

$$A = -RT\ln\left(\frac{C_a}{C_e}\right) \tag{2.12}$$

where C_o and C_e are the initial and final concentrations of the adsorbate solution, and T = the absolute temperature at which the adsorption occurred.

This parameter adds values to the data acquired by using modified biomass as the adsorbent in adsorption experiments. Adsorbate packing on the adsorbent surface is measured using adsorption density. The following equation can be used to determine the adsorption density (ρ) value of the adsorption process:

$$\rho = Z_r C_e e^{-\left[\frac{\Delta G0}{RT}\right]} \tag{2.13}$$

where ρ = adsorption density, Z = valency of adsorbate, R = effective radius of adsorbed ion, C_e = equilibrium concentration of adsorbate solution, R = universal gas constant, T = absolute temperature.

The ability of an adsorbate to remain in the adsorbent indefinitely is described by the metric known as occlusion probability (probability of adsorption). This is a property of the adsorbent/adsorbent system independent of the system operating temperature and performs best when the value is between 0 and 1 1

($0 < S^* < 1$). The following equation can be used to evaluate the likelihood of closure:

$$\ln(1-\theta) = \ln S^* + \frac{E_a}{RT} \tag{2.14}$$

where θ = surface coverage and E_a = activation energy.

The least energy necessary to start a chemical reaction is known as activation energy. A negative E_a for adsorption processes indicates that lower temperatures are more favourable, in which case the adsorption process is referred to as exothermic. On the other hand, a positive E_a denotes the presence of an energy barrier during the adsorption process. To put it another way, this adsorption process is known as endothermic since it requires energy (temperature increase) to be produced by the system. The Arrhenius equation can be used to calculate the activation energy of the adsorption process.

$$\ln k_2 = -\frac{E_a}{RT} + \ln k_0 \tag{2.15}$$

where k_0 = Arrhenius factor. A plot of $\ln k_2$ against $1/T$ gives a straight line from which the activation energy (E_a) can be evaluated (slope of the linear graph).

2.7 COMPUTATIONAL MODELLING, SIMULATION, AND OPTIMISATION OF THE ADSORPTION PROCESS

Computational modelling of adsorption processes in aqueous media is helpful for understanding and optimising the separation of solutes from liquid solutions. There are various parameters involved in adsorption modelling, such as the initial concentration of the adsorbate, the contact time between the adsorbent and the adsorbate, the temperature and pH of the solution, the surface area and porosity of the adsorbent, and the type and strength of the interactions between the adsorbent and the adsorbate. These parameters affect the equilibrium and kinetics of adsorption, which different models can describe. These models are based on different assumptions and empirical observations, and they can be used to fit experimental data and estimate essential parameters such as the maximum adsorption capacity, the adsorption energy, and the heterogeneity of the adsorption sites.

Computational modelling of adsorption processes in aqueous media can help evaluate the performance of different adsorbents for specific applications, such as water purification, wastewater treatment, biotechnology, and so on (Ibrahim *et al.*, 2022). It can also help to design and optimise new adsorbents with tailored properties and functionalities. Computational modelling can be done at different levels of complexity and accuracy, depending on the available data and computational resources.

One of the main challenges of computational modelling of interactions in aqueous medium is accurately describing water's complex and heterogeneous nature and its interactions with other molecules. Water has a high polarity, a

significant dipole moment, and a strong hydrogen bonding network, giving rise to various structural and dynamical anomalies. Water can adopt different phases and forms depending on the temperature, pressure, and content. Water can also influence the conformation, stability, reactivity, and function of biomolecules and other solutes. Different levels of theory and methods can be used to model interactions in an aqueous medium, depending on the system size, complexity, and accuracy required. Some of the most common methods are:

- **Molecular mechanics (MM):** This method uses classical mechanics to model the atoms and bonds as point charges and springs. MM is fast and suitable for large systems, but it relies on empirical parameters and cannot capture quantum effects or bond breaking/formation.
- **Quantum mechanics (QM):** This method uses quantum mechanics to model the electrons and nuclei as wave functions and operators, respectively. QM is accurate and can capture quantum effects and bond breaking/formation, but it is computationally expensive and suitable for small systems.
- **Quantum mechanics/molecular mechanics (QM/MM):** This method combines QM and MM to model different system regions with different levels of theory. QM/MM is a compromise between accuracy and efficiency, and it can handle systems with both covalent and non-covalent interactions between solute and solvent.
- **Molecular dynamics (MD):** This method uses Newton's laws of motion to simulate the trajectories of atoms over time. MD can capture the dynamics and thermodynamics of a system, but it requires a potential energy function (force field) to describe the interactions between atoms.
- **Monte Carlo (MC):** This method uses random sampling to explore the configuration space of a system. MC can capture a system's thermodynamics and equilibrium properties, but does not account for the dynamics or time evolution.

To perform computational modelling of interactions in aqueous medium, one needs to choose an appropriate method, model, force field, boundary conditions, simulation parameters, and analytical tools. The choice depends on the research question, system size, complexity, accuracy required, computational resources available, and prior knowledge or assumptions. Some examples of research topics that involve computational modelling of interactions in aqueous medium are:

- **Solvation effects:** How does water affect the structure, stability, reactivity, and function of solutes?
- **Hydrophobic effects:** How does water drive the aggregation or folding of non-polar molecules or regions?
- **Hydrophilic effects:** How does water mediate the recognition or binding of polar molecules or regions?
- **Ion effects:** How does water modulate the charge distribution, electrostatic potential, and solvation-free energy of ions?
- **Proton transfer:** How does water facilitate or hinder the transfer of protons between molecules or within a molecule?

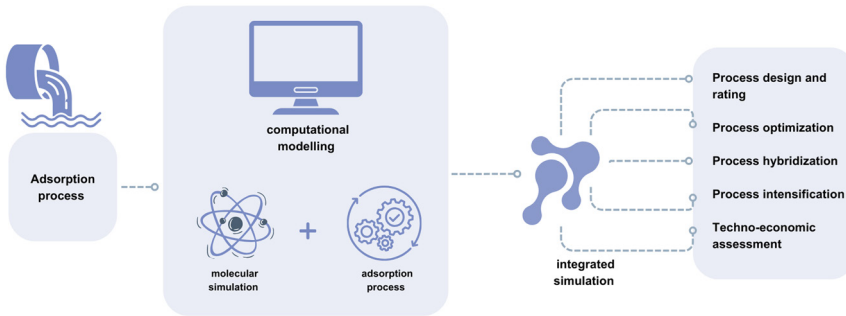


Figure 2.9 Use of integrated simulations (molecular and process simulation) for the adsorption process.

- **Water structure:** How does water organise itself around solutes or interfaces? What are the structural motifs and fluctuations of water?
- **Water dynamics:** How does water move around solutes or interfaces? What are the dynamical properties and timescales of water?

Computational modelling of interactions in aqueous medium is a powerful tool that can complement experimental studies and provide insights into molecular mechanisms and phenomena that are difficult or impossible to observe directly. However, computational modelling also has limitations and uncertainties that must be considered and validated. Computational modelling is not a substitute for experiments but a partner that can enhance our understanding of chemistry in an aqueous medium.

The use of integrated simulations (molecular and process simulation) for the adsorption process is shown in Figure 2.9.

2.8 SUMMARY

The adsorption process includes several technical aspects that can be analysed regarding process improvement. Many studies have focused on determining pollutant removal efficiency by adsorption methods. Factors affecting the adsorption of a pollutant material and the kinetics of adsorption are discussed. Finally, the thermodynamics that govern the adsorption of pollutant material in an aqueous medium are discussed in the final section. Using a solid and trustworthy model can save time and money on experiments. However, picking a model type is challenging and requires knowledge and experience.

This chapter provides an in-depth analysis of the adsorption process and its application in (waste)water treatment, starting with an overview of adsorption principles and the factors influencing adsorption efficiency. Various methods for adsorbent characterisation, including spectroscopic, microscopic, and thermal analyses, are presented to underscore the importance of adsorbent properties in the adsorption process. The chapter categorises adsorption types by interaction (physical and chemical) and mode of operation (batch

and continuous fixed-bed systems), offering insight into practical applications. Furthermore, it discusses empirical adsorption models, focusing on isotherms, kinetics, and thermodynamics, which aid in predicting adsorption behaviours. Finally, computational modelling and simulation are introduced as tools to optimise the adsorption process. This chapter emphasises the role of adsorption in achieving effective (waste)water treatment and pollutant removal.

doi: 10.2166/9781789063943 _0053

Chapter 3

Computational techniques for simulation and optimisation of adsorption processes

3.1 INTRODUCTION

The comprehension and regulation of interfacial interactions are paramount in scientific fields such as materials science, chemistry, biology, physics, and engineering. Given that an interface comprises at least two adjacent surfaces at the nanoscale, the nature of interfacial interactions becomes highly intricate. A range of frequencies can be employed to characterise phenomena such as chemical reactions, adsorption, desorption, translocation, and conformational changes. The development of catalysts, dispersants, lubricants, adsorbents, and mineral powders, among others, relies significantly on the adsorption of contaminants onto the surfaces of adsorbents.

The adsorption process, as elaborated in Chapter 2, is a surface phenomenon characterised by interfacial interactions that are significantly affected by a range of operational parameters. These include the duration of contact between the adsorbent and the adsorbate, the size of the adsorbent particles, the concentration of the adsorbate, and the pH level of the solution, among others. Even under static conditions, the heterogeneous nature of the surface at the nanoscale, the type of medium (whether aqueous, air, or organic solvents), and the properties of the adsorbed molecules – such as their chemical structure and adsorption conformations – are crucial in determining the interfacial interactions between the adsorbate and the adsorbent surface.

In (waste)water treatment facilities, the establishment of an automated and optimised adsorption treatment process presents significant challenges due to several factors: (i) the inherent complexity of the adsorption mechanism, (ii) the non-linear relationships among operational parameters, and (iii) the

© 2026 IWAP. This is an Open Access book chapter distributed under the terms of the Creative Commons Attribution Licence (CC BY-NC-ND 4.0) which permits copying and redistribution for non-commercial purposes with no derivatives, provided the work is properly cited (https://creativecommons.org/licenses/by-nc-nd/4.0/). The chapter is from the book *Computational Techniques for Modelling and Simulating Adsorption Processes for (Waste)Water Treatment*, A. Yadav and P. Labhasetwar (Authors).

sudden fluctuations in adsorbate concentrations. Consequently, it is essential to comprehend, quantify, and optimise the interactions among these operational variables by applying mathematical models. This approach can effectively reduce the need for extensive and time-consuming experimental trials, thereby conserving time and resources and minimising delays in analysis. One can forecast the adsorption capacity of a solid material for use in an adsorption process by developing computational techniques. It is possible to carry out these computational operations utilising a variety of modelling methodologies.

It is challenging for experiments to analyse their effects on interfacial interactions thoroughly. The constraints inherent in experimental methodologies indicate that numerous chemical and physical characteristics of interfaces remain elusive despite considerable progress in experimental and measurement techniques. The evolution of computational methods in quantum chemistry, molecular simulations, and the creation of multi-scale models presents substantial opportunities for researchers investigating these interfaces.

The computational modelling and simulations are compatible with experiments to serve as a link between experiments and theoretical calculations. Additionally, simulation is a rough representation of an integrated complex system used to study the system's behaviour and performance over time. Simulations have various uses, including production, economics, safety engineering, and technology performance or optimisation simulation. Using simulations have several benefits, including confirming the outcomes of other analytical techniques and revealing unexpected phenomena while evaluating system behaviour. Approaches for modelling and simulating the adsorption process are depicted in Figure 3.1.

In the past few decades, much research has been conducted on adsorption processes because they are considered one of the most energy-efficient separation methods for treating contaminated water. The choice of specific adsorbent materials and their adsorption equilibrium features greatly influences the adsorption process. Both experimental data and molecular modelling can be used to determine the equilibrium parameters, such as adsorption isotherms. Depending on the material and adsorbate of interest, experiments need to synthesise a particular type of adsorbent for measuring the isotherms,

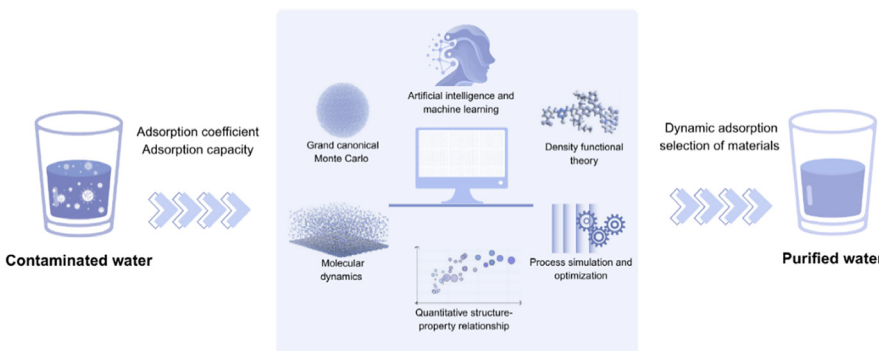


Figure 3.1 Approaches for modelling and simulating the adsorption process.

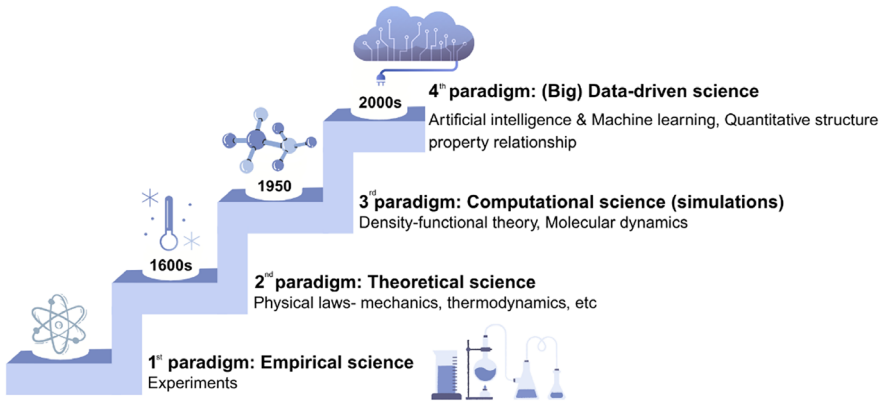


Figure 3.2 Four science paradigms – empirical, theoretical, computational, and data-driven.

which might be expensive. In recent years, several efforts have been made to combine process modelling to identify high-performing adsorbent materials. It is possible because of the increasing computing power and the accessibility of immense data. An efficient investigation of many scenarios under different environmental or operational conditions is made possible by a priori modelling research, which is expensive and time-consuming in experiments. These studies concentrated on creating streamlined screening techniques for several adsorbent materials based on model reduction and data-driven methodologies. The four paradigms of science, that is, empirical, theoretical, computational, and data-driven (Karpatne *et al.*, 2022), are shown in Figure 3.2.

This chapter briefly introduces computational techniques that aid in simulating and optimising adsorption processes. The chapter aims to highlight both the potential and limitations of these tools by discussing common challenges – such as reproducibility, data reliability, and standardisation – and to showcase recent advancements making computational approaches more effective for optimising adsorption processes in industrial and environmental applications.

3.2 HIERARCHICAL MODELLING OF ADSORPTION PROCESSES

Computational modelling has revolutionised the study and optimisation of adsorption processes by allowing scientists and engineers to simulate complex interactions at multiple scales, from molecular to system-wide. Adsorption, a process where molecules adhere to a surface, is critical in environmental management, water purification, gas separation, and energy storage. However, adsorption mechanisms are often complex, involving various thermodynamic, kinetic, and molecular interactions that are challenging to study experimentally. Computational modelling is a powerful tool to bridge this gap, offering insights into adsorption behaviours and providing predictive frameworks that guide process optimisation.

Researchers can use computational methods to rapidly model adsorption systems, reduce experimental costs, and optimise process parameters before practical implementation. These techniques support the development of new materials with enhanced adsorption capacities and the design of efficient adsorption processes for specific applications, making computational modelling an indispensable part of modern adsorption studies.

One effective strategy in computational adsorption modelling is the hierarchical approach, which examines adsorption at different scales. This multi-scale framework enables studying adsorption processes from the molecular level, where fundamental interactions occur, to the process level, where these interactions impact system performance.

In recent years, multi-scale and multi-physics computational methods have been developed to illuminate the underlying molecular mechanisms in experimental adsorption processes (Coasne, 2016; Coasne *et al.*, 2013). These computer modelling frameworks could benefit researchers by offering a controlled, affordable, and reliable environment. Theoretical models that were successfully developed and subsequently put into operation over time to comprehend and investigate the materials on a large scale serve as the foundation for the simulations. The models were developed to encompass a variety of computational techniques, including first-principles calculations, molecular dynamics (MD), mesoscopic modelling, finite-element analysis, quantum and classical mechanics, kinetic theory, and continuum models (Figure 3.3). Each of these methodologies addresses specific temporal and spatial scales. A hierarchical (top-down/bottom-up) or concurrent multi-scale strategy can facilitate the integration of multiple resolutions. Quantum mechanics elucidates the characteristics of the electronic structure, particularly

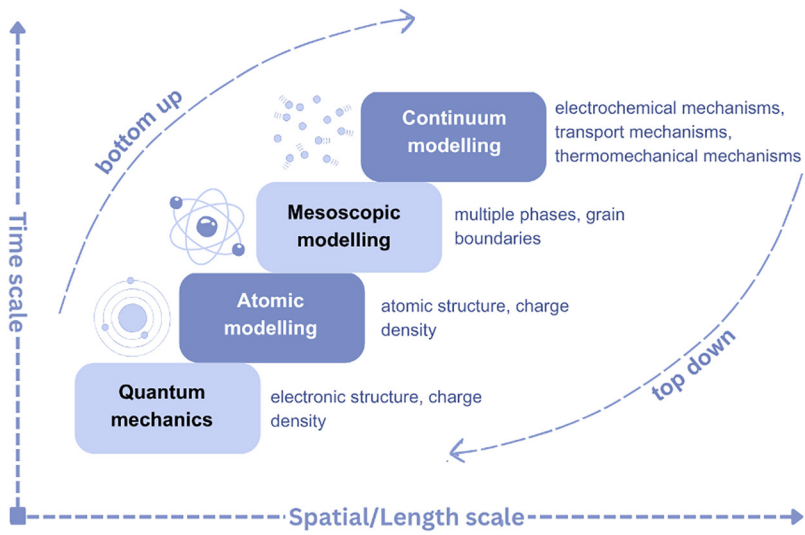


Figure 3.3 Multi-scale approach in adsorption modelling.

emphasising the charge density of water. In atomistic modelling, further MD simulations can yield structural and thermodynamic properties of bulk water phases, potentially allowing for the incorporating of classical force field parameters in specific multi-scale frameworks. The wettability of a surface design is indicated by its contact angle, while interfacial tension and viscosity serve as essential parameters for mesoscopic modelling. Physical quantities derived from lower scales can enhance the accuracy of modelling inputs at the continuum level, thereby addressing critical aspects of the adsorption process.

The so-called first principles/*ab initio* calculations, in which the system characteristics are acquired from the most basic knowledge about the matter at the electronic level, are a reliable methodology for analysing various materials' characteristics. The molecular Schrödinger equation can be solved using the *ab initio* method without any empirical or semi-empirical parameters, so all conclusions are obtained directly from theoretical principles. However, it does not necessarily mean that the solution is exact; rather, it indicates that the particular approximation is strictly specified based on fundamental principles and that its error margin can be qualitatively predicted in advance. This method only applies at the picosecond and nanoscale scales due to computational resource constraints. Therefore, it is possible that first principles cannot directly obtain some essential characteristics in the adsorption process, such as mass transfer. Combining some already-known approaches into multi-scale modelling is an excellent approach to the multi-scale phenomenon in adsorption processes.

Several multi-scale methodologies have been established to examine various systems and their characteristics; however, they have already been used in various scientific domains. The multi-scale strategy necessitates a bridging component to connect theoretical models across different levels of resolution, a common requirement for such strategies. In implementing a multi-scale approach, the initial task involves selecting methodologies that can be suitably resolved according to the relevant temporal and spatial scales. The physical quantities derived from these methodologies are subsequently transferred and utilised as inputs for other scales. Multi-scale approaches are generally categorised into hierarchical and concurrent methods. Hierarchical multi-scale techniques primarily establish connections between the models through a direct upscaling or downscaling process, facilitating the transfer of information from one scale to another. Conversely, concurrent multi-scale methods enable real-time information exchange between fine and coarse scales during simulation. The molecular modelling (from electronic to mesoscale) inside the multi-scale framework may help process design for various objectives.

Theoretical models are mathematical representations of the physical phenomena that determine how molecules and materials behave. They are founded on fundamental ideas like quantum mechanics or classical mechanics, but frequently include simplifications or assumptions to make them feasible. The computational solution may contain errors or uncertainties due to these assumptions.

The hierarchical approach provides a more comprehensive understanding of adsorption, allowing researchers to develop and refine adsorption models that account for complexities at each scale.

3.2.1 Molecular-level modelling

At this level, molecular simulations, such as density functional theory (DFT) and molecular dynamics (MD), are commonly employed to understand the interactions between adsorbate molecules and adsorbent surfaces. These models provide insights into adsorption energetics, structure, and kinetics, helping to identify ideal conditions and materials for specific adsorption goals.

3.2.2 Mesoscale and macroscale modelling

Mesoscale simulations, including coarse-grained modelling techniques, allow researchers to bridge the molecular and process levels, capturing collective behaviours that impact adsorption efficiency. At the macroscale, adsorption processes are evaluated using system-wide models that include mass transfer, thermodynamics, and reactor dynamics, enabling the prediction and optimisation of adsorption in real-world applications.

3.3 OVERVIEW OF COMPUTATIONAL METHODS

Depending on their complexity, there are several computational methods to simulate adsorption processes. These methods are to be appropriately selected for a specific set of problems, particularly in the case of water and wastewater treatment. The methods that are discussed in this book are briefly introduced in this section.

Table 3.1 provides a detailed comparison of the discussed computational techniques, outlining their operational scales, primary purposes, key outputs, strengths, and inherent limitations (Malloum *et al.*, 2023). This comparative perspective not only aids in selecting appropriate methodologies for specific adsorption studies but also highlights opportunities for integrating multiple techniques to achieve more robust and holistic process insights.

3.3.1 Density functional theory calculations

Density functional theory (DFT) is a quantum mechanical modelling approach widely used to study adsorption at the atomic and molecular levels. It calculates the electronic structure of adsorbents and adsorbates, allowing scientists to investigate adsorption energetics and optimise material properties. DFT helps identify preferred adsorption sites, predict adsorption capacities, and evaluate material stability, guiding the design of more effective adsorbents (Aguayo-Villarreal *et al.*, 2020). The first principles and DFT are based on the standard QM methodology, that is, calculations used in these methods are typical QM methodologies. The DFT method uses a quantum chemical description to simulate the interactions between adsorbent and adsorbate molecules and their macroscopic gas adsorption properties. DFT is a robust and cost-effective methodology that uncovers the fundamental properties of materials, encompassing aspects such as energy, geometric configuration, electronic structure, and optical features. This approach provides essential theoretical insights and forecasts pertinent to material design. Furthermore, it yields critical and significant data at the atomic, molecular, and unit cell levels, facilitating a comprehensive understanding of the results. Although it has significant

Table 3.1 Comparison of computational techniques for adsorption processes.

Technique	Scale/Domain	Main Purpose of Adsorption Studies	Key Outputs/ Insights	Strengths	Limitations
DFT	Atomic and electronic scale	Investigates adsorption energetics, sites, and stability	Electronic structures, adsorption energies	Accurate quantum-level predictions identify optimal adsorption sites	Computationally intensive; limited to small systems (a few hundred atoms)
MD	Atomistic scale (time evolution)	Studies the dynamic behaviour of adsorption, kinetics	Adsorption conformations, diffusion, energies over time	Captures time-dependent molecular motion, computes thermodynamic properties	Short timescales (ns), sampling limitations, depend on force fields
GCMC	Statistical ensemble level	Models adsorption equilibria, calculates isotherms	Adsorption isotherms at various P, T, μ	Effective for equilibrium adsorption, flexible with changing molecule numbers	Assumes equilibrium, limited dynamics, and relies on the quality of potential models
QSPR	Molecular descriptor level	Predicts adsorption properties from structural features	Correlations between structure and adsorption	Reduces the need for detailed molecular simulations and efficient screening	Depends heavily on the quality and scope of training data, purely statistical
AI/ML	Data-driven, multi-scale	Predicts adsorption capacities, isotherms, and kinetics from data	Non-linear predictive models, optimal adsorbents	Handles extensive data, uncovers complex patterns, and is adaptable	'Black-box' needs large datasets, issues with explainability, and reproducibility
Process simulation & optimisation	Process/system level	Predicts and optimises adsorption under real conditions	Breakthrough curves, optimal process conditions	Bridges lab to industrial scale, captures full process interactions	Needs accurate inputs, may require heavy calibration, and is complex for multi-component systems

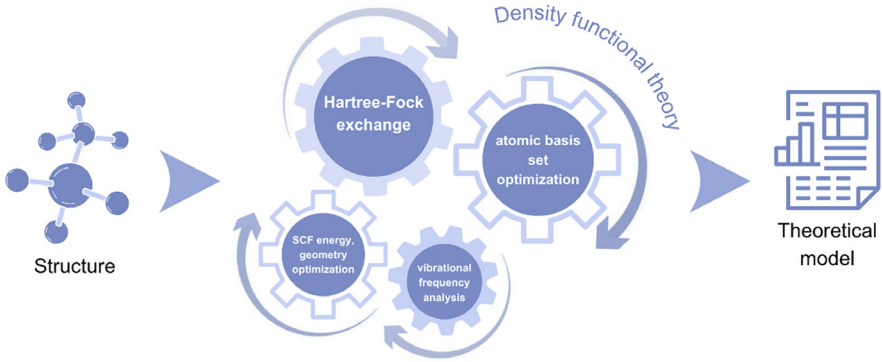


Figure 3.4 Density functional theory calculations.

drawbacks, this method determines the ground state electronic structures for systems containing up to several hundred atoms while maintaining an acceptable balance between accuracy and computational cost. It is helpful for more than just giving direct information on electronic structure; it makes post-processing possible, such as creating simulated scanning tunnelling microscope images, which can reveal additional details about a system and build a close connection to experimental work (Figure 3.4).

3.3.2 Molecular dynamics and grand canonical Monte Carlo simulations

MD and grand canonical Monte Carlo are popular methods for studying the dynamic behaviour of molecules in adsorption processes. MD simulations track the movement of atoms and molecules over time, providing insights into adsorption kinetics and stability under various conditions (Hira *et al.*, 2023). GCMC simulations, on the other hand, are beneficial for modelling adsorption equilibria, as they allow for the calculation of adsorption isotherms by simulating the system at constant temperature and chemical potential (Di and Do, 2006). MD and GCMC enable a thorough analysis of adsorption behaviour, helping optimise process conditions and design efficient adsorbent materials.

Quantum mechanics, molecular mechanics, or a combination of both are used by MD simulations to solve Newton's equations of motion and analyse the behaviour of time-dependent systems. MD simulations reveal various factors, including electrostatic interactions, binding energy, Gibbs free energy, adsorption energy, and loading value, which affect the mechanism of the adsorption process.

The primary advantage of MD over molecular mechanics is that it produces conformations less reliant on the starting structure. However, these simulations have some drawbacks, such as sampling the adsorption and desorption of large organic molecules in various conformations and charge distributions across short time scales (usually tens of nanoseconds). Figure 3.5 provides an overview of molecular simulation methodologies that incorporate particular sampling

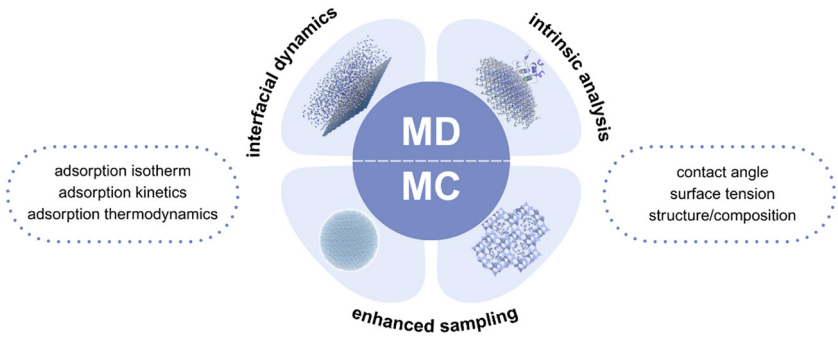


Figure 3.5 Molecular dynamics and grand canonical Monte Carlo simulations in adsorption processes.

approaches, such as the grand canonical ensemble and enhanced sampling, as well as post-processing techniques like intrinsic surface analysis, which are pertinent to interfacial science.

The central idea in the GCMC is typical: resolving complex problems using random numbers, covering several approaches. Contaminant adsorption on the adsorbent can be predicted using Monte Carlo simulations. A convenient way to execute simulation calculations if the system is affected by external factors is to use a grand canonical simulation approach, which allows the number of molecules or particles to change. Adsorption isotherms reveal the behaviour of the adsorbent for the contaminant through these calculations.

3.3.3 Quantitative structure–property relationship analysis

Quantitative structure–property relationship (QSPR) modelling establishes relationships between molecular structures and adsorption properties. This approach enables researchers to predict adsorption behaviours based on structural attributes, reducing the need for extensive trial-and-error experimentation (Li *et al.*, 2020). QSPR is especially useful in screening adsorbent materials for specific applications, as it helps identify promising candidates without requiring detailed molecular-level simulations.

QSPR uses mathematical models to illustrate a variety of potential correlations between molecule structure (or associated characteristics) and chemical activity. It is a flexible tool for descriptive investigation of the relationship between a compound's molecular structure and its physical and chemical properties. The descriptors for hydrophobicity, topology, electronic characteristics, and steric effects are obtained through empirical methods or computational techniques (Figure 3.6).

3.3.4 Artificial intelligence and machine learning

Artificial intelligence (AI) and machine learning (ML) techniques are gaining traction in adsorption modelling because they can handle large datasets and uncover complex patterns (Zhao *et al.*, 2025). ML models, trained on existing

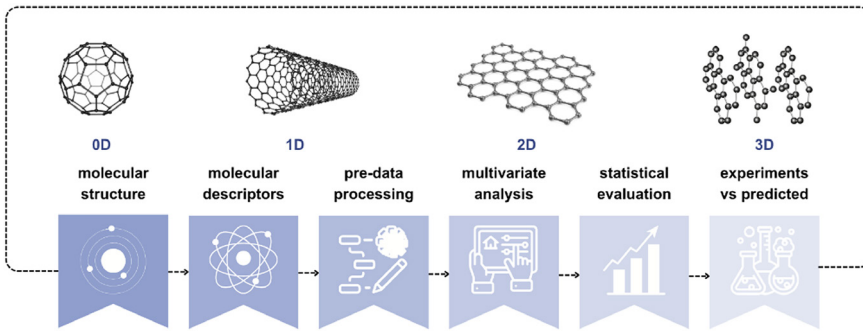


Figure 3.6 Quantitative structure–property relationship analysis model.

adsorption data, can accurately predict adsorption capacities, isotherms, and kinetic parameters. By identifying non-linear relationships and optimising multi-variable processes, AI/ML approaches offer powerful tools for advancing adsorption research and enhancing process efficiency.

An efficient method that might be used to examine the complex relationship between adsorption capabilities and adsorbent parameters is the data-driven ML approach. AI, which entails training machines to mimic human intelligence based on knowledge and experience obtained, is one of the subgroups encompassing ML. ML uses an algorithm to train and generate predictions without being explicitly programmed. Without making any assumptions about what is true, ML has been utilised to explore the complex interactions between adsorbent parameters (such as surface area, total pore volume, average pore diameter, and elemental composition), adsorption factors, and their adsorption performances. Additionally, predictive models for contaminants on adsorbent could be developed via ML. To increase the dependability and performance of the adsorption process, ML can assist researchers in making intelligent and successful decisions on choosing the best adsorbent (Figure 3.7).

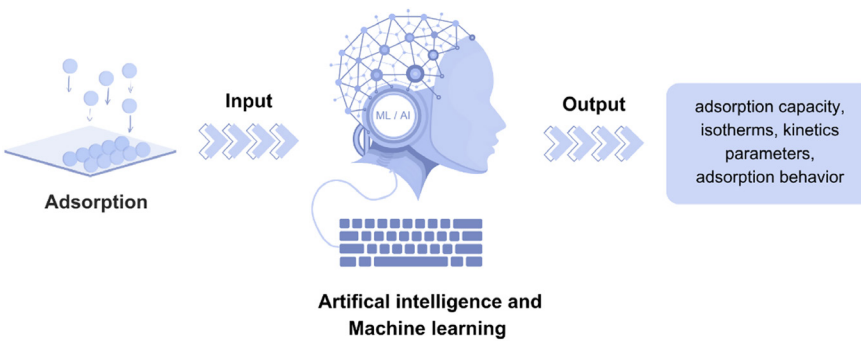


Figure 3.7 Artificial intelligence/Machine learning model.

3.3.5 Process simulation and optimisation

Beyond molecular modelling, process-level simulations play a critical role in optimising adsorption systems. Process simulations enable the prediction of adsorption performance under different operating conditions and facilitate optimisation by identifying ideal configurations for maximising adsorption efficiency (Weber and Smith 1987). The adsorption process is governed by several factors (e.g., pH, time, initial concentration, temperature, and adsorbent mass). Because of this, it is crucial to pick a suitable mathematical model for system prediction and optimisation. Computational fluid dynamics (CFD), response surface methodology (RSM), and artificial neural networks (ANN) are a couple of the methods used most frequently in adsorption literature studies.

CFD studies allow the scalability from atomic absorption calculations with adsorbent to units prepared for industrial use, bridging nanoscale and macroscale calculations. CFD facilitates the prediction of adsorption rates by analysing mass balance and tracking the temporal changes in the concentration of the adsorbent through breakthrough curves. By employing the CFD model for this purpose, one can derive the adsorption rate predictions, which subsequently contribute to determining the mass transfer capacity coefficient and the equilibrium concentration (Figure 3.8). RSM and ANN offer a possible solution for systems where the mathematical relationship between the parameters and the responses is confusing (Figure 3.9). RSM designs and optimises experiments to establish the best operating conditions or regions of interest. RSM encompasses a predetermined series of structured experiments to achieve a specific response through constrained trials. This statistical approach is particularly suitable for experiments involving multiple factors, as it elucidates the relationships among

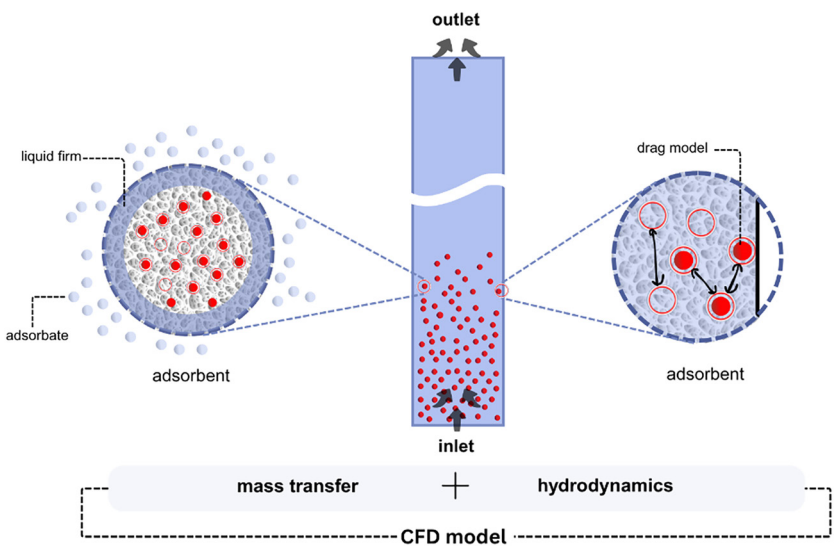


Figure 3.8 Computational fluid dynamics application in the adsorption process.

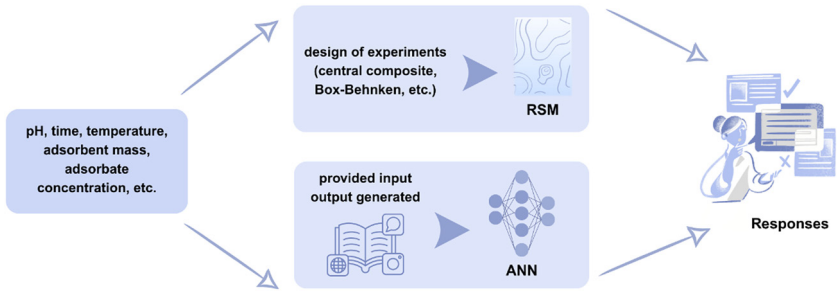


Figure 3.9 Response surface methodology and artificial neural networks used for the optimisation of the adsorption process.

various parameters to identify optimal operational conditions. ANNs are multilayer algorithms that get their inspiration from the human brain's functions. These mathematical methods, which are dependable and robust, may link non-linearity between input and output variables from a series of experiments.

3.4 CHALLENGES IN USING COMPUTATIONAL TOOLS IN THE ADSORPTION PROCESS

Computational tools and techniques offer several advantages over conventional models and established knowledge. While acknowledging these successes is crucial, it is equally important to address the specific challenges (Figure 3.10)

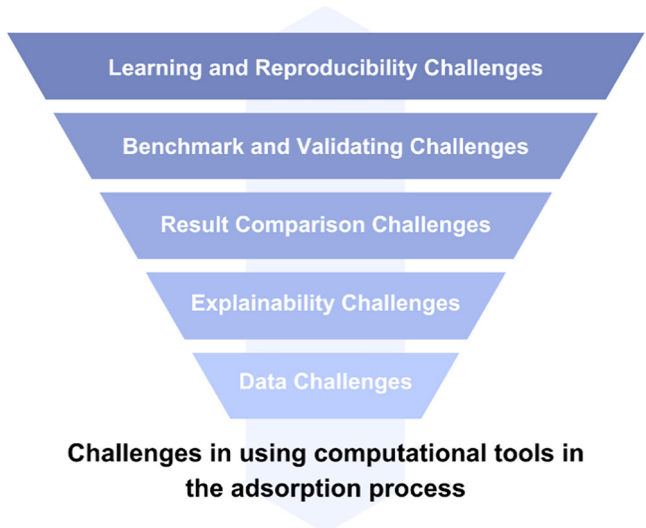


Figure 3.10 Challenges in using computational tools in the adsorption process.

inherent in this domain that must be considered to facilitate broader adoption in water-related applications (Dotto and McKay, 2020; Farmahini et al, 2018).

3.4.1 Learning and reproducibility challenges

Due to variations in computational setups, software, and parameter choices, it can be challenging to reproduce adsorption modelling results consistently. Ensuring reproducibility is vital for scientific progress, making it necessary to establish standardised methodologies in computational adsorption research.

Numerous computational methodologies exhibit significant challenges in reproducibility, primarily due to their reliance on randomly initialised weights and customised activation functions that are often optimised for datasets with characteristics closely aligned to those of the original training and testing data. This limitation complicates the ability of organisations to implement a single model across diverse sectors within their industry and hinders researchers' efforts to replicate and validate prior methodologies and findings. The specific code utilised in developing computational models is often omitted from scholarly publications, which tend to provide only broad outlines of their methodologies. Although there are various justifications for not disclosing the precise code – such as proprietary concerns – this practice does little to enhance public trust, understanding of the systems, or the ability to verify results, further entrenching computational tools in a 'black-box' paradigm.

3.4.2 Data challenges

Reliable data are essential for accurate modelling. However, experimental data for adsorption can vary in quality and may be difficult to obtain for specific materials or conditions. This makes model validation and reproducibility challenging, especially when data from different sources are not standardised.

A significant challenge to consider is the heavy reliance of these models on the chosen datasets. The training phase is often the most critical aspect in creating an effective model, and selecting a suitable dataset is far from trivial. Consequently, minor variations in natural or treatment processes that were not accounted for during the training phase can render a previously effective model ineffective, as it may struggle to interpret new information for which it was not adequately prepared. This issue is further complicated by the reality that many real-world systems do not possess the comprehensive datasets required to support these models. Although researchers and academics can curate their datasets, numerous communities that could greatly benefit from these intelligent systems often lack the necessary data management and storage capabilities to implement them effectively. Thus, while larger municipalities and organisations may find ways to address these data management challenges, smaller populations may remain disadvantaged due to insufficient information.

The challenge associated with data selection also encompasses an issue of specificity. Since data are frequently curated for particular conditions and geographical contexts, applying established models to new environments becomes increasingly challenging. This situation complicates the process of regulatory adoption considerably. The unique characteristics of these datasets, tied to their specific locations and circumstances, pose significant obstacles

to the standardisation often necessary for compliance with local and national regulations. The current landscape of computational tools, which focuses on the meticulous selection of datasets exceptionally suited to their distinct attributes, represents a considerable barrier that must be addressed to facilitate the acceptance of these advanced tools within regulatory frameworks.

3.4.3 Benchmarking and validating challenges

Validating models against experimental results is essential to ensure accuracy, but discrepancies between simulations and real-world data can pose challenges. Developing reliable benchmarks and standards for comparing computational models is critical to enhancing their reliability.

Integrating computational modelling with experimental data presents a significant opportunity for the water sector to enhance the optimisation and governance of water monitoring and management practices. There is a pressing need for innovative algorithms to tackle specific water treatment and management challenges, including water quality assessment, leakage detection, and process optimisation, thereby facilitating informed decision-making. By employing hybrid computational techniques, the accuracy of predictions can be improved, resulting in decreased energy consumption and operational costs.

3.4.4 Result comparison challenges

This issue mirrors the challenges discussed in the standardisation section above. Nevertheless, it specifically pertains to the methodologies researchers utilise in conducting and disseminating their findings and their criteria for success. Researchers frequently apply various statistical techniques to assess the accuracy and precision of their models. These techniques encompass, but are not limited to, the correlation coefficient (R), the coefficient of determination (R^2), mean absolute error (MAE), mean squared error (MSE), root mean squared error (RMSE), normalised root mean squared error (NRMSE), Pearson correlation coefficient (PCC), Nash–Sutcliffe efficiency coefficient (NSE), and relative error (RE). The primary challenge arises from the absence of a universally accepted statistical method among researchers. This issue is further compounded by data availability and reproducibility difficulties, often resulting in incomplete or unpublished raw data, thereby hindering independent statistical analysis. Consequently, this situation complicates the ability to effectively compare results from studies that employ different statistical methods, even when those studies utilise the same computational models.

3.4.5 Explainability challenges

Advanced methods like AI/ML can yield highly accurate predictions, but their ‘black-box’ nature makes it challenging to interpret results. Explainable AI is an area of active research that aims to improve interpretability, helping researchers understand the rationale behind model predictions and ensuring that insights are scientifically meaningful.

It is unrealistic to anticipate that these technologies will be flawless, just as it is unreasonable to expect absolute perfection from operators and other

professionals in the field. The concern lies not in whether these systems will fail but determining when such failures might occur, particularly in critical sectors like water treatment. The intricate and seemingly unpredictable nature of specific models poses a challenge in terms of public comprehension; however, the public needs to be informed about the capabilities and limitations of these technologies. From a legal standpoint, current legislation in many jurisdictions complicates attributing responsibility and providing restitution in the event of failures.

3.5 RECENT ADVANCES IN COMPUTATIONAL TOOLS

In recent years, there have been significant advances in the computational modelling of adsorption processes, both in methods and applications. The development and validation of more accurate and efficient methods to simulate the adsorption equilibrium and kinetics, such as GCMC, MD, DFT, and so on. These methods can capture the molecular interactions and structural changes that occur during adsorption and account for the effects of temperature, pressure, concentration, and so on. The application of computational modelling is to design and optimise novel adsorbents with tailored properties, such as pore size, shape, functionality, and so on. Computational modelling can help screen and select potential adsorbents from a large pool of candidates and predict their performance under different conditions. Computational modelling can help modify and improve existing adsorbents by introducing functional groups, defects, dopants, and so on. Integrating computational modelling with experimental data and ML techniques enhances the models' reliability and applicability. Computational modelling can help interpret and explain experimental results and provide insights and guidance for further experiments. ML techniques can help extract useful information from large and complex datasets and generate predictive models based on data-driven approaches.

The results of these recent advances are better than those of the old studies in several ways, such as:

- They provide more accurate and realistic predictions of the adsorption behaviour and mechanisms, which can help improve the understanding and optimisation of the adsorption processes.
- They enable the design and discovery of new and improved adsorbents with desired properties and performance, which can help expand the range and efficiency of the adsorption applications.
- They facilitate the integration and synergy of computational modelling with experimental and data-driven approaches, which can help enhance the reliability and applicability of the models.

The recent advances in methods and applications have improved the accuracy, efficiency, and utility of computational modelling for adsorption processes. Computational modelling can be crucial in advancing the science and technology of adsorption for water treatment and other applications.

Advancements in computational power and algorithms have significantly improved the accuracy and efficiency of adsorption modelling. Emerging techniques, such as hybrid models that combine molecular simulations with ML, are expanding the predictive capabilities of computational adsorption. Additionally, high-throughput screening methods enable rapid evaluation of thousands of materials, accelerating the discovery of high-performance adsorbents. As computational resources evolve, integrating AI, quantum computing, and data-driven approaches is expected to further transform adsorption modelling and optimisation, enabling increasingly precise control over adsorption processes and facilitating materials development for sustainable applications.

3.6 SUMMARY

This chapter comprehensively explored computational techniques employed to model, simulate, and optimise adsorption processes, particularly in the context of (waste)water treatment. Recognising the inherent complexity of adsorption – stemming from intricate interfacial interactions, non-linear parameter relationships, and variable contaminant concentrations – the chapter highlighted computational tools' indispensable role in advancing scientific understanding and practical applications.

Beginning with a discussion on hierarchical and multi-scale modelling approaches, the chapter underscored how adsorption phenomena can be examined across various scales, from the atomic to the process level. This multi-tiered perspective allows researchers to decode fundamental molecular interactions while optimising system-wide performance.

In conclusion, computational modelling of adsorption processes is a rapidly evolving field that has significantly progressed in recent years. A range of computational methodologies was then systematically introduced, each tailored to address different aspects of adsorption processes. Techniques such as DFT and MD delve into the electronic and atomistic realms, providing insights into adsorption energetics, configurations, and kinetics. GCMC simulations effectively model adsorption equilibria, while QSPR analyses facilitate rapid screening by linking molecular descriptors to adsorption behaviours. Complementing these, AI/ML techniques offer powerful data-driven frameworks that capture complex, often non-linear patterns inherent in adsorption data. Finally, process-level tools – including CFD, RSM, and ANN – enable the prediction and optimisation of adsorption performance under realistic operating conditions.

While these computational tools have markedly advanced adsorption science and engineering, the chapter also acknowledges prevailing challenges related to data quality, reproducibility, benchmarking, and model interpretability. Addressing these issues remains critical to ensuring broader adoption and regulatory acceptance, particularly in the water sector.

Recent developments – such as hybrid multi-scale models, the convergence of molecular simulations with ML, and the emergence of high-throughput screening frameworks – are driving the field towards more accurate, efficient,

and predictive modelling capabilities. These advancements are expected to accelerate the design of tailored adsorbent materials and optimised process configurations, ultimately contributing to more sustainable and energy-efficient water treatment solutions.

In summary, by consolidating foundational principles, methodological nuances, comparative analyses, and future perspectives, this chapter underscores the transformative potential of computational techniques in shaping next-generation adsorption processes.

doi: 10.2166/9781789063943 _0071

Chapter 4

Density functional theory calculations for the adsorption process

4.1 INTRODUCTION

The adsorption process depends on an understanding of and ability to control interfacial interactions. Using experiments to understand the effects of interfacial interactions is exceptionally challenging. The constraints of experimental approaches mean that despite enormous progress on the experimental side, many chemical and physical aspects of adsorption phenomena remain unknown. With the advancement of computational techniques, such as in quantum chemistry, molecular simulations, and the development of multiscale models, there is much scope for researchers at the interfaces. Studying the chemical reactivity, structure–activity relationship, and interfacial chemical interactions during adsorption is made possible by first-principle calculations. The first-principles method can be used directly without a force field to study the properties of interfacial surfaces. First-principle calculations in the past were computationally intensive and expensive, and were rarely used for studying the adsorption process due to the constraints of available computing resources (Zhao *et al.*, 2018). First-principle calculations, particularly those based on the density functional theory (DFT), have been extensively used to analyse adsorption processes in recent years owing to the significant development in high-performance computing (HPC) equipment, computational techniques and software packages.

DFT is a computer quantum mechanical modelling technique used in physics, chemistry, and materials science to study many-body systems' electronic structure (or nuclear structure), especially atoms, molecules, and condensed phases. DFT is a universal approach that can be applied to many systems, including periodic and non-periodic systems. It is a formally exact theory, meaning that it is based on well-defined mathematical principles and that it can, in principle, provide an exact description of the electronic structure of a

© 2026 IWAP. This is an Open Access book chapter distributed under the terms of the Creative Commons Attribution Licence (CC BY-NC-ND 4.0) which permits copying and redistribution for non-commercial purposes with no derivatives, provided the work is properly cited (https://creativecommons.org/licenses/by-nc-nd/4.0/). The chapter is from the book *Computational Techniques for Modelling and Simulating Adsorption Processes for (Waste)Water Treatment*, A. Yadav and P. Labhasetwar (Authors).

many-body system (van Mourik *et al.*, 2014). In practice, DFT is implemented using approximate functions, which introduce some calculation errors, but these errors can often be well controlled. DFT has become a widely used method for studying the electronic structure of many-body systems due to its computational efficiency and accuracy. It has been applied to various systems, including atoms, molecules, solids, and extended systems, such as surfaces and interfaces. DFT is currently a widely utilised method for determining the electrical characteristics of matter. It provides a numerical description of material properties using the basic principles of quantum mechanics. By employing functions that have spatial dependence on the electron density, DFT can be used to identify the parameters of a many-electron system.

This chapter introduces the DFT and the concepts on which the formalism is built. The discussion is then extended to how the adsorption processes can be modelled using the DFT formalism (with appropriate commercially available codes) and the factors governing the adsorption processes from the purview of the DFT. Furthermore, DFT calculations for adsorption interactions are discussed. Moreover, the software packages used in DFT calculations have also been added. For a better understanding of the adsorption processes related to calculations, the case studies are discussed in detail.

4.2 HISTORY AND EARLY DEVELOPMENTS

Due to the constraints of computer power, first-principle computations were rarely employed in the past to examine interfacial features because they were time-consuming and expensive. Since the advent of HPC resources, computational and software tools, first-principle simulations, especially those based on the DFT, have been extensively employed to study interfacial features. DFT calculations enable an understanding of chemical reactivity, structure–activity relationships, and chemical interactions at interfaces. Later, complicated systems were discovered as material science developed, where the classic DFT formalisms failed to produce reliable findings as the system's complexity increased, prompting the need for new formalisms and theories. Although they yield reliable findings, conventional functionals cannot fully explain the band structure of materials. However, the description becomes impractical when trying to find an approximate solution to the Schrödinger equation for systems with many electrons because the computational difficulties increase as the number of electrons increases.

The history and early developments in DFT for the adsorption process are depicted in Figure 4.1. DFT's intuitive roots go back to the ground-breaking Hohenberg–Kohn–Sham articles from 1964 to 1965. Hohenberg, Kohn, and Sham established a rigorous theory that gave Thomas, Fermi, Dirac, and Slater intuitive leaps of understanding legitimacy in their major articles from 1964 to 1965 (Kohn & Sham, 1965; Lieb & Simon, 1977). Although the work of Hohenberg–Kohn and Kohn–Sham was published in the 1960s, the 1980s saw a significant increase in the acknowledgement of its significance. This delay in acceptance by the general public, particularly by chemists, was primarily caused by two factors. The first was the expansion of the scientific community's

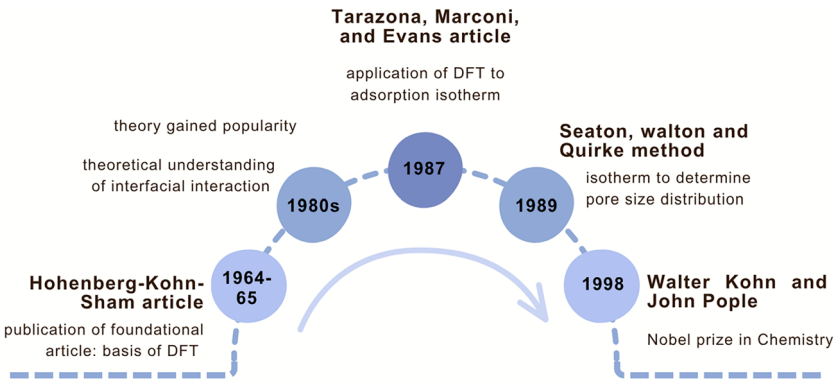


Figure 4.1 History and early developments in density functional theory for the adsorption process.

computational capability, and the second was the ongoing development of theoretical approaches that have allowed solving more complicated issues using algorithms with greater predictive power. Much progress was made in the 1980s towards the theoretical understanding of interfacial interactions. In 1987, Tarazona, Marconi, and Evans (Tarazona *et al.*, 1987) published a study titled 'Phase Equilibria of Fluid Interfaces and Confined Fluids-Non-local versus Local Density Functions,' which played a significant part in defining the application of DFT to the comprehension of adsorption isotherms. This was a significant advancement in the field of adsorption. Hence, the theory, now called DFT, sidesteps the requirement for direct calculation and offers the quantum mechanical description of more complex systems. Walter Kohn and John Pople earned the Nobel Prize in Chemistry in 1998 for their development of DFT (Kohn & Sham, 1965). It has developed into a sophisticated and precise theory for systems with a single interacting electron or many interacting electrons.

4.3 DENSITY FUNCTIONAL THEORY

Quantum mechanics, also called quantum physics or quantum theory, is one of the methods used to explain how electrons and atomic nuclei move in any environment. Wave–particle duality, uncertainty principle, and quantum entanglement are some of the unusual characteristics of electrons that traditional physics cannot explain. The majority of a material's properties are controlled by electron motion. Newton's second law ($F = ma$) in classical mechanics predicts the course a particular system takes given some known initial conditions. Schrödinger's equation is the equivalent of Newton's law in quantum physics. The wave function of the system, also known as the 'state function,' is described by an equation that is generally a linear partial differential equation and not a straightforward algebraic one. By resolving the Schrödinger equation, which explains the quantum behaviour of atoms and molecules, we may comprehend a variety of features of materials (Figure 4.2).

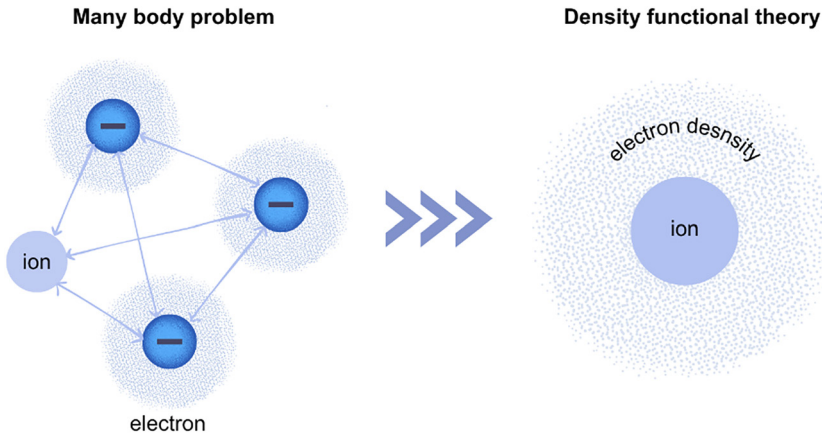


Figure 4.2 Schematic illustration of transforming a many-electron system to an electron density.

Compared to classical molecular dynamics, which lacks force fields and relies on underlying physical laws. Finding the ground-state energy is meant by 'solving the Schrödinger equation' in this context. DFT is an incredibly successful method for solving the Schrödinger equation. DFT has quickly changed with the development of computer technology from a specialised trade practised by a few chemists and physicists to a frequently used tool by many researchers in chemistry, materials science, physics, geology, and other fields.

Two fundamental mathematical theorems that form the basis of DFT are (Zhao *et al.*, 2018):

- Overall energy of a system of electrons and nuclei, or the ground-state energy from Schrödinger's equation, is a unique electron density function.
- The actual electron density that minimises the energy of the overall function is related to the complete solution of the Schrödinger equation.

4.3.1 Exchange-correlation energy

Since the exchange-correlation function lacks an analytical solution, approximations are used in reality, although DFT is theoretically precise. The sources of exchange and correlation are the Pauli principle and dynamic Coulomb interactions between electrons, respectively. Local density approximation (LDA) and generalised gradient approximation (GGA) are the two primary approximations of $E_{xc}[\rho]$ (Gritsenko *et al.*, 2018).

4.3.2 Spin polarisation

Further technical considerations are needed to account for spin polarisation in systems that exhibit magnetism. Generally, this is considered in compounds containing transition metal oxides and metallic systems with Fe, Co, Mn, and Ni. Due to this, it is necessary to use two distinct variables, which are frequently indicated by the symbols $\rho^{\uparrow}$ and $\rho^{\downarrow}$, where $\rho = \rho^{\uparrow} + \rho^{\downarrow}$. Mathematically,

$$E_{xc}^{\mathrm{GGA}}\left[\rho^{\uparrow},\rho^{\downarrow}\right]=\int\varepsilon_{xc}\left(\rho^{\uparrow}(\boldsymbol{r}),\rho^{\downarrow}(\boldsymbol{r}),\nabla\rho^{\uparrow}(\boldsymbol{r}),\nabla\rho^{\downarrow}(\boldsymbol{r})\right)d\boldsymbol{r} \tag{4.1}$$

The interaction between $\rho^{\uparrow}$ and $\rho^{\downarrow}$ must be considered in addition to the two independent calculations. As a result, spin-polarised computations are significantly more expensive than conventional DFT calculations, generally costing over twice as much (Isaacs & Wolverton, 2018).

4.3.3 Dispersion corrections

The development of reliable dispersion correction is a relatively recent addition to the DFT toolbox, which is still ongoing. Long-range electron correlations, also known as electron dispersion forces, cannot be precisely characterised because exchange-correlation functionals like LDA and GGA are approximate (Gritsenko *et al.*, 2016). This is particularly so since instantaneous density fluctuations are ignored when calculating the exchange-correlation energy, and only local features are used.

The most popular and affordable method to consider van der Wall forces is to compute the DFT energy and then add a pairwise additive dispersion correction energy term (E_{disp}). The dispersion strategy behaves asymptotically for two particles separated by $-1/r^6$. The following is a general expression for E_{disp}:

$$E_{\mathrm{disp}}=\sum_{A,B}C_{AB}^{6}/r_{AB}^{6} \tag{4.2}$$

where C_{AB}^{6} is the atom pair A and B's dispersion coefficient, and $r_{AB}{}^{6}$ is the distance between atoms A and B.

4.3.4 Hybrid functionals

Various functionals that combine Hartree–Fock and DFT are referred to as hybrid functionals. By incorporating a component of Hartree–Fock-derived precise exchange, they aim to enhance the formulation for exchange-correlation energy (Park, 2021). For work on molecular DFT in the gas phase, the B3LYP functional is utilised.

4.4 DENSITY FUNCTIONAL THEORY CALCULATION FOR ADSORPTION INTERACTIONS

The DFT calculations are primarily governed by several components such as adsorption energy (E_{ads}), FMO, reactivity descriptors, distortion energy, and spin density. These components *interalia* also depend on corresponding factors as shown in Figure 4.3.

4.4.1 Adsorption energy

The E_{ads} shows the strength of the interaction between the surface and adsorbate, with a minimum E_{ads} of -0.5 eV per molecule, which commonly identifies chemisorption. This measurement can shed light on whether the species is physiosorbed or chemisorbed. One may investigate the interactions

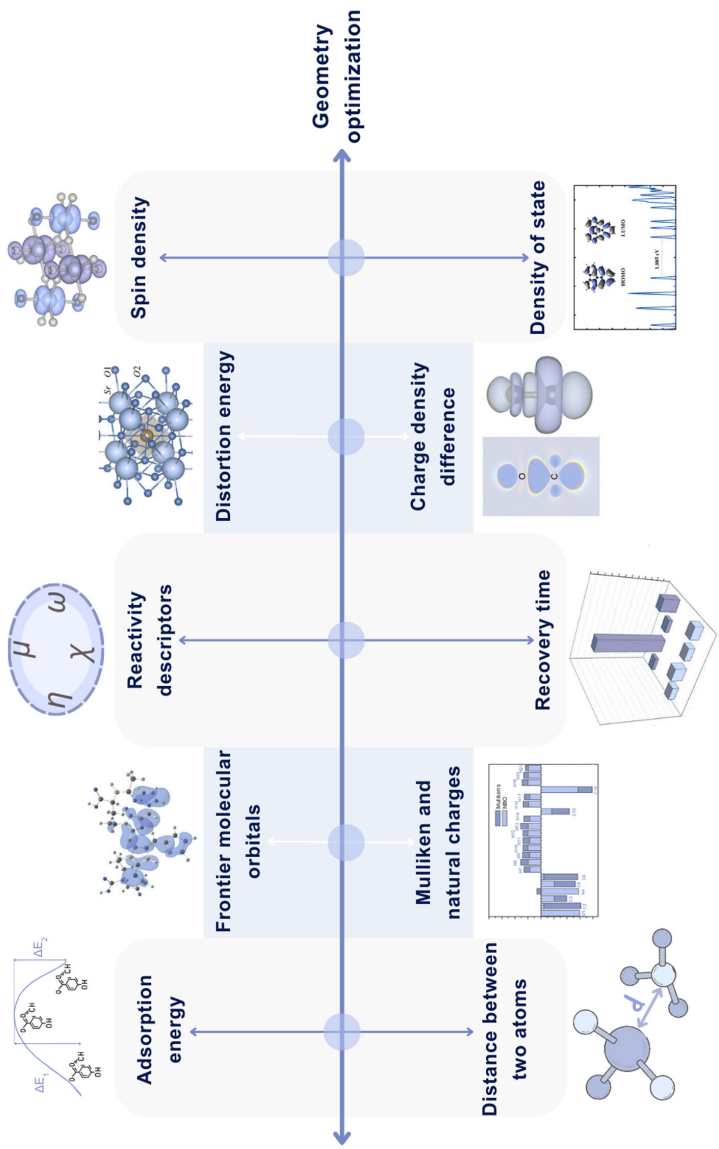


Figure 4.3 Components of density functional theory calculations.

between the adsorbed molecule and the adsorbate surface by calculating the E_{ads} in DFT simulations. Negative E_{ads} indicates an exothermic reaction, and a higher absolute value of E_{ads} denotes a more intense contact between molecules and surfaces. Due to the variations in methods utilised, E_{ads} for computational studies is typically inconsistent across different methods. Nonetheless, the same method's E_{ads} can characterise the adsorption capacity. Further considered are the adsorption circumstances (liquid or in a vacuum), the location, and the coverage. E_{ads} is typically used to study the differences in how molecules change with various functional groups adsorb to the same surface (Sinanoğlu & Pitzer, 1960).

For the case of an explicit solution, E_{ads} is computed by

$$E_{ads} = E_{adsorbate-adsorbent} - \left(E_{adsorbate} + E_{adsorbent}\right) \tag{4.3}$$

where $E_{adsorbate-adsorbent}$ is the energy of the system with the adsorbate adsorbed on the adsorbent, $E_{adsorbate}$ is the energy of the adsorbate and $E_{adsorbent}$ is the energy of the adsorbent.

4.4.2 Distance between two atoms

The adsorption mode and strength can be calculated based on the separation between the two adsorption sites. Distance is a crucial factor, particularly in the formation of chemical bonds and hydrogen bonds. As a result, every initial confirmation that might be evaluated must be optimised appropriately. The stable conformation can be the one with the lowest energy. The strength of the contact between two atoms was dependent on their distance from one another. The distance between two specific sites can be used to determine adsorption models' adsorption capacity, conformation, and even mechanism. (Huang *et al.*, 2024)

4.4.3 Frontier molecular orbitals

Quantum-chemical parameters are used to investigate reactive atoms' atomic charges, the frontier molecular orbitals (FMO) distribution and energy, and the chemically reactive nature of an adsorbed molecule with solid surfaces. The FMO, or highest occupied molecular orbital (HOMO) and lowest unoccupied molecular orbital (LUMO), gives information about the likelihood that an electron would be excited from the HOMO to the LUMO, which results in a chemical reaction in a particular molecule. The FMO distribution reveals the potential locations for chemical reactions, whereas the potential locations for molecule adsorption processes on mineral surfaces are revealed by the FMO energy (Zhao *et al.*, 2018).

The energy of HOMO (E_{HOMO}) indicates a molecule's ability to release electrons, whereas the energy of LUMO (E_{LUMO}) indicates a molecule's ability to accept electrons. Lower E_{LUMO} indicates the high potential for electrons accepting nature, whereas higher E_{HOMO} indicates a greater tendency of the molecule or atom to transfer electrons to acceptors. Because it is easier to transfer electrons from a high-lying HOMO to a low-lying LUMO and to create the activated complex of any possible reaction, an energy gap that is less denotes low kinetic stability and higher chemical reactivity.

4.4.4 Mulliken and natural charges

An optimised geometry or system can generate atomic charges from quantum-chemical parameters, including Mulliken and natural charges. It has been discovered essential in illuminating a reagent's chemical reactivity (Geerlings and Proft, 2002).

4.4.5 Reactivity descriptors

Tjalling Koopmans introduced Koopmans' theorem in 1934, providing a cornerstone concept in quantum chemistry (Koopmans, 1934). According to the theorem, in the context of closed-shell Hartree–Fock theory, the first ionisation energy of a molecule is approximately equal to the negative of the energy of its HOMO. This theorem assumes frozen orbitals – meaning it neglects relaxation or electron correlation effects after electron removal, simplifying calculations considerably.

Koopmans' theorem provides a practical method to estimate orbital energies (ε_i) from molecular orbital calculations, particularly through Hartree–Fock or DFT approaches. These energies are derived from the spin-orbital wave functions and incorporate contributions from kinetic energy, electron–nuclear attraction, and mean-field electron–electron repulsion.

Although originally developed for calculating ionisation potentials in closed-shell systems, Koopmans' theorem has been extended to approximate electron affinities by associating the LUMO with the orbital into which an electron would be added. This offers an efficient means to derive reactivity information from a single-point calculation, avoiding the need to compute energies of the neutral and ionic species separately. The FMOs – namely, the HOMO and LUMO – play a critical role in determining a molecule's chemical reactivity. Their energy gap ($\mathrm{HLG} = E_{\mathrm{LUMO}} - E_{\mathrm{HOMO}}$) is a key indicator of a molecule's stability and reactivity: a smaller gap typically suggests higher reactivity and lower kinetic stability.

From the HOMO and LUMO energies, global reactivity descriptors can be derived, providing valuable insight into the chemical behaviour of adsorbates and adsorbents in water treatment systems. These descriptors include (Heidar *et al.*, 2021):

- Chemical hardness (η): Measures the resistance of a chemical species to change its electron density. Harder species are less polarisable and more chemically stable.

$$\text{Chemical hardness}\,(\eta) = \frac{-E_{\mathrm{HOMO}} + E_{\mathrm{LUMO}}}{2} \tag{4.4}$$

- Chemical potential (μ): Indicates the tendency of electrons to escape from a system. A more negative μ implies a stronger ability to attract electrons (i.e., electrophilicity).

$$\text{Chemical potential}\,(\mu) = \frac{-E_{\mathrm{HOMO}} - E_{\mathrm{LUMO}}}{2} \tag{4.5}$$

- Electrophilicity index (ω): Quantifies the stabilisation energy of a molecule when it acquires an additional electronic charge from the environment.

It is particularly useful for predicting the reactivity of adsorbents towards electron-rich contaminants.

$$\text{Electrophilicity index}\,(\omega) = \frac{\mu^2}{2\eta} \tag{4.6}$$

These descriptors are widely used in conceptual DFT and adsorption modelling to assess the interaction strength and selectivity of materials like activated carbon, graphene, or metal–organic frameworks towards various water pollutants. They also assist in screening and optimising materials for targeted adsorption using computational high-throughput techniques.

4.4.6 Recovery time

In adsorption-based water treatment systems, recovery time (τ) is an important kinetic parameter that reflects the desorption capability or the rate at which an adsorbed species leaves the surface. It directly affects the regeneration efficiency and reusability of the adsorbent material. τ is commonly estimated using an Arrhenius-type equation derived from transition state theory (Zhao *et al.*, 2020)

$$\tau = v_0^{-1} e^{\left(\frac{-E_{ads}}{kT}\right)} \tag{4.7}$$

where v_0, T, E_{ads}, and K denote the attempt frequency (typically 10^{12}–10^{13} s^{-1}), temperature, E_{ads} and Boltzmann constant, respectively (Lim, 2022). The equation suggests a direct relation between τ and E_{ads}.

This expression highlights the exponential relationship between E_{ads} and τ. A highly negative E_{ads} implies stronger binding and a longer τ. Conversely, weaker interactions result in shorter τ, indicating faster desorption.

In practical terms, an optimal adsorbent material should exhibit a moderate E_{ads} – strong enough to ensure high pollutant uptake but not so strong that regeneration becomes difficult or energy-intensive. For example, materials with very long τ may require heating or chemical regeneration, which could undermine the sustainability of the treatment process.

The v_0 represents the intrinsic oscillation frequency of the adsorbate–surface system and is typically assumed to be in the range of 10^{12}–10^{13} s^{-1} based on vibrational analysis. However, computational modelling often approximates it as 10^{12} s^{-1}, especially in studies involving physisorption on low-energy surfaces (Arrhenius, 1889).

4.4.7 Distortion energy

When a molecule is adsorbed on an adsorbate surface instead of its ideal isolated position in the gas phase, it frequently adopts a different shape. The distortion energy (E_{dist}) measures the displacement of the molecule's adsorbed shape from its isolated gas-phase optimised structure (Steele, 1993). Positive E_{dist} values indicate that energy was obtained during deformation away from the conformation of the isolated gas-phase molecule. When combined with additional data like E_{ads}, the distortion energy can offer supplementary

information about the underlying adsorption mechanism. For example, if it improves the overlap between the orbitals of the adsorbate and the surface, molecular deformation at the metal surface may result.

4.4.8 Charge density difference

Although the distribution of charge density (ρ) in the adsorbate–adsorbent system can be investigated, the charge density difference ($\Delta\rho$) may be a more helpful metric, and it is determined analogous to the E_{ads} (Geerlings *et al.*, 2003), that is

$$\Delta\rho = \rho_{surf+molec} - \left(\rho_{surf} + \rho_{molec}\right) \tag{4.8}$$

where $\rho_{surf+molec}$ is the combined adsorbate-surface system charge density, ρ_{surf} is the charge density associated with the clean surface in adsorbed configuration, and ρ_{molec} is the charge density associated with the isolated gas-phase adsorbate in the adsorbed configuration.

The charge density differential visually represents the charge transfer interactions between the adsorbate and the surface. Typically, decreased (increased) electron density regions are related to the adsorbate's HOMO-LUMO orbitals, which can donate (back-donate) electron density.

4.4.9 Spin density

The spin density shows how spin is distributed in the adsorbate-surface system. This is especially intriguing for adsorption onto iron surfaces, where interactions with the ferromagnetic surface can cause non-spin-polarised adsorbates to acquire spin-polarisation (Cao and Nørskov, 2023). The spin density is best understood graphically, much like the difference in charge densities. The spin density supplies the 'difference' compared to the gas-phase molecule because none of the investigated adsorbates carry spin in the gas phase.

4.4.10 Density of states

The number of occupied states at various energies can be determined using the density of states (DOS). Understanding how the adsorbate's electronic structure and surface changes can be highly beneficial to understand the DOS for the adsorbate-surface components before and after adsorption. In the case of the partial DOS (PDOS), where the DOS can be projected upon a particular atom, orbital (s, p, or d), or a combination of both, this idea is especially relevant. In scenarios in which it is expected that particular atoms and their orbitals play an active role in the adsorption process and would, as a result, exhibit a change in the occupancy of energy levels, projecting onto such atoms and their orbitals can be beneficial (Toriyama *et al.*, 2022). Certain DOS bands can be associated with specific molecular orbitals in terms of molecules, and their shift post-adsorption may indicate that those orbitals are well aligned and, therefore, interact favourably with the surface orbitals.

4.4.11 Geometry optimisation

In an adsorption process, the structural and geometrical features of adsorbate and adsorbent molecules shed light on the pathway through which the adsorption process may occur. Geometry optimisation is performed using

DFT to get the most appropriate stable structure with the minimum possible ground state energy, which involves moving the atoms of a molecule. The molecule's energy (or the energy of any chemical species) can be expressed as a function of the atoms' coordinates. The rotational and translational degrees of freedom are eliminated as the 3N Cartesian coordinates are transformed into internal coordinates (3N-6 for non-linear molecules and 3N-5 for linear molecules) (Reveles & Köster, 2004). Most DFT software typically performs the optimisation in internal coordinates. Bonds, angles, dihedrals, and so on, are considered internal coordinates. Further iterations are performed for the optimisation. After each optimisation iteration, quasi-Newton algorithms also update the Hessian matrix (Bučko *et al.*, 2005).

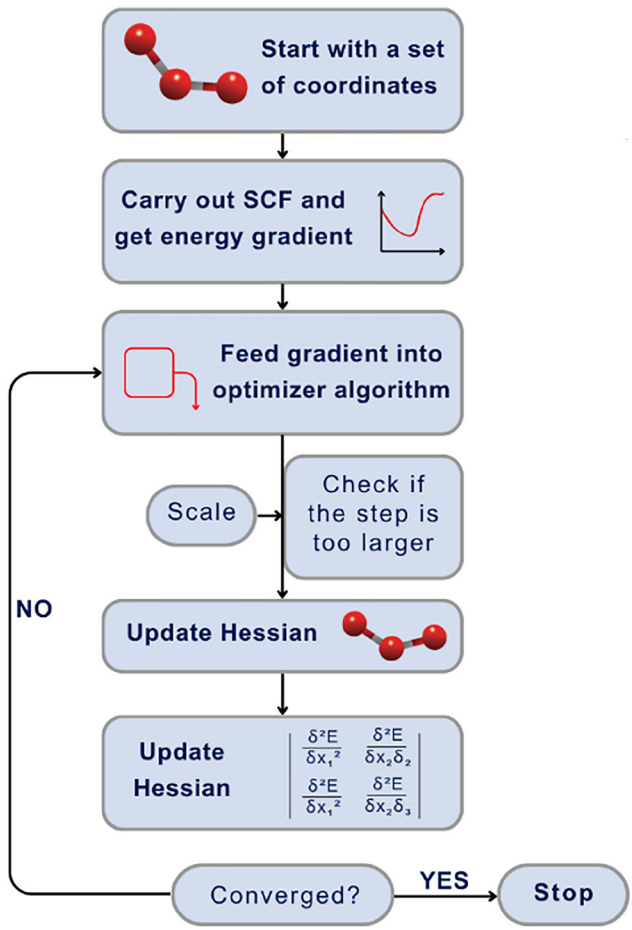


Figure 4.4 Flowchart illustrating the geometry optimisation procedure in density functional theory.

Geometry optimisation calculations involve iteration over a series of inner and outer loops. The outer loop, called the ionic or geometric loop, uses the converged result of the inner loop, that is, electronic energy minimisation, to obtain the forces on the ionic coordinates. These indicate how the atomic positions should be changed to get closer to the ground-state configuration. The ground state is considered to have been reached once further ionic steps do not significantly change user-defined force, energy, and ionic displacement tolerances. The following are the brief general steps for geometry optimisation:

A series of inner and outer loops is iterated in geometry optimisation calculations. The outer loop, known as the ionic or geometric loop, utilises the converged outcome of the inner loop, which involves electronic energy minimisation, to calculate the forces acting on the ionic coordinates. These forces provide insight into adjusting atomic positions to move closer to the ground-state configuration. The ground state is reached when subsequent ionic adjustments no longer cause substantial changes in user-defined force, energy, and ionic displacement tolerances (Irons *et al.*, 2021).

Figure 4.4 summarises general steps for geometry optimisation, detailing iterative steps from initial coordinate setup through SCF calculations, gradient and Hessian updates, step scaling, and convergence checks to achieve the minimum energy configuration. Until a specific convergence criterion is fulfilled, the optimisation process repeats using the above steps.

4.5 SOFTWARE PACKAGES FOR DENSITY FUNCTIONAL THEORY COMPUTATIONS

A wide array of software packages has been developed to perform DFT calculations, as shown in Figure 4.5, each tailored to meet specific research needs across chemistry, physics, and materials science. These tools enable researchers to investigate electronic structures, optimise geometries, compute E_{ads}, and simulate dynamic behaviours of atoms and molecules. The availability of open-source and commercial DFT software has significantly expanded the accessibility of quantum-level modelling, making it possible to simulate systems ranging from small organic molecules to large periodic materials. Selection of an appropriate software package typically depends on the type of system (molecular or periodic), desired accuracy, computational resources, and specific features such as integration with solvation models, relativistic corrections, or post-DFT methods.

ORCA is a widely used quantum chemistry package that offers a rich suite of methods for DFT and post-Hartree–Fock calculations. Developed by the Max Planck Institute, it is especially effective for molecular systems and is known for its accuracy in computing electronic structures, spectroscopic properties, and transition metal complexes. Its ease of use and efficiency on modest computational resources make it popular in academic and industrial research.

SCM's ADF (Amsterdam density functional) is another specialised software that provides a highly accurate implementation of DFT, particularly for molecular and periodic systems. It supports relativistic corrections and excels in modelling transition metals, catalysis, and solvent effects.



Figure 4.5 Software for density functional theory calculations.

SIESTA (Spanish initiative for electronic simulations with thousands of atoms) is tailored for large-scale simulations of periodic systems using numerical atomic orbitals as basis sets. It is particularly suited for systems involving hundreds or thousands of atoms, making it a powerful tool for studying materials, surfaces, and nanostructures relevant to adsorption phenomena.

CASTEP (Cambridge serial total energy package) is a plane-wave pseudopotential DFT code designed for first-principles calculations of solids, surfaces, and interfaces. It is often used in materials science for geometry optimisation, phonon calculations, and electronic properties of crystalline systems.

VASP (Vienna ab initio simulation package) is a high-performance code widely regarded for its robustness and accuracy in simulating periodic systems. It employs a plane-wave basis set and projector augmented-wave (PAW) method, and is extensively used for modelling adsorption on surfaces, band structure calculations, and ab initio molecular dynamics.

Quantum ESPRESSO (Quantum opEn-Source Package for Research in Electronic Structure, Simulation, and Optimisation) is an open-source suite based on plane-wave DFT and pseudopotentials. It is modular, extensible, and widely used for surface chemistry, solid-state physics, and E_{ads} calculations, especially when integrated with post-processing tools for property prediction.

Gaussian is one of the most established quantum chemistry packages, frequently used for DFT and semi-empirical calculations in molecular systems. It is especially powerful for computing molecular orbitals, reaction mechanisms,

and vibrational frequencies, and is widely adopted in organic, inorganic, and biological chemistry.

Materials Studio, developed by BIOVIA, is a commercial software platform integrating various computational tools, including DFT through the CASTEP engine. It provides a user-friendly graphical interface for simulating molecular and materials properties, and is commonly used in industrial settings for designing adsorbents and analysing surface interactions.

ABINIT is an open-source software suite capable of performing DFT calculations for molecules and periodic systems. It supports norm-conserving pseudopotentials and plane-wave basis sets and is suitable for electronic structure calculations, phonons, and excited-state properties.

CP2K is optimised for large-scale simulations of condensed-phase systems and is particularly suitable for ab initio molecular dynamics. It uses a mixed Gaussian and plane-wave approach, offering a balance of speed and accuracy, and is often employed in modelling solvent effects, adsorption in aqueous environments, and surface chemistry.

4.6 CASE STUDIES

DFT can give accurate information about the electronic and geometric properties of adsorbates (the adsorbed molecules) and substrates (the surfaces they are adsorbed on). To use DFT, we need to create a model of the adsorption system, which usually consists of the substrate material and one or more adsorbate molecules on top of it. The slab should be thick enough to represent the bulk properties of the substrate, and it should have periodic boundary conditions along the surface plane. The adsorbate molecules should be placed in a reasonable configuration on the surface, depending on the symmetry and chemistry of the system.

4.6.1 Case study I: Adsorption of pesticides on boron nitride nanosheets

In this case study, the adsorption of pesticides (acetamiprid, clothianidin, imidacloprid, thiacloprid, and triallate) on boron nitride (BN) was studied using DFT (Dindorkar *et al.*, 2022).

4.6.2 Structural properties

Figure 4.6 illustrates the optimised geometries of the isolated pesticide molecules and pristine BN. The BN exhibited an average B–N bond length of 1.45 Å, with nearly perfect hexagonal symmetry reflected by B–N–B and N–B–N bond angles close to 120°. The pesticides showed diverse structural features: acetamiprid, clothianidin, and imidacloprid were non-planar with C–N, C–C, and C–Cl bond lengths of approximately 1.37, 1.45, and 1.29 Å respectively, while lufenuron displayed a planar structure with C–F, C–O, and C–Cl bonds of 1.38, 1.41, and 1.81 Å. Thiacloprid and triallate exhibited slight angular distortions due to CH_2 and CH_3 groups nearby.

Upon adsorption on BN (Figure 4.7), a clear reorientation was observed. Most pesticide molecules aligned their aromatic rings parallel to the BNN plane, promoting π–π stacking interactions, except for triallate, which instead

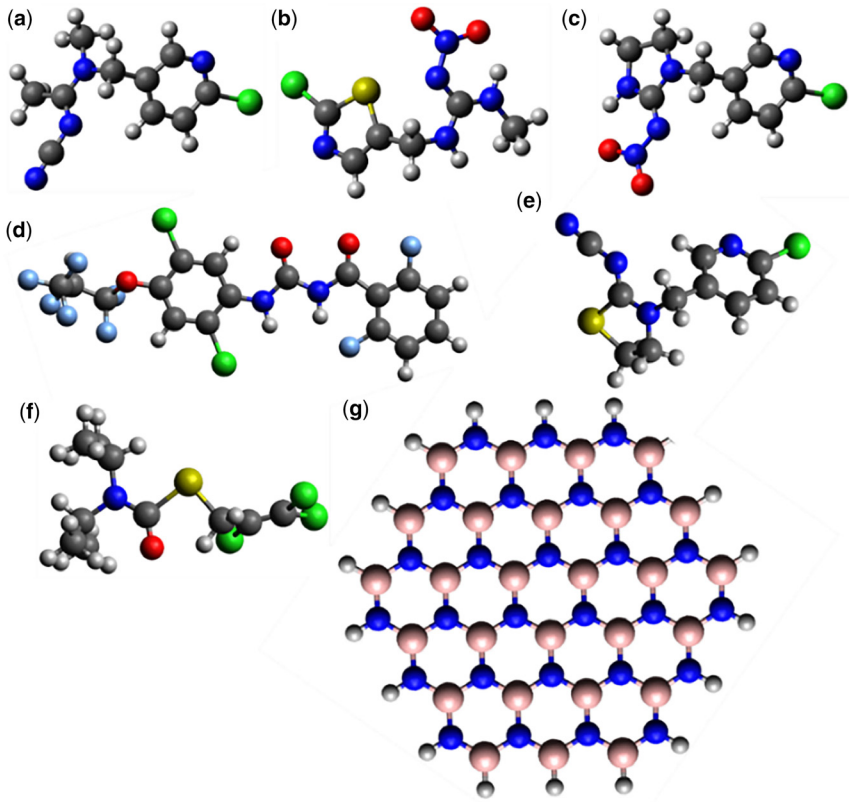


Figure 4.6 Optimised geometries of (a) Acetamiprid, (b) Clothianidin, (c) Imidacloprid, (d) Lufenuron, (e) Thiacloprid, (f) Tri-allate, (g) BN. (Dindorkar *et al.*, 2022).

oriented its C–Cl bonds parallel to the surface, with chlorine atoms closest to BN. The closest approach was found for lufenuron at 2.13 Å, indicating strong physisorption, while triallate maintained the largest separation of 3.31 Å, suggesting weaker interaction.

4.6.2.1 Adsorption energy and recovery time

E_{ads} calculations (Table 4.1) confirmed these observations, yielding negative values across all pesticides, indicating exothermic, spontaneous adsorption. Imidacloprid showed the strongest adsorption with an E_{ads} of −47.21 kJ/mol, followed by clothianidin, thiacloprid, and acetamiprid. Triallate showed the weakest interaction at −18.12 kJ/mol. These trends were reflected in the calculated τ, where acetamiprid, lufenuron, and triallate exhibited rapid desorption on the order of 10^{-9} s, while clothianidin and imidacloprid, due to their stronger binding, had longer τ up to 10^{-4} s, suggesting that BN would be especially sensitive towards these molecules.

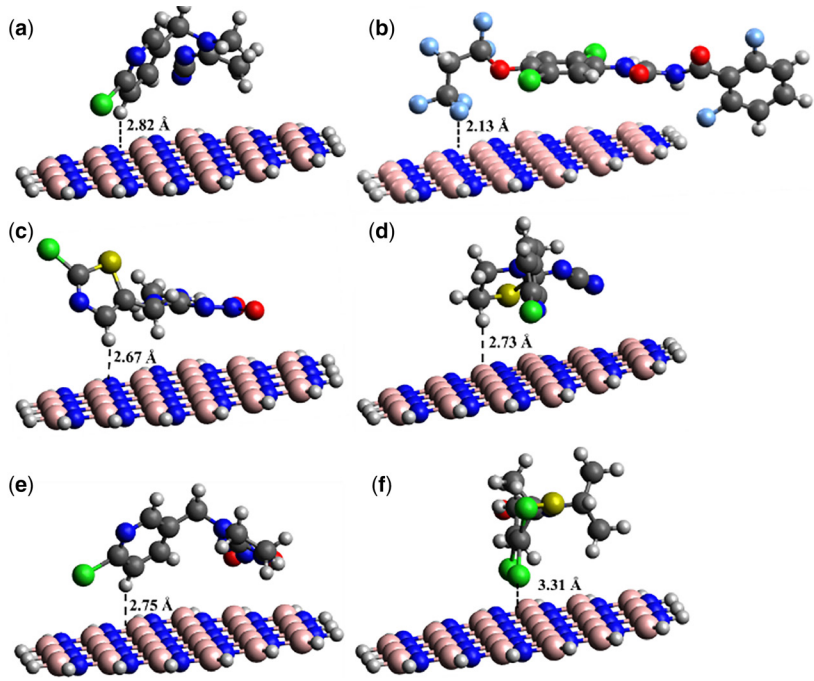


Figure 4.7 Optimised geometries of (a) Acetamiprid adsorbed BN, (b) Clothianidin adsorbed BN, (c) Imidacloprid adsorbed BN, (d) Lufenuron adsorbed BN, (e) Thiacloprid adsorbed BN, (f) Tri-allate adsorbed BN. (Dindorkar *et al.*, 2022).

Table 4.1 Reactivity descriptors, shortest distance, adsorption energy, and recovery time of the clusters before and after adsorption.

	ΔE (kJ mol^{-1})	HOMO (eV)	LUMO (eV)	HLG (eV)	η (eV)	μ (eV)	ω (eV)	Shortest Distance (Å)	Recovery Time (s)
Acetamiprid	–	–6.36	–1.19	5.17	2.59	3.78	2.76	–	–
Clothianidin	–	–6.91	–1.88	5.03	2.52	4.40	3.84	–	–
Imidacloprid	–	–6.63	–1.85	4.78	2.39	4.24	3.76	–	–
Lufenuron	–	–6.63	–1.86	4.77	2.39	4.25	3.78	–	–
Thiacloprid	–	–6.68	–1.21	5.47	2.74	3.95	2.85	–	–
Tri-allate	–	–6.81	–1.42	5.39	2.70	4.12	3.14	–	–
Acetamiprid-BN	–19.71	–6.36	–1.20	5.16	2.58	3.78	2.77	2.82	3×10^{-9}
Clothianidin-BN	–42.57	–6.42	–2.05	4.37	2.19	4.24	4.10	2.13	3×10^{-5}
Imidacloprid-BN	–47.21	–6.43	–2.12	4.31	2.16	4.28	4.24	2.67	2×10^{-4}
Lufenuron-BN	–19.74	–6.23	–2.16	4.07	2.04	4.20	4.32	2.73	3×10^{-9}
Thiacloprid-BN	–26.30	–6.42	–1.26	5.16	2.58	3.84	2.86	2.75	4×10^{-8}
Tri-allate-BN	–18.12	–6.48	–1.37	5.11	2.56	3.93	3.01	3.31	1×10^{-9}

4.6.2.2 Electronic properties

Figure 4.8 displays the HOMO and LUMO distributions of the isolated pesticide molecules, revealing HOMOs mainly localised on aromatic rings or aliphatic chains, and LUMOs on complementary regions, consistent with typical π–electron delocalisation and electrophilic centres. Upon adsorption on BN (Figure 4.9), the HOMOs generally shifted to the BNN surface, especially highlighting charge transfer, except in acetamiprid where the HOMO largely retained its molecular character. LUMOs largely remained on the pesticide molecules, indicating that the adsorption process involved interaction of pesticide HOMOs with the LUMO states of BN.

The reduction in the HOMO–LUMO gap by approximately 0.5 eV for most systems, attributed to the emergence of new energy levels near −2.0 eV, signalling moderate electronic interaction, with acetamiprid showing minimal change consistent with its more localised HOMO. This moderate shift indicated that although adsorption affected the electronic properties, it did not drastically disrupt the electronic structure of BN, which is desirable for maintaining stability in sensing applications.

4.6.2.3 Reactivity descriptors

Reactivity descriptors presented in Table 4.1 revealed that adsorption resulted in slight decreases in η (by $\sim$0.1–0.3 eV) and marginal increases in ω (by $\sim$0.4 eV), suggesting stabilisation of the adsorbed complexes without significant alteration in their reactivity.

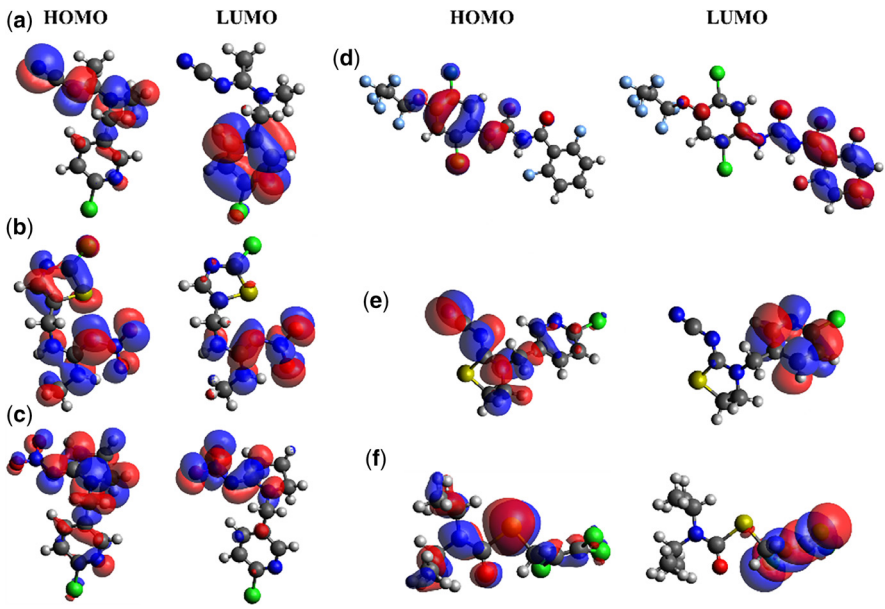


Figure 4.8 Highest occupied molecular orbitals and the lowest unoccupied molecular orbitals distributions of (a) Acetamiprid, (b) Clothianidin, (c) Imidacloprid, (d) Lufenuron, (e) Thiacloprid, (f) Triallate. (Dindorkar *et al.*, 2022).

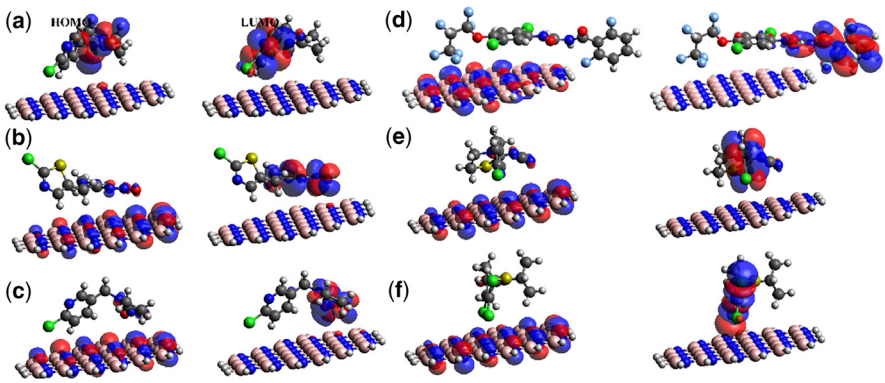


Figure 4.9 Highest occupied molecular orbitals and the lowest unoccupied molecular orbitals distributions of (a) Acetamiprid adsorbed BN, (b) Clothianidin adsorbed BN, (c) Imidacloprid adsorbed BN, (d) Lufenuron adsorbed BN, (e) Thiacloprid adsorbed BN, (f) Triallate adsorbed BN. (Dindorkar *et al.*, 2022).

4.6.2.4 Reduced density gradient scatter and non-covalent interaction plots

The reduced density gradient (RDG) plot and non-covalent interaction (NCI) isosurfaces (Figure 4.10) for the free molecules confirmed the presence of van der Waals forces (green surfaces) along with minor H-bonds and dipole interactions (blue), and limited steric repulsion (red). After adsorption (Figure 4.11), green regions dominated, indicating that van der Waals forces were primarily responsible for binding, with minimal repulsion. Overall, these combined results demonstrate that BN offer an effective platform for the adsorption of neonicotinoid and related pesticides through weak physical interactions, maintaining a balance between sufficient adsorption for detection and fast recovery for reuse.

4.6.3 Case study II: Adsorption of pharmaceutical and personal care products on graphene, boron nitride, and boron carbon nitride nanosheets

In this case study, the first principle DFT calculations were used to study and compare the adsorptive removal of triclosan and triclocarban using graphene (GRA), BN, and boron carbon nitride (BCN) (Dindorkar *et al.*, 2023).

4.6.3.1 Structural properties

Figure 4.12 shows the optimised structures of TCS and TCC along with the adsorbent nanosheets. TCC was found to possess coplanar benzene rings, while TCS adopted a non-planar geometry due to free rotation across its N–C–N linkage, enhancing its configurational flexibility. BCN exhibited slightly varied bond lengths (1.36–1.47 Å) due to the mixture of C–C, C–N, C–B, and B–N bonds.

Upon adsorption, the molecules assumed distinct orientations depending on the adsorbent (Figure 4.13). TCC aligned parallel to BN and BCN surfaces, promoting π–π stacking, while on GRA it adopted a nearly perpendicular orientation, with its α-hydrogen atom (adjacent to the chloro group) interacting closest at 2.39 Å, indicating local C–H$\cdots\pi$ interactions. TCS lay closest to GRA

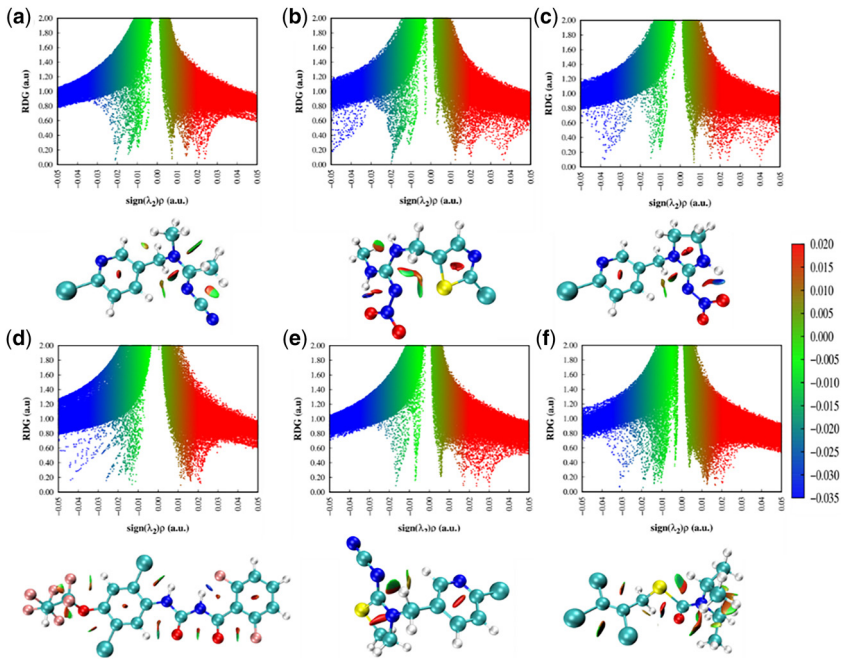


Figure 4.10 Reduced density gradient plot and non-covalent interactions isosurfaces of (a) Acetamiprid, (b) Clothianidin, (c) Imidacloprid, (d) Lufenuron, (e) Thiacloprid (f) Tri-allate, (g) BN. (Dindorkar *et al.*, 2022).

at just 2.25 Å, followed by BCN and BN, suggesting stronger adsorption with GRA due to π–π interactions with the delocalised graphene surface.

4.6.3.2 Adsorption energy and recovery time

E_{ads} in Table 4.2 were consistently negative, confirming spontaneous physisorption, with TCS showing the strongest adsorption on GRA at −28.46 kJ/mol, followed by BCN and BN. The calculated τ indicated rapid desorption across all systems, typically in the sub-nanosecond range, though slightly slower on GRA due to stronger interaction. This suggests a favourable balance between adsorption capacity and ease of regeneration for GRA and BCN, while BN's weaker adsorption could enable faster reusability but with reduced affinity.

4.6.3.3 Electronic properties

Electronic structure analysis (Figure 4.14) revealed that the LUMOs of BN and BCN were localised over electron-deficient boron atoms, while HOMOs concentrated on nitrogen and carbon atoms, providing complementary sites for electron donation. The HOMOs of TCS and TCC were localised near electronegative O and Cl atoms, consistent with their nucleophilic tendencies. After adsorption (Figure 4.15), HOMO and LUMO distributions remained

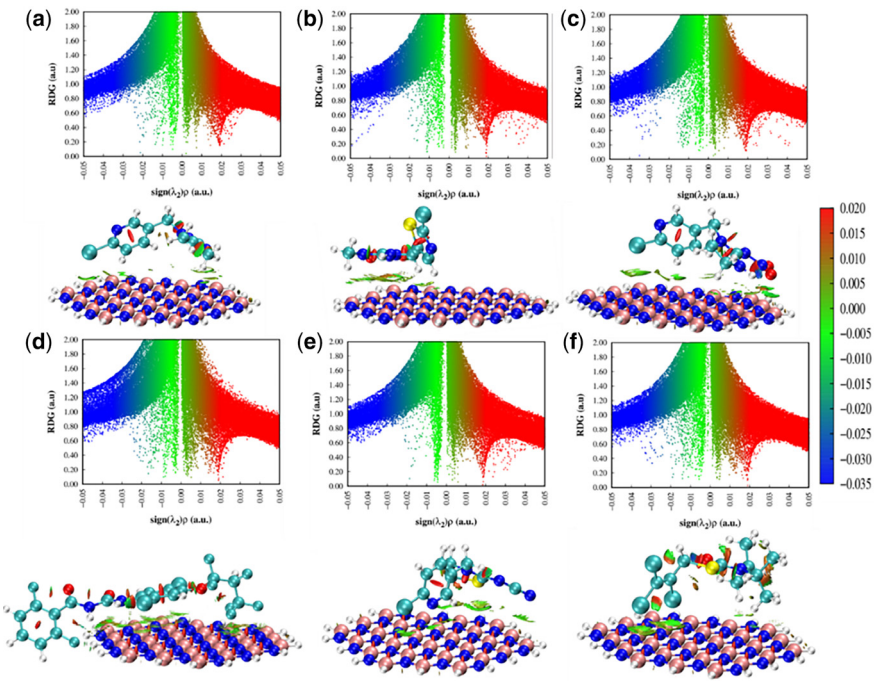


Figure 4.11 Reduced density gradient plot and non-covalent interactions isosurfaces of (a) Acetamiprid adsorbed BN, (b) Clothianidin adsorbed BN, (c) Imidacloprid adsorbed BN, (d) Lufenuron adsorbed BN, (e) Thiacloprid adsorbed BN, (f) Tri-allate adsorbed BN. (Dindorkar *et al.*, 2022).

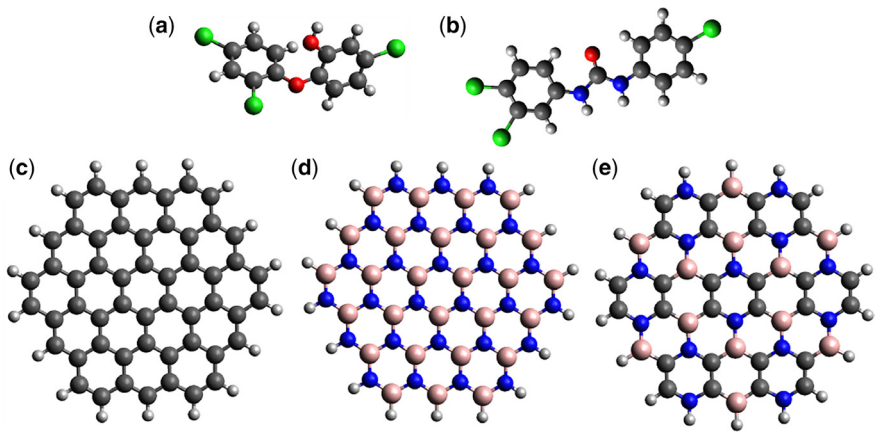


Figure 4.12 Optimised geometries of (a) TCS, (b) TCC, (c) GRA, (d) BN, (e) BCN. (Dindorkar *et al.*, 2023).

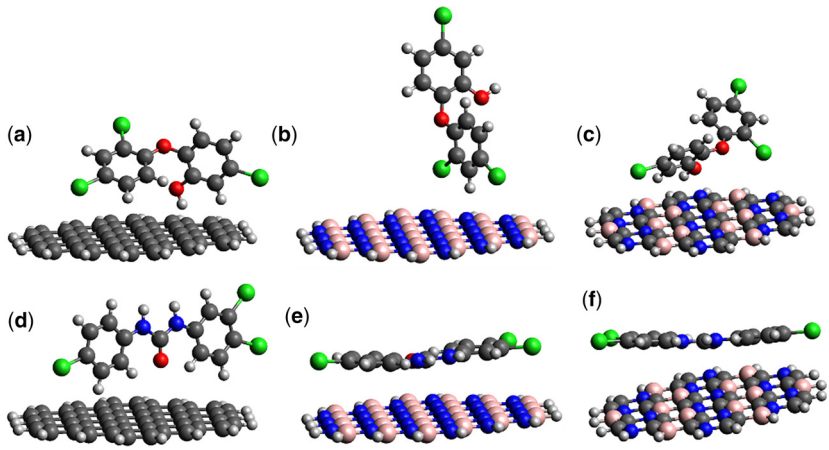


Figure 4.13 Optimised geometries of different clusters (a) TCS-GRA, (b) TCC-GRA, (c) TCS-BN, (d) TCC-BN, (e) TCS-BCN, (f) TCC-BCN. (Dindorkar *et al.*, 2023).

Table 4.2 Reactivity descriptors, shortest distance, adsorption energy, and recovery time of the clusters before and after adsorption.

	TCS	TCC	BN-TCS	BN-TCC	BCN-TCS	BCN-TCC	GRA-TCS	GRA-TCC
ΔE (kJ/mol)	–	–	−10.67	−7.58	−22.9	−11.96	−28.46	−18.96
HOMO (eV)	−0.86	−0.91	−0.87	−0.94	−3.97	−3.9	−2.59	−2.55
LUMO (eV)	−6.53	−6.13	−6.48	−6.13	−2.89	−2.83	−5.46	−5.43
HLG (eV)	5.67	5.22	5.61	5.19	1.08	1.07	2.87	2.88
η (eV)	7.39	7.04	7.35	7.07	6.86	6.73	8.05	7.98
μ (eV)	3.69	3.52	3.67	3.54	3.43	3.36	4.02	3.99
ω (eV)	0.92	0.88	0.92	0.88	0.86	0.84	1.01	0.99
Shortest distance (Å)			2.95	3.21	2.39	2.48	2.25	2.13
Recovery time (s)			3×10^{-9}	3×10^{-5}	2×10^{-4}	3×10^{-9}	4×10^{-8}	1×10^{-9}

largely unchanged on GRA and BCN, indicating minimal perturbation to their electronic structures, whereas BN exhibited significant band gap reduction due to new energy levels forming near −1 eV, especially in TCS adsorption. This was corroborated by the DOS plots, which showed a pronounced narrowing of the band gap for BN upon adsorption, suggesting potential for electronic sensing.

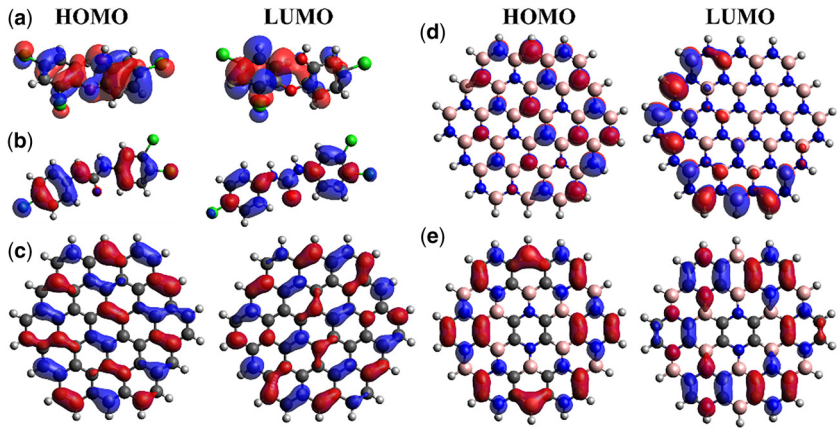


Figure 4.14 Highest occupied molecular orbitals and the lowest unoccupied molecular orbitals distribution for optimised structure of (a) TCS, (b) TCC, (c) GRA, (d) BN, (e) BCN. (Dindorkar *et al.*, 2023).

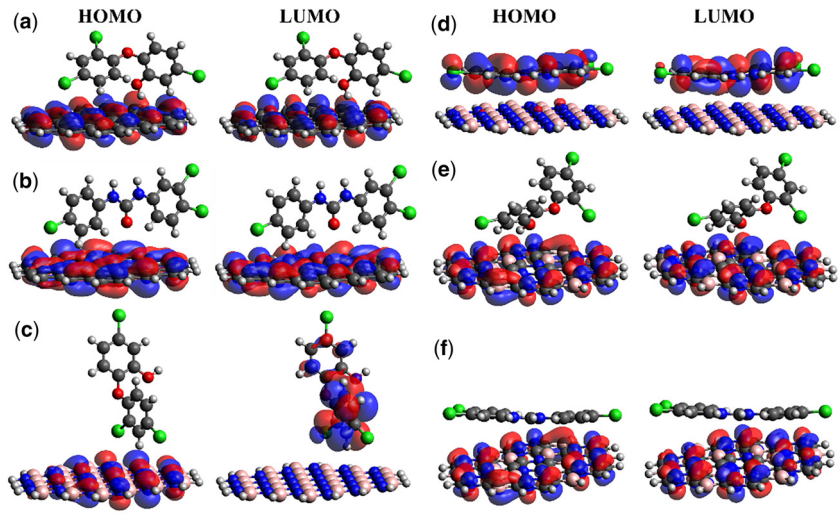


Figure 4.15 Highest occupied molecular orbitals and the lowest unoccupied molecular orbitals distribution for the optimised structure of different clusters (a) TCS-GRA, (b) TCC-GRA, (c) TCS-BN, (d) TCC-BN, (e) TCS-BCN, (f) TCC-BCN. (Dindorkar *et al.*, 2023).

4.6.3.4 Reactivity descriptors

Reactivity descriptors (Table 4.2) revealed that adsorption slightly increased the η of TCS and TCC on GRA, reflecting enhanced stability, while a minor decrease was seen for BN and BCN. The μ were highest ($\sim$4 eV) on GRA, indicating stronger adsorption driving forces.

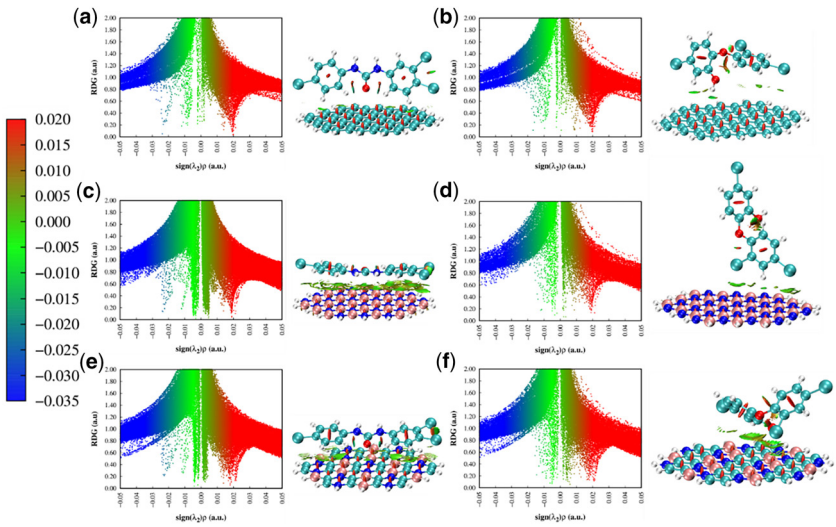


Figure 4.16 Reduced density gradient plot and non-covalent interactions isosurfaces in different clusters (a) TCS-GRA, (b) TCC-GRA, (c) TCS-BN, (d) TCC-BN, (e) TCS-BCN, (f) TCC-BCN. (Dindorkar *et al.*, 2023).

4.6.3.5 Reduced density gradient scatter and non-covalent interaction plots

The RDG and NCI plots (Figure 4.16) confirmed that adsorption was primarily governed by van der Waals interactions (green surfaces), with limited H-bonding (blue) or steric hindrance (red). The relatively undisturbed electronic structure of GRA and BCN after adsorption, coupled with moderate E_{ads} and short τ, suggests they are well-suited for water purification applications. Meanwhile, BN's substantial electronic perturbation highlights its potential use in sensor devices where changes in electronic signals upon adsorption are advantageous.

4.7 SUMMARY

Various experimental techniques have been developed to study the various aspects of the adsorption process. These experiments find adsorption strength, heights, geometry, pattern, electronic structure, and vibrational properties. Computational methods can provide a level of detail that is difficult to obtain via experimental methods, thereby enhancing these experiments. DFT approaches, in particular, are effective alternatives to conventional theoretical studies and molecular simulations in first-principle calculations. They work together to connect the structural and thermodynamic properties of the material with the microscopic features of the adsorption process. The adaptability of DFT in problem-solving and its widespread use by researchers in chemistry, physics, chemical engineering, and materials science demonstrate its value. DFT is an adequate theoretical tool for calculating the adsorbate/adsorbent structure and its surface adsorption. Further, the first-principles calculation method based on

DFT can analyse the interaction mechanism of the adsorbate and adsorbent at the molecular/atomic level.

The basics of DFT calculation were introduced in this chapter to enable the readers to understand and perform DFT for their adsorption model. Two case studies were also presented. This chapter provided a detailed exploration of DFT and its applications in studying adsorption processes. It outlines the theoretical aspects of DFT, describes the computation of adsorption-related properties, and discusses critical metrics, such as E_{ads}, charge density difference, and DOS, essential for understanding adsorption mechanisms. Furthermore, it reviews software packages used for DFT calculations and presents case studies on adsorption behaviours on nanosheet materials. The case studies reveal insights into structural and electronic properties and reactivity descriptors, offering a robust framework for evaluating adsorption phenomena and facilitating advancements in adsorption-based applications.

doi: 10.2166/9781789063943 _0095

Chapter 5

Molecular dynamics and grand canonical Monte Carlo simulations of adsorption processes

5.1 INTRODUCTION

Adsorption, the accumulation of atoms, ions, or molecules from a phase (gas or liquid) onto the surface of a solid or porous material, is a fundamental process that underpins numerous industrial, environmental, and biological applications. It plays a critical role in water and air purification, the separation of gases, the storage of energy carriers such as hydrogen and methane, the catalysis of chemical reactions, and even emerging biomedical technologies. The efficiency and selectivity of adsorption processes hinge on complex interactions at the molecular scale, where surface chemistry, pore architecture, and fluid properties converge in intricate ways.

While experiments remain the cornerstone for measuring adsorption capacities, kinetics, and thermodynamics, they often fall short of revealing detailed microscopic mechanisms. Techniques such as spectroscopy and calorimetry can provide indirect evidence of adsorbate configurations or energy changes, yet they struggle to map out molecular trajectories, identify transient intermediates, or capture cooperative and competitive adsorption in multi-component systems. Moreover, manipulating experimental conditions to isolate specific contributions – such as pore-size effects, surface heterogeneity, or solvent interactions – can be challenging.

Molecular simulations have thus emerged as indispensable partners to experiments, offering a 'virtual laboratory' to probe adsorption phenomena under controlled, idealised, or even extreme conditions. Two computational approaches have become especially prominent (Ekberg *et al.*, 2022). Molecular dynamics (MD) simulations solve Newton's equations of motion to provide time-resolved trajectories of atoms and molecules, thereby elucidating diffusion, clustering, and

© 2026 IWAP. This is an Open Access book chapter distributed under the terms of the Creative Commons Attribution Licence (CC BY-NC-ND 4.0) which permits copying and redistribution for non-commercial purposes with no derivatives, provided the work is properly cited (https://creativecommons.org/licenses/by-nc-nd/4.0/). The chapter is from the book *Computational Techniques for Modelling and Simulating Adsorption Processes for (Waste)Water Treatment*, A. Yadav and P. Labhasetwar (Authors).

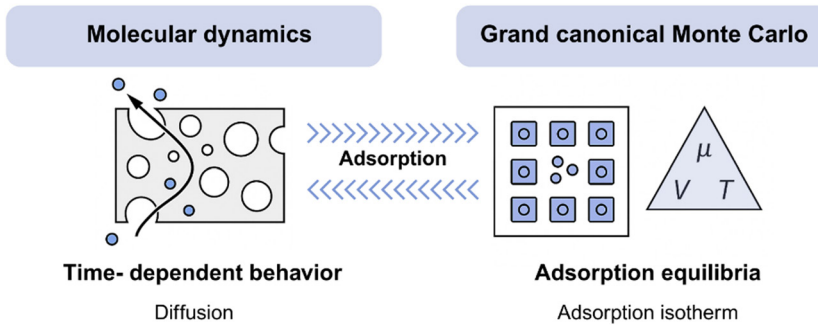


Figure 5.1 Complementary roles of molecular dynamics and grand canonical Monte Carlo simulations in adsorption studies.

conformational dynamics within adsorbent materials. In contrast, grand canonical Monte Carlo (GCMC) simulations operate by sampling different numbers of adsorbate molecules at fixed chemical potential, temperature, and volume, making them uniquely suited to predict adsorption isotherms, identify preferred adsorption sites, and study phase transitions such as capillary condensation.

Figure 5.1 illustrates how MD and GCMC complement each other in studying adsorption processes. While MD reveals adsorbates' temporal evolution and transport behaviour – tracking how molecules navigate pores or rearrange on surfaces – GCMC directly captures equilibrium uptake and the statistical likelihood of adsorption configurations under varying chemical potentials. Together, they form a powerful toolkit for understanding both adsorption's equilibrium and dynamic facets.

This chapter aims to provide a comprehensive overview of how MD and GCMC simulations are employed to investigate adsorption phenomena. It begins with a discussion of the statistical mechanics framework underlying these methods, followed by examining interatomic potentials and force fields crucial for accurately modelling adsorbent–adsorbate systems. Subsequent sections cover practical aspects of representing adsorbents and solvents, setting up simulation workflows, and employing state-of-the-art software packages. The chapter concludes with selected case studies, current challenges, and perspectives on future advances, offering readers both foundational knowledge and practical guidance to apply these computational tools effectively in adsorption research.

5.2 HISTORY AND EARLY DEVELOPMENTS

The rise of molecular simulations as a scientific discipline dates to the mid-20th century, when advances in theoretical physics aligned with the emergence of digital computing. Two main approaches emerged: MC and MD, each providing a distinct but complementary way to investigate many-particle systems. MC methods, rooted in probability and statistical mechanics, allowed researchers to compute ensemble averages by generating random configurations. The name 'Monte Carlo,' coined by Metropolis and Ulam, underscored the stochastic nature of these techniques. Initially used to solve problems in neutron transport,

MC quickly evolved to study thermodynamic properties of model systems such as Ising lattices and simple fluids.

In contrast, MD offered a mechanical perspective by numerically integrating Newton's equations of motion to follow how particles move over time. This approach provided insight into equilibrium and dynamic behaviours, like diffusion and structural relaxation. A landmark study by Alder and Wainwright (1957) used MD to simulate hard spheres, revealing unexpected features such as a dip in the velocity autocorrelation function that pointed to the 'caging' effect in dense liquids (Alder & Wainwright, 1957).

The 1960s and 1970s saw rapid progress. Rahman's (1964) simulation of liquid argon, employing the Lennard–Jones potential, was the first realistic MD study of a molecular fluid (Rahman, 1964). Verlet soon introduced his celebrated integration algorithm and neighbour list method, greatly enhancing the efficiency of MD. Rahman and Stillinger's (1971) study of liquid water uncovered a dynamic hydrogen-bonded network, overturning earlier views of water diffusion as a series of discrete jumps (Rahman & Stillinger, 1971). In parallel, MD was extended to biomolecules by Karplus, Levitt, and Warshel, paving the way for protein folding simulations – work that would later earn them the Nobel Prize in Chemistry (Warshel & Karplus, 1972).

Meanwhile, MC techniques have also advanced. The Metropolis algorithm, formalised in 1953, became the backbone of modern MC sampling (Metropolis *et al.*, 1953). In the 1980s, Panagiotopoulos introduced Gibbs ensemble MC to compute phase equilibria without explicit interfaces, while GCMC approaches emerged as essential tools for studying adsorption, enabling direct control of chemical potential to predict isotherms and pore filling (Panagiotopoulos, 1992).

These foundational decades made molecular simulations indispensable across physics, chemistry, and materials science, bridging theoretical models with experimental observations. As computational power has grown, so has the ambition of simulations, which tackle complex systems from nanoporous materials and catalytic surfaces to planetary interiors. Figure 5.2 illustrates this brief history, highlighting the key milestones in developing MD and GCMC simulations.

5.3 FUNDAMENTALS OF MOLECULAR SIMULATIONS

Molecular simulations derive their power from statistical mechanics, which provides the rigorous link between the discrete, atomistic world and the continuum-level thermodynamic properties we observe experimentally. At their heart, these simulations generate representative microscopic configurations (microstates) of a system under specific constraints, and from these, compute macroscopic quantities via ensemble averages (Alavi, 2020; Zhou and Liu, 2022).

This framework rests on ensembles – large hypothetical collections of identically prepared systems representing the probability landscape of all possible microstates under given thermodynamic conditions. Different ensembles are defined depending on which variables are held constant and which are allowed to fluctuate, each suited to studying particular physical scenarios. This chapter focuses on four such ensembles most relevant to adsorption simulations: the microcanonical (NVE), canonical (NVT), isothermal–isobaric (NPT), and grand canonical (μVT) ensembles (Lustig, 1994). Figure 5.3 schematically

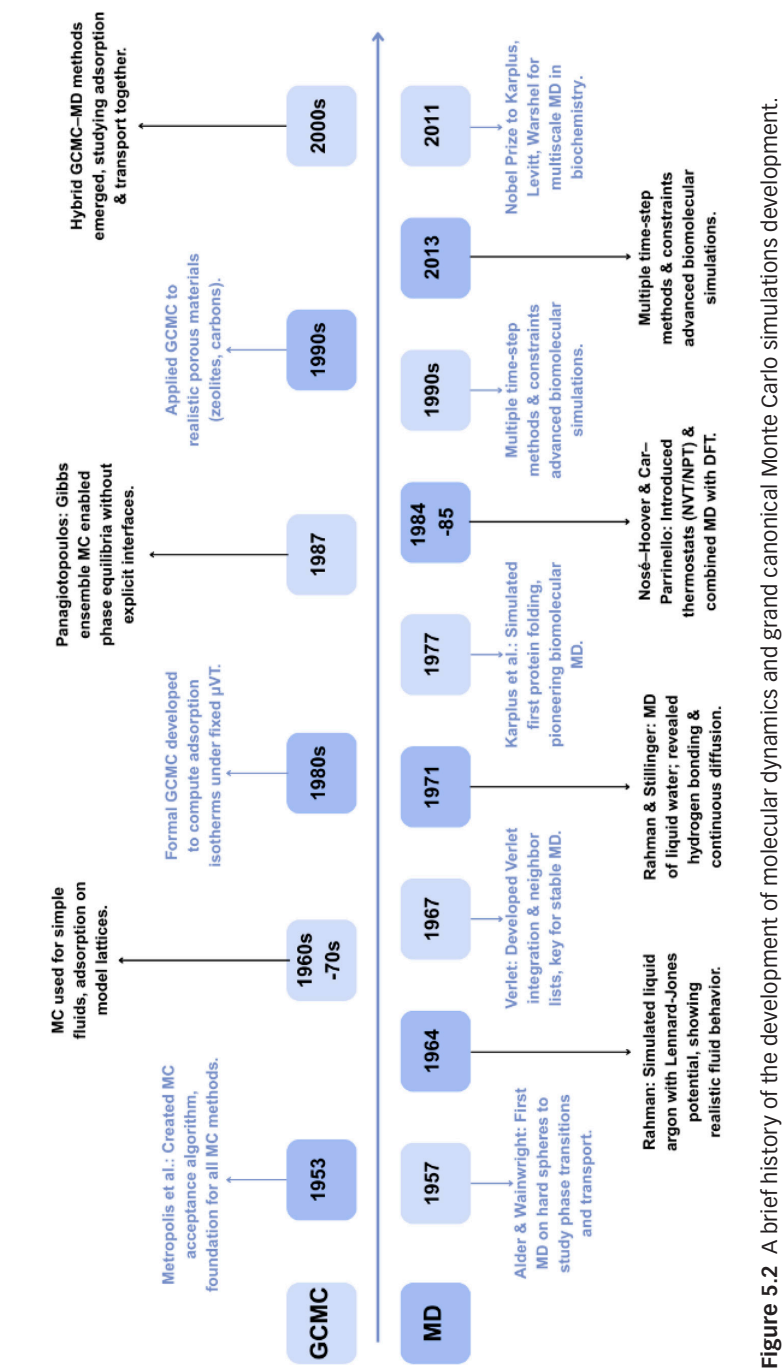


Figure 5.2 A brief history of the development of molecular dynamics and grand canonical Monte Carlo simulations development.

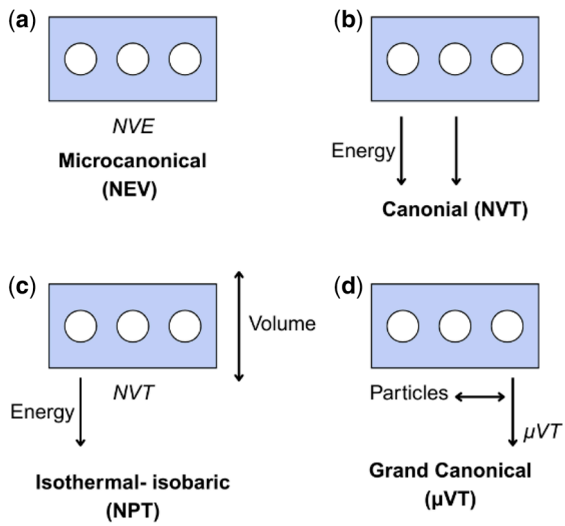


Figure 5.3 Schematic of four molecular simulation ensembles: NVE (fixed E), NVT (fixed T), NPT (fixed P, T with volume fluctuations), and μVT (particle exchange at fixed μ).

illustrates these ensembles, emphasising the differences in what exchanges are allowed (energy, volume, particles) and the corresponding fixed parameters characterising each ensemble.

5.3.1 Statistical mechanics and ensembles

In any molecular simulation, the goal is to sample a set of microstates according to the probability distribution prescribed by the chosen ensemble. These distributions stem directly from the principles of statistical mechanics, ensuring that calculated averages reflect the physical reality under the specified macroscopic constraints. The ensemble selection thus determines not only the modelled thermodynamic conditions but also the types of fluctuations that occur in the system (in energy, volume, or particle number).

5.3.1.1 Microcanonical ensemble (NVE)

The microcanonical ensemble describes an isolated system with a fixed number of particles (N), volume (V), and total energy (E). There is no exchange of energy or particles with any surroundings. Every microstate accessible under these constraints is equally probable, making this ensemble foundational for linking microscopic dynamics to entropy. Mathematically, the microcanonical ensemble leads to the microcanonical partition function:

$$\Omega(N,V,E) = \sum_{\text{states}} \delta(H - E) \tag{5.1}$$

where H is the Hamiltonian of the system. This ensemble provides direct insight into the density of states and entropy.

Integrating Newton's equations of motion under conservative forces in MD inherently conserves energy, making MD naturally suited for NVE simulations. Such simulations often probe intrinsic dynamical properties – vibrational spectra, collision cascades, or how local perturbations propagate through a lattice. In adsorption studies, short NVE segments may characterise how quickly energy redistributes after an adsorption event.

5.3.1.2 Canonical ensemble (NVT)

The canonical ensemble represents systems at constant N, V, and temperature (T), with the system able to exchange energy with an external reservoir (a heat bath). This means the energy of the system fluctuates, and the Boltzmann distribution gives the probability of observing a microstate with energy E:

$$P(E) = \frac{e^{-\beta E}}{Z}, \quad \beta = \frac{1}{kBT} \tag{5.2}$$

where Z is the canonical partition function, summing over all microstates.

Maintaining a precise temperature is crucial for simulating adsorption at conditions matching experiments. In practice, MD simulations achieve NVT sampling by employing thermostats. Popular choices include the Nosé–Hoover thermostat, which modifies the system's equations of motion to mimic coupling to an external heat bath, and stochastic approaches like Langevin dynamics. These methods enable the exploration of temperature-dependent adsorption phenomena such as structural reorganisation or desorption kinetics.

5.3.1.3 Isothermal–isobaric ensemble (NPT)

The isothermal–isobaric ensemble holds N, T, and pressure (P) constant, allowing the system volume to fluctuate to maintain equilibrium with an external pressure reservoir. The probability of observing a microstate in this ensemble includes both energy and volume contributions:

$$P(E,V) = \frac{e^{-\beta(E+PV)}}{\Delta} \tag{5.3}$$

where Δ is the isothermal–isobaric partition function.

This ensemble is critical for systems that undergo volume changes, such as swelling clays, flexible MOFs, or responsive polymer membranes. NPT simulations use barostats like the Parrinello–Rahman or Berendsen algorithms, which dynamically adjust the simulation box to control pressure. In adsorption studies, simulating under NPT conditions helps model realistic scenarios where adsorption induces structural deformations of the adsorbent framework.

5.3.1.4 Grand canonical ensemble (μVT)

The grand canonical ensemble maintains chemical potential (μ), volume (V), and temperature (T) constant, while the number of particles (N) is allowed to fluctuate due to exchange with a reservoir. The probability of finding the system with N particles and energy E is given by

$$P(N,E) = \frac{e^{-\beta(E-\mu N)}}{\Xi} \tag{5.4}$$

where Ξ is the grand partition function.

This ensemble is the natural framework for studying adsorption processes, as it directly models the physical situation of a porous adsorbent in equilibrium with a fluid reservoir at given μ (or, equivalently, a fixed bulk concentration or gas pressure). GCMC simulations implement this by trial insertions and deletions of particles, accepting or rejecting moves based on the chemical potential and energy change. This enables the direct computation of adsorption isotherms, pore filling sequences, and even cooperative adsorption transitions, which are otherwise difficult to extract purely from MD.

5.3.2 Molecular dynamics: theory and algorithms

MD simulations are among the most versatile tools in modern adsorption research. They provide a computational microscope, enabling researchers to watch how atoms and molecules move and interact over time under conditions that mimic real experiments. Unlike purely statistical methods focusing only on equilibrium averages, MD captures the actual time evolution of systems, opening the door to investigating structural preferences and kinetic processes (Toxvaerd, 1991).

At its core, MD solves the classical many-body problem by following how each atom in a system responds to the forces exerted by its neighbours. Although rooted in Newtonian mechanics, the method can incorporate sophisticated potentials to approximate quantum effects or complex environmental influences. For adsorption studies, this means MD can reveal where molecules prefer to adsorb on a surface or within pores, how they get there, how long they stay, and how they move around once adsorbed. The standard MD workflow is illustrated in Figure 5.4. Starting from an initial configuration, forces are computed from the interatomic potential, velocities and positions are updated using an integration algorithm, and periodic boundary conditions are applied. This cycle repeats across millions of steps to generate trajectories, which are then analysed to extract equilibrium and dynamic properties relevant to adsorption, such as diffusion coefficients, residence times, and structural rearrangements.

5.3.2.1 Integration of equations of motion

The theoretical foundation of MD lies in Newton's laws: each atom moves according to the forces derived from its interactions with all other atoms in the system. These forces arise from a force field, which encapsulates bonded interactions (bonds, angles, dihedrals) and non-bonded interactions (van der Waals and electrostatics). In practice, numerical methods are employed since analytical solutions to these coupled motions are impossible for realistic systems (Harrison *et al.*, 2018).

The standard MD workflow involves:

- **Force calculation:** Determining the force on each atom based on its current position and the positions of all other atoms.

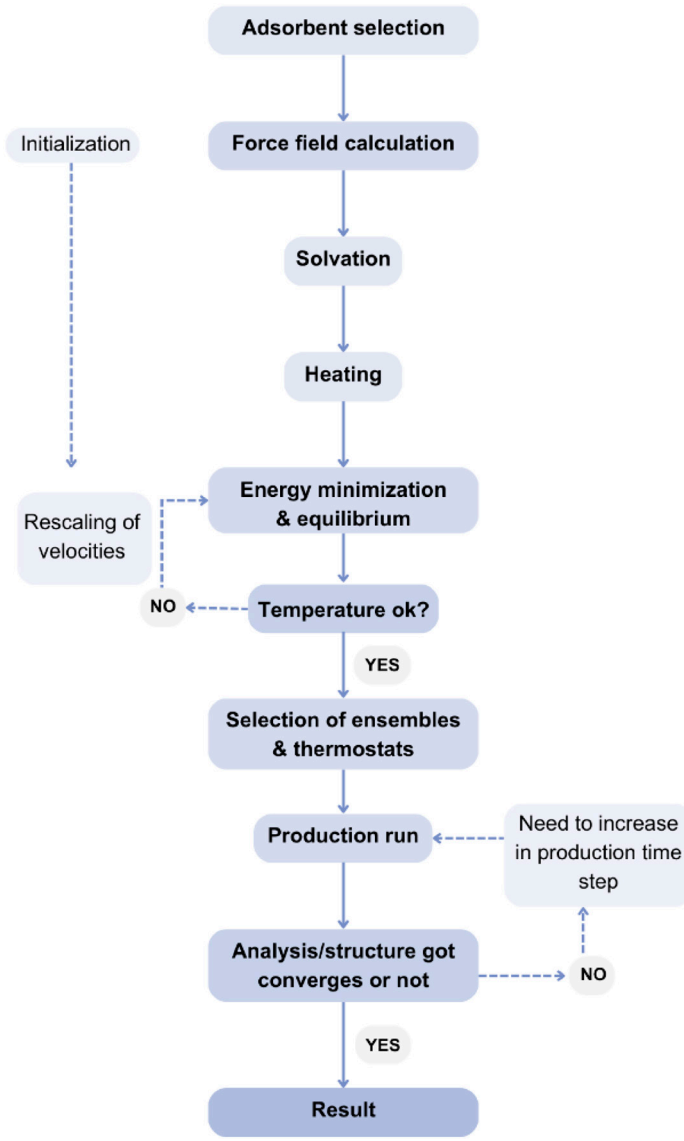


Figure 5.4 Workflow of a typical molecular dynamics simulation.

- **Integration:** Updating velocities and positions using an algorithm like the velocity-Verlet or leapfrog method. These integrators are favoured for their simplicity, stability, and reasonable energy conservation over long trajectories.
- **Thermostatting or barostatting:** Adjusting velocities (thermostats) or the simulation box dimensions (barostats) to maintain target temperature

or pressure, enabling sampling of the canonical (NVT) or isothermal–isobaric (NPT) ensembles.
- **Periodic boundary conditions:** Applying artificial wrapping of atoms that exit one side of the simulation box back into the opposite side, to mimic an infinite system and eliminate surface effects.
- **Data collection:** Recording configurations, velocities, and energies at intervals for later analysis.

The choice of time step is crucial. It must be small enough to capture the fastest motions, typically bond vibrations involving hydrogen atoms. As a rule of thumb, adsorption simulations involving water or organic adsorbates use time steps of 1–2 fs. To use larger time steps (e.g. up to 4 fs), constraints like SHAKE or LINCS are often applied to keep bond lengths involving hydrogens fixed.

Because adsorption processes can involve phenomena on longer timescales – such as rearrangement of large frameworks, slow diffusion in narrow pores, or rare desorption events – strategies like multiple time-step algorithms or enhanced sampling (covered later in the chapter) may also be employed.

5.3.2.2 Sampling dynamic properties

Once an MD trajectory is generated, it serves as a rich data source for extracting structural and dynamic information. This is particularly valuable in adsorption research, where kinetics can matter as much as equilibrium loading.

Diffusion and mobility in porous systems

A primary application of MD in adsorption is to determine how easily adsorbates move within pores. For example, water or organic contaminants inside mesoporous silica or MOFs may show quite different diffusion characteristics depending on pore size, connectivity, or surface functionalisation.

One can compute self-diffusion coefficients by tracking the mean-squared displacement (MSD) of molecules over time. In nanoporous carbons, for instance, simulations often reveal that diffusion becomes sub-linear (indicative of hindered or anomalous diffusion) at higher loadings or in ultra-micropores, directly affecting adsorption kinetics in breakthrough experiments.

Residence times and site-specific retention

MD also allows calculation of residence times – how long a molecule stays adsorbed at a particular site before moving on. This is critical for understanding selectivity. In competitive adsorption, molecules with similar affinities in static isotherms may differ dramatically in how long they occupy critical adsorption sites.

For example, studies of CO_2 and CH_4 co-adsorption in certain MOFs have shown that although equilibrium uptake may be comparable, CO_2 often has longer residence times at open metal sites, improving its separation under flow conditions.

Molecular reorientation and confinement effects

Inside narrow pores, adsorbed molecules often adopt preferred orientations or form structured hydrogen-bond networks that differ from bulk phases.

MD captures these details by computing orientational correlation functions or local pair distributions, helping to explain shifts seen in infrared or NMR experiments.

In hydrophobic carbons, water molecules may form transient clusters that rearrange frequently, whereas in hydrophilic silica, they may lock into more stable hydrogen-bonded cages. Such microscopic rearrangements underlie macroscopic hysteresis in adsorption–desorption cycles.

Framework dynamics and coupling to adsorption

Many modern adsorbents, such as flexible MOFs or layered clays, respond dynamically to guest molecules. Adsorption can induce breathing or swelling transitions, opening or closing pores. MD can capture this coupled host–guest dynamics, revealing how uptake drives structural transformations that can further influence selectivity or capacity.

5.3.3 Monte Carlo and grand canonical Monte Carlo methods

MC methods are foundational in molecular simulation, offering a fundamentally different approach from MD. While MD follows the explicit time evolution of atomic positions under Newtonian mechanics, MC methods explore the configurational landscape through probabilistic sampling instead. By generating sequences of statistically representative microstates and calculating ensemble averages, MC provides a direct route to thermodynamic properties without tracking real-time trajectories (Lustig, 1994). This is particularly valuable for adsorption studies, where equilibrium phenomena – such as the distribution of adsorbates within pores, adsorption isotherms, and site occupancies – are often the primary focus.

The strength of MC techniques lies in their ability to efficiently sample the regions of phase space that most significantly contribute to equilibrium properties (Tylianakis and Froudakis, 2009). Unlike MD, which may require a long time to observe rare events or to cross energy barriers, MC methods can propose large, non-physical jumps in configuration space. This allows them to quickly explore diverse molecular arrangements, dramatically improving convergence, especially in systems where kinetic bottlenecks or strong local minima would slow down MD. Figure 5.5 shows the workflow of a typical MC simulation.

5.3.3.1 Metropolis algorithm and importance sampling

The formal framework for modern MC simulations was established with the Metropolis algorithm, introduced in 1953 by Metropolis (Hastings, 1970; Metropolis *et al.*, 1953). This algorithm provides a robust scheme for generating microstates that are distributed according to the statistical weights dictated by the chosen ensemble, most commonly the canonical ensemble in early applications. Rather than randomly sampling all possible configurations with equal frequency, which would waste effort on highly improbable states, the Metropolis approach implements importance sampling. In this scheme,

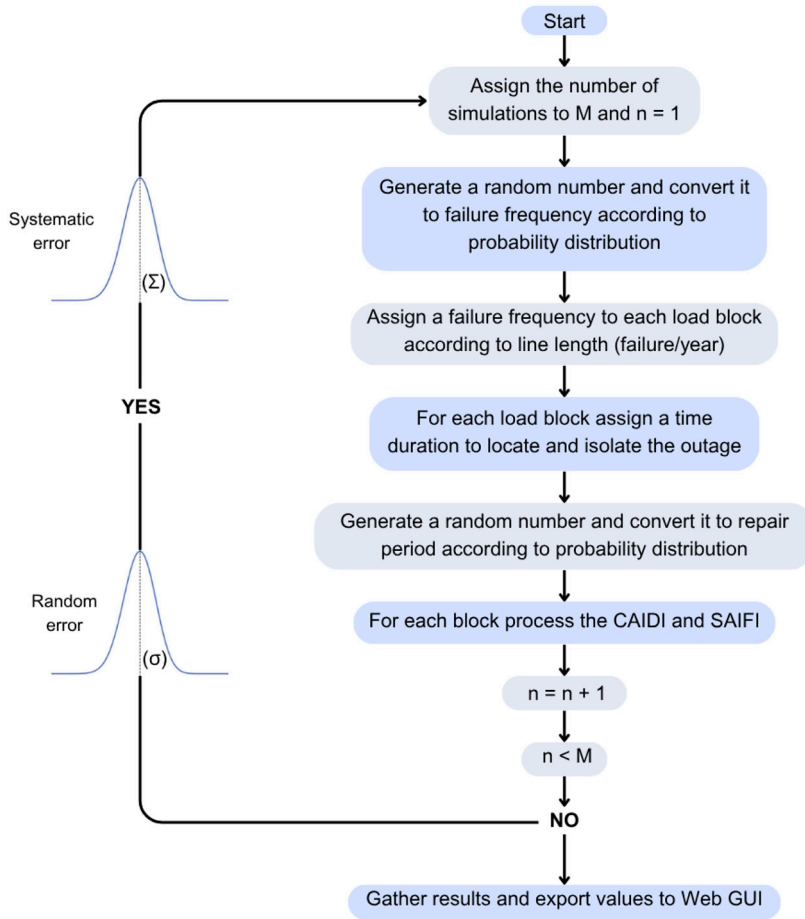


Figure 5.5 Workflow of a typical grand canonical Monte Carlo simulation.

the algorithm preferentially explores those microstates that contribute most significantly to thermodynamic averages.

At each step, the Metropolis algorithm proposes a trial change to the current configuration, such as moving a molecule or altering its orientation. The change in system energy resulting from this move is then evaluated. If the new configuration lowers the system energy, it is automatically accepted. If it increases the energy, it may still be accepted, with a probability that decreases exponentially with the energy rise. This acceptance criterion allows the system to escape local minima and ensures that, over many iterations, configurations are sampled according to the Boltzmann distribution.

This concept of importance sampling is crucial for adsorption studies. It ensures that computational resources are concentrated on physically relevant configurations – such as those where adsorbate molecules occupy energetically favourable sites on a surface or within pores – while occasionally sampling higher-energy arrangements that contribute to entropy and thermal fluctuations. The approach rapidly converges observables like adsorption site occupancies, local densities, and configurational entropy.

5.3.3.2 Grand canonical Monte Carlo for adsorption studies

Among the most powerful MC frameworks for adsorption phenomena is the GCMC method, which operates under the grand canonical ensemble. In this statistical ensemble, the system maintains constant chemical potential (μ), volume (V), and temperature (T), while allowing the number of particles (N) to fluctuate. This mirrors the conditions of many experimental adsorption measurements, where a porous adsorbent equilibrates with a gas reservoir at a fixed pressure, or a liquid solution maintains a constant solute concentration.

In GCMC simulations, trial moves include attempts to insert new molecules into the system, remove existing ones, or adjust their positions and orientations. Each move is evaluated using a statistical acceptance rule that incorporates the chemical potential, ensuring that the simulation samples microstates according to the grand canonical distribution over time. This direct particle exchange mechanism allows GCMC to rapidly explore different adsorption loadings, capturing the equilibrium distribution of adsorbates under the specified thermodynamic conditions.

One of the principal advantages of GCMC for adsorption is that it directly yields equilibrium adsorption isotherms – plots of the amount adsorbed versus chemical potential or external pressure – without the need to perform multiple simulations at different fixed particle numbers. It also captures fluctuations in occupancy that reveal important thermodynamic information, such as the heat of adsorption. In systems where adsorption involves cooperative effects, such as stepwise pore filling or capillary condensation, GCMC readily captures these transitions, providing microscopic insight into how adsorbates organise within the host material.

Moreover, GCMC is well-suited to studying competitive adsorption in multi-component systems. By assigning different chemical potentials to multiple species, one can simulate mixtures of gases or solutes and predict selectivity, directly linking molecular interactions with macroscopic separation performance.

Because randomly inserting large or flexible molecules into crowded or narrow pores often leads to steric clashes and rejected moves, modern GCMC implementations frequently incorporate advanced techniques such as configurational bias MC. This method builds molecules piecewise inside the pore to avoid overlaps, significantly improving sampling efficiency. Additional biasing strategies may also be employed to enhance exploration of rarely visited, high-energy configurations, which is important for accurately capturing phase transitions or pore-filling thresholds.

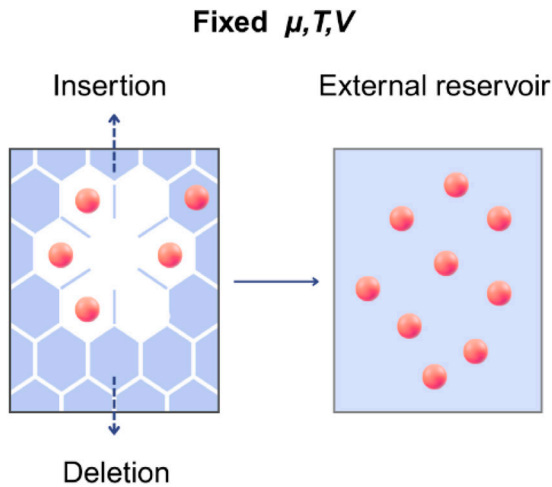


Figure 5.6 Schematic representation of grand canonical Monte Carlo sampling in an adsorption simulation.

Figure 5.6 illustrates the essential concept of GCMC in adsorption: the system dynamically samples configurations with varying numbers of adsorbed molecules by performing trial insertions and deletions, ultimately building up the equilibrium distribution dictated by the imposed chemical potential. This approach offers a virtual experiment that complements laboratory adsorption measurements, providing atomistic-level insight otherwise difficult to achieve.

5.4 INTERATOMIC POTENTIALS AND FORCE FIELDS

The mathematical model that describes how atoms interact is at the heart of any molecular simulation. This is encoded in a force field or interatomic potential – a collection of analytical functions and parameters that together determine the forces acting on each atom based on its position relative to others. The choice and quality of this force field are critical, as they directly dictate the realism and predictive power of MD and MC simulations in adsorption studies (McCready *et al.*, 2024).

Force fields typically partition the total potential energy of a system into contributions from bonded interactions, which hold molecules together, and non-bonded interactions, which govern the forces between molecules or between adsorbates and the adsorbent surface. Advanced treatments also incorporate schemes for accurately handling long-range electrostatic interactions, which are essential for charged systems. Figure 5.7 provides a conceptual overview of these main components, illustrating how bonds, angles, torsions, and non-bonded forces work together to shape the behaviour of molecular systems.

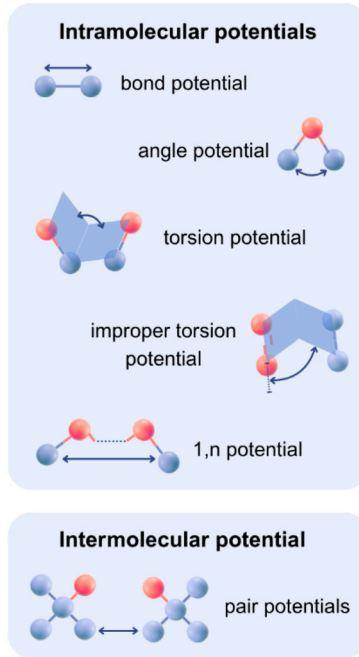


Figure 5.7 Schematic depiction of the main components of molecular force fields.

5.4.1 Bonded interactions: bonds, angles, torsions

Bonded interactions model the internal connectivity of molecules, maintaining their structural integrity. They are typically divided into three primary components.

5.4.1.1 Bond stretching

This term describes the potential energy associated with the length of a bond between two atoms deviating from its equilibrium distance. A simple harmonic potential often represents it, effectively acting like a spring that resists compression or extension.

5.4.1.2 Angle bending

Three connected atoms define an angle. Deviations from the preferred (equilibrium) angles increase the system's energy. This is also commonly modelled using a harmonic potential, penalising bending away from the ideal geometry.

5.4.1.3 Dihedral (torsional) rotations

When considering four sequentially bonded atoms, the rotation around the central bond defines a dihedral angle. Unlike bonds and angles, torsional potentials are typically modelled with periodic functions that capture the energy barriers associated with rotating around bonds, reflecting phenomena such as gauche and trans conformations in hydrocarbons.

Together, these bonded interactions ensure that molecules retain their characteristic shapes and internal flexibilities, crucial when studying adsorption phenomena involving flexible organic contaminants or functional groups on adsorbent surfaces.

5.4.2 Non-bonded interactions: van der Waals and electrostatics

Non-bonded interactions govern how atoms and molecules influence each other when covalent bonds do not directly connect them. In adsorption studies, these forces largely determine how adsorbates interact with the adsorbent surfaces and how molecules pack within pores (Fischer & Wendland, 2023).

5.4.2.1 van der Waals interactions

These encompass short-range attractive and repulsive forces arising from instantaneous and induced dipoles. They are most commonly modelled using the Lennard–Jones (12-6) potential, which captures both the steep repulsion at very close distances (due to Pauli exclusion) and the gentler attraction at intermediate ranges (due to London dispersion forces). The balance of these forces is essential for phenomena like physisorption in porous carbons or the organisation of gas molecules in MOF cavities.

5.4.2.2 Electrostatic interactions

Electrostatic forces arise from the interactions of partial charges assigned to atoms, accounting for attractions between oppositely charged sites and repulsions between like charges. These interactions often have longer ranges compared to van der Waals forces and are critical for modelling adsorption in systems involving polar molecules or charged surfaces, such as water in zeolites or ion-exchange processes in clays.

5.4.3 Long-range treatments: Ewald summation and particle mesh Ewald

Because electrostatic interactions decay slowly with distance (proportional to 1/r), simple cutoffs can introduce significant errors. This is particularly problematic in periodic systems like crystals or extended porous materials, where long-range Coulomb interactions have substantial cumulative effects (de Souza & Ornstein, 1997).

To address this, molecular simulations employ specialised algorithms such as:

- **Ewald summation:** This classical method splits the electrostatic interaction into a rapidly converging real-space sum and a complementary sum in reciprocal space, efficiently handling infinite periodic arrays of charges.
- **Particle mesh Ewald (PME):** A more modern, scalable variant, PME accelerates the reciprocal space calculations by mapping charges onto a grid and using fast Fourier transforms. This has become the standard in large biomolecular and materials simulations, enabling accurate and efficient computation of long-range interactions even in systems with thousands to millions of atoms.

Correct treatment of these long-range forces is essential in adsorption studies. For example, in simulating water uptake in charged frameworks like

aluminosilicate zeolites, ignoring proper electrostatics would dramatically underestimate adsorption strength and fail to capture cooperative hydrogen bonding networks.

5.4.4 Specialised force fields for adsorption systems

Beyond general-purpose force fields like OPLS, AMBER, or CHARMM, which were initially developed for biomolecules, adsorption studies often require force fields specifically parameterised to capture interactions in inorganic materials or hybrid frameworks.

For example, ClayFF is tailored for modelling clay minerals and layered silicates, incorporating parameters that reproduce structural flexibility and hydration behaviour. Dreiding and UFF (Universal force field) are generic force fields applicable across various elements and structures, often used for simulating MOFs, COFs, and other porous frameworks. COMPASS and CVFF are employed in simulations where a balance between organic and inorganic interactions is needed, such as functionalised silica or mixed-matrix systems.

Additionally, adsorption simulations increasingly rely on polarisable force fields or incorporate machine-learned potentials that dynamically adjust to local environments, improving accuracy for systems where induction effects are significant, like water clusters near charged defect sites.

Choosing the right force field is not merely a technical detail; it fundamentally determines how faithfully a simulation captures the energetics and dynamics of adsorption. Poorly parameterised interactions can lead to misleading adsorption capacities, selectivity, or kinetics predictions.

5.5 MODELLING ADSORBENTS AND FLUIDS

An essential step in setting up molecular simulations of adsorption processes is carefully constructing realistic models of both the adsorbent and the fluid phase. (Wadi *et al.*, 2023) The quality of these models directly influences the accuracy of predictions, from adsorption isotherms and heats of adsorption to diffusion pathways and competitive selectivity. Capturing the structural complexity of porous materials and the detailed behaviour of solvent molecules or gas adsorbates is thus a cornerstone of molecular-level adsorption studies (Salahshoori *et al.*, 2024).

5.5.1 Structural models of adsorbents

5.5.1.1 Zeolites, carbons, metal organic frameworks, covalent organic frameworks, 2D materials

Modern adsorption simulations span various adsorbent materials, each with distinct structural motifs and challenges.

Zeolites, for example, are crystalline aluminosilicate frameworks with well-defined microporous channels and cages. Their periodic structures are typically built from crystallographic data (such as CIF files) in structural databases. These models preserve atomistic detail, including framework charges associated with aluminium substitutions, which necessitate counterions and careful treatment of long-range electrostatics (Ioannidou *et al.*, 2022).

Activated carbons, by contrast, are inherently amorphous. They are often represented by computationally generated models mimicking disordered pore

networks or extracting representative fragments from larger graphitic structures. Such models capture the broad distribution of pore sizes and the irregular geometry leading to complex adsorption isotherms often observed experimentally. Molecular simulations typically rely on experimentally determined unit cells replicated to form sufficiently large simulation boxes. The modular chemistry of these materials allows simulations to explore how subtle changes in linkers or functional groups impact adsorption capacity and selectivity.

5.5.1.2 Introducing functional groups and defects

In real-world materials, ideal crystalline structures are often perturbed by defects, vacancies, or additional functional groups deliberately introduced to tune adsorption properties. Simulating these features is critical for realistic predictions.

Functional groups – carboxyl, hydroxyl, or amine moieties – can be grafted onto carbon surfaces or MOF linkers within the simulation model to explore how they enhance interactions with polar or charged adsorbates. Similarly, introducing oxygenated groups into graphene or carbon models captures the hydrophilicity of oxidised carbons, often used in water treatment.

Defects play an equally pivotal role. Missing linker defects in MOFs, undercoordinated metal sites, or vacancy clusters in carbons can create high-energy adsorption sites that significantly alter isotherms and heats of adsorption. By explicitly modelling such features, simulations can reveal local environments that disproportionately influence adsorption behaviour, guiding synthesis strategies aimed at defect engineering for improved performance.

5.5.2 Water and solvent models

Accurately capturing the behaviour of fluids – whether water, organic solvents, or gases – is just as important as modelling the solid adsorbent. In many adsorption applications, especially those involving aqueous systems, the solvent plays a dominant role by mediating adsorbate–adsorbent interactions and structuring itself near pore walls.

5.5.2.1 SPC, TIP3P, TIP4P, SPC/E

Water is the most common solvent in environmental and catalytic adsorption studies, and its complex hydrogen-bonding network demands careful modelling. Several standard rigid water models are widely used in molecular simulations (Linse & Hub, 2021; Nagata *et al.*, 2016):

- The SPC (Simple Point Charge) model is one of the earliest, representing water as three charged sites arranged with fixed geometry. While computationally efficient, it underestimates some dynamical properties like self-diffusion.
- TIP3P (Transferable Intermolecular Potential with 3 Points) improves upon SPC, slightly adjusting charges and geometry better to match experimental liquid densities and heats of vaporisation.
- TIP4P and its improved variant TIP4P/2005 add a fourth virtual site carrying the negative charge, positioned near the oxygen, to more accurately reproduce the water dipole moment and radial distribution functions.

- SPC/E (Extended SPC) modifies SPC by including a self-polarisation correction, offering improved dielectric properties and diffusion coefficients closer to experimental values.

Choosing among these models depends on the balance between computational efficiency and fidelity needed for the adsorption study. For example, TIP4P-based models are often preferred when fine details of hydrogen bonding within narrow hydrophilic pores are critical, such as in zeolites or layered clays.

5.5.2.2 Polarisable and advanced water models

Despite their success, standard water models treat the charge distribution as fixed, neglecting polarisation effects that become significant near charged surfaces or under confinement. To address this, polarisable water models, such as those incorporating Drude oscillators or fluctuating charge schemes, allow the water dipole moment to adjust dynamically in response to local electric fields. This captures stronger adsorption near charged or highly polar surfaces, particularly important in ion-exchange processes or adsorption within highly polar frameworks (Bachmann & van Gunsteren, 2014).

Advanced many-body water models, such as MB-pol or neural network potentials trained on quantum mechanical data, provide near-chemical accuracy for specialised studies. While computationally more demanding, they reveal subtle structuring and entropic contributions to adsorption phenomena, especially in systems where traditional force fields fail to capture cooperative effects (Vega & Abascal, 2011).

Figure 5.8 schematically contrasts simple rigid water models with polarisable models, illustrating how the latter adapt to local fields near charged adsorbent sites. Rigid point-charge models like SPC and TIP3P have fixed charge distributions, while polarisable models dynamically adjust dipoles in response to local electric fields, better representing adsorption near charged or highly polar sites.

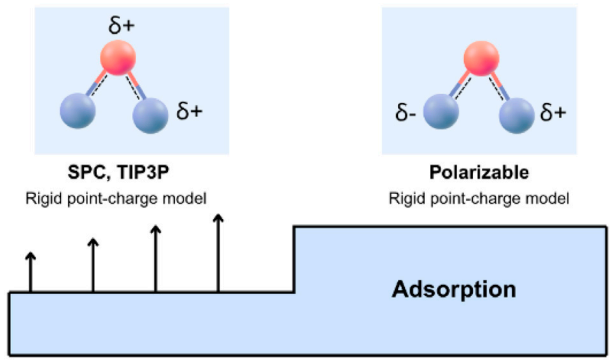


Figure 5.8 Comparison of common water models in molecular simulations.

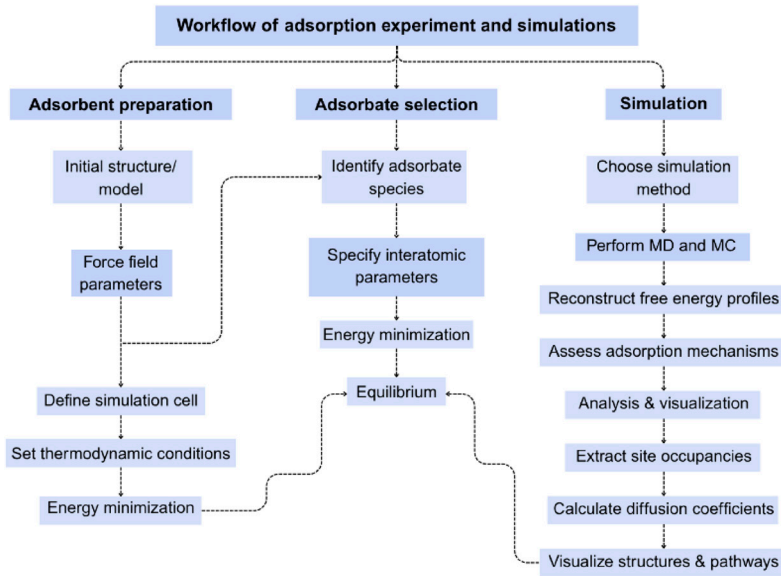


Figure 5.9 Workflow of a typical molecular dynamics/grand canonical Monte Carlo simulation for adsorption.

5.6 SIMULATION WORKFLOWS AND ANALYSES

Designing molecular simulations that reliably capture adsorption phenomena requires careful attention to the force fields and structural models and the practical workflows by which simulations are constructed, executed, and analysed (Gelpi *et al.*, 2015). Each step – from building the initial system, through running controlled simulations, to extracting meaningful observables – plays a critical role in ensuring that the results are both physically meaningful and comparable to experiments.

This section outlines the typical workflows (see Figure 5.9) for MD and GCMC simulations in adsorption studies, followed by a discussion of common analysis techniques used to interpret the resulting data.

5.6.1 Molecular dynamics workflows

MD workflows for adsorption studies encompass the full pipeline from constructing atomistic models of adsorbent–adsorbate systems to executing simulations under controlled thermodynamic conditions. This process generates equilibrium structures and captures the detailed time-dependent motions essential for analysing adsorption kinetics and transport phenomena.

5.6.1.1 System preparation and solvation

The first step in an MD simulation is assembling the system. For adsorption studies, this generally means importing a structural model of the adsorbent, such

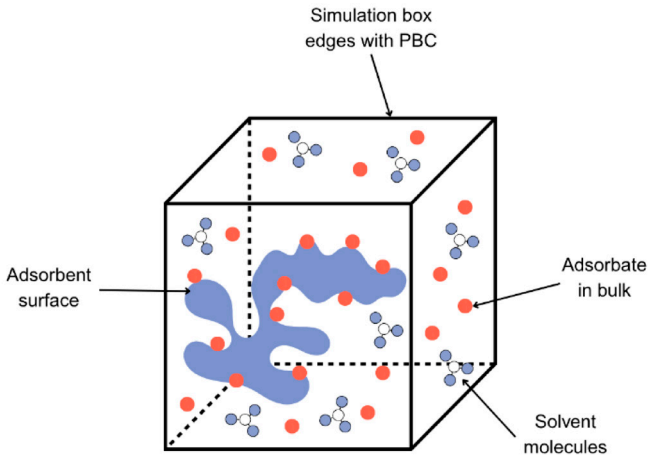


Figure 5.10 The MD simulation box of a porous adsorbent solvated with water and adsorbate molecules is ready for energy minimisation and equilibration.

as a MOF unit cell replicated into a sufficiently large supercell, or an amorphous carbon structure generated to reflect experimental pore-size distributions.

Next, adsorbate molecules (e.g., water, gases, or organic solutes) are introduced. This often involves solvating the adsorbent with thousands of water molecules for aqueous systems. Tools like PACKMOL or built-in solvation commands in simulation packages help distribute solvent and adsorbates uniformly around or inside the porous material, ensuring realistic starting conditions. At this stage, counterions may also be added to neutralise charged frameworks (such as aluminosilicate zeolites), or pH-dependent species are set, based on experimental conditions.

Figure 5.10 illustrates a typical prepared simulation box, showing an adsorbent immersed in a solvent environment, ready for energy minimisation. Such detailed initial setups are critical for realistic adsorption simulations.

5.6.1.2 Equilibration, production runs, data sampling

Once the system is built, it minimises energy, removing any steric clashes or unrealistic overlaps introduced during solvation. A multi-stage equilibration protocol follows this. Initially, simulations may be performed under constant volume (NVT) to stabilise temperature, then under constant pressure (NPT) to allow the system volume to adjust and reach the target pressure, reproducing experimental conditions.

During equilibration, thermostats (like Nosé–Hoover or Langevin) maintain temperature, while barostats (like Parrinello–Rahman) regulate pressure. Depending on system size and complexity, these phases typically last hundreds of picoseconds to a few nanoseconds (Basconi & Shirts, 2013).

Following equilibration, the production run generates the main trajectory data. This phase may span tens to hundreds of nanoseconds, during which

positions, velocities, and energies are saved at regular intervals for analysis. Careful data sampling – collecting snapshots frequently enough to capture relevant dynamics, but not so often as accumulating redundant data – is essential for robust statistical averaging.

5.6.1.3 Analysis: radial distribution function, mean-squared displacement, coordination numbers

The trajectory data from MD simulations is rich in information. To interpret adsorption behaviour, several analyses are commonly performed:

- The radial distribution function (RDF), g(r), quantifies how particle density varies as a function of distance from a reference atom. Peaks in g(r) indicate preferred adsorption distances, revealing the structural organisation of adsorbates near surface sites.
- MSD tracks how far molecules migrate over time, providing diffusion coefficients. This is critical for understanding transport within pores and assessing how easily adsorbates move through adsorbents.
- Coordination numbers measure the average number of neighbouring atoms within a specified cutoff, offering insight into hydration shells around ions, or local clustering of adsorbates in pores.

Additional analyses might include velocity autocorrelation functions (to probe molecular friction), residence time distributions (to assess how long molecules stay adsorbed), and hydrogen bond statistics (to understand solvent structuring).

These analyses together build a comprehensive microscopic picture of adsorption, going far beyond simple uptake values.

5.6.2 Grand canonical Monte Carlo workflows

GCMC workflows take a different approach, focusing on efficiently sampling equilibrium states by directly allowing the number of adsorbed molecules to fluctuate under fixed chemical potential and temperature. These simulations provide a powerful means to predict adsorption isotherms, heats of adsorption, and competitive uptake in multi-component systems.

5.6.2.1 Setting chemical potential and temperature

GCMC simulations begin by specifying the chemical potential (μ), temperature (T), and volume (V) of the system. The chemical potential typically corresponds to an experimental gas pressure (via an equation of state) or a solution concentration.

The adsorbent structure – often a periodic cell of an MOF, zeolite, or carbon model – is loaded into the simulation, and parameters controlling the range and frequency of insertion, deletion, and move attempts are set. Proper selection of these parameters balances sampling efficiency with acceptance rates.

Because adsorption involves fluctuating numbers of particles, careful calibration is needed to relate μ to experimental pressures, ensuring that the simulation conditions directly correspond to lab adsorption measurements.

5.6.2.2 Adsorption isotherms and heat of adsorption

A primary output of GCMC is the adsorption isotherm, which shows how the average number of adsorbed molecules varies with chemical potential or pressure. By systematically varying μ (or equivalently, running multiple GCMC simulations at different imposed pressures), one constructs a curve analogous to experimental volumetric or gravimetric isotherms.

Additionally, fluctuations in particle number and energy allow calculation of the isosteric heat of adsorption, indicating how strongly the adsorbates bind to the adsorbent. This is key for understanding the balance of enthalpic versus entropic contributions to adsorption, and helps identify whether adsorption is primarily driven by strong site-specific interactions or by entropy-favoured filling of larger pore spaces.

5.6.2.3 Multi-component and competitive adsorption

GCMC workflows are also readily extended to multi-component adsorption by assigning separate chemical potentials to different species. This makes it possible to simulate competitive adsorption from gas mixtures, or co-adsorption of solvents and contaminants in water treatment studies.

By analysing the equilibrium occupancies of each species, one can directly predict selectivity, providing a molecular-level explanation for why certain adsorbents preferentially uptake CO_2 over CH_4, or why specific dyes outcompete heavy metals on functionalised carbons.

Figure 5.11 schematically illustrates a typical GCMC workflow for multi-component adsorption, showing trial insertions and deletions of different coloured species into a porous framework, ultimately building up a picture of competitive site occupation. Trial insertions and deletions of different molecular species at fixed chemical potentials allow direct sampling of competitive adsorption, providing insight into mixture selectivity and site preferences.

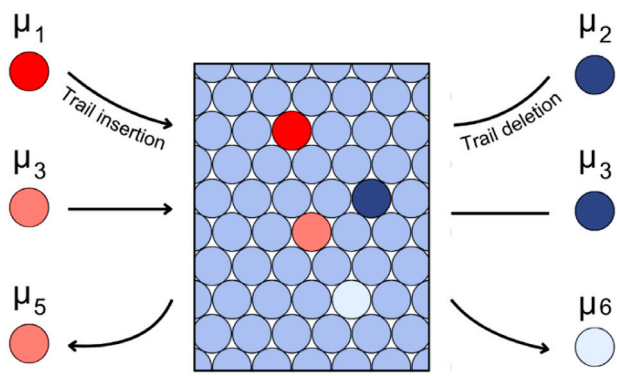


Figure 5.11 Schematic of a grand canonical Monte Carlo simulation for multi-component adsorption.

5.7 ADVANCED SIMULATION TECHNIQUES: HYBRID MOLECULAR DYNAMICS–GRAND CANONICAL MONTE CARLO APPROACHES

As molecular simulations of adsorption evolve beyond simple equilibrium studies, new computational strategies have emerged to tackle increasingly complex systems and capture phenomena that conventional methods struggle to reach. These advanced simulation techniques extend the capabilities of standard MD and GCMC, allowing researchers to explore rare events, simulate coupled processes, and achieve chemical accuracy in systems where traditional force fields may fall short. They form a crucial frontier in adsorption research, bridging the gap between atomistic modelling and the nuanced realities of experimental observations.

Traditional MD simulations operate at fixed particle numbers, while GCMC allows fluctuations by inserting and deleting molecules. However, many adsorption processes involve equilibrium loading under a reservoir pressure (best handled by GCMC) and subsequent dynamics such as diffusion and rearrangement (captured by MD). Hybrid approaches integrate these strengths.

In hybrid MD–GCMC simulations, a typical workflow alternates between GCMC moves (insertion, deletion) that adjust the number of adsorbate molecules to maintain equilibrium at a specified chemical potential, and MD segments that allow the system to evolve under Newtonian dynamics, equilibrating local

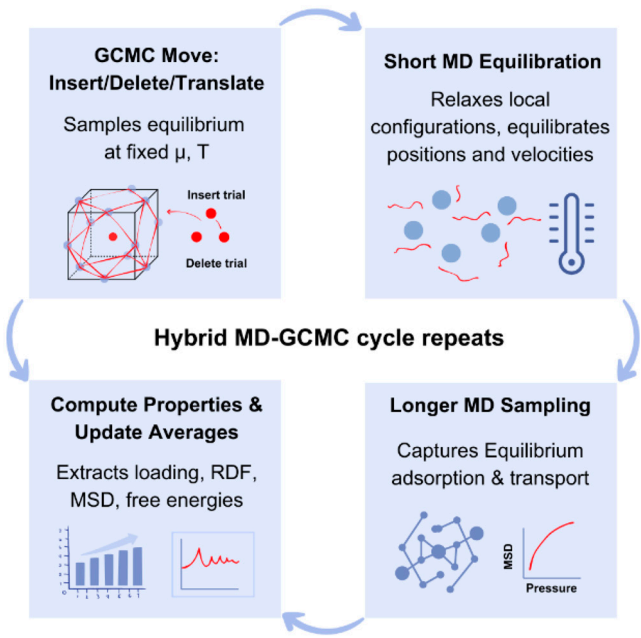


Figure 5.12 Schematic of a hybrid molecular dynamics-grand canonical Monte Carlo simulation cycle.

structures and exploring dynamic rearrangements. This coupling accurately captures both equilibrium loadings and realistic molecular motions within the adsorbent.

Such hybrid techniques are potent in flexible frameworks like certain metal-organic frameworks (MOFs) or polymers, where adsorption may induce structural responses that affect further adsorption. They are also critical for systems exhibiting coupled mass transfer and equilibrium, such as the hydration of clays or organic dye adsorption in soft polymeric matrices.

Figure 5.12 illustrates a schematic hybrid MD–GCMC cycle, where GCMC steps adjust adsorbate concentration, followed by MD evolution to equilibrate positions and framework conformations. GCMC moves insert or delete molecules to maintain equilibrium at a fixed chemical potential, followed by MD evolution that equilibrates local structures and captures dynamic rearrangements within the adsorbent framework.

5.8 SOFTWARE PACKAGES FOR MOLECULAR DYNAMICS AND GRAND CANONICAL MONTE CARLO SIMULATIONS

MD and GCMC simulations are essential computational tools for studying adsorption phenomena at the atomic scale. MD simulations provide detailed insight into molecules' time-dependent behaviour, transport properties, and structural evolution in adsorbent–adsorbate systems. In contrast, GCMC simulations are compelling for modelling equilibrium adsorption, enabling the prediction of adsorption isotherms and capacities under varying chemical potentials or gas pressures. A range of software packages as shown in Figure 5.13 has been developed to perform these simulations, each offering specific advantages in terms of computational efficiency, scalability, and applicability to different materials and adsorbates.

Materials Studio, a commercial software suite by BIOVIA, supports MD and GCMC simulations through integrated modules such as Forcite and Sorption. It provides a graphical interface, making it accessible to users across disciplines. The platform is particularly effective for simulating adsorption in crystalline materials, including zeolites, MOFs, and polymers.

CP2K is a powerful open-source package capable of performing atomistic simulations of condensed-phase systems using a hybrid Gaussian and plane-wave approach. While it is primarily used for ab initio MD simulations, CP2K can also be applied to study adsorption at liquid–solid interfaces, which is relevant for aqueous-phase contaminant removal.

LAMMPS (Large-scale Atomic/Molecular Massively Parallel Simulator) is a highly flexible and scalable MD engine for modelling molecular, biomolecular, and materials systems. It supports a variety of force fields and can be extended to perform hybrid MD–GCMC simulations using additional plugins or coupling frameworks. LAMMPS is especially useful for large-scale simulations involving porous adsorbents or polymeric materials.

QBOX is another open-source package designed to perform first-principles MD simulations based on density functional theory. It is optimised for

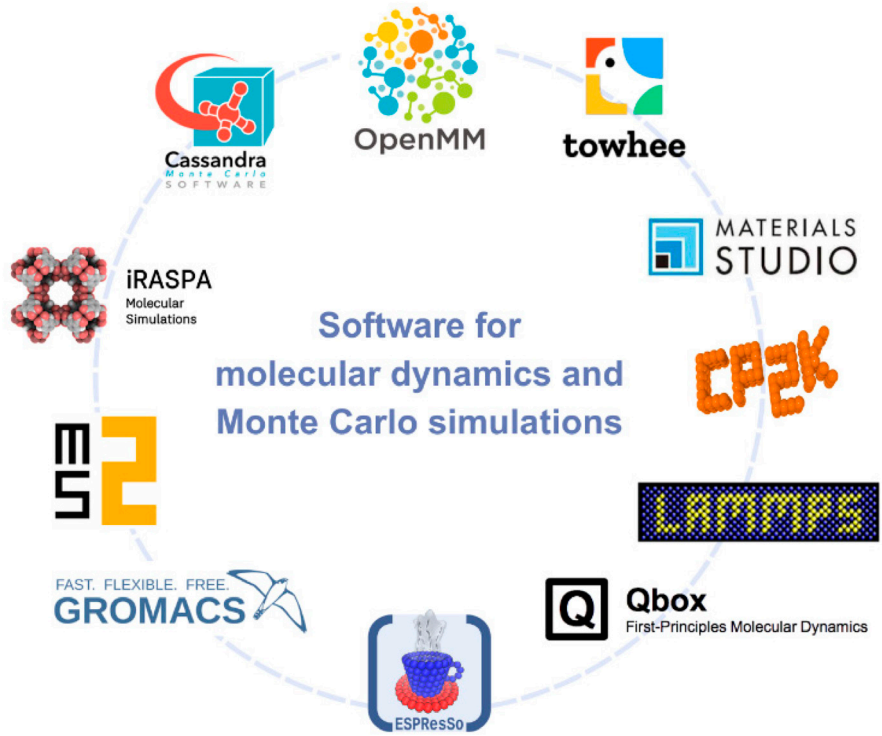


Figure 5.13 Software packages for molecular dynamics and grand canonical Monte Carlo simulations.

high-performance computing environments and can simulate the dynamic interactions of molecules with surfaces or within confined pores.

Quantum ESPRESSO, though primarily a DFT package, also includes limited functionality for performing ab initio MD simulations. It is best suited for studying adsorption mechanisms on crystalline surfaces where quantum-level accuracy is required.

GROMACS is a widely used MD software package known for its speed and efficiency in simulating biochemical and soft matter systems. Though originally developed for biomolecular simulations, it has been effectively applied to study the adsorption and diffusion of small molecules in porous media. GROMACS can also be adapted for GCMC simulations using custom scripts or coupling with external MC modules.

MS2 (Molecular simulation 2) is a specialised package for fluid phase equilibria and adsorption studies. It supports both MD and GCMC simulations and is particularly useful for calculating adsorption isotherms, diffusivities, and thermodynamic properties of fluids in nanoporous materials.

IRMOF Adsorption Structure and Properties Analyser (IRASPA) provides a user-friendly graphical interface for visualising and analysing adsorption simulations. It is compatible with output from various MD and GCMC packages, serving as a post-processing and visualisation tool, especially for porous crystalline frameworks.

OpenMM is a high-performance MD engine primarily aimed at simulating biomolecular systems. However, its flexibility and GPU-acceleration capabilities make it suitable for simulating adsorption of organic and pharmaceutical molecules on nanomaterials or polymeric substrates. Its Python-based scripting environment enables integration with MC methods, making it adaptable for adsorption-related studies.

Cassandra and Towhee are dedicated MC simulation packages widely used for GCMC calculations. Cassandra supports various ensemble types and interaction models and is tailored for modelling adsorption in nanoporous materials. Towhee has been extensively applied to simulate multi-component adsorption equilibria and is valued for its robust implementation of GCMC techniques.

5.9 CASE STUDIES

5.9.1 Case study I

This case study investigates the adsorption behaviour of two-dimensional graphene (GRA), boron nitride (BN), and boron carbon nitride (BCN) nanosheets for the simultaneous removal of arsenic(III) ions and methylene blue dye using MD simulations (Yadav *et al.*, 2022).

The simulation model comprised an aqueous solution placed atop rigid GRA, BN, and BCN sheets, constructed via the Nanostructure Builder plugin in VMD. The final simulation box dimensions were approximately 5.2 nm $\times$ 4.1 nm in the x and y directions, with a height of 150 nm along the z axis. The molecular structure of methylene blue (excluding the chloride ion) was obtained from PubChem.

5.9.1.1 Adsorption system

The simulation model consisted of an aqueous solution placed above rigid GRA, BN, or BCN nanosheets, as shown by the equilibrium snapshots in Figures 5.14–5.16. The box dimensions were approximately 5.2 nm $\times$ 4.1 nm in the lateral directions, with a height of 150 nm to accommodate solute movement. At equilibrium, MB molecules consistently aligned parallel to the surfaces on all three nanosheets, while As(III) ions remained at a slightly greater distance from the surfaces. The equilibrium distance of MB was found to be approximately 3.40 Å from all surfaces, indicating strong physisorption via π–π stacking or dispersion interactions. In contrast, As(III) ions were closest to GRA (3.73 Å), moderately distant from BCN (5.90 Å), and furthest from BN (6.76 Å). These observations (captured in Figures 5.14–5.16) highlight that due to its delocalised electron cloud and negative charge distribution, the GRA surface preferentially attracted both MB and As(III) more effectively than BN and BCN.

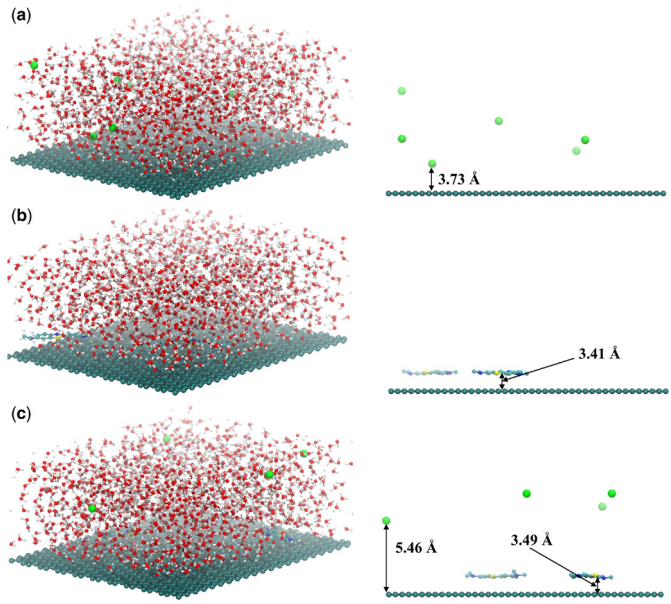


Figure 5.14 Equilibrium configurations of (a) As(III), (b) methylene blue, and (c) As(III) + methylene blue in aqueous solution above the graphene nanosheet (Yadav *et al.*, 2022).

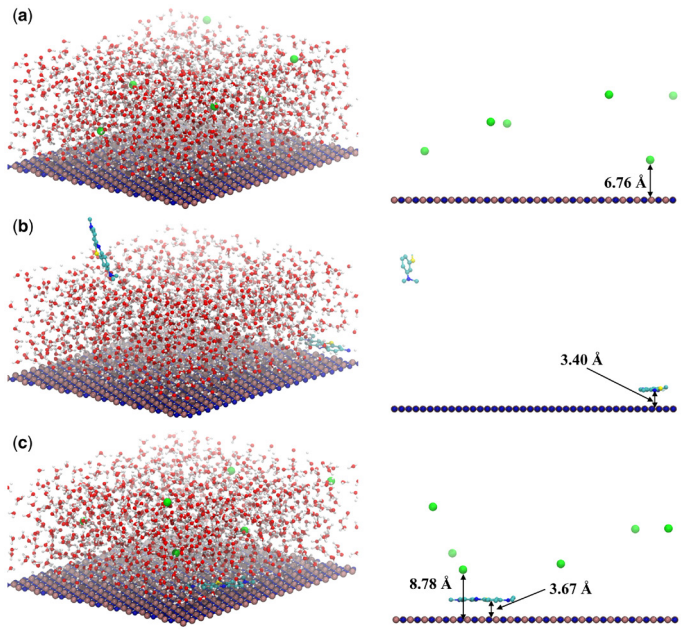


Figure 5.15 Equilibrium configurations of (a) As(III), (b) methylene blue, and (c) As(III) + methylene blue in aqueous solution above the boron nitride nanosheet (Yadav *et al.*, 2022).

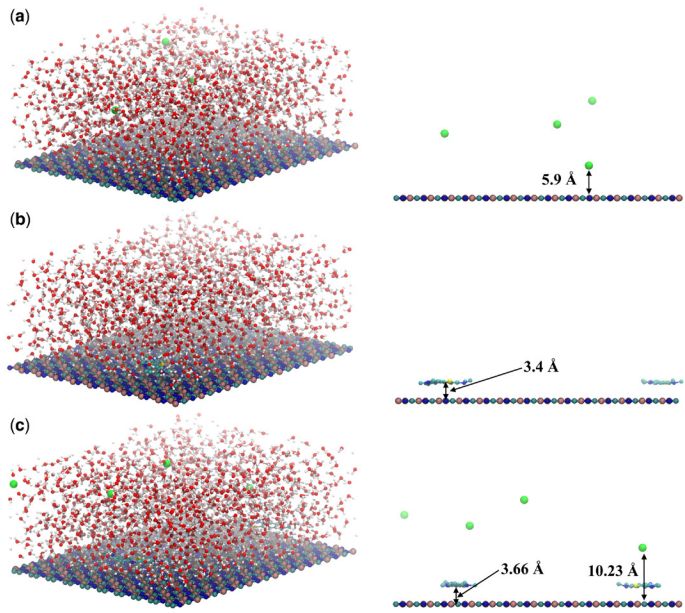


Figure 5.16 Equilibrium configurations of (a) As(III), (b) methylene blue, and (c) As(III) + methylene blue in aqueous solution above the boron carbon nitride nanosheet (Yadav *et al.*, 2022).

5.9.1.2 Radial distribution function

The RDF provided more profound insights into molecular structuring near the adsorbent surfaces. Figure 5.17 presents the RDF of oxygen–oxygen (O_W-O_W) pairs in water, showing well-defined first peaks across systems, with subtle differences. In BN systems containing MB, the first peak shifted slightly inward (to ~2.5 Å) and was less intense, suggesting slightly altered water structuring due to MB presence. The OW-OW first peak height was nearly halved for BCN systems with As(III), indicating a lower density of structured water around As(III) compared to systems with MB.

Further, the O_W-As RDFs (Figure 5.18) revealed a prominent peak near 3 Å, consistent across surfaces and suggesting that hydration shells around As(III) were similarly structured whether adsorbed singly or together with MB, except for BCN, where the peak was notably diminished, indicating less dense solvation. The RDFs for As–As pairs (Figure 5.19) exhibited peaks in the 8–10 Å range for all systems, showing that As(III) ions remained dispersed, with little tendency to cluster regardless of co-adsorption with MB.

The RDFs of MB–O_W pairs (Figure 5.20) revealed maxima at ~3.5 Å, uniform across surfaces and essentially unchanged between single MB adsorption and binary systems, indicating stable solvation structures around MB even in the presence of As(III). Taken together, these RDF trends suggest that while MB consistently adsorbs close to the surfaces and maintains hydration shells, As(III) adsorption and solvation are more sensitive to the surface type, with GRA facilitating tighter adsorption.

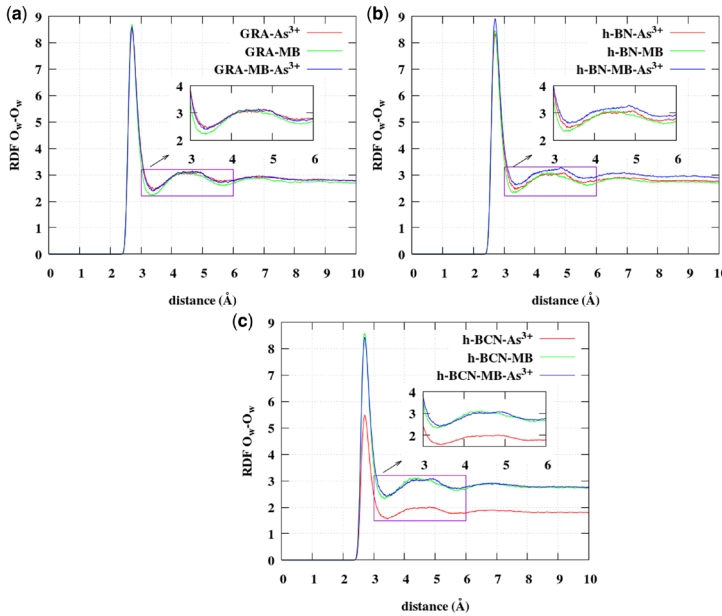


Figure 5.17 The radial distribution function for O_W-O_W atoms of water molecules on (a) GRA, (b) BN, and (c) BCN nanosheets (Yadav *et al.*, 2022).

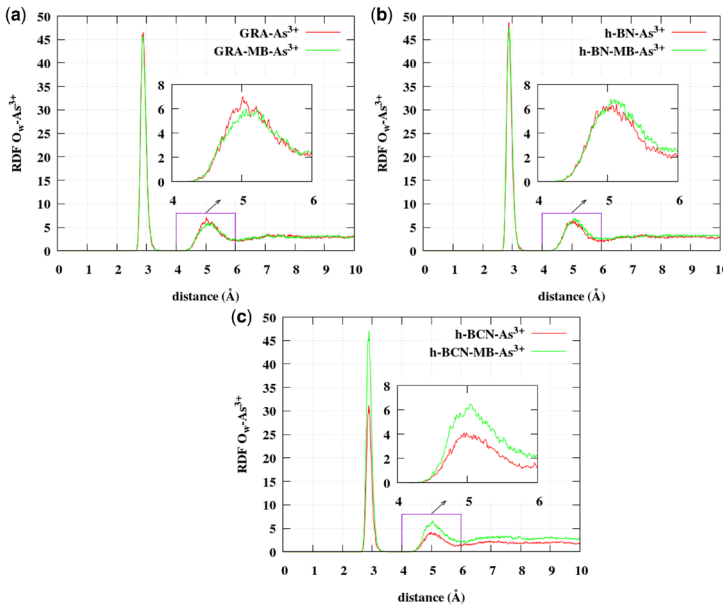


Figure 5.18 The radial distribution function for O_W-As on (a) graphene, (b) hexagonal boron nitride, and (c) hexagonal boron carbon nitride nanosheets (Yadav *et al.*, 2022).

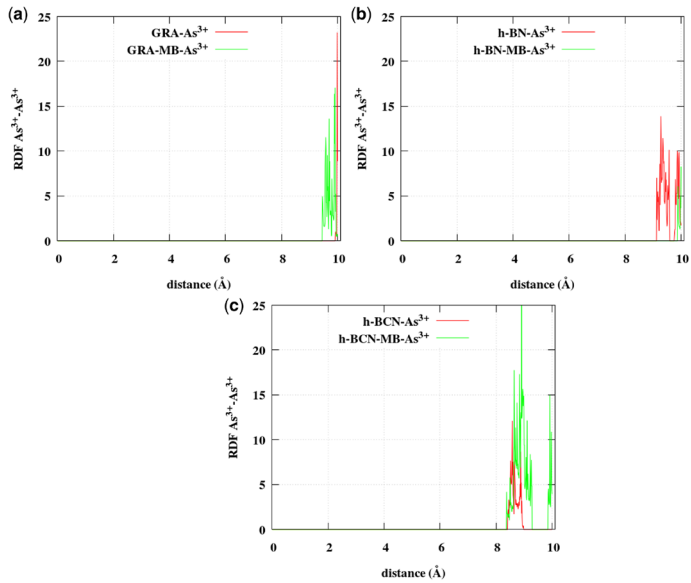


Figure 5.19 The radial distribution function for the As-As pair on (a) graphene, (b) hexagonal boron nitride, and (c) hexagonal boron carbon nitride nanosheets (Yadav *et al.*, 2022).

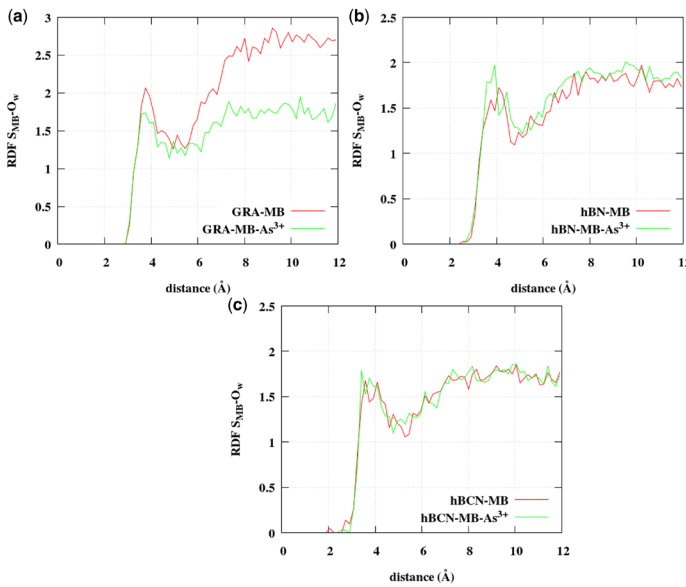


Figure 5.20 The radial distribution function for the S_{MB}-O_w pair on (a) graphene, (b) hexagonal boron nitride, and (c) hexagonal boron carbon nitride nanosheets (Yadav *et al.*, 2022).

The coordination number derived from RDF integrations showed that approximately 12 water molecules surrounded each As(III) ion within 3–4.5 Å on all surfaces, consistent with efficient packing typical of non-hydrogen-bonded liquids. This arrangement limits the closer approach of another As(III), reflected in the As-As RDF peaks at ∼9 Å.

5.9.1.3 Mean-squared displacement

The mobility of species was assessed by MSD analysis (Figures 5.21 and 5.22). The MSD plots revealed that MB exhibited the highest diffusion across all systems, attributed to hydrogen bonding with water that promotes its migration. Interestingly, the diffusion coefficients (derived from the slopes of MSD vs time) showed that on GRA, As(III) diffused more rapidly in the binary system than in the single As(III) system, while for BN and BCN, the order was reversed (As(III) $<$ MB + As(III)). The mobility of water itself was notably reduced after MB adsorption on all surfaces, indicating that MB's interactions with water slightly restricted overall fluid movement.

5.9.1.4 Potential mean force

To probe the thermodynamic favourability, the PMF profiles were computed as a function of the distance between adsorbates and surfaces (Figure 5.23). These plots displayed typical Lennard–Jones-like profiles with clear minima at ∼4 Å, consistent with RDF observations. Notably, the depth of the PMF

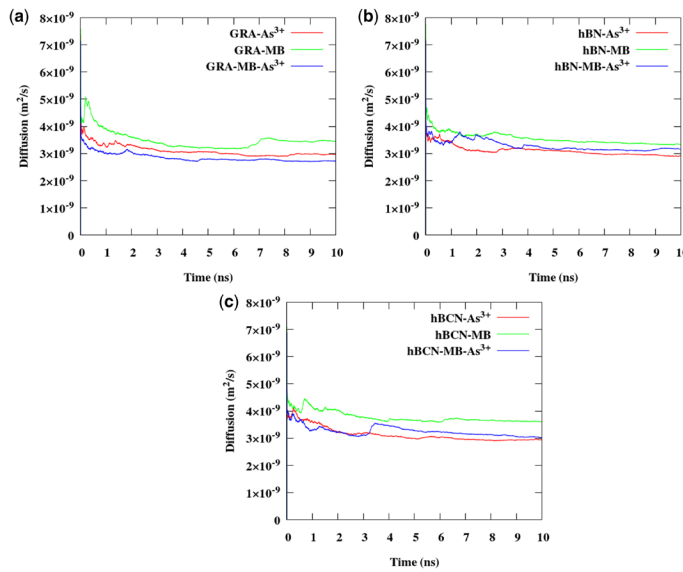


Figure 5.21 The diffusion coefficients of the water molecules as a function of time on (a) graphene, (b) hexagonal boron nitride, and (c) hexagonal boron carbon nitride nanosheets (Yadav *et al.*, 2022).

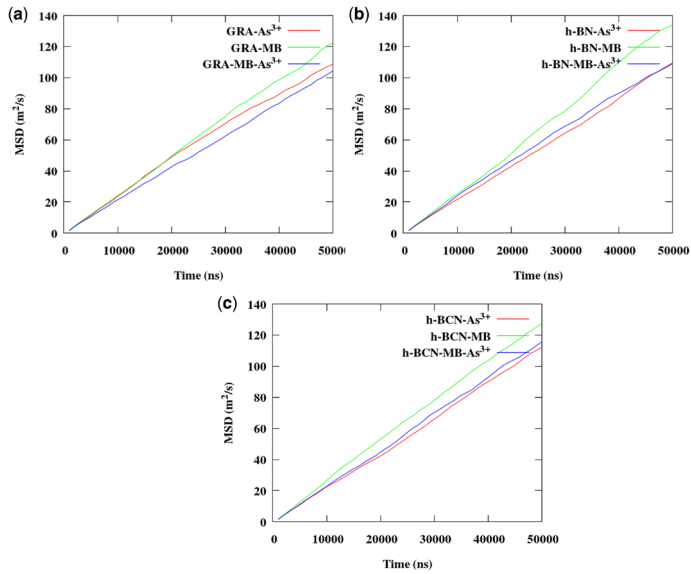


Figure 5.22 MSD plots for the sheet/water/methylene blue, sheet/water/As(III), and the sheet/water/ methylene blue +As(III) systems on (a) graphene, (b) hexagonal boron nitride, and (c) hexagonal boron carbon nitride nanosheets (Yadav *et al.*, 2022).

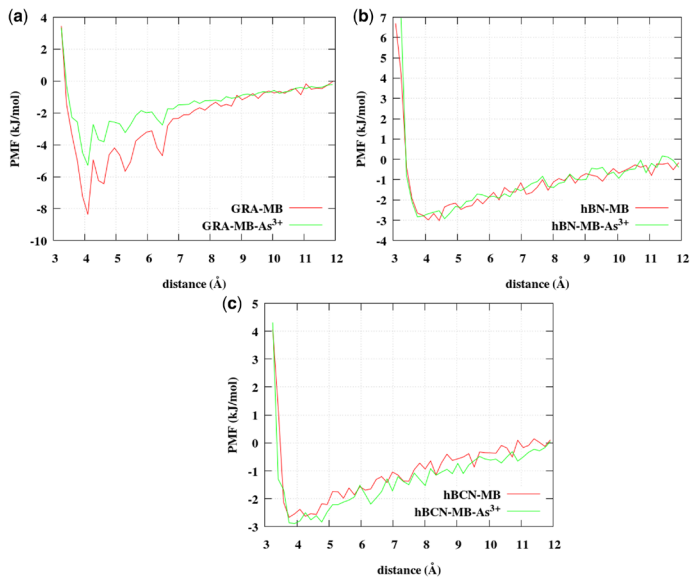


Figure 5.23 PMF plots for (a) graphene, (b) hexagonal boron nitride, and (c) hexagonal boron carbon nitride nanosheets (Yadav *et al.*, 2022).

minimum for MB on GRA was ~8.3 kJ/mol, roughly twice that seen for BN and BCN systems (~3 kJ/mol), indicating a stronger stabilisation of MB on GRA. Simultaneous adsorption of MB and As(III) on GRA also showed a relatively deep PMF minimum, though slightly shallower than MB alone, implying that co-adsorption remains highly favourable on GRA. The BN and BCN systems showed similar PMF depths for single and binary adsorption, reinforcing that these surfaces were less selective.

5.9.2 Case study II

This case study investigated the adsorption affinity of methylene blue dye and norfloxacin antibiotic on polyvinylidene fluoride (PVDF) and PVDF-silica composite using MD.

The basic model consists of an aqueous solution placed over GRA, BN, and BCN nanosheets generated using the Nanostructure Builder plugin in VMD. The final dimensions of the simulation box were ~5.2 nm and ~4.1 nm along the x and y directions, respectively, while the box size along the z-direction was set to 150 nm. The molecular structure for methylene blue without the chloride ion was obtained from PubChem.

The initial simulation system, a mixture of water molecules and As(III) ions/methylene blue, was placed over the nanosheet. Periodic boundary conditions were used in the three spatial directions. The initial system configuration was subjected to energy minimisation and thermal equilibrium for 0.1 ns at 298 K. The system pressure was set to 1 atm by maintaining an equivalent force on the top piston wall for 2 ns. After the pressure equilibration, the piston wall was removed, and the resulting system configuration was run for 10 ns. A time step of 1 fs is used to integrate the equations of motion. The PPPM method is used to compute long-range interactions. A large-scale atomic/molecular massively parallel simulator package was used for simulations.

5.9.2.1 Adsorption system

The simulation models consisted of a pristine PVDF surface or a PVDF–silica composite, constructed using standard polymer building tools and equilibrated to mimic experimental densities. An aqueous phase containing either methylene blue or norfloxacin was placed above these surfaces, with the final simulation box dimensions chosen to provide adequate bulk water above the adsorbent, avoiding finite-size artefacts.

Energy minimisation and thermal equilibration were carried out similarly to the earlier case study, followed by production runs under NPT conditions at 298 K and 1 atm for 10 ns, allowing the contaminants to diffuse, interact, and equilibrate with the surfaces. Periodic boundary conditions and the PPPM method were applied to handle long-range electrostatics.

Snapshots of the equilibrium configurations are shown in Figure 5.24, highlighting how methylene blue and norfloxacin approach and align differently on the PVDF and PVDF–silica surfaces. The presence of silica appears to slightly enhance adsorption, potentially due to additional polar sites introduced by silica that can interact via hydrogen bonding or electrostatic attractions.

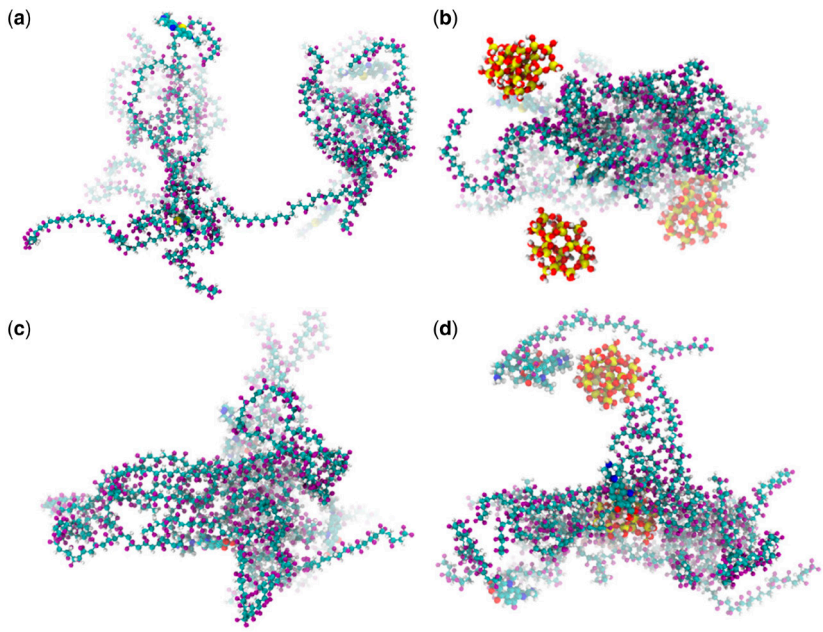


Figure 5.24 Snapshot of the adsorption system containing (a) methylene blue + polyvinylidene fluoride, (b) methylene blue + polyvinylidene fluoride-silica composite, (c) norfloxacin + polyvinylidene fluoride, and (d) norfloxacin + polyvinylidene fluoride-silica composite.

5.9.2.2 Radial distribution function

The structural organisation of water molecules around the contaminants and near the adsorbent surfaces was analysed through RDFs. As shown in Figure 5.25, the O_W–O_W RDFs (oxygen–oxygen pairs of water molecules) exhibited characteristic first peaks around 2.8 Å, consistent with the hydrogen-bonding network in liquid water.

Further RDF analyses in Figure 5.26 explored interactions of specific contaminant atoms with water oxygen atoms. The RDFs for N_{MB}–O_w (nitrogen in methylene blue to water oxygen) and N_{NFX}–O_w showed prominent peaks near 3.4 Å, indicating structured hydration shells. These structured layers were slightly more pronounced in systems with the PVDF–silica composite, suggesting that the silica may indirectly influence water structuring around adsorbed molecules.

Integration of the RDFs up to the first minimum provided coordination numbers, revealing how many water molecules typically surround key functional sites on the contaminants. For methylene blue and norfloxacin, coordination numbers ranged between 6 and 8 within 4 Å, reflecting stable hydration even upon adsorption. This suggests that adsorption did not fully dehydrate these molecules, which is consistent with physisorption dominated by van der Waals and moderate hydrogen-bond interactions.

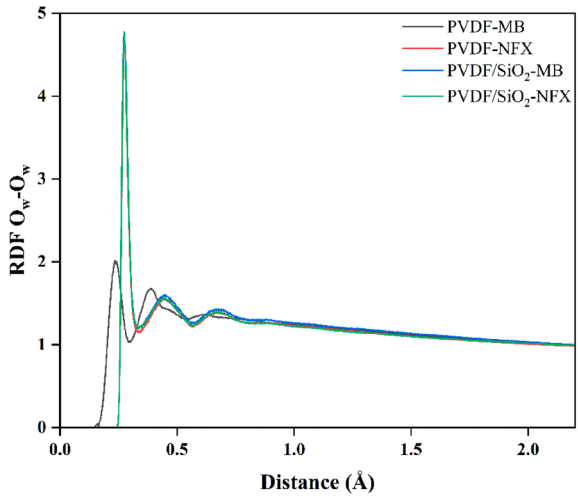


Figure 5.25 The radial distribution function for O_W-O_W atoms of water molecules in different adsorption systems.

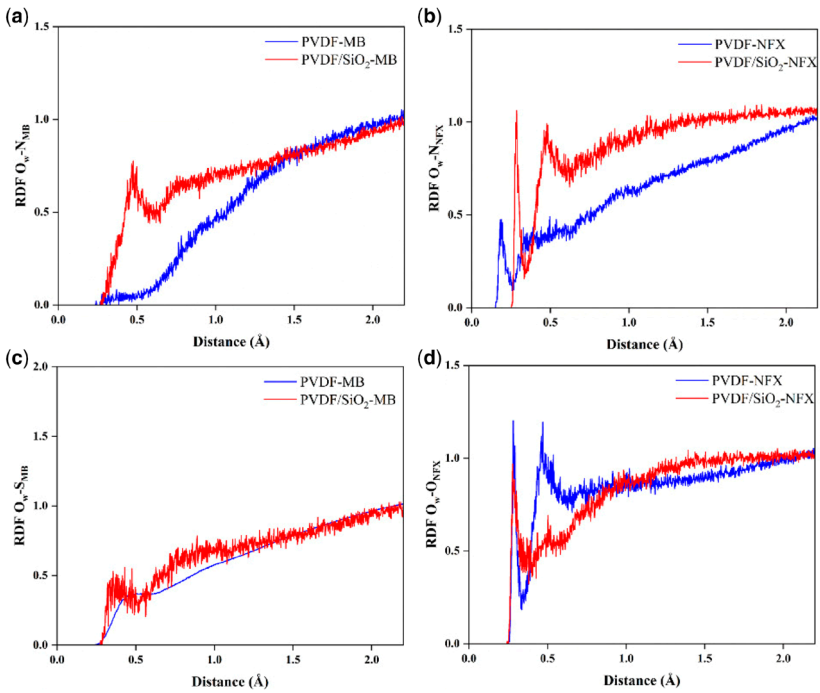


Figure 5.26 The radial distribution function for (a) N_{MB}-O_w, (b) N_{NFX}-O_w, (c) S_{MB}-O_w, and (d) O_{NFX}-O_w pairs in different adsorption systems.

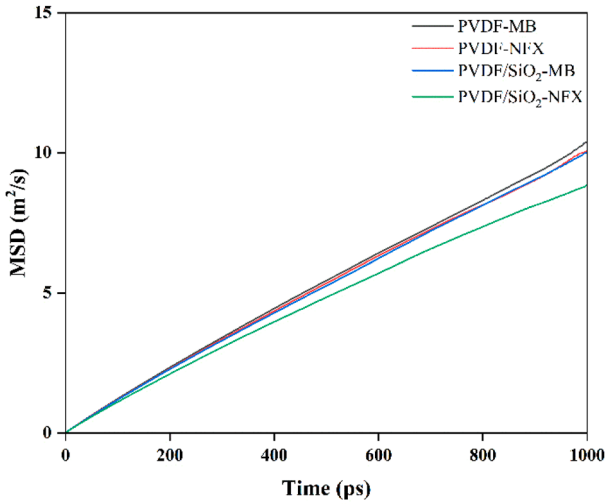


Figure 5.27 Water molecules' MSD plots in different adsorption systems.

5.9.2.3 Mean-squared displacement

The dynamic behaviour of water and the contaminants was evaluated through MSD analyses. As illustrated in Figure 5.27, the MSD plots showed that water mobility was slightly reduced in adsorbed contaminants, with diffusion coefficients ranging from $\sim 1.46 \times 10^{-5}$ to $\sim 1.65 \times 10^{-5}$ $cm^2\ s^{-1}$. Among these, systems with the PVDF–silica composite exhibited marginally lower water diffusivities, possibly due to stronger water structuring near the silica sites.

Comparisons of contaminant mobility revealed that methylene blue, more planar and prone to π–surface interactions, exhibited lower mobility upon adsorption than norfloxacin. This observation aligns with practical expectations, where planar dyes often adsorb more tightly onto hydrophobic or semi-polar surfaces.

5.10 SUMMARY

MD simulations provide a fundamental framework for studying the behaviour of atoms and molecules under well-defined thermodynamic conditions. By integrating Newton's equations of motion, MD captures the time evolution of particle positions and velocities, allowing direct observation of processes such as diffusion, adsorption kinetics, and dynamic restructuring within porous materials. This time-resolved perspective makes MD especially powerful for understanding how adsorbates migrate through channels, stabilise at specific binding sites, and respond to thermal fluctuations or framework flexibility.

In contrast, GCMC simulations adopt a statistical sampling approach, focusing on equilibrium properties under fixed chemical potential, temperature, and volume conditions. By permitting the number of adsorbed molecules to

Table 5.1 Comparison of molecular simulation methods.

Feature	MD	GCMC	Hybrid MD–GCMC
Ensemble	NVE, NVT, NPT	μVT (grand canonical)	Coupled
Key control parameters	T, P, N	μ, T, V	μ, T, P, N
Tracks real-time dynamics	Yes	No (sample equilibrium only)	Yes + sampling
Computes adsorption isotherms	Indirect/requires multiple runs	Directly	Efficient
Suitable for diffusion studies	Excellent	Not applicable	Yes
Typical output	MSD, RDF, velocity correlations	Isotherms, site occupancies, and heats	Both
Best for	Kinetics, transport, structural rearrangements	Equilibrium adsorption, selectivity	Complex systems

fluctuate through trial insertion and deletion moves, GCMC efficiently explores the configurational space that determines adsorption isotherms, heats of adsorption, and site occupancies. This ensemble-based methodology bypasses the timescale limitations inherent in MD, directly yielding equilibrium loadings and revealing cooperative or competitive adsorption behaviours in single- and multi-component systems. Table 5.1 compares both molecular simulation methods.

Taken together, these computational strategies offer complementary insights into adsorption phenomena. This chapter explored the fundamentals of molecular simulations, beginning with the statistical mechanical foundations and everyday ensembles, followed by detailed discussions on MD and MC methods, including their algorithms, workflows, and typical analyses. It then examined how interatomic potentials and force fields are constructed to capture bonded and non-bonded interactions, and how realistic models of adsorbents and fluid phases are developed. Finally, it highlighted advanced techniques such as hybrid MD–GCMC approaches, enhanced sampling methods like metadynamics and umbrella sampling, and the emerging role of machine learning and reactive force fields. Together, these tools form a comprehensive computational framework for understanding and predicting adsorption behaviour at the molecular scale.

doi: 10.2166/9781789063943 _0133

Chapter 6

Quantitative structure–property relationship analysis of adsorption processes

6.1 INTRODUCTION

The exponential growth of industrial and domestic activities has resulted in the discharge of a vast array of pollutants into aquatic systems, posing serious environmental and public health concerns. With more than 85,000 chemicals registered by the U.S. Environmental Protection Agency and approximately 700–1000 new chemicals introduced annually, the complexity of water contamination has dramatically increased (Naidu *et al*., 2021). Managing this diversity of contaminants requires robust treatment techniques and efficient predictive tools to guide the selection and optimisation of these techniques.

Among various treatment methods, adsorption has proven to be one of the most effective and widely adopted processes for removing organic and inorganic contaminants from water and wastewater. However, experimentally investigating the adsorption performance for such an extensive range of pollutants is time-consuming and resource-intensive. This challenge underscores the necessity for computational approaches to predict adsorption behaviour based on the intrinsic properties of contaminants and adsorbents.

Quantitative structure–property relationship (QSPR) modelling has become a powerful tool in this context. By establishing mathematical relationships between the structural features of chemical compounds and their physicochemical or biological properties, QSPR enables the prediction of adsorption performance without exhaustive laboratory experiments. It leverages molecular descriptors, numerical values derived from chemical structures, to correlate with adsorption parameters such as capacity, affinity, and kinetics. This approach accelerates material screening and provides mechanistic insights into adsorption processes, facilitating the rational design of more effective adsorbents.

© 2026 IWAP. This is an Open Access book chapter distributed under the terms of the Creative Commons Attribution Licence (CC BY-NC-ND 4.0) which permits copying and redistribution for non-commercial purposes with no derivatives, provided the work is properly cited (https://creativecommons.org/licenses/by-nc-nd/4.0/). The chapter is from the book *Computational Techniques for Modelling and Simulating Adsorption Processes for (Waste)Water Treatment*, A. Yadav and P. Labhasetwar (Authors).

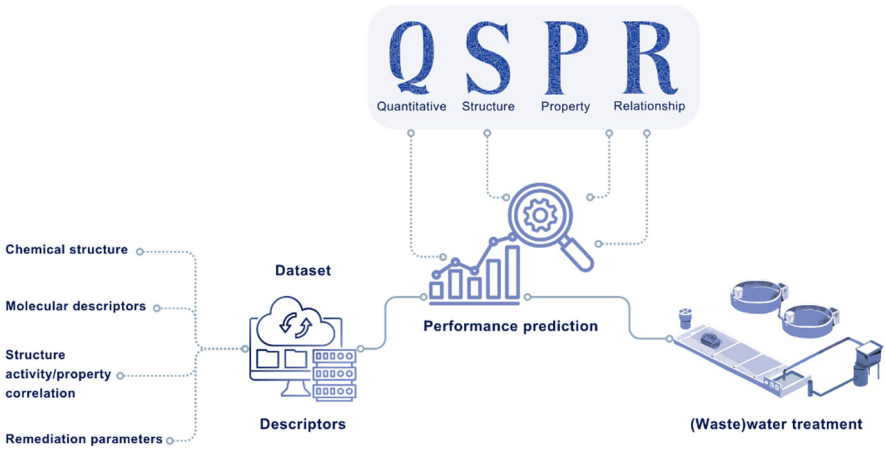


Figure 6.1 Application of quantitative structure–property relationship models to adsorption processes in (waste)water treatment.

Figure 6.1 illustrates the conceptual framework of applying QSPR models to adsorption processes in (waste)water treatment (Awfa *et al.*, 2021). By systematically relating molecular structure information to adsorption behaviour, QSPR can significantly enhance the ability to predict treatment efficacy, optimise process conditions, and ultimately contribute to more sustainable water management strategies.

This chapter examines QSPR analysis in the context of adsorption processes. It first reviews the historical background and core principles of QSPR, then describes molecular descriptors used to represent structural, electronic, and geometric features. The chapter outlines the recommended workflow for building robust QSPR models, covering data handling, descriptor selection, validation, and applicability domains. It further discusses specialised approaches for adsorption modelling, advanced strategies such as hybrid and multitask frameworks, and methods incorporating defects and material stability.

6.2 HISTORY AND EARLY DEVELOPMENTS

The origins of QSPR can be traced back to the 1960s, when Corwin Hansch and co-workers laid the foundation for what would become a cornerstone of computational chemistry and predictive modelling. Initially formulated under the broader concept of quantitative structure–activity relationships (QSAR), these models were designed to establish statistical correlations between the chemical structures of compounds and their biological activities, primarily to aid pharmaceutical research and drug discovery.

Early QSPR and QSAR studies were relatively simple, relying on linear regression techniques to correlate a small number of molecular descriptors such as hydrophobicity parameters (log P), electronic properties (Hammett

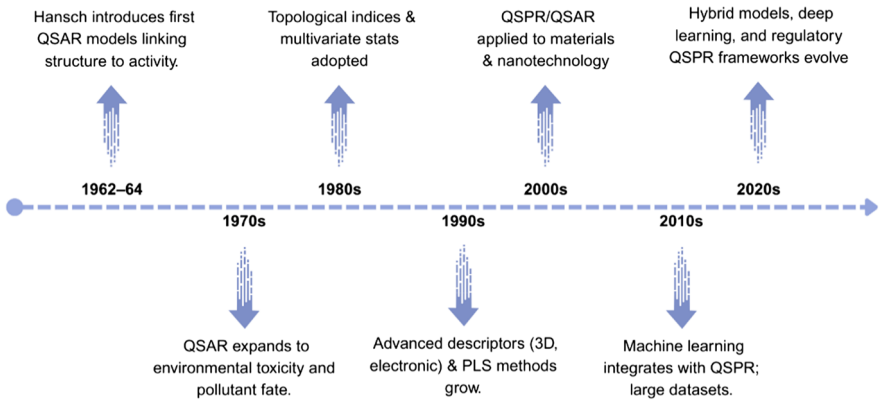


Figure 6.2 A brief history of quantitative structure–property relationship development.

constants), and steric factors with biological or physicochemical endpoints. These pioneering efforts demonstrated the immense potential of mathematical models to reduce experimental workload and systematically explore structure–property landscapes.

Through the 1970s and 1980s, the methodology evolved steadily, expanding from drug design into environmental sciences and toxicology, where researchers began applying QSPR principles to predict the behaviour and fate of environmental contaminants. The increasing computational power in the following decades further propelled QSPR/QSAR methodologies. By the 1990s and early 2000s, advances in chemoinformatics and the developing of sophisticated molecular descriptors enabled more complex multivariate models, accommodating larger chemical datasets with diverse structures.

Currently, QSPR modelling encompasses many techniques, ranging from traditional multiple linear regression (MLR) to machine learning approaches capable of handling high-dimensional descriptor spaces and non-linear relationships. This evolution has broadened the application scope to materials science and catalysis and enhanced the models' predictive power and mechanistic understanding.

Figure 6.2 provides a concise timeline summarising the key milestones in developing QSPR and QSAR methodologies. This historical progression underscores how a concept that began with simple linear correlations has matured into a sophisticated set of tools that continue to drive innovation across multiple scientific disciplines.

6.3 QUANTITATIVE STRUCTURE–PROPERTY RELATIONSHIP ANALYSIS

QSPR analysis is a computational technique that establishes mathematical correlations between molecular structures and their associated physicochemical properties (Roy *et al.*, 2015). These properties may include solubility, boiling point, adsorption capacity, reactivity, toxicity, or transport behaviour in various

environments. QSPR models are built on the assumption that the behaviour of a molecule can be explained by its structural attributes, which are quantified through mathematical descriptors.

The goal of QSPR is not only to predict properties of known molecules but also to infer the behaviour of untested or hypothetical compounds, enabling virtual screening and rational design in fields such as water treatment, drug development, catalysis, and nanomaterial synthesis. In environmental systems, QSPR is critical in estimating parameters for complex processes such as adsorption, especially when experimental data are sparse or difficult to obtain.

Figure 6.3 outlines the general workflow of a typical QSPR model development process. The approach involves collecting relevant molecular and property data, calculating molecular descriptors, building statistical or machine learning models, validating those models for accuracy and reliability, and applying them for property prediction of new compounds.

6.3.1 Basic concepts

At the heart of QSPR is the premise that every chemical compound can be uniquely characterised by its molecular structure, and this structure encodes sufficient information to predict a wide range of physical, chemical, and environmental properties (Dickenson *et al.*, 2010). By transforming chemical structure information into numerical descriptors, QSPR enables the construction of models that can relate structure to property quantitatively. A QSPR model generally follows this form:

$$Y_i = f(X_1, X_2, ..., X_n) + \varepsilon \tag{6.1}$$

where Y is the property or response of interest, X_1, X_2, $\ldots X_n$ are the selected molecular descriptors, f represents the mathematical function linking descriptors

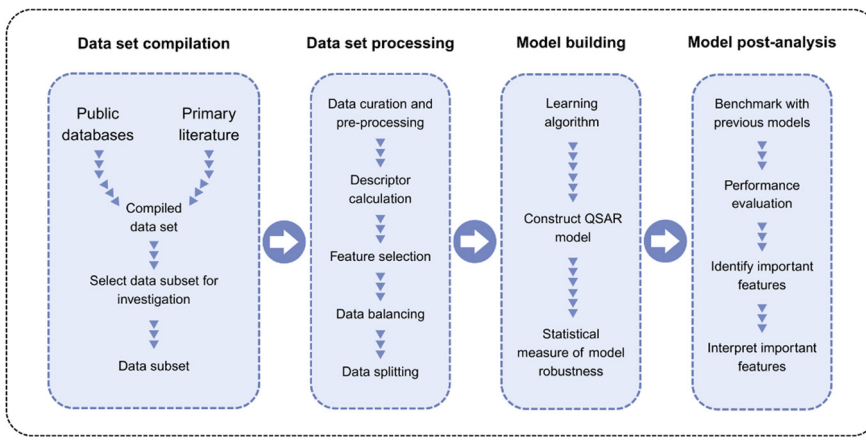


Figure 6.3 Typical workflow of quantitative structure–property relationship model development.

to the property (which may be as simple as multiple linear regression or as complex as a neural network), and ε is the error term accounting for variability not captured by the model.

The strength and utility of a QSPR model depend on the appropriateness of the selected descriptors, the mathematical method used for modelling, and the robustness of its validation. The descriptors bridge molecular structure and macroscopic properties, and their selection is crucial for interpretability and predictive power.

QSPR differs from QSAR primarily in its endpoint: while QSAR models target biological activities (e.g., enzyme inhibition, toxicity), QSPR models predict physicochemical or material properties, such as adsorption equilibrium constants or degradation rates. However, the modelling process and conceptual foundations are often interchangeable. The endpoint is the dependent variable obtained from an experiment, which is modelled using the following general equation:

$$\text{Endpoint (property)} = f(\text{chemical structure}) \tag{6.2}$$

6.3.2 Principles underpinning quantitative structure–property relationship

Two central assumptions form the theoretical foundation of QSPR:

(1) **Similarity Principle:** Compounds with similar molecular structures exhibit similar physicochemical behaviour under comparable environmental conditions. This enables the extrapolation of properties from known compounds to structurally similar but untested ones.
(2) **Structure–Property Dependence:** A compound's properties are determined by its structural, electronic, steric, and topological features. Therefore, systematic variations in molecular structure will induce corresponding variations in measurable properties.

These principles allow QSPR models to function as predictive tools across diverse chemical domains. The statistical correlation does not imply causation, but well-constructed models can offer mechanistic hypotheses, highlight structure–property trends, and guide experimental work.

Furthermore, the validity of a QSPR model heavily depends on its applicability domain, the chemical space for which the model was trained, and its reliability. Predictions outside this domain can be misleading; hence, defining and monitoring this space is crucial for model development (discussed further in Section 6.4.4).

6.3.3 Molecular descriptors

Molecular descriptors are the numerical values that capture molecules' structural, electronic, topological, and geometrical features. These descriptors are calculated using algorithms that translate chemical representations (e.g., SMILES strings, InChI, molecular graphs) into quantitative features. They form the basis for correlating structure with property in QSPR models. Descriptors are commonly categorised into several broad classes based on the level of molecular detail they represent as presented in Table 6.1 (Bolboaca *et al.*, 2013).

Table 6.1 Summary of descriptor classes used in quantitative structure–property relationship analysis for adsorption processes.

Descriptor Class	Typical Examples	How Computed	Relevance to Adsorption
1D (Constitutional)	Molecular weight, atom counts, bond counts	Direct from the molecular formula	Baseline size and composition affect diffusion and basic sterics.
2D (Topological/ Graph-based)	Wiener index, Balaban index, substructure counts, electrotopological states	Derived from 2D molecular graphs, adjacency matrices	It captures connectivity, branching, and aromaticity, which are important for molecular packing and surface contact.
3D (Geometric/ Spatial)	Molecular volume, surface area, shape indices, radius of gyration	Computed from optimised 3D structures via molecular mechanics or quantum chemistry	Reflects steric compatibility with pore sizes and adsorption sites.
Electronic	HOMO-LUMO gap, dipole moment, partial charges, polarisability	Quantum chemical calculations (e.g., DFT, semi-empirical)	Governs electrostatic interactions, π–π stacking, and Charge transfer in adsorption.
Thermodynamic	Heat of formation, Gibbs free energy, and solvation energy	Calculated via quantum chemistry or empirical methods	Indicates stability and energetic favourability of adsorption under various conditions.

6.3.3.1 1D descriptors

1D descriptors are the simplest and most intuitive, typically involving straightforward counts or sums derived from the molecular formula. Examples include molecular weight, the total number of atoms, the number of heteroatoms (like nitrogen or oxygen), or counts of specific bond types. Because they do not incorporate information about atom connectivity or spatial arrangement, they are computationally trivial to calculate but often insufficient to capture the nuances needed for detailed property prediction.

6.3.3.2 2D descriptors

2D descriptors advance this by incorporating information from the molecule's two-dimensional graph representation, capturing how atoms are connected. Topological indices, such as the Wiener index (which sums the shortest path lengths between all pairs of atoms) or the Balaban index (which integrates connectivity

and cyclicity), quantify the overall shape and branching of the molecule. Other 2D descriptors include counts of specific substructures (like aromatic rings or aliphatic chains) and electrotopological state indices that combine electronic and topological characteristics. These descriptors are particularly useful in studies of adsorption where molecular branching and functional group distribution influence how molecules interact with adsorbent surfaces.

6.3.3.3 3D descriptors

3D descriptors incorporate spatial geometry, providing a three-dimensional perspective on molecular size and shape. These include descriptors like the radius of gyration, molecular volume, surface area, and shape indices that quantify how compact or elongated a molecule is. For example, Jurs descriptors combine surface area and partial charges to capture how molecular polarity is distributed in space. Such 3D descriptors are critical when modelling processes like adsorption, where steric compatibility with pore structures or surface features of adsorbents can dictate adsorption efficiency.

6.3.3.4 Electronic descriptors

Electronic descriptors delve into the electronic environment of molecules. They quantify properties such as the energies of the highest occupied and lowest unoccupied molecular orbitals (HOMO and LUMO), which are indicators of electron donation and acceptance potential, respectively. Examples include total dipole moment, atomic partial charges derived from quantum chemical calculations, and polarisability. These descriptors are essential in adsorption studies where electrostatic interactions or π–π stacking with adsorbent surfaces play significant roles.

6.3.3.5 Thermodynamic descriptors

Thermodynamic descriptors capture energetic aspects of molecules and may include heats of formation, Gibbs free energy, enthalpy, entropy, and solvation energies. They provide insight into the stability of molecules under various conditions and can help models predicting adsorption equilibria, particularly in systems sensitive to temperature or solvent effects. By combining these classes of descriptors, QSPR models can comprehensively represent the molecular features that govern physicochemical properties, enabling robust and interpretable predictions.

Descriptor selection is a critical step in QSPR modelling. The choice of descriptors affects model performance, generalisability, and interpretability. While thousands of descriptors may be available, not all contribute meaningfully to the model. Advanced selection techniques (e.g., principal component analysis (PCA), genetic algorithms, or recursive feature elimination) are used to identify the most informative subset.

It is also important to note that the relevance of a descriptor may be context-dependent. For example, descriptors like molecular surface area, polarity, and hydrophobicity are more relevant in adsorption studies, while in electronic property prediction, orbital energy descriptors dominate. The quality of descriptors also impacts the model's ability to generalise beyond the training set. Descriptors

should ideally be efficiently computable, interpretable, non-redundant, sensitive to small structural changes, and applicable across various compounds.

6.4 MODEL DEVELOPMENT WORKFLOW AND BEST PRACTICES FOR QUANTITATIVE STRUCTURE–PROPERTY RELATIONSHIP MODELLING

Developing a scientifically sound and practically beneficial QSPR model requires more than statistical fitting. It is a multi-stage process integrating principles from chemoinformatics, statistical learning, and domain-specific knowledge. Each phase of model construction – from data curation to descriptor selection, algorithm choice, validation, and interpretability – carries unique challenges and best practices that must be addressed to ensure the resulting model is robust, generalisable, and capable of offering mechanistic insights. In adsorption process modelling, these steps are even more critical due to the interplay of diverse adsorbent surfaces, molecular interactions, and environmental factors. Figure 6.4 illustrates a typical workflow for QSPR model development, highlighting these stages' iterative and interconnected nature (Le *et al.*, 2012; Kulkarni *et al.*, 2019).

6.4.1 OECD principles

A landmark contribution to the formalisation of QSPR and QSAR modelling guidelines comes from the organisation for economic cooperation and development (OECD), which outlined five fundamental principles to ensure that computational models are scientifically credible and suitable for regulatory or industrial use. These principles serve as a benchmark for best practices across chemical, pharmaceutical, and environmental applications. Figure 6.5 illustrate the best practices for QSPR modelling.

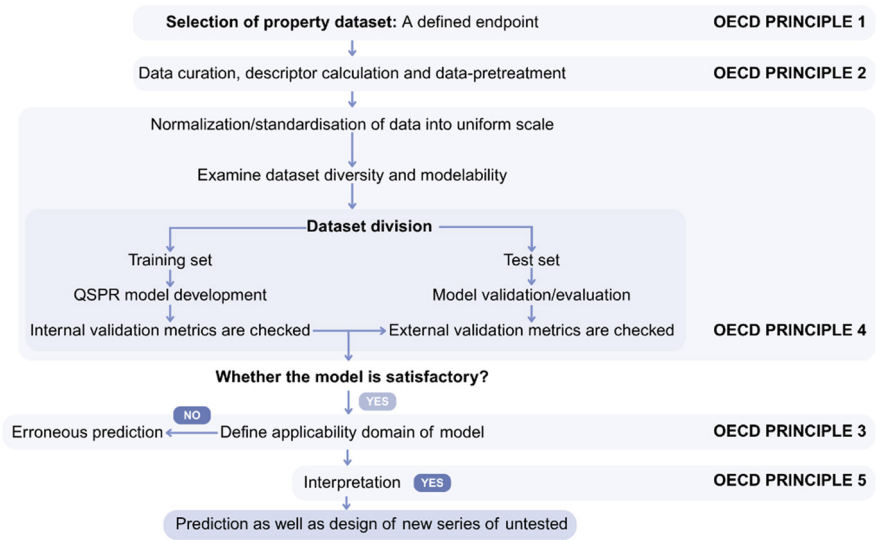


Figure 6.4 Workflow for quantitative structure–property relationship model development.

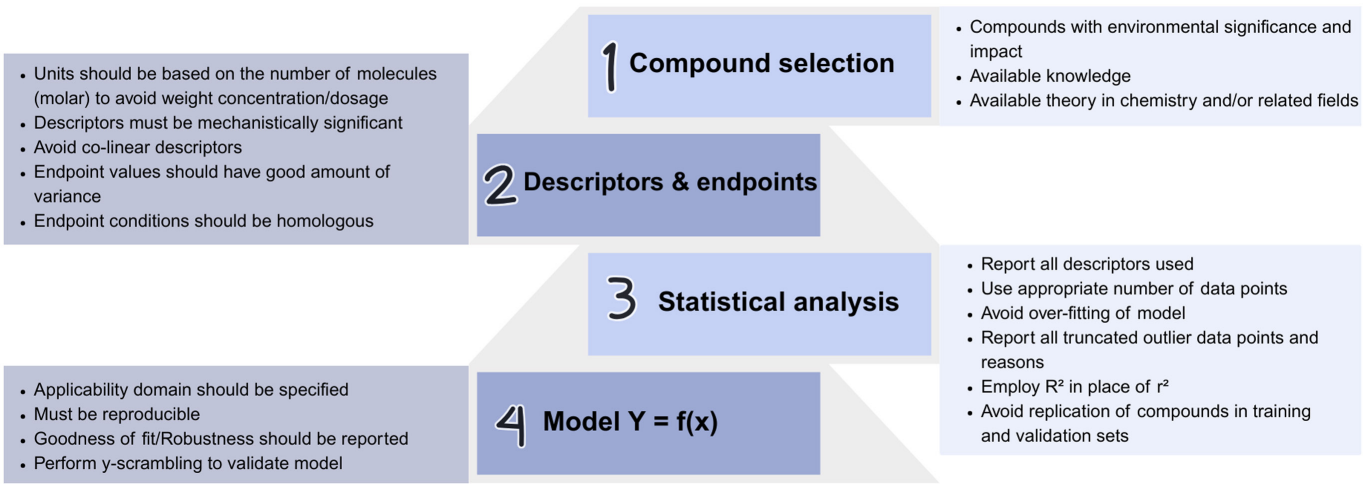


Figure 6.5 Best practices for quantitative structure–property relationship modelling.

The first principle emphasises the need for a well-defined endpoint. This means that the property or activity being predicted must be clearly specified, measured under standardised conditions, and preferably derived from reliable experimental protocols. In adsorption studies, this might involve adsorption capacities measured at a consistent pH and temperature, or equilibrium constants determined using standardised isotherm models.

The second principle insists on an unambiguous algorithm. The mathematical or computational approach linking descriptors to the predicted property should be transparent and reproducible. Whether the model is based on multiple linear regression, support vector machines (SVM), or neural networks, full disclosure of the modelling equations, hyperparameters, and data preprocessing steps is crucial for reproducibility.

The third principle requires a clearly defined domain of applicability, ensuring that the model is only used to predict structurally and chemically similar compounds to those in the training set. Predictions made outside this domain are inherently less reliable.

The fourth principle demands appropriate goodness-of-fit measures, robustness, and predictive power. This typically involves a combination of statistical metrics obtained from internal validation (like cross-validation) and external validation on independent test sets.

Finally, the fifth principle underscores the importance of mechanistic interpretation whenever feasible. Understanding why specific descriptors influence a property enhances scientific trust and allows models to serve as predictive tools and platforms for hypothesis generation and experimental design.

6.4.2 Data considerations

High-quality, well-curated data form the bedrock of any QSPR modelling endeavour. This includes the dependent variables (such as adsorption capacities, rate constants, or equilibrium constants) and the independent molecular structures from which descriptors are computed. Raw datasets often require meticulous preprocessing to address missing values, typographical errors, inconsistent units, and duplicate entries. Outlier detection is also critical, as erroneous or extreme data points can disproportionately influence regression coefficients or distort machine learning models.

In adsorption studies, the heterogeneity of experimental conditions poses additional challenges. Adsorption data reported at different pH values, temperatures, or ionic strengths may not be directly comparable. Careful stratification or standardisation may be necessary to ensure meaningful relationships are captured. Increasingly, researchers rely on publicly available databases such as PubChem or ChEMBL for molecular structures, while adsorption-specific datasets are curated from literature mining or specialised repositories.

The size and diversity of the dataset are equally important. A dataset that is too small or lacks structural variability may lead to overfitting, where the model captures random noise rather than genuine structure–property relationships. Conversely, a large and chemically diverse dataset improves the statistical power of the model and expands its domain of applicability. However, this also heightens the need for rigorous descriptor selection and validation to manage complexity.

6.4.3 Descriptor selection

Descriptor selection is arguably one of the most critical and nuanced steps in QSPR modelling. While modern software packages can compute thousands of descriptors for a single molecule, including constitutional, topological, geometric, electronic, and thermodynamic types, not all will be informative or relevant to the property under investigation. Using too many descriptors, particularly those collinear or redundant, increases the risk of overfitting and hampers interpretability.

Effective descriptor selection balances statistical criteria with chemical intuition. Simple techniques like pairwise correlation analysis help eliminate descriptors that are highly correlated with each other, reducing multicollinearity. More advanced approaches involve principal component analysis (PCA) to capture the primary directions of variance in the dataset or machine learning techniques like recursive feature elimination (RFE), random forests for variable importance ranking, or genetic algorithms that evolve optimal descriptor subsets over successive iterations.

In adsorption-focused QSPR studies, descriptors related to molecular polarity (dipole moment, log P), size (molecular volume, surface area), and electronic features (HOMO-LUMO gap, partial charges) are often prioritised, as they directly influence interactions with adsorbent surfaces. Ideally, the final selected descriptor set should be parsimonious, containing only variables that significantly improve model predictivity while offering insight into the underlying physicochemical mechanisms.

6.4.4 Validation methods

Validation provides the quantitative backbone for assessing the reliability and generalisability of a QSPR model (Figure 6.6). Internal validation methods such as k-fold cross-validation, leave-one-out cross-validation (LOO-CV), or bootstrapping help estimate how the model might perform on unseen data drawn from the same distribution as the training set. These methods partition the dataset into multiple subsets, iteratively training the model on some subsets while testing it on others, generating metrics like average R^2, root mean square error (RMSE), and mean absolute error (MAE) across all folds.

External validation involves applying the finalised model to a completely independent test set not used during model training or hyperparameter tuning. This is often considered the gold standard for evaluating predictive performance. Splitting strategies for forming training and test sets can be random, stratified to preserve the distribution of the property values, or even based on temporal sequencing if the data span multiple studies over time.

Advanced protocols such as double cross-validation or y-randomisation (where the response variable is shuffled to test for spurious correlations) further bolster confidence in the model by demonstrating its robustness and ensuring it is not simply fitting noise. Reporting multiple complementary metrics – including Q^2 (predictive squared correlation coefficient), RMSE, and coverage within the applicability domain – provides a more comprehensive picture of model performance [5].

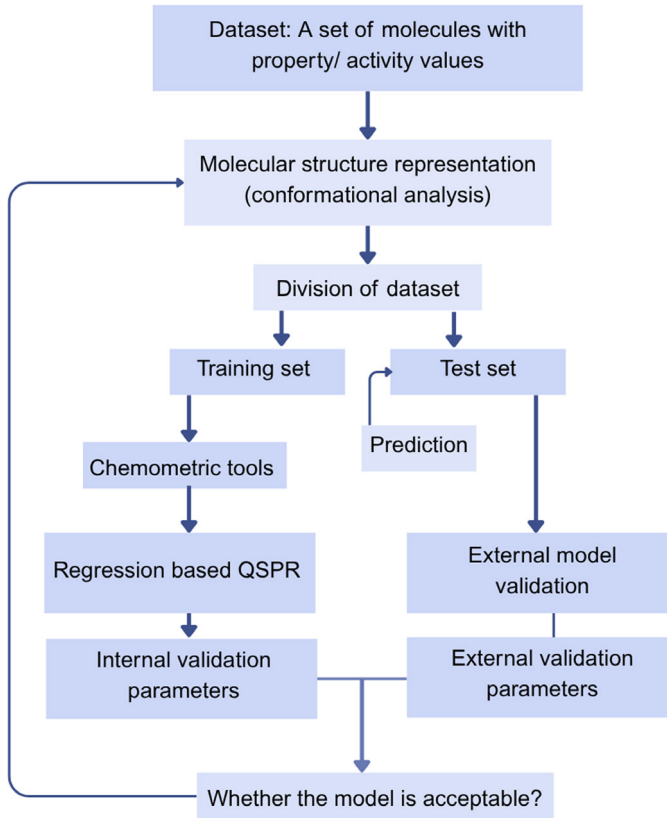


Figure 6.6 Steps of validation methods for the quantitative structure–property relationship model.

6.4.5 Multitask modelling

Many real-world applications in adsorption and environmental chemistry involve optimising or predicting multiple interrelated properties simultaneously, such as adsorption capacity, rate constants, and thermodynamic parameters. Multitask modelling frameworks allow for the simultaneous prediction of several endpoints using shared representations, effectively leveraging correlations among different properties to improve overall predictive power (Figure 6.7).

Traditional chemometric approaches might involve partial least-squares (PLS) regression extended to handle multiple dependent variables. Modern machine learning advances have brought forward multitask neural networks, which use common hidden layers to learn relevant features across tasks while maintaining task-specific output layers. Such approaches enhance prediction accuracy and reveal deeper structure–property relationships that might be missed when modelling each property in isolation.

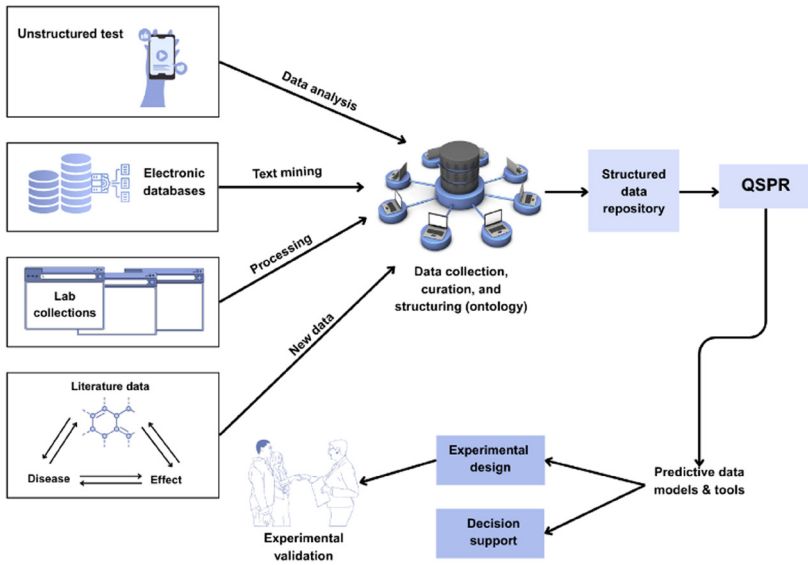


Figure 6.7 Multitask modelling in quantitative structure–property relationship.

6.4.6 Applicability domain and predictive reliability

A critical, often underappreciated aspect of QSPR modelling is defining the model's applicability domain (AD), the chemical space over which the model's predictions are considered reliable. Predictions made for compounds outside this domain are prone to large errors and may lack physical or chemical meaning.

Methods for defining the applicability domain include distance-based approaches (like leverage or Mahalanobis distance). These bounding box methods define descriptor ranges and probability density estimations that assess whether a new compound lies within the high-density region of the training data. Visual tools such as Williams plots, which plot standardised residuals against leverage, are frequently used to identify outliers and influential points. Ensuring that new predictions lie within the AD safeguards the trustworthiness of QSPR applications, particularly in regulatory or process optimisation contexts.

6.4.7 Interpretability

Beyond predictive accuracy, interpretability is a hallmark of well-constructed QSPR models, enabling researchers to glean mechanistic insights into how molecular structure governs adsorption behaviour or other properties. In simpler models like multiple linear regression, the regression coefficients directly indicate the direction and magnitude of each descriptor's influence. For more complex machine learning models, interpretation may require post-hoc tools such as feature importance scores from random forests, partial dependence plots that show how a property varies with a descriptor while holding others constant, or Shapley values that fairly attribute contributions across correlated features.

Interpretability fosters scientific understanding and enhances stakeholder confidence, making the model outcomes actionable for guiding experimental design, selecting candidate molecules, or optimising process conditions. In adsorption process modelling, this can reveal how increased molecular polarity or specific functional groups enhance affinity towards hydrophilic or hydrophobic adsorbents, thereby providing a rational basis for material design.

6.5 QUANTITATIVE STRUCTURE–PROPERTY RELATIONSHIP MODELLING OF ADSORPTION PROCESSES

The QSPR approach offers a powerful avenue to systematically explore, understand, and predict the adsorption behaviour of organic and inorganic contaminants on various adsorbent materials (Le *et al.*, 2012). Unlike classical single-phase applications of QSPR, adsorption inherently involves complex interactions at the interface of two distinct phases: the adsorbate molecule and the adsorbent surface. This added layer of complexity necessitates careful consideration of not just the adsorbates' molecular features but also the adsorbent material's physicochemical characteristics and the surrounding solution environment. As the diversity of emerging contaminants and novel adsorbent materials grows, QSPR methodologies have become indispensable for rapidly screening potential systems, prioritising experimental efforts, and deriving mechanistic insights that would otherwise require extensive trial-and-error laboratory campaigns (Figure 6.8).

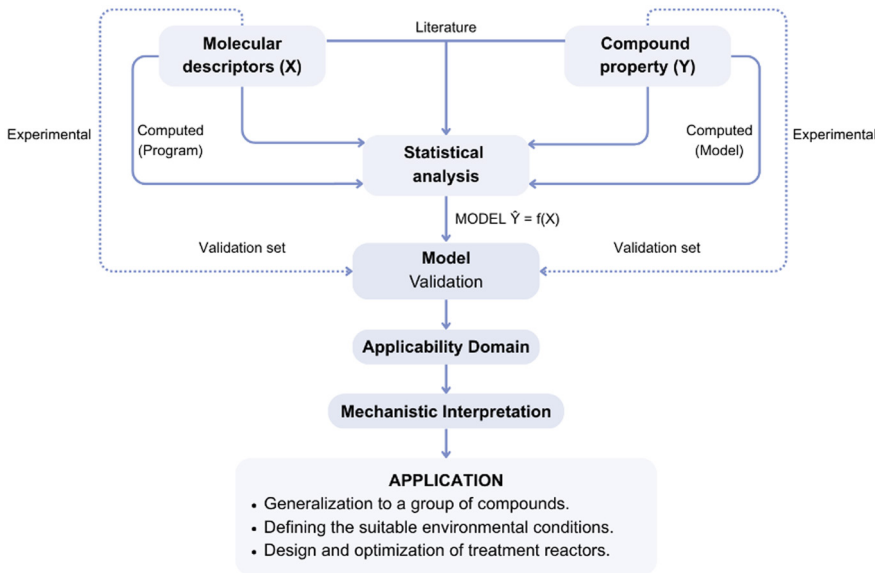


Figure 6.8 Simplified flow diagram of typical quantitative structure–property relationship models of water treatment applications.

6.5.1 Adsorbent and adsorbate specifics

In adsorption studies, both the molecular properties of the species being removed (the adsorbate) and the characteristics of the material capturing them (the adsorbent) play critical roles. Unlike traditional QSPR contexts, such as predicting boiling points or solubility, that involve intrinsic properties of isolated molecules, adsorption is governed by interfacial phenomena that depend heavily on the mutual compatibility of adsorbate and adsorbent.

On the adsorbate side, molecular properties such as size, shape, polarity, and electronic structure largely determine how the molecule interacts with a given surface. For instance, hydrophobic pollutants with high log P values generally exhibit stronger affinities towards hydrophobic adsorbents like raw activated carbons, whereas highly polar or charged molecules may interact preferentially with functionalised surfaces bearing complementary charges or polar groups. Electronic features, such as partial charges and frontier molecular orbital energies (HOMO-LUMO levels), also dictate susceptibility to π–π stacking interactions and electrostatic attractions with surface functionalities.

Meanwhile, adsorbent properties encompass various textural, chemical, and electronic characteristics. Textural parameters, such as Brunauer–Emmett–Teller (BET) surface area, total pore volume, and pore-size distribution, directly influence the accessibility and accommodation of adsorbate molecules within the porous matrix. Chemical surface properties, including the nature and density of functional groups, surface acidity/basicity, and zeta potential, modulate adsorption through hydrogen bonding, acid–base interactions, and electrostatics. For example, an adsorbent functionalised with amino groups may preferentially bind anionic contaminants via electrostatic attractions. Even subtler features, such as defects in crystalline frameworks (common in MOFs or graphene-based materials), can create high-affinity sites that significantly alter adsorption behaviour.

Moreover, adsorption is rarely governed by a single interaction type. It often arises from dispersive forces, hydrogen bonding, π–π interactions, and electrostatics, varying with solution pH, ionic strength, and temperature. As a result, robust QSPR modelling of adsorption processes often integrates the molecular descriptors of adsorbates and experimentally determined or theoretically derived properties of adsorbents, ensuring the models reflect the multifaceted nature of adsorption phenomena.

6.5.2 Types of molecular descriptors in adsorption studies

Because adsorption is fundamentally an interfacial process influenced by a complex interplay of molecular size, shape, electronic structure, and surface compatibility, selecting descriptors becomes especially critical in adsorption-focused QSPR studies. While the broad categories of descriptors, such as 1D, 2D, 3D, electronic, and thermodynamic, remain relevant, specific subsets have proven particularly useful for modelling adsorption behaviour.

Size and shape descriptors (often 3D or hybrid 2D–3D) such as molecular volume, solvent-accessible surface area, aspect ratio, and shape indices are frequently used. These descriptors help capture the steric compatibility of adsorbate molecules with the pore structure or surface roughness of adsorbents.

For instance, a molecule with a large volume relative to average pore diameters may experience steric hindrance, reducing adsorption capacity.

Polarity and hydrophobicity descriptors, notably the octanol–water partition coefficient (log P), dipole moment, and related hydrophilicity indices, are crucial in predicting adsorption onto surfaces with differing polarity profiles. Molecules with high log P values preferentially partition onto hydrophobic surfaces, whereas more polar or charged molecules may rely on hydrogen bonding or ion exchange mechanisms.

Electronic descriptors, such as partial atomic charges, HOMO-LUMO energy gaps, electrophilicity indices, and electrostatic potential maps, are vital for modelling interactions driven by electrostatics or π–π stacking. These are especially important in studies involving graphitic carbons, CNTs, or aromatic MOFs, where delocalised π-electron systems can interact strongly with similarly conjugated adsorbates.

Topological and connectivity indices, like the Wiener index, Kier–Hall indices, or Balaban index, offer a way to quantify branching, cyclicity, and connectivity patterns. While these descriptors are more abstract, they often correlate with steric accessibility and how molecules orient themselves upon adsorption.

Thermodynamic descriptors, such as heats of formation, solvation energies, and Gibbs free energy changes, provide additional layers of predictive power, indicating how favourable interactions may be under given environmental conditions.

In advanced adsorption QSPR studies, hybrid descriptor sets are increasingly used. These combine quantum chemical descriptors of the adsorbate with experimentally measured adsorbent properties (like BET area, pore size, or surface functional group density), or even incorporate computed interaction parameters (like binding energies from docking simulations). This integrative approach enhances the ability of models to capture the synergistic influences governing adsorption.

Figure 6.9 illustrates the major categories of descriptors, including size and shape, polarity and hydrophobicity, electronic, topological and connectivity, thermodynamic, and hybrid descriptors, highlighting the key properties captured by each and their roles in modelling adsorption behaviour.

6.5.3 Steps in developing quantitative structure–property relationship for adsorption

Constructing a QSPR model tailored explicitly to adsorption processes involves a multi-stage workflow that carefully bridges molecular informatics with adsorption science. The process generally unfolds as follows:

The first stage involves comprehensive data acquisition. This includes collecting reliable experimental measurements of adsorption capacities, equilibrium constants from isotherm models (like Langmuir or Freundlich parameters), or kinetic constants (such as pseudo-second-order rate constants). Equally important is gathering detailed structural representations of the adsorbate molecules (such as SMILES strings or 3D optimised geometries) along with physicochemical properties of the adsorbent (e.g., BET surface area, average pore diameter, surface functional group analysis via FTIR or Boehm titration).

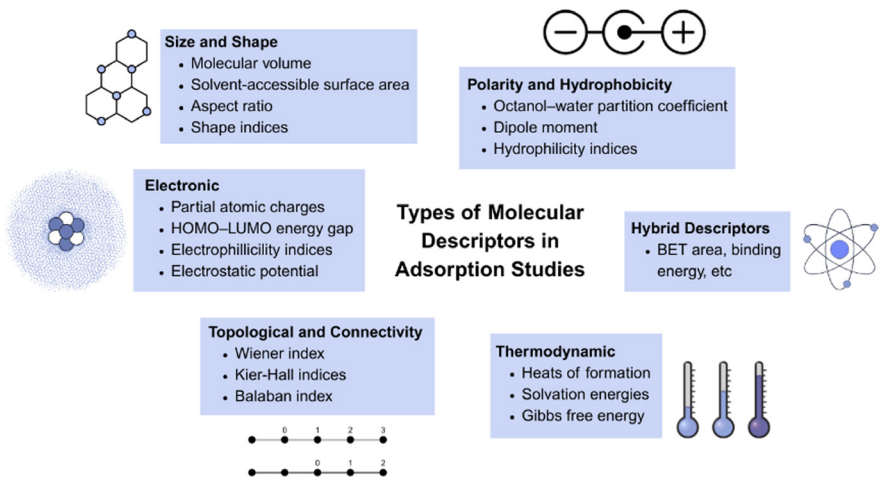


Figure 6.9 Classification of molecular descriptors used in adsorption-focused quantitative structure–property relationship studies.

The second stage focuses on descriptor calculation and preparation. For adsorbates, a suite of molecular descriptors is calculated using cheminformatics toolkits (such as PaDEL-Descriptor, Dragon, or RDKit) or quantum chemistry software (like Gaussian or ORCA for electronic properties). In parallel, adsorbent properties obtained from experimental characterisation are formatted as additional input features. In some cases, composite or interaction descriptors are engineered, for example, by multiplying adsorbate polarity indices with adsorbent surface polarity, to capture synergy explicitly.

Next comes descriptor selection and reduction, where redundant or non-informative variables are pruned through correlation thresholding, PCA, or wrapper methods like recursive feature elimination. This step prevents overfitting and ensures the final model remains interpretable.

The model-building stage employs statistical or machine learning algorithms to establish the quantitative relationship between descriptors and adsorption properties. While multiple linear and partial least-squares regression are popular for their interpretability, more complex systems, especially those involving non-linear dependencies, often benefit from machine learning techniques like support vector regression (SVR), random forests, gradient boosting, or artificial neural networks (ANN). Model hyperparameters are typically optimised using cross-validation schemes to ensure robustness.

Following model construction, rigorous validation is conducted through internal validation techniques such as k-fold cross-validation or leave-one-out validation, combined with external validation on hold-out test sets. Applicability domain analyses (using leverage or distance-based methods) ensure predictions are restricted to chemical spaces well represented in the training data, safeguarding reliability.

Finally, the validated QSPR model is applied to predict adsorption behaviour for new or hypothetical adsorbates and adsorbent combinations. This predictive capability accelerates screening large chemical libraries, prioritises experimental efforts, and often generates new hypotheses regarding the molecular mechanisms underlying adsorption. In modern workflows, this step may be embedded in an iterative design loop, where predictions inform new synthesis or adsorption experiments, whose results refine subsequent models.

Through this structured, meticulous process, QSPR modelling becomes an indispensable tool for navigating the vast combinatorial landscape of potential adsorbate–adsorbent systems, ultimately contributing to more efficient and targeted strategies for water purification, environmental remediation, and material optimisation.

6.6 ADVANCED MODELLING APPROACHES

As adsorption science continues to evolve, so does the need for more sophisticated predictive models capable of addressing the multifaceted complexities inherent in these systems. Classical QSPR approaches, often rooted in linear or modestly non-linear correlations between molecular descriptors and adsorption properties, provide valuable insights but may fall short when faced with the diverse, multi-parametric influences that govern adsorption phenomena (Kulkarni *et al.*, 2019). This is particularly evident when considering variations in adsorbate structure, adsorbent material properties, interfacial effects, and environmental conditions such as pH or competing ions. Advanced modelling strategies have been developed to overcome these limitations, encompassing hybrid and ensemble frameworks, machine learning systems generalising across multiple adsorbent classes, and models that explicitly integrate defects and stability considerations intrinsic to many high-performance materials. These advanced approaches expand the predictive capabilities of QSPR and enable a more nuanced exploration of adsorption processes. Figure 6.10 illustrates advanced modelling strategies in adsorption studies, including hybrid models combining mechanistic and machine learning approaches, consensus models aggregating predictions from multiple algorithms, machine learning frameworks spanning diverse adsorbent classes, and integrating defect and stability considerations to enhance predictive reliability.

6.6.1 Hybrid and consensus models

Hybrid and consensus modelling techniques represent strategic advancements beyond single-model paradigms, designed to enhance the predictive accuracy and generalisability of QSPR analyses. A hybrid model typically combines two or more distinct methodologies within a unified framework, leveraging the individual strengths of each approach. In adsorption, hybrid models may directly integrate mechanistic equations or physics-based adsorption parameters (such as those derived from isotherm or kinetic models) with data-driven statistical or machine learning components. For example, adsorption capacities predicted by classical Langmuir or Freundlich models might be used as intermediate features, combined with molecular descriptors in a multivariate regression

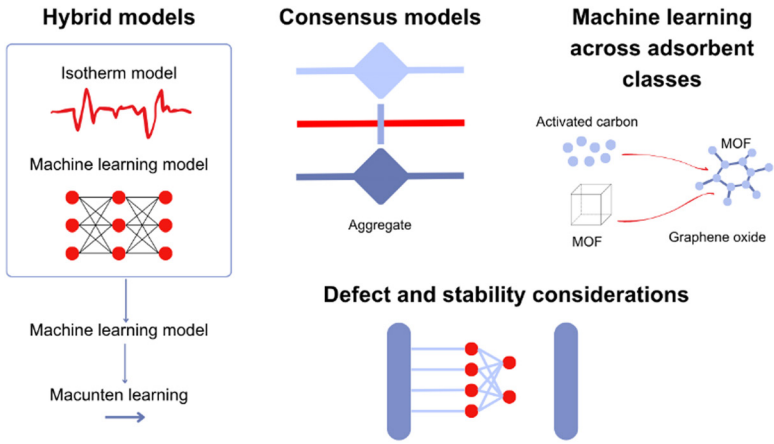


Figure 6.10 Illustration of advanced modelling strategies in adsorption studies.

or neural network, to capture fundamental adsorption thermodynamics and complex structural effects.

Consensus modelling, on the other hand, operates on the principle of aggregating predictions from multiple independent models to produce a final estimate. This ensemble philosophy reduces the risk of overfitting associated with any single modelling approach and delivers more stable and reliable predictions. In adsorption QSPR, consensus models often combine outputs from diverse algorithms such as MLR, SVR, random forests, and ANNs. Each model may capture different facets of the structure–property relationship, and by averaging or otherwise integrating their predictions, the consensus approach achieves improved robustness across chemically diverse datasets.

Studies focusing on the adsorption of pharmaceuticals onto activated carbons, for instance, have demonstrated that consensus models integrating linear regressions with ensemble tree-based methods outperform any single model in predicting removal efficiencies across a wide range of compound classes. This highlights the capacity of hybrid and consensus frameworks to improve quantitative predictions and accommodate the inherently multifactorial nature of adsorption phenomena.

6.6.2 Machine learning across adsorbent classes

Traditional QSPR studies in adsorption often target specific material systems, building models narrowly tailored to individual adsorbent classes such as activated carbons, zeolites, or mesoporous silicas. While effective within their domains, such models lack the flexibility to predict adsorption behaviour across different material platforms, limiting their utility in comparative screening or discovering universal adsorption principles.

Recent advances in machine learning, particularly multitask learning and hierarchical modelling frameworks, have begun to address this limitation. These approaches enable the simultaneous training of models on datasets spanning

multiple adsorbent types, capturing shared adsorption mechanisms while accounting for material-specific interactions. For example, multitask neural networks leverage common hidden layers to learn generalised adsorption-relevant features, while output layers specialise in predicting adsorption capacities or rate constants for different adsorbent families.

A representative study exploring the removal of aromatic contaminants across activated carbons, MOFs, and graphene oxide composites utilised a multitask support vector regression approach. The model identified global structural factors, such as molecular planarity and π-electron density, broadly influencing adsorption, alongside material-dependent effects like pore-size matching and surface charge interactions. This machine learning strategy provides a pathway to develop unified predictive tools, significantly reducing the need for separate, narrowly focused QSPR models.

Moreover, including explicit adsorbent descriptors (such as BET surface area, average pore diameter, or functional group concentration) combined with molecular descriptors allows machine learning algorithms to navigate the complex adsorbent–adsorbate compatibility space. Such integrative models facilitate cross-material screening, identifying optimal adsorbent–adsorbate pairs even in cases involving novel or hybrid materials.

6.6.3 Defect and stability considerations

A critical yet frequently underrepresented dimension in adsorption-focused QSPR models involves explicitly incorporating the influence of material defects and structural stability. Many modern high-capacity adsorbents derive their unique adsorption behaviours not from perfectly ordered structures but from intrinsic or engineered defects. For instance, MOFs with missing linker defects often exhibit unsaturated metal coordination sites that dramatically enhance adsorption affinity for particular organic or ionic species. Similarly, defect sites in graphene oxide or nitrogen-doped carbons introduce localised electronic environments that serve as high-energy binding spots.

Capturing these defect-induced effects within QSPR frameworks typically requires the inclusion of specialised descriptors that quantify defect density, coordination environments, or electronic heterogeneity. These can be derived from advanced characterisation methods such as X-ray photoelectron spectroscopy (XPS) for surface chemical states, positron annihilation lifetime spectroscopy (PALS) for vacancy measurements, or density functional theory (DFT) simulations to compute binding energies at defect sites. Incorporating such descriptors into machine learning or regression models enables predictions that reflect real-world adsorption behaviours more accurately, moving beyond the idealised assumptions of defect-free surfaces.

Equally important is the consideration of adsorbent stability under operational conditions. Adsorption often occurs in aqueous environments that may be acidic, basic, or contain competing ions, all of which can lead to hydrolysis, oxidation, or other structural transformations of the adsorbent. MOFs, for example, are well known for their sensitivity to moisture and pH extremes, which can degrade their frameworks and diminish adsorption performance over time. By including stability-related descriptors, such as hydrothermal

degradation energies computed from molecular dynamics simulations or experimentally determined structural retention indices, QSPR models can prioritise adsorbents with high initial capacities and those likely to maintain performance across the anticipated range of environmental conditions.

Incorporating defect and stability considerations into advanced QSPR models provides a more holistic understanding of adsorption systems. It ensures that predictions extend beyond static equilibrium behaviours to account for dynamic, real-world operational factors, ultimately supporting the selection and design of more durable, application-ready adsorption materials.

6.7 SOFTWARE PACKAGES FOR QUANTITATIVE STRUCTURE–PROPERTY RELATIONSHIP ANALYSIS

QSPR analysis has become an essential approach in adsorption research for predicting adsorption capacities, affinities, and selectivity based on molecular descriptors. By establishing mathematical relationships between the structural features of adsorbates or adsorbents and their observed adsorption behaviour, QSPR models help reduce experimental efforts and accelerate material screening. Several specialised software packages (Figure 6.11) are available to support QSPR (and the closely related QSAR) studies, each offering distinct capabilities for molecular descriptor calculation, model development, and validation.

Open3DQSAR is an open-source suite designed for three-dimensional QSPR and QSAR modelling. It enables alignment-independent comparative molecular field analysis (CoMFA) and related techniques, making it suitable for studying how spatial molecular features influence adsorption on porous materials or functionalised surfaces.



Figure 6.11 Software packages for adsorption process simulation and optimisation.

AlvaDesc is a widely used descriptor calculation tool that can compute thousands of molecular descriptors, including topological, geometrical, electronic, and thermodynamic properties. These descriptors are key inputs for developing QSPR models that relate molecular structures to adsorption parameters such as equilibrium constants or rate coefficients.

Schrödinger's suite, including its QikProp and Phase modules, offers advanced molecular descriptor calculation, pharmacophore modelling, and property prediction capabilities. While initially developed for drug design, it is increasingly applied in materials science to predict adsorption affinities based on structural properties.

COSMOtherm uses quantum chemical COSMO-RS theory to predict thermodynamic properties such as solubility, partition coefficients, and adsorption isotherms. It can evaluate how molecular polarity, charge distribution, and solvent effects influence adsorption, providing a mechanistic layer to QSPR studies.

Spartan, by Wavefunction, provides quantum chemical calculations and molecular mechanics simulations to compute electronic properties and molecular descriptors. Its user-friendly interface makes it particularly suitable for generating descriptor datasets for QSPR models linked to adsorption processes.

QSAR DataBank (QSARDB) is a platform for storing, sharing, and validating QSAR/QSPR models. Researchers working on adsorption can leverage this resource to benchmark models, ensure reproducibility, and explore descriptor–property relationships developed by the broader scientific community.

Scigress combines molecular modelling and cheminformatics tools, enabling users to compute various molecular descriptors and visualise molecular interactions. It facilitates building QSPR models by integrating descriptor calculation with regression and statistical analysis tools.

QSPRPred is a specialised platform designed for building and validating QSPR models using machine learning techniques. It automates descriptor selection, model training, and performance validation, streamlining the process of correlating molecular structures with adsorption capacities or efficiencies.

6.8 SUMMARY

Adsorption represents one of the most effective and widely implemented methods for removing diverse contaminants from aqueous systems, owing to its operational flexibility, economic viability, and broad applicability to various classes of pollutants. However, the intricate dependence of adsorption performance on the interplay between adsorbate molecular characteristics, adsorbent surface properties, and environmental conditions often complicates efforts to predict system behaviour solely through experimental investigations. In this context, QSPR modelling has emerged as a crucial computational strategy, offering a means to systematically correlate molecular structures with measurable physicochemical properties. By converting detailed structural information into mathematical predictions, QSPR enables more efficient exploration of chemical spaces, reduces experimental workloads, and supports the rational design of adsorption processes.

This chapter comprehensively examined QSPR methodologies as applied to adsorption systems. The discussion began with the historical progression and foundational concepts underlying QSPR, followed by an overview of key molecular descriptors that quantify structural, topological, geometric, electronic, and thermodynamic features relevant to adsorption behaviour. Special attention was given to the distinctive requirements of adsorption modelling, where descriptors for adsorbates and adsorbents must often be integrated to capture interfacial phenomena adequately. The chapter also explored advanced modelling strategies, including hybrid and consensus approaches, multitask machine learning frameworks that span multiple adsorbent classes, and techniques that explicitly incorporate material defects and stability considerations. Through these elements, QSPR modelling is positioned not only as a predictive tool but also as a means of deepening understanding of adsorption mechanisms, ultimately guiding the development of more effective and resilient adsorption systems across environmental and industrial applications.

doi: 10.2166/9781789063943 _0157

Chapter 7

Artificial intelligence and machine learning in adsorption processes

7.1 INTRODUCTION

Adsorption methods are extensively used in (waste)water as physical and chemical treatments for eliminating pollutants. Adsorption moves a target molecule (or adsorbate) using an exothermic mass-transfer surface mechanism from a fluid to a solid surface. It is often challenging for (waste)water treatment plants to accurately calculate the essential factors and eventual elimination due to the complexity of the interactions that determine the effectiveness of an adsorption process. Minimising this complexity improves the adsorption process's effectiveness, ensures that the water is being treated optimally, and enhances the lifespan of an adsorbent. Researchers have discovered models that use artificial intelligence and machine learning (AI/ML) to accurately predict the adsorption process's key aspects, helping optimise the process.

AI allows computers to perform tasks and draw conclusions that would require an intelligent human in the same situation. In contrast, ML refers to intelligent systems that can adapt their behaviour to newly presented information during the system-training stage. Because of their application in various industries, AI and ML are well-known and excellent tools for solving real-world problems. AI and ML methods, which have already demonstrated promise in various applications in forecasting, classification, regression, and optimisation, can benefit practically all trans-disciplinary areas. The powers of AI to choose, learn from, and adjust to a system based on previous data are the leading causes of its current success. The algorithms developed by AI-based systems that combine intelligence, flexibility, and intentionality have increased the significance of AI over time. Treating water has become simpler because of the easy design, flexibility, generalisation, and minimal implementation of AI.

© 2026 IWAP. This is an Open Access book chapter distributed under the terms of the Creative Commons Attribution Licence (CC BY-NC-ND 4.0) which permits copying and redistribution for non-commercial purposes with no derivatives, provided the work is properly cited (https://creativecommons.org/licenses/by-nc-nd/4.0/). The chapter is from the book *Computational Techniques for Modelling and Simulating Adsorption Processes for (Waste)Water Treatment*, A. Yadav and P. Labhasetwar (Authors).

The emergence of AI and ML applications in academic communities across all sectors, including those exploring (waste)water treatments, is partly due to their potential to enhance and promote comprehension.

This chapter summarises various AI and ML techniques and their water treatment applications, primarily focusing on adsorption. The initial sections are devoted to the foundations of various techniques and algorithms for building such AI/ML models. The second half of the chapter discusses the AI/ML techniques and their importance in studying adsorption processes. The choice and the validation of AI/ML models are also discussed. Software packages for developing and testing such models are listed, and several case studies are discussed to better understand the practical applications better.

7.2 HISTORY AND THE EARLY DEVELOPMENTS

The term AI was coined in the 1950s and is currently used to define 'the capability of a machine to simulate intelligent human behaviour (Haenlein & Kaplan, 2019)'. ML, a critical computer science component, has become prominent in recent years (Figure 7.1). Integrating AI and ML into adsorption science has been a gradual yet transformative journey, rooted in key historical developments of computational intelligence. These milestones have progressively shaped the capabilities of modern adsorption process modelling, simulation, and optimisation.

The conceptual origin dates to 1943, when McCulloch and Pitts (McCulloch and Pitts, 1943) introduced the first computational model of a neural network. This early theoretical framework laid the foundation for ANNs, later proving pivotal in modelling non-linear and complex adsorption systems. In 1950, Alan

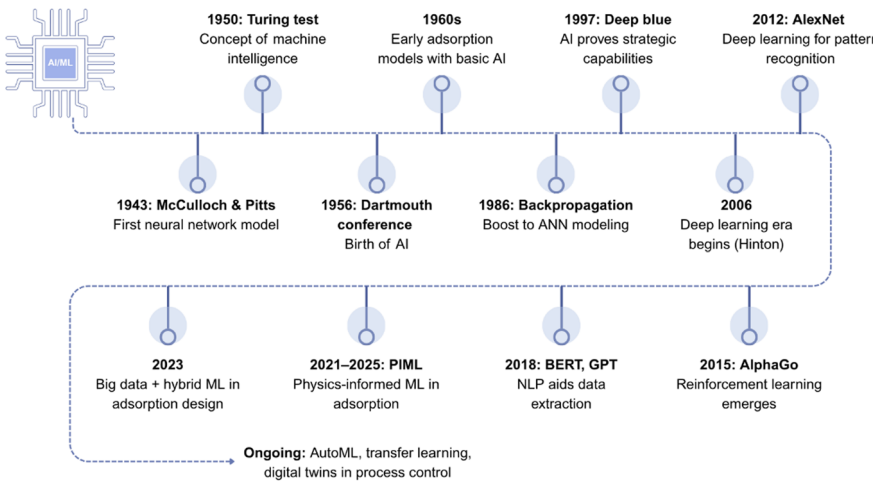


Figure 7.1 Milestone events of artificial intelligence/machine learning applications in the adsorption process.

Turing's (Turing, 1950) proposal of the Turing Test spurred widespread interest in machine intelligence, sowing the seeds for algorithmic approaches to problem-solving in scientific domains, including chemical engineering. The formal birth of AI occurred in 1956 at Dartmouth, USA, Conference, initiating decades of innovation in symbolic reasoning, learning algorithms, and intelligent systems (Newell and Simon, 1956). By the 1960s, early computational tools and rule-based models emerged in adsorption studies, using empirical equations and simulation frameworks to describe isotherms and kinetics.

A significant leap occurred in 1986 with the popularisation of the backpropagation algorithm, revitalising ANNs and enabling their application to complex adsorption modelling (Rumelhart et al., 1986). In 1997, the success of IBM's Deep Blue in defeating world chess champion Garry Kasparov underscored AI's problem-solving capabilities and indirectly inspired its adoption in engineering optimisation problems (Goodman and Keene, 1997). The advent of deep learning 2006, led by Geoffrey Hinton, marked a turning point. Deep belief networks and later architectures allowed for hierarchical feature extraction from complex datasets, highly applicable to the multi-parametric nature of adsorption systems. The 2012 success of AlexNet (Alex *et al.*, 2012) demonstrated the power of convolutional neural networks (CNNs), encouraging their use in pattern recognition and material characterisation tasks within adsorption studies.

Recent years (2021–2025) have seen the integration of physics-informed ML (PIML), enabling the fusion of domain knowledge with data-driven models for better interpretability and generalisation. By 2023, adsorption research had embraced hybrid and ensemble learning approaches, fueled by big data availability and increased computational power. AutoML, transfer learning, and digital twins are currently being explored for real-time optimisation and control in industrial adsorption systems.

7.3 ARTIFICIAL INTELLIGENCE AND MACHINE LEARNING ALGORITHMS

The primary and well-known area of computer science that works with creating intelligent systems and finding solutions to issues akin to the human intelligence system is known as AI. A major goal of the system when applying AI is to improve computer skills related to human knowledge, such as learning, problem-solving, reasoning, and perception. ML techniques are utilised to solve regression and classification issues by building prediction models based on process data. In other words, a complete application of ML technique consists of the following steps: (i) estimating the non-linear relationship between system input parameters and target output from a given data set; and (ii) using the estimated non-linear relationship to forecast the system's new output. Because the goal of ML is prediction rather than estimation, it can be used to predict algal blooms, water quality, and pipe network problems.

Four categories of ML can be distinguished based on the properties of data sets and their accompanying labels: supervised, unsupervised, semi-supervised, and reinforcement learning. The most popular kind of ML used for adsorption is supervised learning. Output variables for unsupervised learning lack

corresponding labels. Therefore, clustering frequently uses such techniques. With more input than output variables, semi-supervised learning combines both supervised and unsupervised learning benefits. Reinforcement learning is a type of ML that interacts with the environment and can adjust parameters in response to feedback from the environment. Figure 7.2 presents a summary of the standard algorithms and assessment indicators of ML for adsorption. Subsections that follow address the main AI/ML approaches.

7.3.1 Supervised learning

7.3.1.1 Artificial neural networks

ANNs are computational models inspired by the structure and function of biological neurons in the human brain (Abiodun *et al.*, 2018). They are particularly well-suited for modelling complex, non-linear systems such as adsorption processes, where traditional mathematical models may struggle to capture intricate relationships between multiple variables.

In an ANN, individual computational units called *neurons* or *nodes* are organised into layers. The basic structure includes three main types of layers:

- **Input layer:** This layer receives raw data (e.g., adsorbent properties, temperature, pH, contact time, initial concentration).
- **Hidden layers:** These intermediate layers process the input data through weighted connections and activation functions to extract patterns and non-linear interactions. The number and size of hidden layers influence the network's capacity to model complexity.
- **Output layer:** This layer provides the final prediction or classification, such as Q, R, or breakthrough time.

Each connection between neurons carries a *weight*, determining the strength and direction of the signal passed between nodes. These weights are iteratively adjusted during the training phase using optimisation techniques such as backpropagation and gradient descent to minimise a *cost function* (e.g., mean-squared error or cross-entropy loss).

A typical ANN model may consist of one or more hidden layers. ANNs have been widely and successfully applied in adsorption research due to their ability to model complex, non-linear systems. They are beneficial for predicting Q under varying operational conditions, such as changes in temperature, pH, contact time, and initial concentration. ANNs have also been employed to model the dynamic behaviour of adsorption processes in both batch and continuous systems, capturing the temporal evolution and breakthrough profiles effectively. Additionally, these networks serve as powerful tools for process optimisation, allowing researchers to map multi-input systems to single or multiple outputs, thereby identifying optimal operating conditions. Furthermore, ANNs are valuable for conducting sensitivity analysis, helping to determine which process parameters significantly influence adsorption performance. Figure 7.3 illustrates a basic feed-forward ANN architecture with two hidden layers, showcasing the flow of information from input variables to predicted output values.

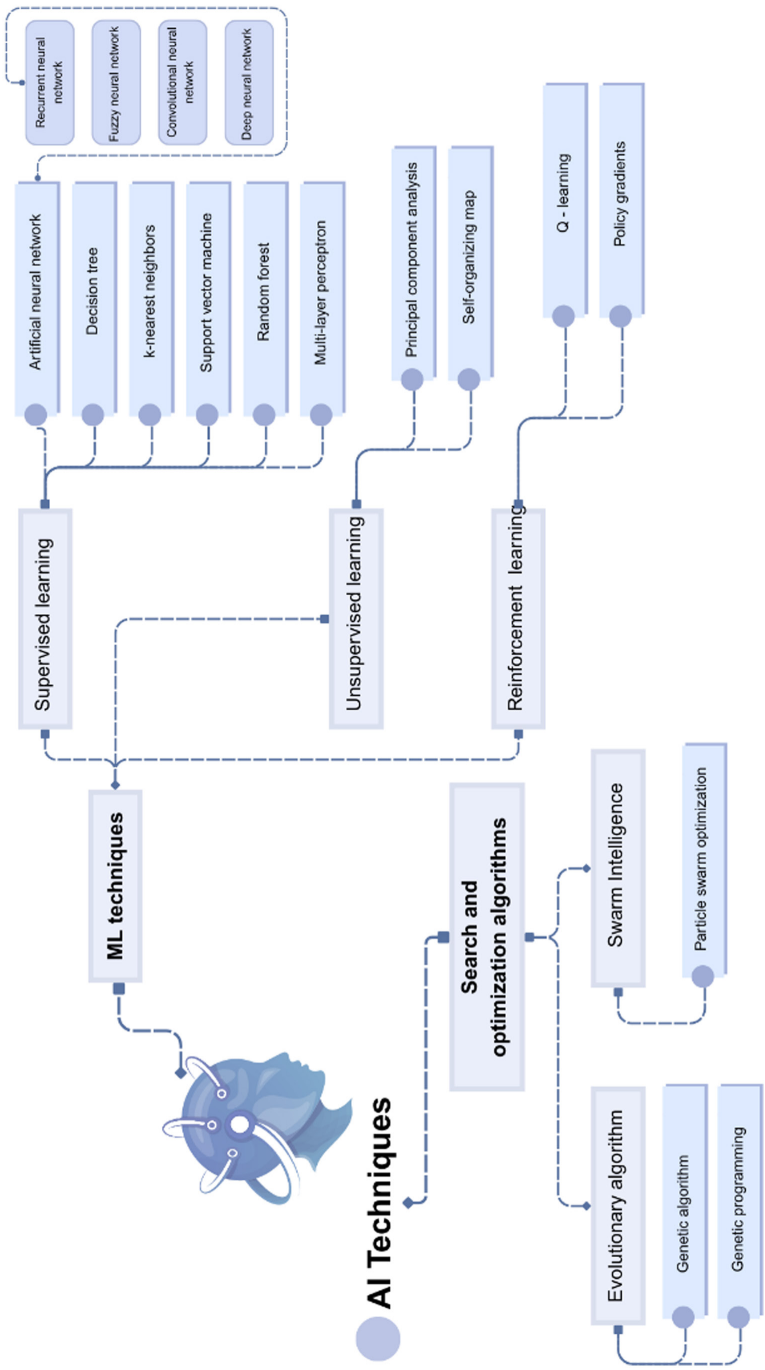


Figure 7.2 Artificial intelligence/machine learning algorithms used in water treatment.

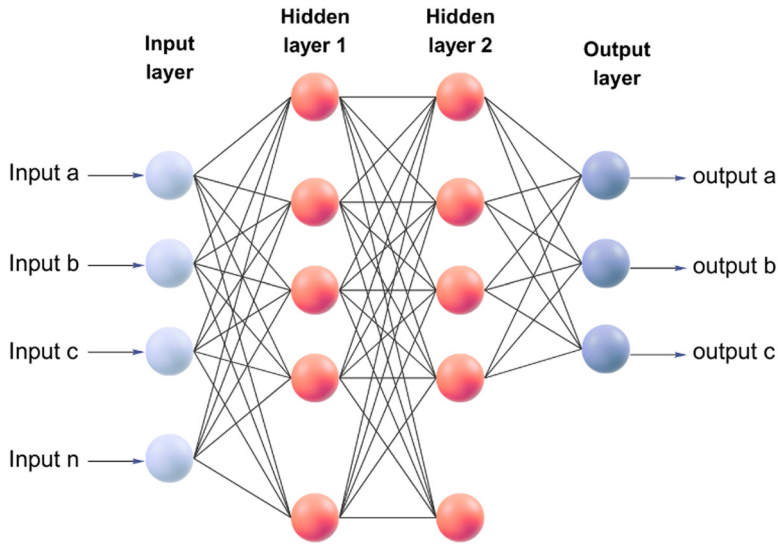


Figure 7.3 Artificial neural network architecture with four layers: an input layer, two hidden layers, and an output layer.

Fuzzy neural network

Figure 7.4 illustrates how fuzzy logic and neural networks were combined to develop the AI technology known as fuzzy neural network (FNN). FNN manipulates the fuzzy set and fuzzy rule parameters that comprise a fuzzy system using neural network approximation techniques. FNN is mainly used

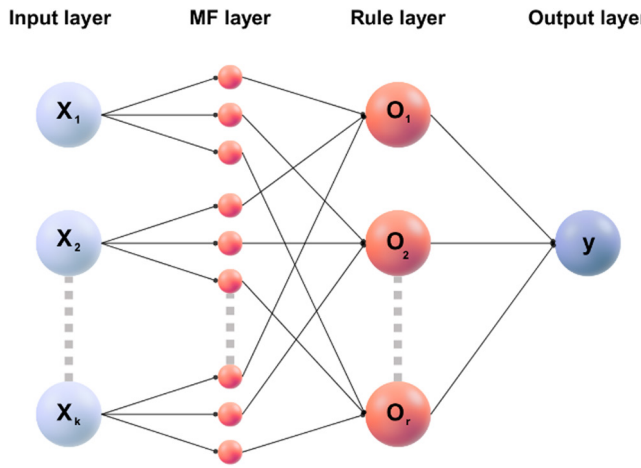


Figure 7.4 Basic fuzzy neural network architecture.

for pattern recognition, regression, and density estimation when there is no mathematical model for a given problem.

Convoluted neural network

Convoluted neural networks (CNNs), also known as feed-forward neural networks (FFNNs), are ANN types that use convolution instead of ordinary matrix multiplication in at least one of their layers. CNN is most employed in natural language processing, financial time-series analysis, image/video recognition and classification. 'Local sparse connections amongst consecutive layers, weight sharing, and pooling' are the three core concepts used by CNN. While pooling minimises feature size, the first two approaches reduce the number of training parameters. In Figure 7.5, the conventional CNN layout is displayed. The two components of CNN are classification layers (completely connected and output layers), which make decisions based on parameters gathered in earlier levels, and hidden layers (convolutional and pooling layers), which extract challenging traits.

Deep neural network

As shown in Figure 7.6, a deep neural network (DNN) has input and output layers and several hidden layers. With additional hidden layers and neurons, DNN is frequently used for learning complex models and high-dimensional data processing. However, DNN requires more computational power and makes training more challenging. If the datasets have enough data, DNN performs better than other ANNs.

Recurrent neural network

Recurrent neural networks (RNNs) are like other ANNs, except that they have an extra memory state allowing neurons to share the same parameters. Information is transported from the input layer to the output layer in an RNN, a type of FFNN. It stores the results of a certain layer and links them to the input to forecast the results. RNNs process variable-length input sequences by using their internal state (memory). Long short-term memory (LSTM), which

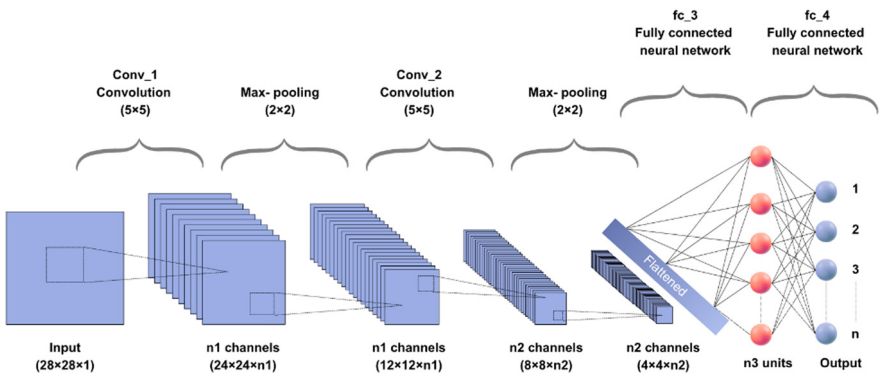


Figure 7.5 Basic convoluted neural network architecture.

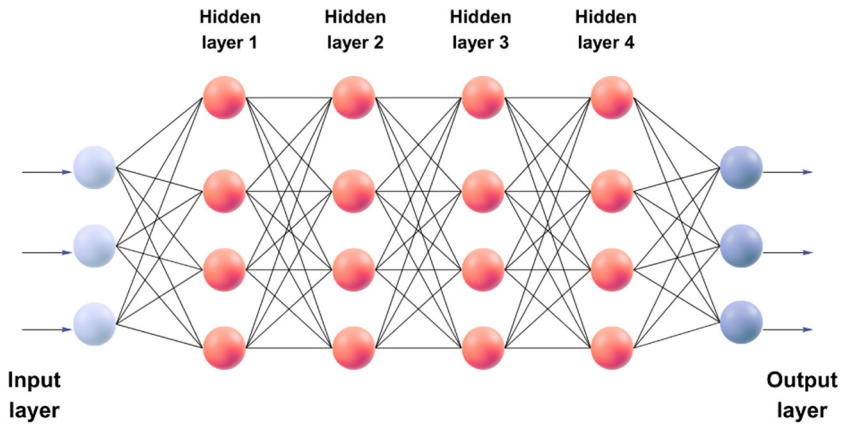


Figure 7.6 Common deep neural network with three input layers, four hidden layers, and two output layers.

has three gates (the input, output, and forget gate) to calculate the hidden state, is a type of RNN that is frequently utilised. Figure 7.7 depicts a straightforward example of an RNN, where nodes from different neural network levels are compressed to generate an RNN of a single layer.

7.3.1.2 Decision tree

A decision tree (DT) is a non-parametric, supervised learning algorithm widely used for regression and classification tasks in data-driven modelling (Charbuty and Abdulazeez, 2021). It is particularly favoured for its interpretability, simplicity, and ability to handle numerical and categorical data. By learning

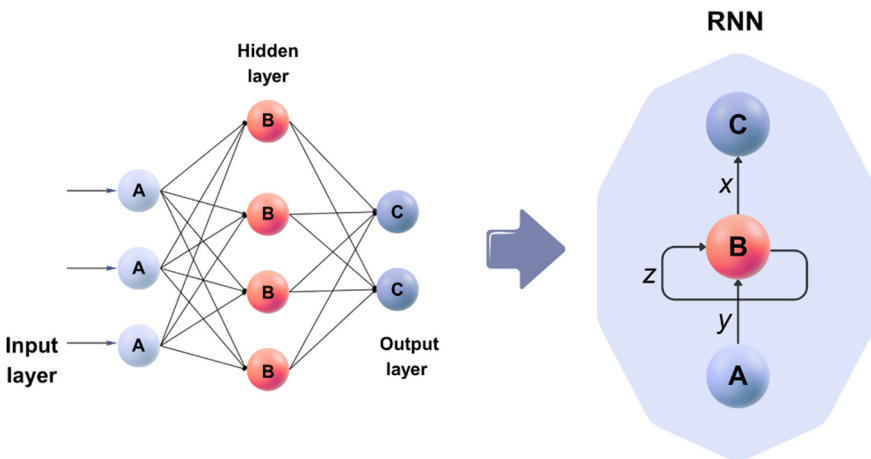


Figure 7.7 Recurrent neural network architecture.

from experimental datasets, DTs in adsorption studies often predict process outcomes such as Q, removal efficiency, or breakthrough time. Structurally, a DT resembles an inverted tree, where each internal node represents a test or decision based on a specific input feature (e.g., pH, adsorbent dose, or contact time), each branch represents a possible outcome of the test, and each leaf node corresponds to a final prediction or class label. This hierarchical, rule-based structure allows DTs to effectively capture non-linear relationships and interaction effects among variables.

DTs' key strengths are their ability to explore all relevant paths – from the root node to the leaf nodes – to identify the most optimal solution based on a predefined criterion, such as minimising error in regression tasks or maximising information gain in classification. Despite their simplicity, DTs can lead to highly accurate models; however, they may also be prone to overfitting if not properly pruned or regularised. Figure 7.8 illustrates a sample DT used in an adsorption modelling context, demonstrating how various input features are split to arrive at a predicted outcome. Due to their transparency and logical structure, DTs are often used as building blocks for more advanced ensemble methods like Random Forests and Gradient Boosted Trees, which offer improved accuracy and robustness.

7.3.1.3 k-Nearest neighbours

The k-nearest neighbours (k-NN) algorithm is one of the simplest yet effective supervised learning techniques, widely used for classification and regression tasks (Dhanabal and Chandramathi, 2011). The core principle of k-NN assumes that similar data points exist in proximity within a feature space. When a new data point is introduced, the algorithm identifies the 'k' closest data points from the training dataset and assigns the new instance to the most common class among its nearest neighbours (for classification) or computes an average of the

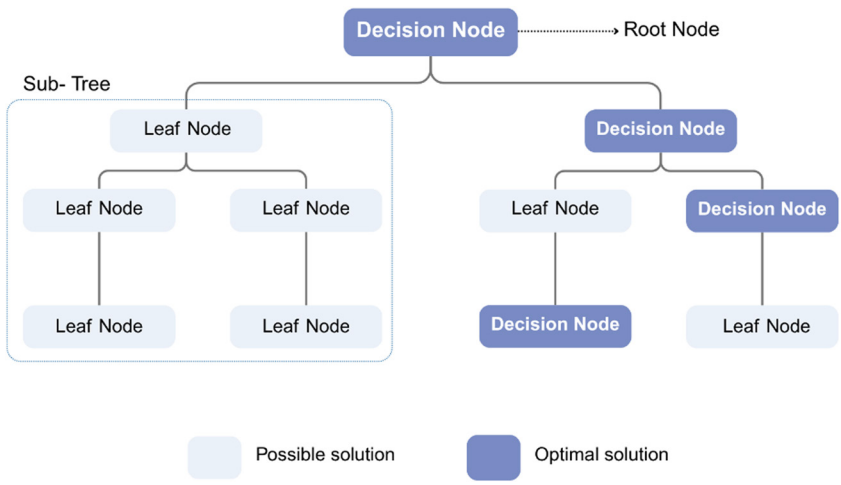


Figure 7.8 Decision tree architecture.

neighbours' values (for regression). k-NN is a non-parametric algorithm that does not assume any underlying data distribution. It is also known as a lazy learner because it does not build a predictive model during training; instead, it stores the entire dataset and performs classification or regression at the time of prediction using distance-based similarity metrics. This makes k-NN computationally inexpensive during training but relatively intensive during prediction, especially for large datasets.

The performance of the k-NN algorithm heavily depends on several key parameters, including the choice of k (the number of neighbours), the distance metric used, and the decision rule applied. A very small value of k may lead to overfitting, capturing noise in the data, while a very large value may oversimplify the model, leading to underfitting. In adsorption studies, k-NN can classify adsorbent types, predict adsorption capacities under varying conditions, or group similar experimental setups. For instance, if adsorption data points are labelled as belonging to two classes – high- or low-performance adsorbents – a new experimental condition can be classified based on the majority class of its nearest neighbours using an appropriate distance metric. As illustrated in Figure 7.9, if most of the nearest neighbours of a new data point belong to class Z, the new point is classified into Z based on Euclidean distance.

Despite its simplicity, k-NN remains a powerful pattern recognition and prediction tool, especially when combined with effective feature scaling and dimensionality reduction techniques like principal component analysis (PCA). However, its sensitivity to irrelevant or highly correlated features necessitates proper data pre-processing to achieve optimal results.

7.3.1.4 Support vector machine

Support vector machine (SVM) is a widely used AI technique for solving classification and regression problems (Kumar *et al.*, 2019). It is a supervised learning algorithm that relies on labelled training data to learn how to distinguish between different classes or predict continuous values. SVM's fundamental idea is to project input data into a high-dimensional feature space, which makes

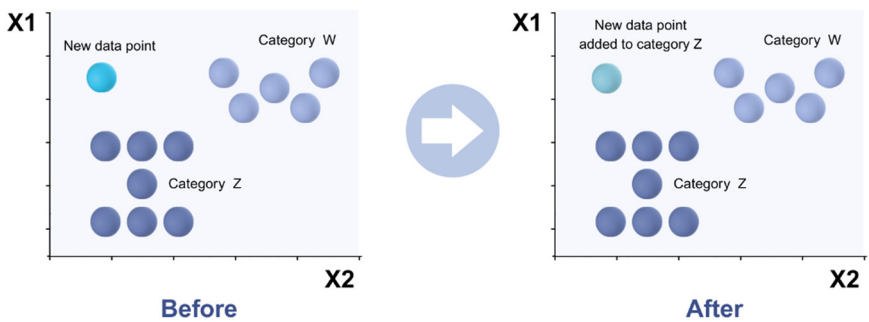


Figure 7.9 An example of the k-nearest neighbour technique before and after a classification problem.

it simpler to identify distinct class boundaries. This is accomplished through mathematical functions called kernel functions, which include radial basis function (RBF), polynomial, and linear kernels. The structure and complexity of the dataset determine which kernel should be used.

SVM works by constructing a hyperplane that best separates the data points of different classes in the feature space. The objective is to maximise the margin – the distance between the hyperplane and the closest data points from each class, known as support vectors. These support vectors are critical, as they determine the orientation and position of the optimal hyperplane. As shown in Figure 7.10, when the classes are linearly separable, SVM draws a straight line (or hyperplane in higher dimensions) to separate them. Each class contributes at least one support vector closest to the decision boundary.

Depending on the nature of the training data, SVM models can be classified as linearly separable or non-linearly separable. In cases where the data is linearly separable, a hard margin approach is applied, which aims for perfect classification with no tolerance for misclassification. However, the data is not perfectly separable in most practical scenarios, especially in experimental variability adsorption studies. A soft margin approach is used in such cases, allowing a limited degree of misclassification to improve the model's generalisation ability. This is achieved by introducing slack variables that permit specific data points to fall within the margin or even on the wrong side of the hyperplane.

To handle non-linearly separable data, SVM employs kernel tricks to map the data into a higher-dimensional space where a linear separation becomes feasible. This transformation allows SVM to maintain computational efficiency while effectively modelling complex, non-linear relationships in the data. The kernel method also reduces the dimensionality of the input vector, making the model suitable for high-dimensional datasets commonly encountered in adsorption modelling.

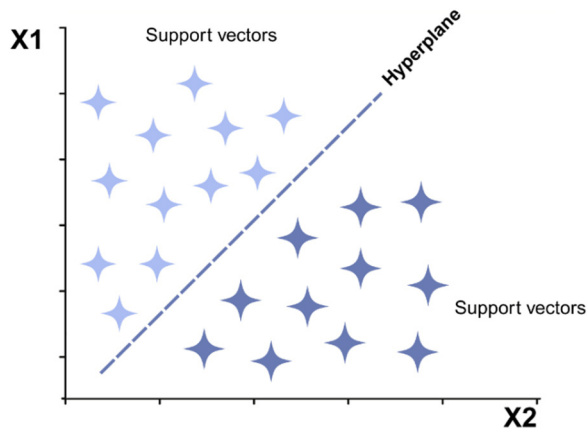


Figure 7.10 An example of support vector machine classification with a linear hyperplane.

7.3.1.5 Random Forest

Random Forest (RF) is a robust, ensemble-based ML algorithm that handles classification and regression problems (Salman *et al.*, 2024). As a non-linear algorithm, RF operates by constructing a collection of DTs, hence the name 'forest'. The central idea is that a group of weak learners (individual DTs) can be combined to form a strong learner, significantly improving prediction accuracy and model generalisation. In RF, multiple DTs are generated by training each tree on a different random subset of the original dataset using a technique known as bootstrap aggregation or bagging. Each DT makes a prediction, and the final output is determined through majority voting (for classification tasks) or averaging (for regression tasks). This ensemble approach reduces the risk of overfitting, a common drawback of single DTs, by diluting the noise from individual models.

As illustrated in Figure 7.11, the RF algorithm takes random samples from the dataset to build multiple trees independently. The results from these trees are then aggregated to produce a final, more accurate and stable prediction. Unlike individual DTs, RF grows each tree to the maximum possible depth using a greedy algorithm without applying pruning. Despite this, the ensemble effect ensures that the overall model remains well-regularised. One of the key strengths of RF is its ability to handle high-dimensional data and assess the importance of individual features (or descriptors), which is particularly beneficial in adsorption modelling where numerous input variables – such as pH, adsorbent dose, temperature, and surface area – can influence performance. RF can help identify the most influential factors affecting adsorption behaviour, thus aiding in feature selection and model simplification.

7.3.1.6 Multi-layer perceptron

The multi-layer perceptron (MLP) is a fundamental architecture in ANN and has become a cornerstone of modern supervised learning approaches

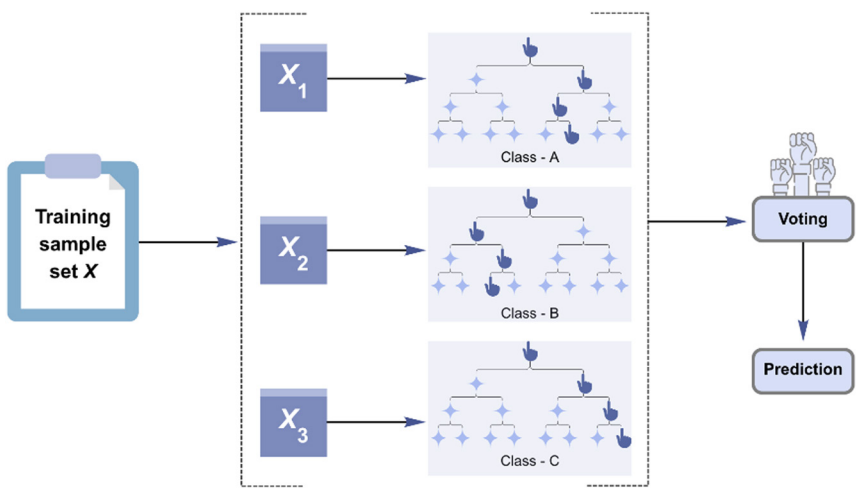


Figure 7.11 Random forest architecture and working procedure.

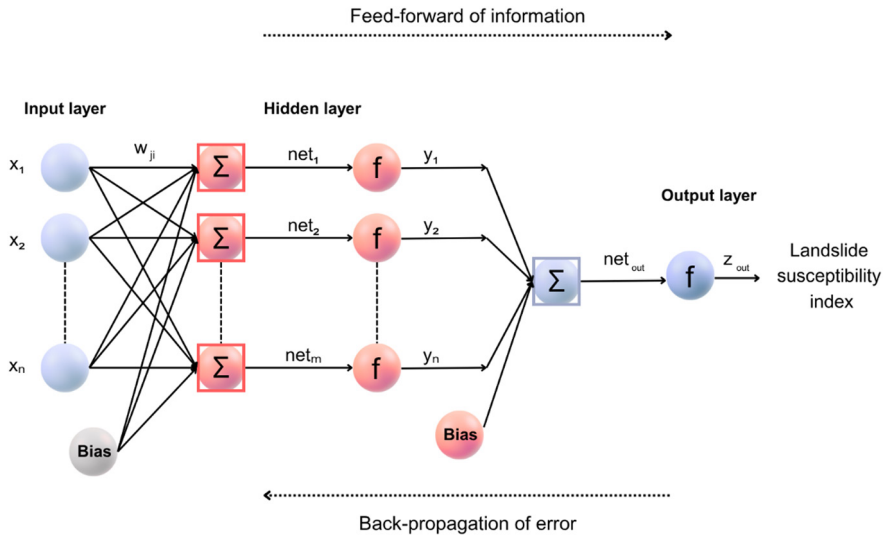


Figure 7.12 Illustration of a multilayer perceptron used to model complex relationships in adsorption systems.

(Figure 7.12). An MLP consists of an input layer, one or more hidden layers, and an output layer, where each layer comprises interconnected processing units called neurons. These neurons are organised feed-forward, meaning the data moves from the input layer to the output layer without forming any loops. After applying a bias term and computing a weighted sum of the input signals from the preceding layer, each neuron sends the output through a non-linear activation function, such as the hyperbolic tangent, sigmoid, or rectified linear unit (ReLU). Thanks to this non-linearity, the MLP can simulate extremely intricate and non-linear relationships between inputs and outputs, which are typical in real-world systems like adsorption processes.

In adsorption, MLPs are particularly effective for modelling and predicting process behaviour under varying operational conditions. They can learn functional relationships between a wide range of input parameters – such as initial solute concentration, solution pH, adsorbent dosage, contact time, and temperature – and output responses like adsorption capacity, breakthrough time, or percentage removal. For example, researchers have successfully applied MLPs to simulate dye removal efficiency using adsorbents or to predict the performance of modified adsorbents under multivariate conditions. These models can be trained using experimental datasets, and once validated, they offer a fast and efficient way to perform predictive simulations without resorting to time-consuming laboratory trials or complex mechanistic models.

Training an MLP involves adjusting weights and biases using optimisation algorithms such as stochastic gradient descent or Adam. The learning is carried out via the backpropagation algorithm, which propagates the prediction error

backwards through the network to update parameters and reduce the loss function, typically the mean-squared error in regression-based adsorption studies. While MLPs offer high predictive accuracy and flexibility in handling non-linear problems, they have certain limitations. One challenge is their tendency to overfit when trained on small or noisy datasets, which can be mitigated through cross-validation, dropout regularisation, or early stopping. Moreover, unlike simpler algorithms, MLPs are often criticised for being 'black-box' models, making it difficult to interpret the internal representation of knowledge or the relative importance of individual variables.

Despite these challenges, the multi-layer perceptron remains a powerful and widely used tool for modelling adsorption systems. It has also been integrated with other AI techniques, such as genetic algorithms or particle swarm optimisation, to form hybrid models that enhance prediction accuracy and process optimisation. In adsorption science and engineering, MLPs offer a pragmatic and effective alternative to conventional mechanistic models, especially in cases where the system behaviour is governed by complex interactions that are difficult to capture analytically.

7.3.2 Unsupervised learning

7.3.2.1 Principal component analysis

PCA is a potent statistical method for data visualisation, pattern recognition, and dimensionality reduction. It transforms a large set of correlated variables into a smaller set of uncorrelated variables termed principal components, while keeping as much of the original data variance as feasible. In adsorption studies, PCA is widely employed to analyse multivariate experimental data, reduce redundancy, and identify the most influential variables affecting adsorption performance (Greenacre *et al.*, 2022). A flowchart has been presented in Figure 7.13. PCA works by computing the covariance matrix of the data and extracting its eigenvalues and eigenvectors. The eigenvectors represent the directions (principal components) along which the data varies the most, and the corresponding eigenvalues indicate the amount of variance captured by each principal component. By projecting the original data onto these components, PCA enables researchers to explore high-dimensional adsorption datasets in two or three dimensions without significant loss of information.

In adsorption research, PCA proves particularly valuable for handling complex and high-dimensional experimental data. It helps identify the most dominant process variables – such as pH, initial concentration, contact time, and temperature – significantly influencing adsorption behaviour (Safwat *et al.*, 2022). By reducing the number of variables without losing critical information, PCA simplifies datasets obtained from batch or column studies, making them easier to interpret and model. Additionally, PCA aids in uncovering hidden patterns, clusters, and outliers within the data, offering deeper insight into system behaviour. It is also commonly used as a pre-processing step before applying ML algorithms, helping to eliminate multicollinearity, reduce noise, and prevent overfitting, ultimately enhancing model accuracy and robustness. Despite its strengths, PCA assumes linear relationships and may not fully capture non-linear interactions between variables. However, when used with

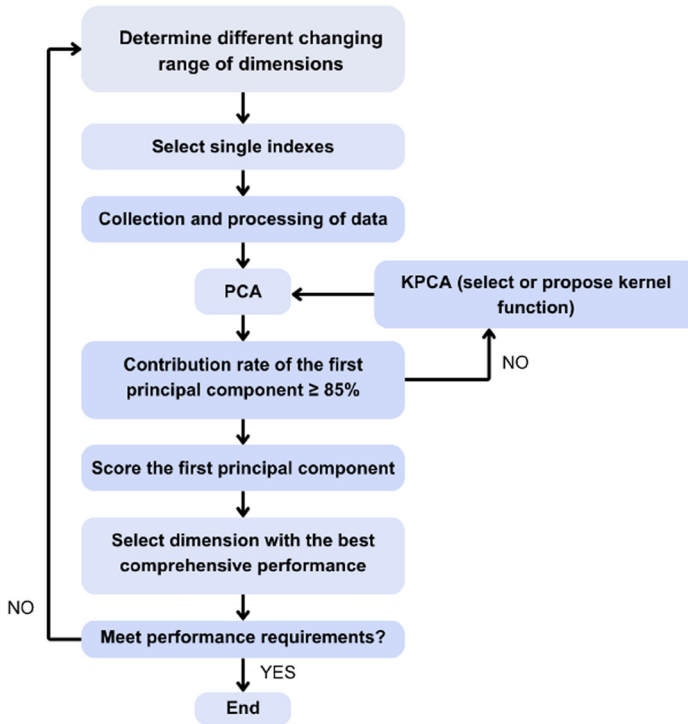


Figure 7.13 Principal component analysis flowchart.

non-linear models such as ANNs or SVMs, PCA is an effective pre-processing tool, enhancing model performance and reducing computation time.

7.3.2.2 Self-organising map

Self-organising map (SOM) is an unsupervised learning algorithm and one of the most widely used AI techniques for data clustering, visualisation, and dimensionality reduction. Developed by Teuvo Kohonen, SOM is a type of ANN that projects high-dimensional data onto a lower-dimensional (typically two-dimensional) map while preserving the topological structure of the data (Brereton, 2012). This capability is particularly useful for exploratory data analysis and pattern recognition in complex systems such as adsorption processes. A SOM consists of two layers: the input layer, which receives multi-dimensional data, and the output layer, also known as the feature map or map layer, which is typically arranged as a grid of neurons. Each neuron in the map layer is associated with a weight vector with the same dimensionality as the input data. During training, input vectors are presented to the network, and the neuron whose weight vector is like the input (called the Best Matching Unit, or BMU) is identified. The BMU and its neighbouring neurons then adjust their weights to become more like the input vector, gradually organising the map to reflect the structure of the input space.

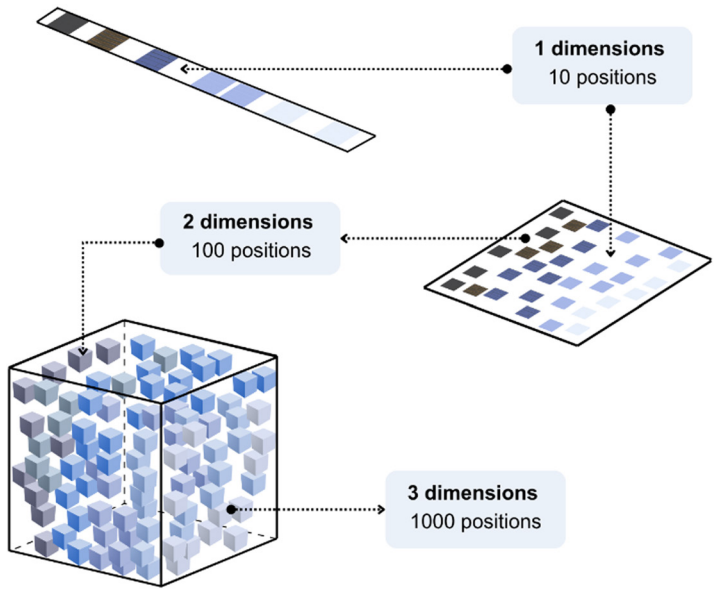


Figure 7.14 Self-organising map dimensionality reduction.

As illustrated in Figure 7.14, SOM can group similar data points, forming distinct clusters based on inherent patterns in the dataset. This makes it highly effective for clustering experimental adsorption data, such as grouping adsorbents with similar performance profiles or identifying trends across operating conditions. Additionally, SOM reduces the dimensionality of complex datasets, which is particularly valuable when dealing with numerous experimental parameters. By simplifying the input space, SOM improves the interpretability of data and assists in identifying key variables influencing adsorption behaviour. One of the key advantages of SOM is its unsupervised nature, which means it does not require labelled training data. It is ideal for uncovering hidden structures and relationships in datasets without prior assumptions. However, the performance of SOM can be influenced by parameters such as map size, learning rate, and neighbourhood function, which must be carefully selected for optimal results.

7.3.3 Reinforcement learning

A novel approach to ML called reinforcement learning (RL) uses interactions with the environment and feedback in the form of rewards or penalties to teach an agent how to behave optimally (Kaelbling *et al.*, 1996) (Figure 7.15). RL enables the agent to learn a policy that maximises long-term cumulative reward through trial-and-error decision-making, unlike supervised learning, which trains models on a predetermined dataset. In adsorption processes, RL holds potential for dynamic control and optimisation where process parameters must be adjusted in real-time or staged sequences. Examples include switching

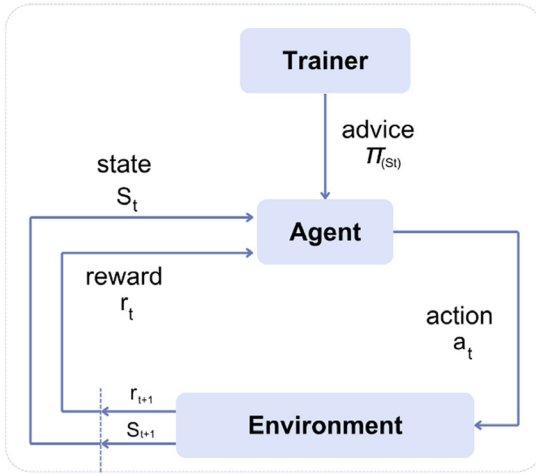


Figure 7.15 Reinforcement learning framework illustrating agent–environment interaction in an adsorption process.

between adsorption and desorption phases, adjusting flow rates in multi-bed systems, or optimising operating strategies under varying influent conditions.

An RL system consists of an environment (such as the adsorption column or reactor), possible states (e.g., concentration levels, flow rate settings), actions the agent can take, and a reward mechanism that provides feedback based on the performance outcome. The agent iteratively interacts with the environment and refines its decisions based on previous experience. This makes RL particularly useful in cases where the system is partially observable, non-linear, or stochastic, often in real adsorption systems.

7.3.3.1 Q-learning

Q-learning is one of the most widely used reinforcement learning algorithms, known for its simplicity and effectiveness. It works by learning a value function that estimates how good a specific action is in a particular state, even without a complete model of the environment (Clifton and Laber, 2020). Over time, the agent builds a decision map that guides it to select actions that lead to the highest cumulative reward. In adsorption-related applications, Q-learning can identify optimal strategies for operating adsorptive columns, such as determining the best times for switching columns or initiating regeneration cycles to extend efficiency.

For example, in a semi-continuous adsorption system handling wastewater treatment, Q-learning could be used to develop a control policy that decides when to introduce fresh adsorbent based on current concentration levels and flow dynamics. It adapts its decision-making as more feedback is collected, making it especially useful for applications with complex dynamics or uncertainty in influent characteristics.

7.3.3.2 Policy gradients

Policy gradient methods form another important class of reinforcement learning algorithms. Instead of learning the value of actions indirectly, as in Q-learning, policy gradient methods aim to learn the decision-making strategy, or policy, directly that maps states to actions (Sumiea *et al.*, 2024). This is particularly advantageous when dealing with environments that require fine-grained control or where the action space is continuous, such as regulating inflow concentrations or adjusting temperature profiles in an adsorption process.

In adsorption systems, policy gradients can be applied to tune parameters continuously during operation to improve system performance, such as maximising adsorption capacity or minimising breakthrough time. These highly flexible methods are often implemented with neural networks, making them suitable for integration with other deep learning architectures. The ability to learn complex, adaptive control strategies makes policy gradients an emerging tool in intelligent process engineering.

7.3.4 Hybrid artificial intelligence techniques

In addition to the individual AI methods, hybrid AI techniques have emerged as powerful tools by combining the strengths of multiple algorithms to enhance performance, accuracy, and adaptability. These approaches integrate different AI models to overcome the limitations of standalone methods and leverage their complementary capabilities. Researchers across various domains, including environmental engineering and water treatment, have increasingly adopted hybrid AI strategies to solve complex, non-linear, and data-intensive problems.

In adsorption processes, hybrid models are particularly valuable for improving prediction accuracy, optimising system parameters, and enhancing model robustness. Commonly used hybrid approaches include the combination of genetic algorithm (GA), particle swarm optimisation (PSO), RNN, and SVM. As illustrated in Figure 7.16, these techniques are often integrated to form powerful modelling frameworks, for example, using GA or PSO to optimise the hyperparameters of an SVM or training an RNN with optimised weights derived from an evolutionary algorithm.

Such hybrid systems have shown great promise in adsorption-based water and wastewater treatment applications, offering improved generalisation, faster convergence, and better handling of noisy or sparse data. By intelligently fusing multiple algorithms, hybrid AI techniques provide a flexible and adaptive approach to tackle the multi-dimensional challenges of modern adsorption system design and analysis.

7.3.5 Search and optimisation algorithms

7.3.5.1 Evolutionary algorithms

Genetic algorithm

The GA is a powerful heuristic optimisation technique inspired by natural selection and genetics principles. It is widely used to solve both constrained and unconstrained optimisation problems, particularly in systems where the solution space is complex, non-linear, or poorly defined – common characteristics in adsorption process modelling and parameter optimisation (Jong *et al.*, 1988).

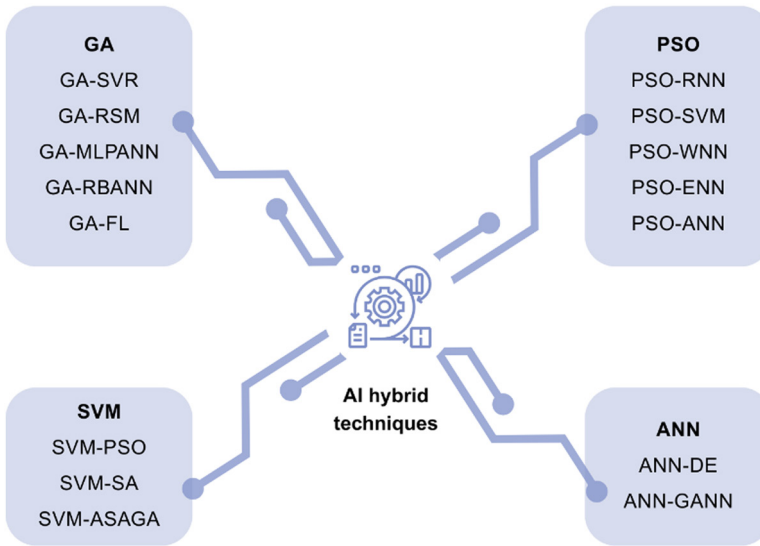


Figure 7.16 Artificial intelligence hybrid techniques.

A flowchart has been presented in Figure 7.17 for your reference. The algorithm begins by generating an initial population of potential solutions, often represented as chromosomes or strings, typically created randomly. Each chromosome encodes a possible solution to the problem, and its fitness is evaluated based on a predefined objective or fitness function. GA then iteratively evolves this population through three core genetic operations: selection, crossover (recombination), and mutation.

- Selection involves choosing the fittest individuals from the current population to pass their genes to the next generation.
- Crossover mimics biological reproduction by combining parts of two parent solutions to produce new offspring, introducing diversity and promoting better solution space exploration.
- Mutation introduces random alterations in individual genes, helping the algorithm avoid local optima and maintain genetic diversity within the population.

The process is repeated over several generations, with the population gradually evolving towards an optimal or near-optimal solution. The recursive nature of GA allows it to search vast and complex solution spaces efficiently, even when traditional gradient-based methods may fail.

GA has been successfully applied in adsorption studies to optimise experimental conditions (e.g., temperature, pH, adsorbent dose), tune ML model parameters, and fit complex isotherm or kinetic models. Its ability to handle multi-objective optimisation also makes it suitable for balancing trade-offs, such as maximising Q while minimising energy input or cost.

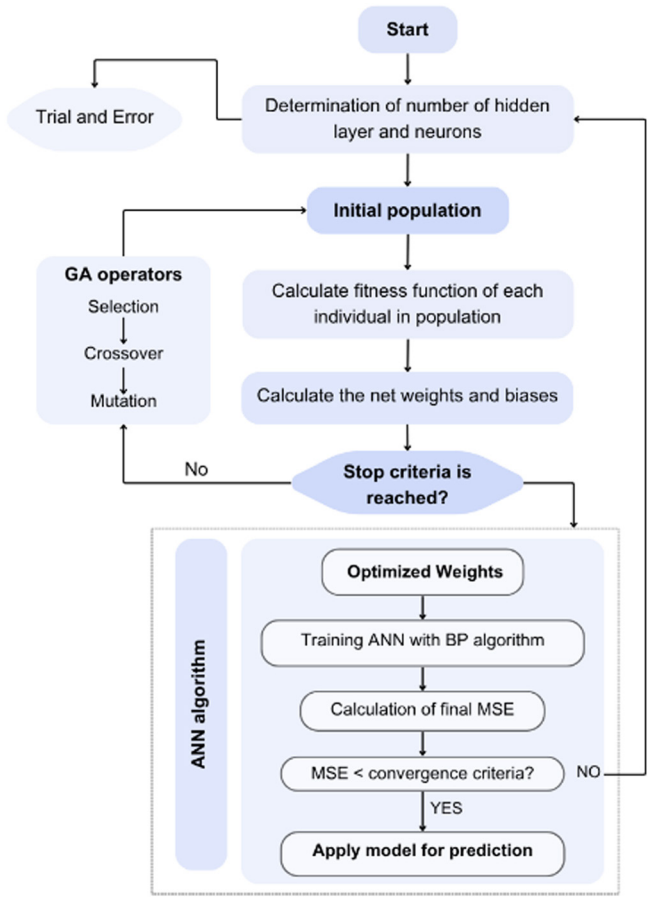


Figure 7.17 Genetic algorithm flowchart.

One of the advantages of GA is its flexibility in handling diverse types of variables (binary, categorical, or continuous), and its independence from the need for derivative information. However, carefully selecting population size, mutation rate, and crossover probability is crucial for achieving efficient convergence.

Genetic programming

Genetic programming (GP) is an evolutionary computation technique and an extension of GA, where the goal is to evolve computer programs or symbolic expressions that solve a specific problem (Zhang *et al.*, 2021). Unlike GA, which typically operates on fixed-length strings or numerical representations, GP evolves entire mathematical models, functions, or tree-like structures capable of capturing complex relationships among variables. This makes GP especially valuable for symbolic regression, model discovery, and non-linear system

modelling, which are highly relevant in adsorption science. GP begins with the random generation of an initial population of candidate programs, usually represented as tree structures, where nodes represent operations (e.g., addition, multiplication, logarithmic, or exponential functions) and leaves represent input variables or constants (Figure 7.18). These program trees are evaluated using a fitness function that quantifies how well each candidate solves the problem. GP then applies evolutionary operations such as selection, crossover, and mutation – like GA – to iteratively evolve the population towards better-performing solutions.

One of the major strengths of GP is its ability to automatically discover mathematical expressions or predictive models without requiring predefined model structures. This capability is particularly advantageous in adsorption research, where physical models such as isotherms or kinetics may not fully capture real-world systems' non-linear and multivariable nature. GP can be used to derive empirical correlations for Q, breakthrough behaviour, or rate constants directly from experimental data. For example, GP can generate interpretable equations describing how pH, temperature, contact time, and adsorbent dose influence adsorption performance. The resulting symbolic expressions provide accurate predictions and insight into the system's underlying behaviour, aiding scientific understanding and process design.

Despite its flexibility and power, GP can be computationally expensive and prone to bloat – a phenomenon where evolved programs become excessively

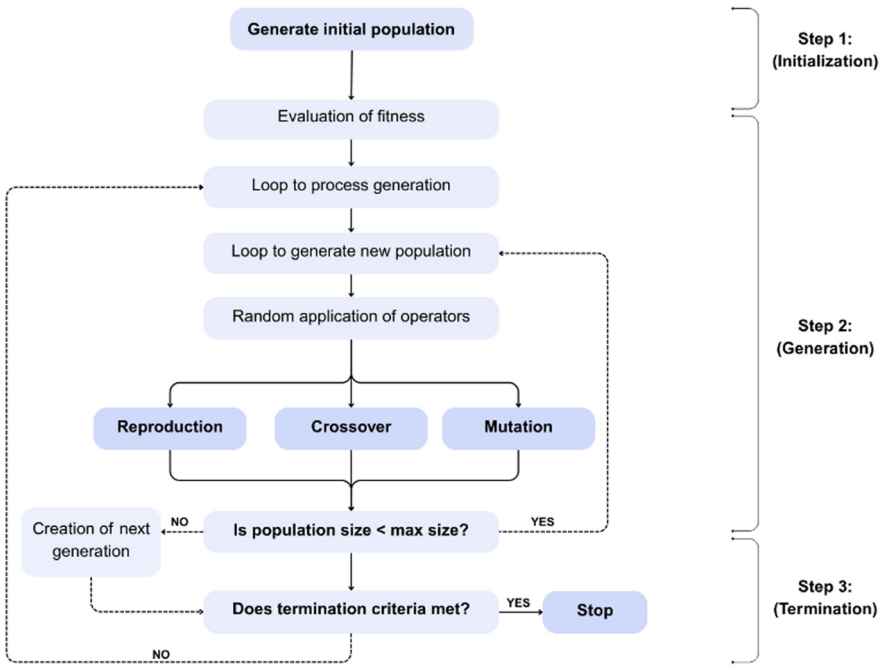


Figure 7.18 Genetic programming flowchart.

large without corresponding improvements in fitness. Strategies such as tree size control, parsimony pressure, or elitism are often employed to manage this issue.

7.3.5.2 Swarm intelligence

Particle swarm optimisation

Particle swarm optimisation (PSO) is a widely used, population-based AI technique to solve complex optimisation problems. Inspired by the social behaviour of birds flocking or fish schooling, PSO mimics individuals' collective movement and decision-making – called particles – within a population or swarm as they search for an optimal solution in a defined space (Gad, 2022). This algorithm is particularly valued for its simplicity, convergence efficiency, and ability to handle non-linear, multi-dimensional problems, making it highly applicable to adsorption process modelling and parameter optimisation.

In PSO, each particle represents a potential solution and is characterised by its position and velocity in the search space. The particles move through the solution space by adjusting their velocity and position iteratively based on two key experiences: their own best-known position (personal best or pBest) and the global best-known position (gBest) identified by the swarm. At every iteration, particles update their velocities based on these two guiding positions, encouraging convergence towards the best solution while maintaining exploration of the search space. The flowchart is provided in Figure 7.19. Mathematically, the position and velocity of each particle are updated using a set of equations influenced by inertia, cognitive, and social components. This balance allows particles to explore new areas (exploration) while refining

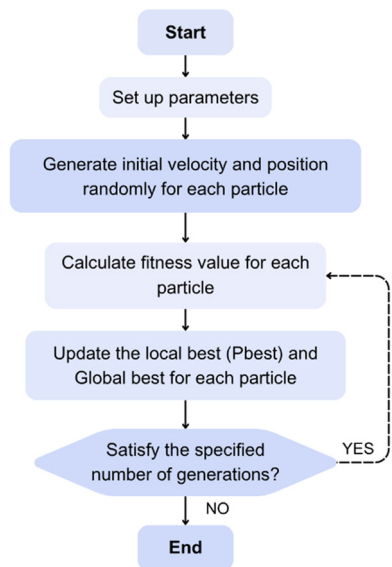


Figure 7.19 Particle swarm optimisation flowchart.

promising solutions (exploitation). The iterative process continues until a termination criterion is met, such as a maximum number of iterations or a satisfactory objective function value.

In adsorption studies, PSO has been used to optimise operating conditions – including pH, contact time, adsorbent dosage, and temperature – to maximise Q or removal efficiency. It is also employed for training ML models, tuning parameters in hybrid modelling approaches, and solving multi-objective optimisation problems where trade-offs between competing outcomes must be evaluated. One of PSO's key advantages is that it does not require gradient information, making it suitable for complex, non-differentiable, or noisy objective functions often encountered in experimental data. Furthermore, it typically requires fewer parameters to adjust than other evolutionary algorithms and can converge quickly to a high-quality solution.

7.3.6 Fuzzy logic

Fuzzy logic is an AI technique miming human reasoning and decision-making in uncertain, imprecise, or vague environments (Lu *et al.*, 2024). Unlike traditional binary logic, which classifies information into strictly true or false categories, fuzzy logic allows for degrees of truth – ranging between 0 and 1 – enabling it to model systems that involve ambiguity and complexity,

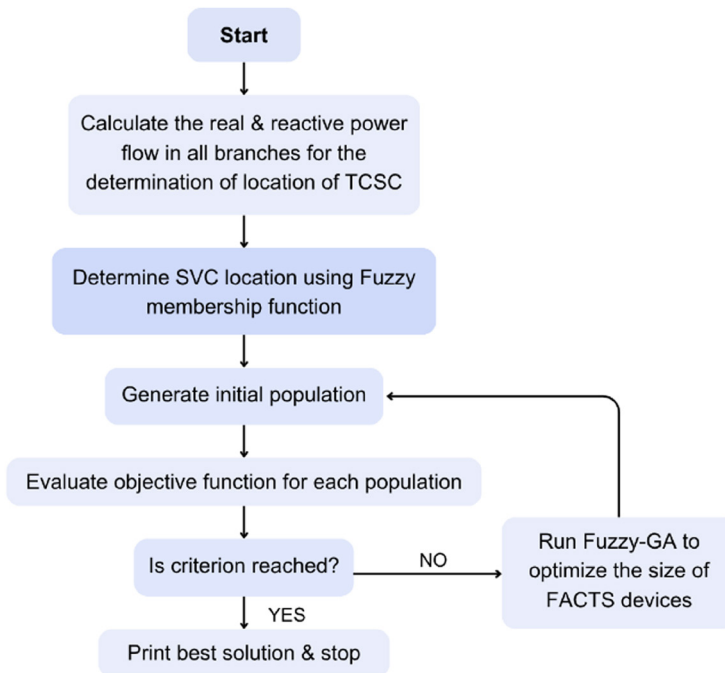


Figure 7.20 Fuzzy logic flowchart.

Table 7.1. Comparison of artificial intelligence/machine learning techniques in adsorption studies.

AI/ML Technique	Applications	Advantages	Limitations
DT	Classification of adsorbents, prediction of Q	Easy to interpret, handles both numerical and categorical data	Prone to overfitting, sensitive to small data variations
ANN	Non-linear modelling of adsorption isotherms and kinetics, process optimisation	Can model complex relationships, high prediction accuracy	Requires large datasets, low interpretability (black box)
k-NN	Prediction of adsorption outcomes based on similar cases	Simple to implement, no training phase required	Computationally expensive for large datasets, sensitive to noisy or irrelevant features
SVM	Classification of adsorbent types, regression modelling of adsorption parameters	Effective in high-dimensional spaces, it works well with small datasets	Requires careful kernel selection, less interpretable
RF	Prediction of adsorption performance, feature importance ranking	Reduces overfitting, handles missing data, identifies key variables	Slower for large datasets, less interpretable than individual trees
SOM	Clustering of adsorbents and experimental conditions, data visualisation	Useful for pattern recognition and dimensionality reduction	Requires careful tuning of map parameters, interpretability can be subjective
PCA	Dimensionality reduction, pre-processing for machine learning models	Reduces data complexity, helps visualise variable influence	Assumes linearity, does not capture non-linear relationships
GA	Optimisation of adsorption conditions, model parameter tuning	Global optimisation ability, handles complex and multi-modal functions	Computationally intensive, sensitive to parameter settings
GP	Symbolic regression for deriving adsorption models, model discovery	Produces interpretable mathematical models, flexible modelling framework	Can produce overly complex solutions (bloat), slow convergence
PSO	Parameter optimisation in adsorption systems, ANN/SVM tuning	Easy to implement, fast convergence, few parameters to tune	Can get trapped in local optima, less effective for discrete problems

see Figure 7.20. This characteristic makes fuzzy logic particularly suitable for adsorption processes, which often involve uncertainties in experimental conditions, measurement variability, and non-linear interactions between process parameters.

At its core, fuzzy logic operates on fuzzy sets, where elements can partially belong to more than one set, with a certain membership degree. For example, instead of assigning a temperature as 'high' or 'low', fuzzy logic can define it as *partially high* and *partially medium* with associated membership values. The fuzzy logic system typically includes four main components:

- Fuzzification – Converts crisp input values (e.g., pH, contact time, dosage) into fuzzy sets using membership functions.
- Rule base – Contains a set of 'if–then' rules that represent expert knowledge or empirical relationships (e.g., *If pH is low and contact time is high, adsorption is moderate*).
- Inference engine – Evaluates the rules based on fuzzy inputs and determines the degree to which each applies.
- Defuzzification – Converts the fuzzy output to a crisp value for practical interpretation and decision making.

In adsorption studies, fuzzy logic has been widely used for process control, parameter estimation, multi-objective decision making, and predictive modelling. For instance, it can help predict Q based on uncertain or incomplete input data, classify adsorbent performance levels, or aid in selecting optimal operating conditions in the presence of conflicting objectives.

One of the key advantages of fuzzy logic is its interpretability, as it provides rule-based outputs that human experts can understand and modify. Moreover, it can handle qualitative information and expert intuition, which are difficult to incorporate into traditional mathematical models. Fuzzy logic is also easily integrated with other AI techniques such as neural networks and GA, leading to hybrid models like neuro-fuzzy systems, which combine learning ability with interpretability.

Overall, fuzzy logic offers a flexible, intuitive, and robust framework for handling uncertainty and complex relationships in adsorption systems, making it a valuable tool for researchers and engineers (Table 7.1).

7.4 SELECTING AN ARTIFICIAL INTELLIGENCE/MACHINE LEARNING MODEL FOR ADSORPTION

The selection of an appropriate AI or ML model for adsorption applications depends on several key factors, including the problem's nature, the dataset's type and size, the descriptors selected, and the computational resources available. A systematic understanding of these considerations ensures the model is accurate, interpretable, and relevant to adsorption system optimisation (Lowe *et al.*, 2022).

7.4.1 Identifying the type of problem

Before choosing an ML algorithm, it is essential to determine the type of problem being addressed. In adsorption studies, most applications fall under three categories:

- Regression, where the goal is to predict continuous numerical outcomes such as Q (mg/g) or R (%).
- Classification, where predictions involve discrete categories, for example, whether an adsorbent is effective or not under specific conditions.
- Clustering, where the algorithm groups similar data points based on patterns in the data without predefined labels, is often used in screening new materials or grouping pollutants.

In most cases, regression tasks dominate, as they align with experimental goals focused on predicting system performance across a range of operational variables.

7.4.2 Constructing the dataset: Top-down vs. bottom-up

The performance of any ML model is highly dependent on the quality and structure of the dataset used (Yuan *et al.*, 2025). Two primary approaches exist for dataset construction in adsorption modelling:

- *Top-Down Approach*: This is the most used strategy in experimental adsorption research. Datasets are constructed using measurable process parameters such as pH, contact time, initial pollutant concentration, adsorbent dosage, temperature, and agitation speed. These are input descriptors, while outputs include performance metrics like Q, R, or breakthrough time. Algorithms such as multiple linear regression (MLR), SVM, DTs, and k-NN are commonly used in this approach. However, the top-down method often suffers from limited dataset size and variability due to experimental constraints.
- *Bottom-Up Approach*: This approach uses computational simulations or quantum chemical calculations (e.g., density functional theory) to derive datasets. Descriptors may include d-band centre, p-band centre, electronegativity, molecular weight, or ionisation energy of the adsorbent or pollutant. Output variables typically include adsorption energy or Gibbs free energy change. Because it allows high-throughput data generation, this approach is well-suited for training data-intensive models such as ANN, RF, adaptive neuro-fuzzy inference systems (ANFIS), and gradient boosting machines.

7.4.3 Selecting input features and target outputs

Any ML model's predictive power and interpretability depend significantly on selecting input features (independent variables) and target outputs (dependent variables). In the top-down approach, input features should be selected based on their known influence on adsorption behaviour, and may include pH, contact time, initial concentration, and adsorbent dose. Output variables are typically chosen as Q or R, due to their direct relevance to performance evaluation.

In the bottom-up strategy, inputs often relate to atomic-scale or molecular descriptors derived from simulation or theoretical calculations, while outputs may involve thermodynamic or electronic properties like adsorption energy. In both approaches, techniques like PCA and sensitivity analysis (SA) can reduce dimensionality and identify the most significant variables.

7.4.4 Matching the model to the dataset

Model selection should consider dataset characteristics, including data volume, noise levels, and the complexity of relationships among variables. Simpler models like MLR, SVM, and DT are preferable for small or moderately sized datasets, especially when model transparency is desired. These models perform well when the relationship between input and output is primarily linear or involves well-understood interactions.

On the other hand, more complex or non-linear relationships, especially common in adsorption systems involving multiple interacting variables, may be better captured by models such as ANN, RF, or ANFIS. These models can learn hidden patterns in high-dimensional data, though they require larger datasets and more computing power. For classification tasks, algorithms like logistic regression, DTs, and ensemble classifiers (e.g., RF or gradient boosting) are widely used.

7.4.5 Evaluating model performance

Regardless of the model chosen, it must be evaluated using appropriate performance metrics. For regression tasks, common metrics include:

- ***R*² (coefficient of determination):** Measures the proportion of variance in the output explained by the model.
- **RMSE (root mean squared error):** Captures the standard deviation of prediction errors, penalising large errors more heavily.
- **MAE (mean absolute error):** Provides the average magnitude of errors without considering direction.

For classification tasks, the following are used:

- **Accuracy:** Measures overall correctness.
- **Precision and Recall:** Evaluate how well the model identifies true positives and minimises false positives/negatives.
- **F1 Score:** Harmonic mean of precision and recall, useful for imbalanced datasets.
- **AUC-ROC:** Indicates the model's ability to distinguish between classes.

Using multiple metrics is recommended to fully understand model performance and avoid misleading conclusions from a single indicator.

7.4.6 Practical guidelines for implementation

To implement ML effectively in adsorption research, it is recommended to start by clearly defining the objective (e.g., prediction, classification, optimisation). Researchers should then select or construct a dataset suited to the problem type and available data, ensuring all variables are relevant and of high quality.

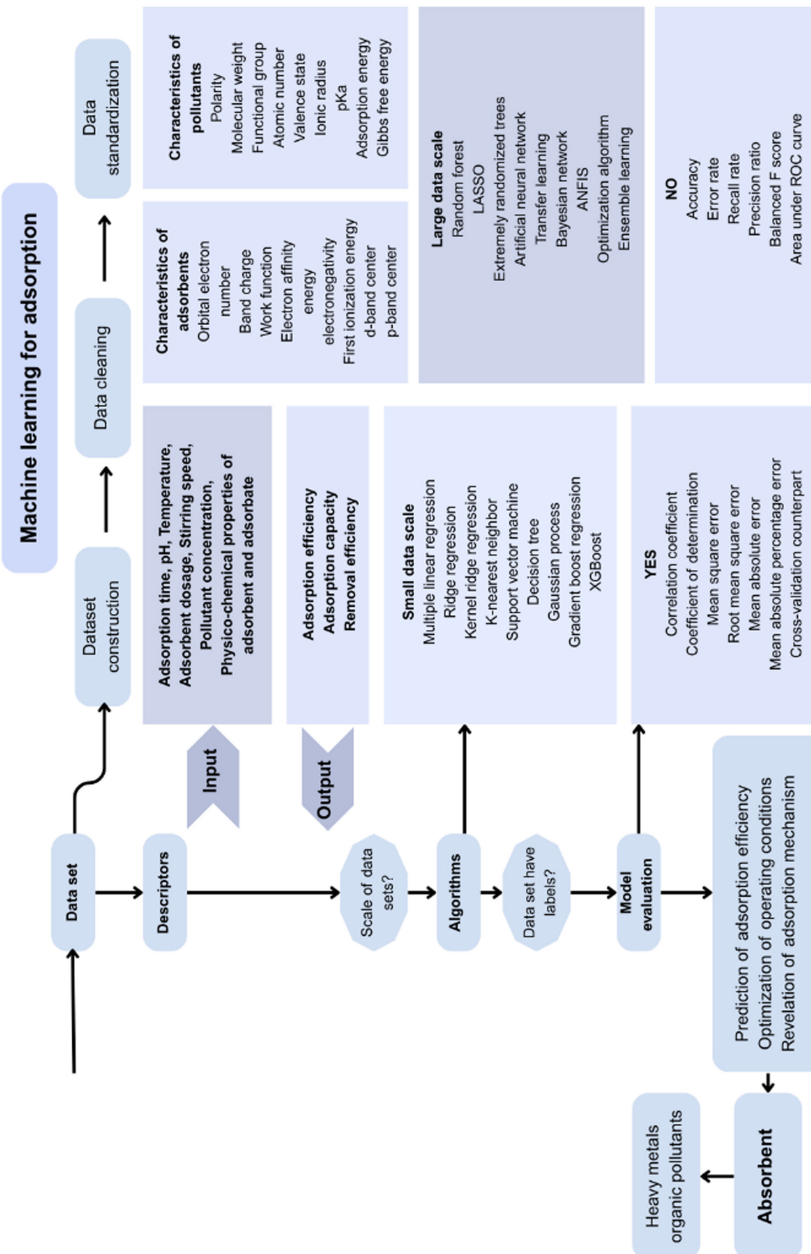


Figure 7.21 Guidelines for artificial intelligence/machine learning applications in adsorption processes.

Feature selection techniques should be applied to enhance model performance and reduce overfitting. Based on the system's complexity and data availability, an appropriate model should be selected, ranging from interpretable linear regression to complex non-linear ANN. Finally, model performance should be validated using robust metrics and cross-validation techniques and compared against baseline or alternative models.

The flowchart in Figure 7.21 summarises the model selection process, offering a quick-reference guide for applying ML techniques effectively in adsorption studies.

7.5 SOFTWARE PACKAGES FOR ARTIFICIAL INTELLIGENCE/ MACHINE LEARNING SIMULATIONS

AI and ML are increasingly being applied to model, predict, and optimise adsorption processes, offering a data-driven alternative to conventional simulations. These approaches can efficiently handle non-linear relationships, large datasets, and multivariate systems common in adsorption studies. Various software platforms and libraries have been developed to implement AI/ML algorithms (see Figure 7.22) that cover different levels of expertise and application complexity, from simple regression models to advanced deep learning architectures.

Google Colab is a cloud-based Python environment that allows users to write and execute ML code interactively without requiring local installation. It supports GPU acceleration and integrates seamlessly with shared AI libraries, making it an ideal platform for prototyping models in adsorption studies, such as adsorption isotherm prediction or material screening.

Python has become the *de facto* programming language for AI/ML due to its simplicity, extensive libraries, and community support. With packages such as Scikit-learn, TensorFlow, and PyTorch, users can implement algorithms ranging



Figure 7.22 Software packages for artificial intelligence/machine learning simulations.

from linear regression and SVMs to DNN and reinforcement learning. These tools are extensively used to develop predictive models, surrogate models for Q, kinetics, and even material informatics.

Scikit-learn is a robust Python library with classification, regression, clustering, and model evaluation tools. It is particularly effective for adsorption applications where interpretable and scalable models are required using structured datasets.

TensorFlow and PyTorch are advanced deep learning frameworks widely used in scientific ML. These platforms enable the development of DNN, convolutional architectures, and sequence models, which can predict adsorption performance based on material descriptors, operating conditions, or molecular fingerprints.

MATLAB also offers a well-developed ML toolbox for classification, regression, clustering, and dimensionality reduction. Its graphical interface and ease of integration with experimental data make it suitable for researchers who prefer low-code environments for building adsorption models.

RapidMiner and Orange Data Mining are visual workflow-based platforms that allow users to perform ML without extensive coding. These tools are especially suitable for those with limited programming backgrounds, enabling easy drag-and-drop creation of classification or regression models to analyse adsorption performance datasets.

KNIME (Konstanz Information Miner) is another visual data analytics platform that supports various ML algorithms and data pre-processing steps. Its modular structure allows seamless integration with Python and R scripts, making it useful for advanced data manipulation, feature engineering, and model validation in adsorption studies.

Weka is a Java-based ML suite that includes a collection of algorithms for data mining tasks. It is particularly well-suited for educational use and quick prototyping of adsorption prediction models using structured input datasets.

7.6 CASE STUDY

In this case study, a research work by Soares *et al.* (de Miranda Ramos Soares *et al.*, 2020) was explored, where ML models were employed to predict the adsorption of methylene blue dye using orange bagasse, a residual agricultural biomass. ML is particularly valuable for modelling adsorption processes due to the non-linear and complex relationships among multiple influencing factors. The dataset was generated through 202 independent batch experiments (each performed in triplicate) to evaluate the Q and R of methylene blue dye from aqueous solutions. Orange bagasse was used as adsorbent, and the temperature, pH, adsorbent dosage, contact time, salinity, initial dye concentration and rotation speed were systematically varied. Post-treatment, the samples were centrifuged, and the remaining dye concentration was measured via UV–vis spectrophotometry. The Q and R were then calculated.

7.6.1 Data exploration

We began with an exploratory analysis using Pearson correlation heatmaps to uncover patterns and gain preliminary insights into the adsorption process (see Figure 7.23). These visualisations mapped the relationships among

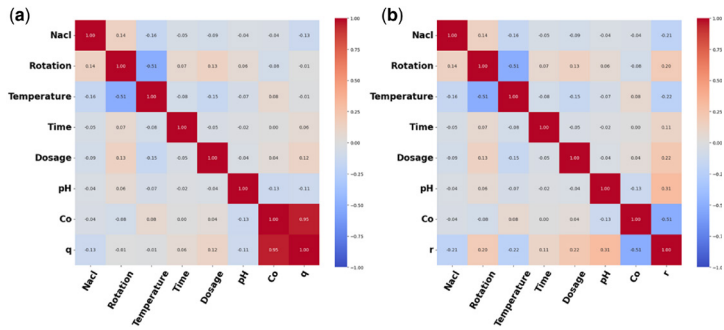


Figure 7.23 Heatmap indicating the relationship between process variables and (a) adsorption capacity, (b) percentage removal.

key experimental variables, such as NaCl concentration, rotation speed, temperature, contact time, adsorbent dosage, pH, and initial dye concentration (C_o) against two response variables: Q and R.

- C_o exhibited a strong positive correlation ($r = 0.95$) with Q, indicating that higher C_o typically leads to greater adsorption per unit mass of orange bagasse.
- However, C_o showed a moderate negative correlation ($r = -0.51$) with R, suggesting a decline in performance due to possible saturation effects at higher dye concentrations.
- Other variables, such as NaCl concentration, contact time, and pH, showed weak correlations with both responses, implying that their linear influence on outcomes is limited in this dataset.
- Temperature and rotation speed displayed a moderate negative correlation, potentially due to the controlled experimental design rather than a causal relationship.

These patterns point towards a non-linear and complex system where interactions among variables may not be fully captured through linear models or simple statistical correlations. Strong, weak, and even inverse relationships suggest that some models may perform better than others depending on their ability to handle non-linearity, variable importance, and noise.

The performance of four distinct ML models, RF, k-NN, SVM, and DT, is determined and compared. Based on the exploratory data analysis results, it is hypothesised that non-linear models with the ability to capture complex interactions will likely outperform simpler models:

- RF is expected to perform well, especially for Q, due to its ability to capture feature importance and handle non-linearity without overfitting on noisy variables.
- SVM may be effective if the right kernel function is chosen, particularly in datasets where certain trends are evident but not linearly separable.
- k-NN might perform adequately, especially in regions of the dataset where local similarity (e.g., similar pH or initial concentration) drives similar responses.
- Decision Trees, while interpretable, may struggle with generalisation – especially for the more variable response, R – but could still reveal clear decision boundaries in simpler relationships.

By comparing their accuracy with both training and testing data, we will evaluate how well our exploratory data analysis guided expectations align with actual model performance. This modelling exercise not only enhances predictive understanding but also serves to verify the insights derived through exploratory analysis.

7.6.2 Random Forest model

The Random Forest model was trained to predict both Q and R. Its performance was evaluated using parity plots and time-series comparisons:

- **Training Set**: Excellent accuracy was observed with $R^2 = 0.9936$ (Q) and $R^2 = 0.9618$ (R).
- **Test Set**: Performance remained strong for Q ($R^2 = 0.9688$), but declined for R ($R^2 = 0.5636$), indicating more variability in removal efficiency under unseen conditions.

The parity plots, shown in Figure 7.24, illustrate the relationship between the measured and RF-predicted values for training and testing datasets. In the training set, the RF model achieved excellent predictive accuracy, as indicated by high coefficients of determination ($R^2 = 0.9936$ for Q and $R^2 = 0.9618$ for R), with most points clustering tightly along the ideal $y = x$ line. This demonstrates that the model effectively learned the underlying patterns in the data. For the testing set, the RF model maintained strong performance for Q ($R^2 = 0.9688$), while the prediction of R was somewhat less accurate ($R^2 = 0.5636$). The lower R^2 for R in the test set suggests that while the model generalises well for Q, there may be more variability or complexity in predicting R under unseen conditions.

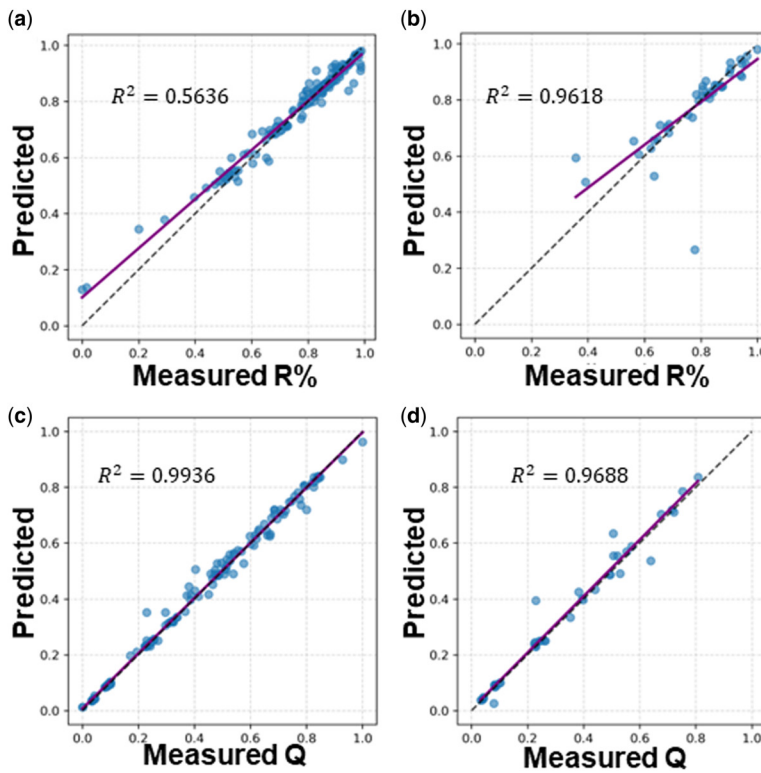


Figure 7.24 Parity plots comparing random forest model predictions to experimental values: (a) percentage removal for the test set, (b) training set, (c) adsorption capacity for the training set, and (d) test set.

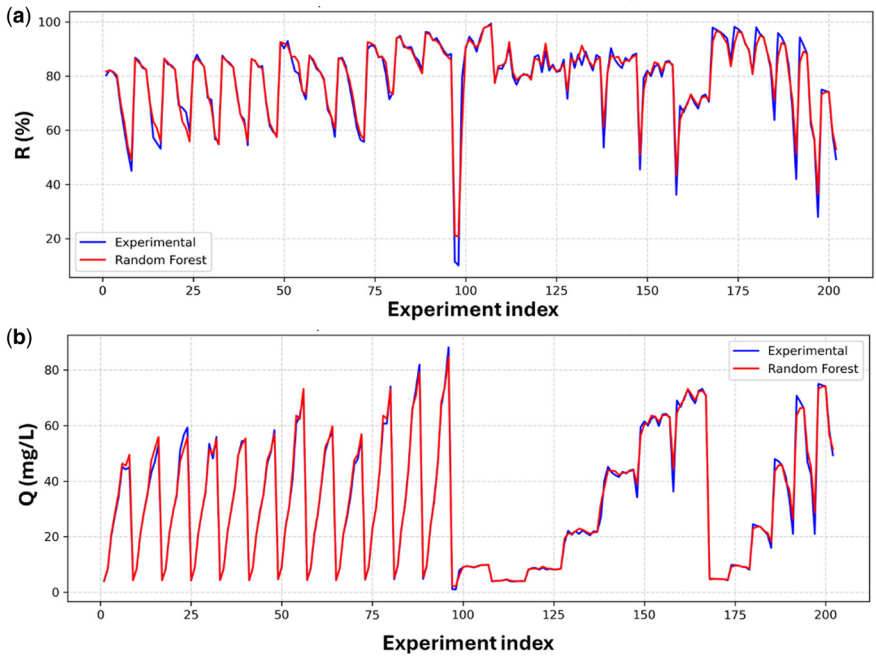


Figure 7.25 Comparison of experimental and random forest model predictions across all adsorption experiments: (a) percentage removal versus experiment index, (b) adsorption capacity versus experiment index.

Figure 7.25 compares the experimental and RF-predicted values of R and Q across all experiments. The close alignment between the blue (experimental) and red (RF prediction) lines for both metrics demonstrates the model's ability to reproduce the experimental trends and fluctuations across various conditions. Minor deviations are observed in certain regions, particularly for R, but overall, the RF model captures the primary dynamics of the adsorption process.

7.6.3 k-Nearest neighbour neural network

The k-NN model was similarly applied to predict Q and R. Performance metrics included:

- **Training Set**: $R^2 = 0.9864$ (R), $R^2 = 0.9982$ (Q)
- **Test Set**: $R^2 = 0.7923$ (R), $R^2 = 0.9521$ (Q)

The parity plots in Figure 7.26 show the relationship between measured and k-NN-predicted values for both R and Q. For R, the k-NN model achieved high accuracy in the training set ($R^2 = 0.9864$), with predictions closely matching the measured data. In the test set Figure 7.23, the predictive power decreased

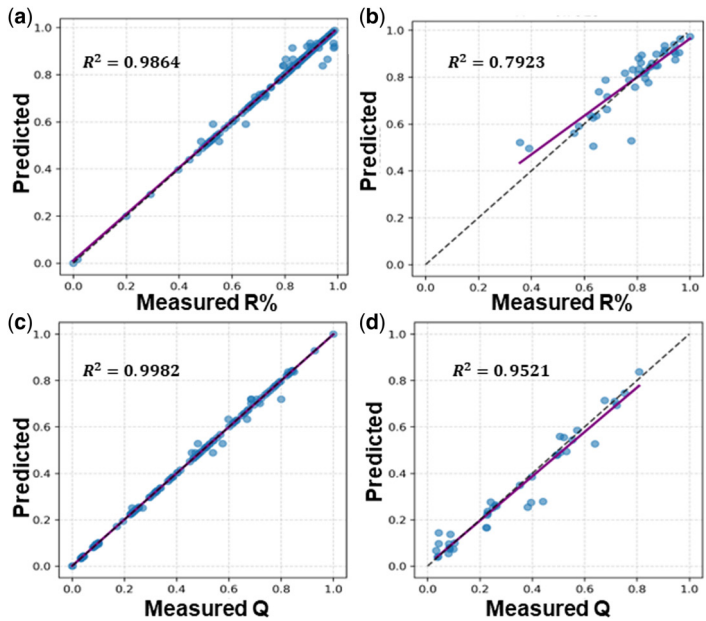


Figure 7.26 Parity plots comparing k-nearest neighbour model predictions to experimental values (a) percentage removal for the training set and (b) the test set, (c) adsorption capacity for the training set, and (d) the test set.

($R^2 = 0.7923$), indicating some loss of generalisation when exposed to unseen data, but still capturing the main trends. For Q, the k-NN model performed exceptionally well in training ($R^2 = 0.9982$) and testing ($R^2 = 0.9521$) sets, with predicted values aligning very closely with experimental results.

Figure 7.27 illustrates the comparison between experimental and predicted values for R and Q across all experiments. The red and blue (experimental) lines overlap substantially for both metrics, demonstrating that the k-NN model can track the experimental variations and capture the underlying patterns in the data. Minor discrepancies are observed, particularly in regions with rapid fluctuations, but the overall agreement is strong.

7.6.4 Decision tree

The DT model produced the following results:

- *Adsorption Capacity:* Strong performance with $R^2 = 0.9689$ (training) and $R^2 = 0.9439$ (testing)
- *Removal Efficiency:* Moderate predictive power with $R^2 = 0.7607$ (training) and $R^2 = 0.3346$ (testing)

The parity plots (Figure 7.28(a–d)) show the relationship between measured and DT-predicted values for both R and Q. For Q, the DT model demonstrates

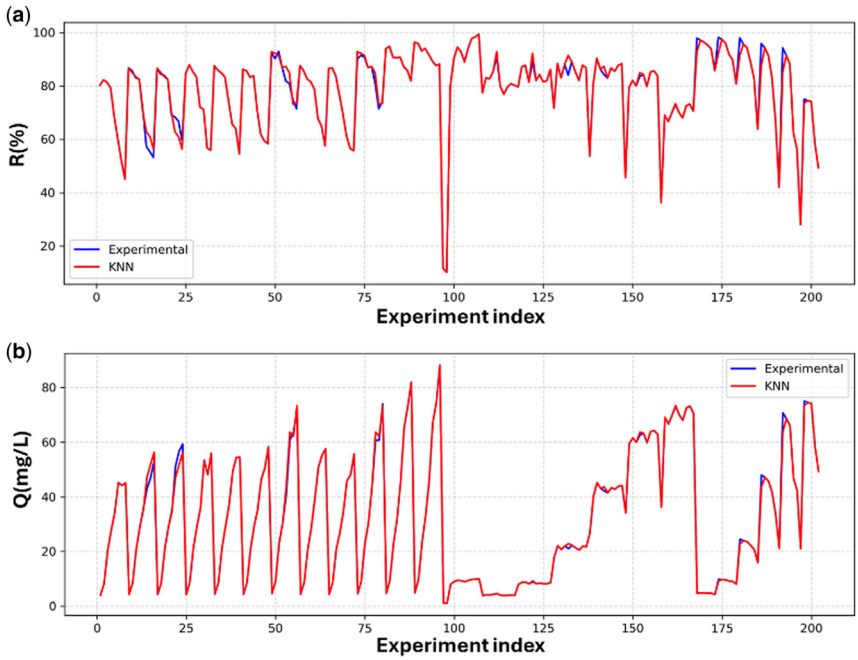


Figure 7.27 Comparison of experimental and k-nearest neighbour model predictions across all adsorption experiments (a) percentage removal versus experiment index, (b) adsorption capacity versus experiment index.

strong predictive performance, with high coefficients of determination in both the training ($R^2 = 0.9689$) and testing ($R^2 = 0.9439$) datasets. The data points are closely aligned along the ideal $y = x$ line, indicating that the model captures the underlying trends in the data and generalises well to unseen samples. For R, the DT model achieves moderate accuracy, with R^2 values of 0.7607 for training and 0.3346 for testing, suggesting that while the model can capture the main trends in the training data, its performance on new data is more limited, likely due to the inherent complexity and variability of the R response.

The time-series plots (see Figure 7.29) further compare experimental and DT-predicted values for R and Q across all experiments. The red (DT prediction) and blue (experimental) lines generally follow similar trends, especially for Q, where the agreement is strong throughout the experimental range. The DT model tracks the main fluctuations for R but exhibits some deviations, particularly in regions with abrupt changes or high variability. The deviations occur because decision trees struggle to capture abrupt, complex variations in removal efficiency due to their piecewise nature, combined with the high sensitivity of R to interacting process variables and possible experimental fluctuations.

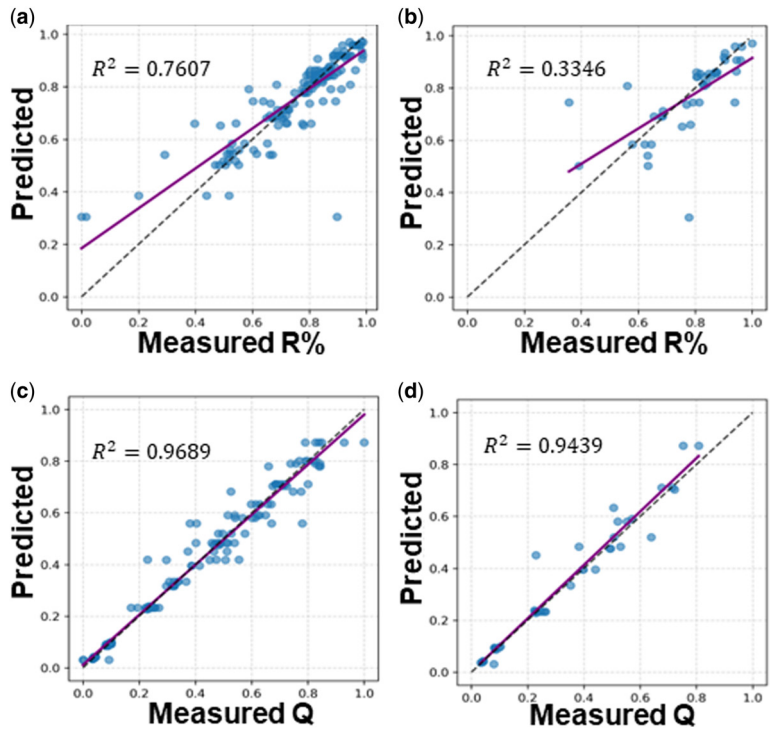


Figure 7.28 Parity plots compare decision tree model predictions to experimental values (a) percentage removal for the training set and (b) the test set, (c) adsorption capacity for the training set, and (d) the test set.

7.6.5 Support vector machine

The SVM model was trained with the same dataset and demonstrated consistent and robust predictive ability:

- **Percentage Removal:** $R^2 = 0.8072$ (test), $R^2 = 0.7840$ (training)
- **Adsorption Capacity:** $R^2 = 0.9524$ (test), $R^2 = 0.9557$ (training)

SVM showed strong capability in modelling both metrics, effectively capturing experimental fluctuations across a broad parameter range.

The parity plots (see Figure 7.30) display the relationship between the measured and SVM-predicted values for both R and Q. For R, the SVM model achieves strong predictive performance, with R^2 values of 0.8072 and 0.7840 for the respective test and training datasets. This indicates that the model can capture the main trends in the data, with most points clustering around the ideal $y = x$ line, though some scatter is present. For Q, the SVM model demonstrates even higher accuracy, as shown by R^2 values of 0.9524 and 0.9557, with the predicted values closely matching the measured data.

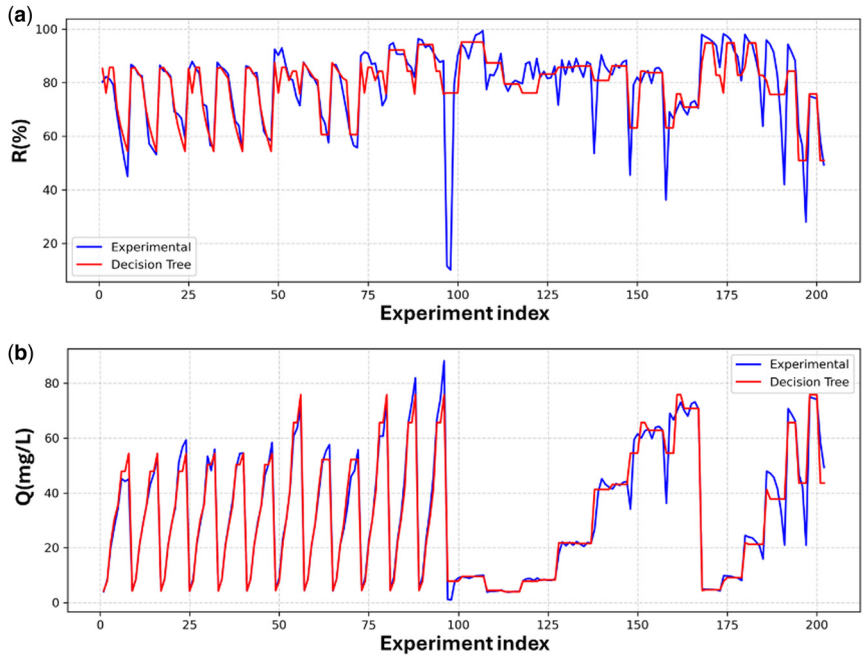


Figure 7.29 Comparison of experimental and decision tree model predictions across all adsorption experiments (a) percentage removal versus experiment index, (b) adsorption capacity versus experiment index.

The time-series plots (Figure 7.31) provide a direct comparison between the experimental (blue) and SVM-predicted (red) values for R and Q across all experiments. Minor deviations are observed, particularly in regions with rapid changes or high variability, but the overall agreement remains strong.

7.6.6 Comparative insights

The comparative analysis of ML models – RF, k-NN, DT, and SVM for predicting the adsorption performance of methylene blue on orange bagasse highlights how different algorithms address the challenges posed by non-linear, multivariable processes. Informed by the exploratory data analysis, which revealed strong correlations (e.g., between initial dye concentration and Q) and complex interactions, we anticipated that models capable of handling non-linear relationships and local variations would perform better. The modelling outcomes confirm many of these expectations.

RF and k-NN consistently demonstrated superior predictive accuracy for Q, which aligns with EDA predictions. RF achieved R^2 values exceeding 0.96 across training and test sets, validating its strength in capturing global patterns and mitigating overfitting through ensemble averaging. k-NN outperformed other models in some scenarios, reaching R^2 values of 0.9982

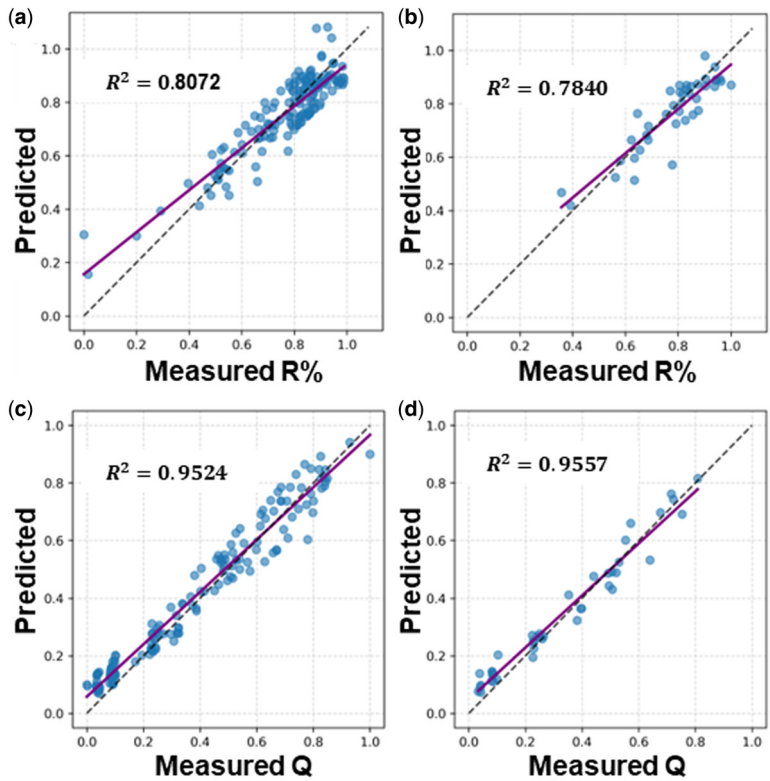


Figure 7.30 Parity plots comparing support vector machine model predictions to experimental values (a) percentage removal for the training set and (b) the test set, (c) adsorption capacity for the training set, and (d) the test set.

(training) and 0.9521 (testing) for Q, showcasing its effectiveness in modelling local data behaviour, especially where subtle shifts in input features influence the outcome.

For R, k-NN emerged as the most reliable model on the test set ($R^2 = 0.7923$), confirming the hypothesis that instance-based approaches are more adaptive when response variables exhibit high variability or are sensitive to local feature space distributions. Though excellent for Q, RF displayed reduced generalisation for R ($R^2 = 0.5636$ in testing), likely due to R's susceptibility to abrupt response shifts not fully captured by tree-based ensemble averaging.

SVM also performed robustly, particularly for Q, with R^2 values above 0.95 in training and testing. For R, it maintained moderate performance ($R^2 \approx 0.80$), suggesting that SVM's kernel-based flexibility allows it to model non-linear separability well when the data distribution is relatively clean. However, it may be less resilient to noise or highly irregular data clusters than k-NN.

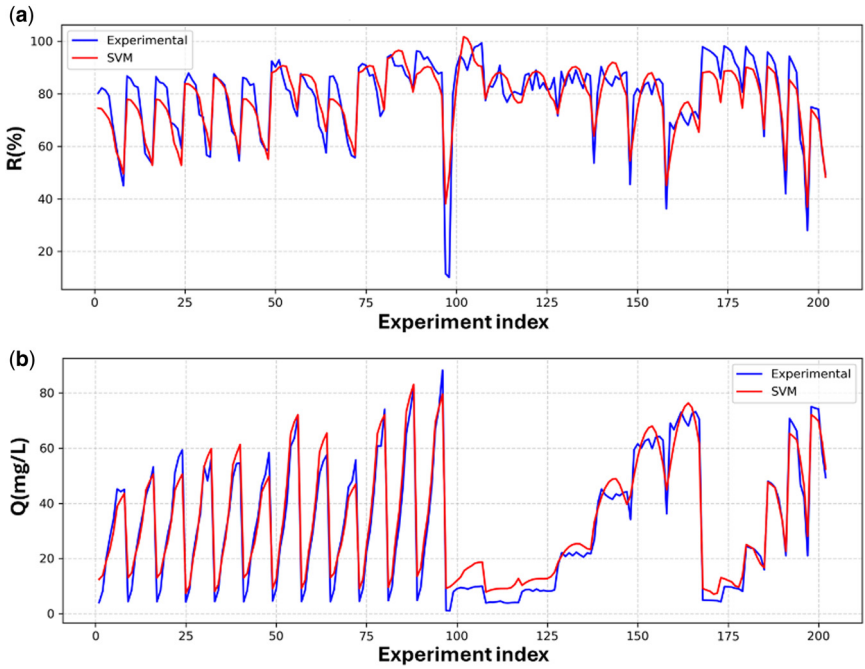


Figure 7.31 Comparison of experimental and support vector machine model predictions across all adsorption experiments (a) percentage removal versus experiment index, (b) adsorption capacity versus experiment index.

In contrast, the DT model lagged in predictive accuracy, especially for R on unseen data ($R^2 = 0.3346$), aligning with the EDA-based prediction that DT may struggle with generalisation. While DT achieved decent performance for Q in both training and testing sets, it appeared to be overfitted to training data. It lacked robustness in modelling complex or noisy variations in R. Nonetheless, its interpretability and speed make it valuable for identifying decision rules and feature importance in preliminary analyses.

These differences stem from each algorithm's underlying mechanism:

- RF and k-NN excel in capturing non-linearity, with RF offering global robustness and k-NN favouring local adaptability.
- SVM performs well on structured, moderately noisy data, especially when relationships are not linearly separable.
- DT is best reserved for simpler or highly interpretable scenarios and may be a first-pass diagnostic tool.

7.7 SUMMARY

AI and ML have become powerful tools for modelling, optimising, and automating adsorption-based water and wastewater treatment processes. This

chapter provided a comprehensive overview of how AI/ML techniques are applied to improve pollutant removal, reduce experimental costs, and offer predictive insights for system performance. many AI/ML models – including ANN, SVM, DTS, RF, and hybrid systems like ANFIS – have successfully predicted the adsorption behaviour of pollutants such as dyes, heavy metals, pharmaceuticals, and pesticides. These models are particularly effective in capturing non-linear relationships and optimising process conditions.

The chapter also outlined a structured approach to selecting appropriate ML models based on problem type (regression, classification, clustering), dataset origin (top-down or bottom-up), and key descriptors. Emphasis was placed on selecting meaningful input variables and evaluating model performance using metrics like R^2, RMSE, and MAE to ensure accuracy and reliability. While AI/ML offer clear advantages, challenges remain, such as limited datasets, risk of overfitting, and lack of standardised benchmarks. Future efforts should improve dataset quality, adopt hybrid AI models, and validate predictions through pilot-scale studies. Establishing standardised frameworks for model comparison will be key to wider adoption. Finally, software tools and case studies were discussed to demonstrate the real-world application of these techniques. AI/ML approaches are rapidly becoming essential for advancing adsorption research and developing more efficient, intelligent water treatment systems.

doi: 10.2166/9781789063943 _0199

Chapter 8

Adsorption process simulation and optimisation

8.1 INTRODUCTION

Adsorption is a multi-parametric physicochemical process governed by a complex interplay of operational variables such as solution pH, contact time, initial solute concentration, system temperature, and adsorbent dosage. The nonlinear and often synergistic interactions among these factors make accurate prediction and optimisation of adsorption performance challenging. Conventional isotherm and kinetic models – such as Langmuir, Freundlich, and pseudo-second-order rate expressions – offer limited explanatory power when applied to systems where multidimensional variable interdependencies are significant. Consequently, there is a growing need for advanced modelling approaches to accommodate nonlinearity, multicollinearity, and variable interactions in process systems.

Optimisation of adsorption processes entails identifying the most favourable set of operational and design parameters that maximise performance metrics such as removal efficiency, adsorption capacity, or energy efficiency. Traditional optimisation via the one-variable-at-a-time (OVAT) method is inherently limited and inefficient, neglects variable interactions, and demands many experimental iterations. In contrast, multivariate optimisation frameworks – particularly those based on response surface methodology (RSM) and artificial neural networks (ANNs) – offer a more rigorous and statistically robust approach to experimental design, model generation, and performance prediction (Elfghi, 2016).

RSM employs polynomial regression models to approximate complex response surfaces, enabling the identification of optimal conditions using a minimal experimental dataset (Anfar *et al*., 2020). Techniques such as central composite design (CCD), Box–Behnken design (BBD), and Plackett–Burman design facilitate structured exploration of the design space. However, RSM

© 2026 IWAP. This is an Open Access book chapter distributed under the terms of the Creative Commons Attribution Licence (CC BY-NC-ND 4.0) which permits copying and redistribution for non-commercial purposes with no derivatives, provided the work is properly cited (https://creativecommons.org/licenses/by-nc-nd/4.0/). The chapter is from the book *Computational Techniques for Modelling and Simulating Adsorption Processes for (Waste)Water Treatment*, A. Yadav and P. Labhasetwar (Authors).

is generally limited to modelling lower-order nonlinearity and requires prior assumptions about the functional form of input–output relationships.

ANNs, on the other hand, provide a data-driven alternative that bypasses the need for predefined mathematical formulations. ANNs can approximate highly nonlinear input–output mappings through supervised learning algorithms by training on empirical datasets (Reynel-Ávila *et al.*, 2022). Their adaptability and predictive accuracy suit them, particularly for complex adsorption systems with incomplete mechanistic understanding or strong variable coupling.

In parallel, computational fluid dynamics (CFD) has revolutionised the simulation of transport phenomena in adsorption systems. CFD solves the fundamental governing equations of fluid mechanics – namely, the Navier–Stokes equations – coupled with scalar transport equations for species, energy, and momentum. CFD simulations provide spatially and temporally resolved insights into flow regimes, boundary layer behaviour, turbulence characteristics, and intra- and interphase mass transfer phenomena (Liu *et al.*, 2024). CFD can model intraparticle diffusion, film resistance, and non-Newtonian fluid behaviour when applied to porous media and multiphase systems, significantly enhancing adsorption equipment's design, scale-up, and operational troubleshooting.

This chapter presents an integrated view of adsorption process modelling and optimisation, focusing on applying CFD for transport modelling and RSM and ANN for process optimisation. Special attention is given to methodological implementation, algorithmic selection, and comparative analysis of predictive accuracy and computational efficiency. A comprehensive framework for simulation and optimisation of adsorption processes is proposed by leveraging mechanistic and data-driven modelling paradigms.

8.2 HISTORY AND EARLY DEVELOPMENTS

The foundation of CFD lies in the mathematical formulation of fluid motion, particularly the Navier–Stokes equations, which were completed in the mid-19th century when Sir George Stokes introduced the viscous terms (Figure 8.1) (Kelvin, 1903). Early progress in numerical fluid mechanics was driven by pioneers such as Lewis Fry Richardson (Richardson, 1911), who proposed the first finite difference method for solving partial differential equations, and the trio Courant, Friedrichs, and Lewy (Courant *et al.*, 1928), who formulated the CFL condition – a stability criterion critical for explicit numerical schemes.

The first significant strides in computer-based fluid modelling were made in the 1950s at Los Alamos National Laboratory, where the T3 group, led by Francis H. Harlow, developed several numerical schemes (e.g., Marker-and-Cell, SHASTA) for simulating transient two-dimensional incompressible flow (Harlow, 2004; Johnson, 1996). This era marked the inception of modern CFD. In 1967, John Hess and Smith introduced one of the first three-dimensional fluid flow models (Hess & Smith, 1967). The development of pressure-based algorithms continued with the seminal work of Brian Spalding and Suhas V. Patankar at Imperial College London. Patankar's introduction of the SIMPLE (Semi-Implicit Method for Pressure-Linked Equations) algorithm in the 1970s (Patankar & Spalding, 1972) became a cornerstone in incompressible flow modelling.

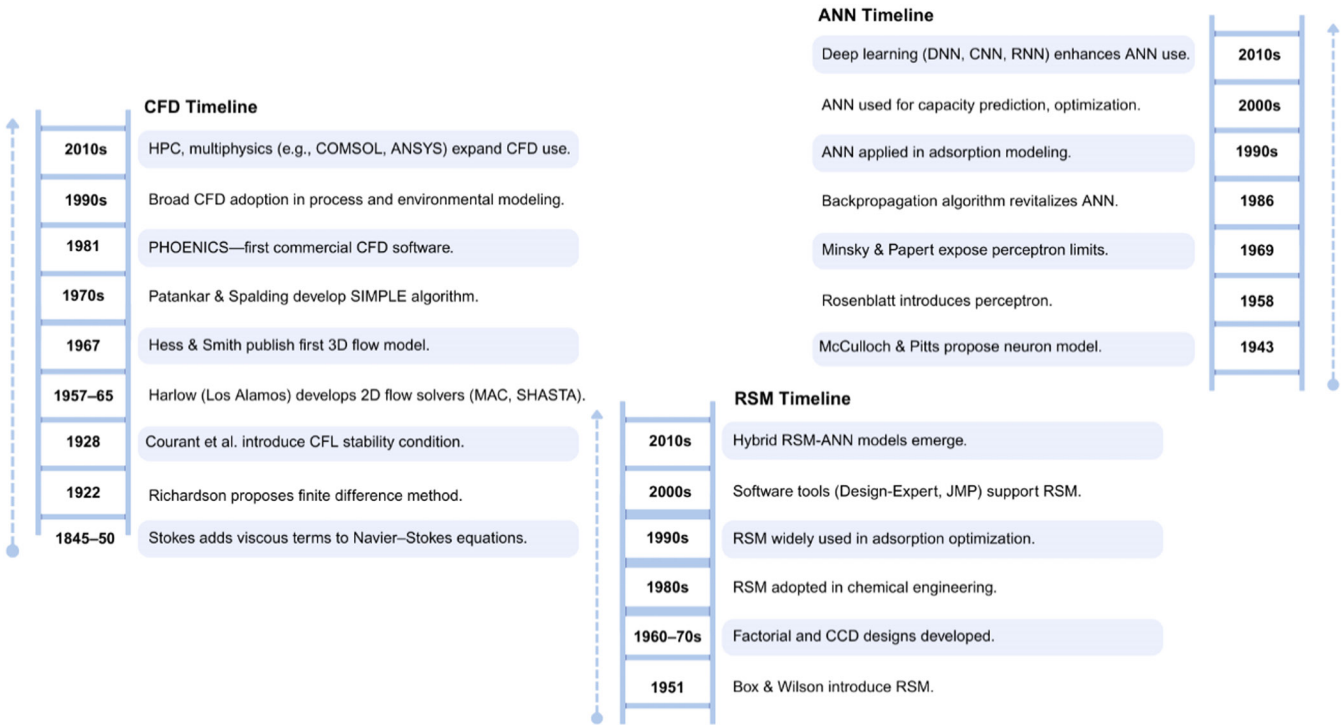


Figure 8.1 A brief history of computational fluid dynamics, artificial neural network and response surface methodology development.

The release of PHOENICS in 1981 marked the beginning of commercial CFD software. Since then, advances in computational hardware, numerical solvers, and turbulence modelling have positioned CFD as a vital tool for simulating momentum, heat, and mass transfer in complex process systems – including adsorption columns, packed beds, and porous media.

Parallel to the evolution of CFD, data-driven modelling and statistical optimisation techniques began to take root, particularly for systems where first-principles modelling proved infeasible or intractable.

RSM emerged from the statistical design of experiments (DoE) field during the 1950s. Initially developed by Box and Wilson (Bučko *et al.*, 2005), RSM was conceived to optimise chemical processes through empirical polynomial regression models, often of second order. The approach gained traction for modelling response variables influenced by several factors and for identifying optimal process settings with a minimal number of experiments. By the 1980s and 1990s, RSM had become a widely adopted technique in adsorption studies, particularly for evaluating sorbent performance, interaction effects, and process robustness under varying operational conditions.

ANNs trace their conceptual origin to McCulloch and Pitts in 1943, who developed a simplified computational model of a biological neuron. The resurgence of interest in ANNs came with the development of the backpropagation algorithm in the 1980s, enabling multilayer networks to learn from data. The capacity of ANNs to model highly nonlinear, multivariate systems made them especially attractive for chemical and environmental engineering applications in the 1990s and 2000s. In adsorption research, ANNs have been used to predict adsorption capacity, simulate breakthrough curves, and optimise multi-variable systems where mechanistic equations are unavailable or too complex.

Today, CFD, RSM, and ANN represent complementary tools within the adsorption research domain. CFD provides spatially resolved, physics-based flow and mass transport simulations, while RSM and ANN offer efficient data-driven models for system-level optimisation. Their integration into the adsorption process modelling and design toolkit reflects physical science and artificial intelligence convergence, enabling high-fidelity simulations, predictive modelling, and optimisation under uncertainty.

8.3 PROCESS SIMULATION OF THE ADSORPTION PROCESS

The behaviour of adsorption systems involving fluid flow, mass transfer, and thermal effects can be modelled using CFD. CFD solves partial differential equations (PDEs) derived from physical laws – conservation of mass, momentum, and energy – along with constitutive laws like Fourier's (heat conduction), Fick's (mass diffusion), and Newton's (viscosity). Due to the complexity of realistic systems, numerical solutions are essential, as analytical ones are limited to idealised scenarios.

CFD handles flow regimes such as steady/unsteady, compressible/incompressible, laminar/turbulent, and single/multiphase. For adsorption,

it enables accurate prediction of flow patterns, pressure drop, temperature profiles, and concentration distributions within columns, packed beds, and porous domains.

One can use mathematical formulations in PDEs with boundary/initial conditions (BCs/ICs) or experimental testing to solve fluid flow problems (Patankar, 2018). The principal laws of physics (mass conservation, momentum conservation, and energy conservation), as well as phenomenological laws like Fourier's law of heat conduction, Fick's law of mass diffusion, Newton's viscosity law, and Hooke's law, are applied to derive the mathematical formulations. Under some simplified assumptions, the mathematical equations regulating the physics of fluid flows are solved analytically; in most cases, however, they are solved numerically. Experiments are frequently costly, slow, sequential, and one-use only.

8.3.1 Stages of computational fluid dynamics modelling

8.3.1.1 Pre-processing

The initial step of the numerical simulation involves defining the solver settings, setting up basic physics, and developing a trustworthy model to describe the domain mesh production. At this point, the computer is informed of the issue, which includes:

- Determining the problem's shape and creating a structured or unstructured mesh that will be used to evaluate the solution at its points (cells);
- Choosing suitable physical models, such as those for turbulence, and supplying the right physical constants, like the fluid viscosity, and
- Providing the problem's ICs/BCs.

8.3.1.2 Solver/solution

The solver is the second phase in the numerical simulation analysis. The numerical schemes, convergence control, and computation are set using the CFD solver. The fundamentals of preprocessing must be understood in order to get good results. The next stage is to set various numerical parameters in the code and set it to run on the computer. This involves spatial discretisation, temporal (time) discretisation, and solution of the resultant systems of algebraic equations.

8.3.2 Post-processing

The last stage of a CFD study is the post-processing phase. At this stage, the results are examined. Quantitative data analysis and flow field visualisation are possible with CFD post-processing. CFD simulation codes can plot and display the flow variables on a line, point, or other plane of interest. Statistical reporting techniques can be used to calculate quantitative outputs such as flux balance, average heat-transfer coefficients, and forces and moments.

This entails, understandably, presenting the generated data. A graphical display on a computer screen, value extraction at mesh points in the domain, animation of the solution's sequential time steps, or using virtual reality to allow the user to enter the solution are examples of post-processing techniques.

8.3.3 Solution algorithms in computational fluid dynamics

Figures 8.2 and 8.3 show working of CFD's two general solution algorithms: pressure-based and density-based (Miettinen and Siikonen, 2015). The pressure-based approach was historically developed for low-speed incompressible flows, while the density-based approach was mainly used for high-speed compressible flows. Although both methods have been extended to solve a wide range of flow conditions (i.e., from incompressible to compressible), the density-based approach may be more accurate in some cases of high-speed compressible flows. In both methods, the velocity field is obtained from the momentum equations. In the pressure-based approach, the pressure field is obtained by solving a Poisson equation for pressure (also known as a pressure-correction equation) derived by manipulating the continuity and momentum equations. In the density-based approach, the continuity equation is used to obtain the density field, while the pressure field is determined from an equation of state.

In any CFD simulation, the reliability and robustness of the numerical solution are governed by four fundamental numerical properties: accuracy, consistency, stability, and convergence.

Accuracy refers to how closely the numerical solution approximates the exact or analytical solution of the governing equations. Although exact

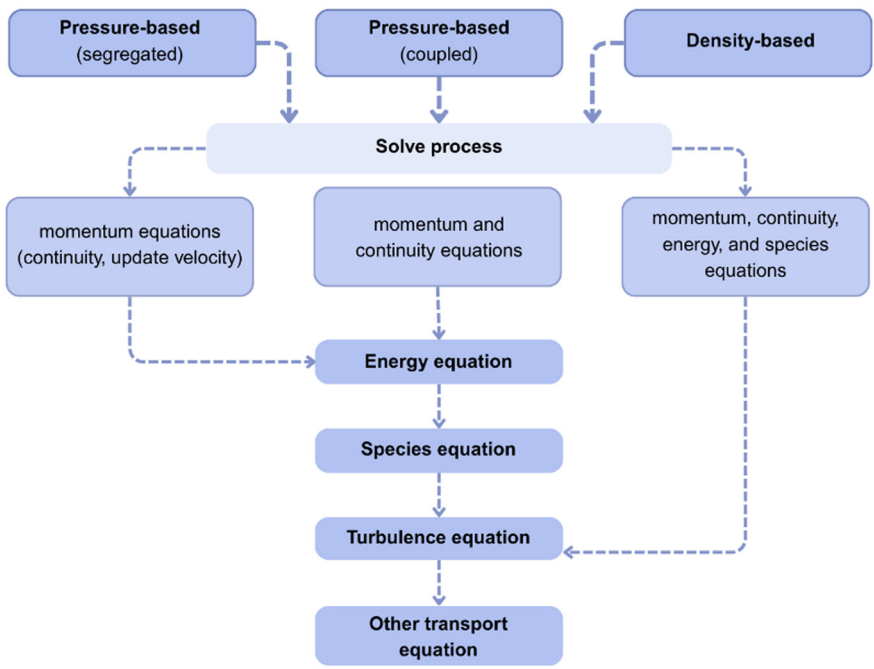


Figure 8.2 Solution algorithms in computational fluid dynamics.

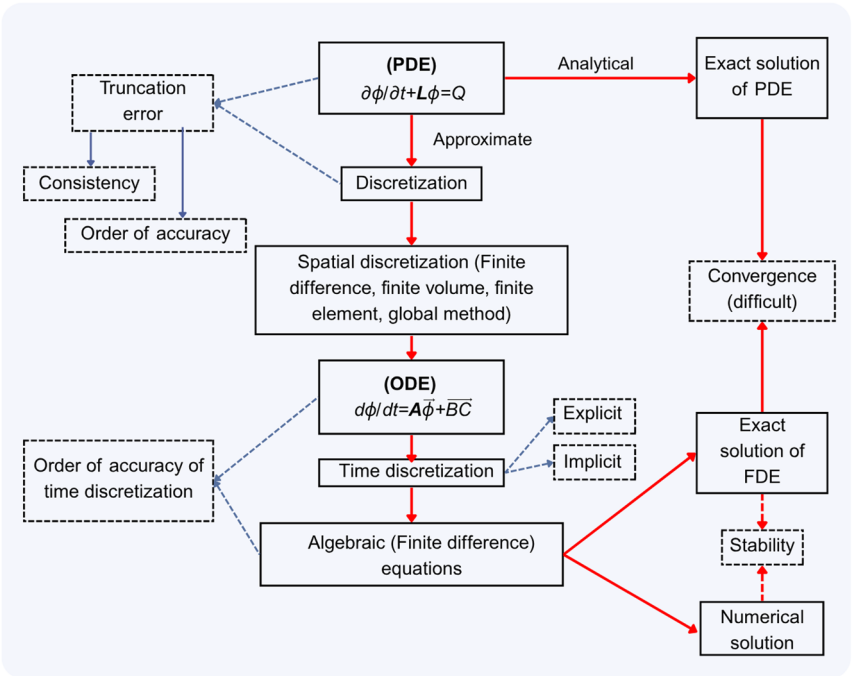


Figure 8.3 Overall solution process for a partial differential equation.

solutions are rarely known for complex systems, accuracy is often assessed by comparing numerical results with experimental data or benchmark solutions. The discretisation method and mesh resolution significantly influence accuracy.

Consistency ensures that the discretised equations approximate the original PDEs as the mesh size (Δx) approaches zero. In other words, as the grid is refined, the numerical scheme must correctly replicate the behaviour described by the continuous governing equations. A scheme that fails this requirement may not yield meaningful results, even on very fine meshes.

Stability is the property that prevents numerical errors – whether due to rounding, truncation, or initial perturbations – from growing uncontrollably during computation. An unstable method may cause divergence or produce physically meaningless results. Stability is often maintained by choosing appropriate time steps, discretisation schemes, and solver settings.

Convergence is achieved when the iterative solution process leads to a steady state where further iterations do not cause significant changes in the solution. Additionally, mesh convergence – or grid independence – is confirmed when refining the mesh no longer alters the numerical results appreciably. A well-designed CFD simulation satisfies all four properties, ensuring the solution is mathematically sound and physically realistic.

8.3.4 Discretisation methods

8.3.4.1 Finite difference method

The finite difference method (FDM) is one of the earliest numerical techniques developed for solving differential equations and has been widely used in early CFD applications (Mazumdar, 2015; Lomax *et al.*, 2002). In FDM, the computational domain is represented by a structured grid of nodes, and derivatives in the governing equations are approximated using finite differences between function values at these nodes. For example, a second-order derivative can be approximated using central difference schemes. The method is relatively easy to implement and computationally efficient for simple geometries with regular boundaries.

However, FDM has significant limitations. Its reliance on structured, orthogonal grids makes it poorly suited for complex geometries, irregular domains, or domains involving multiple materials and BCs. Additionally, it can be challenging to ensure the conservation of mass, momentum, or energy in problems involving non-uniform meshes. Despite these drawbacks, FDM still finds niche applications, especially in academic studies or problems involving rectangular geometries, where grid generation is straightforward.

8.3.4.2 Finite-element method

Finite-element method (FEM) is a more flexible and mathematically rigorous approach compared to FDM (Mazumdar, 2015; Lomax *et al.*, 2002). In FEM, the domain is divided into a finite number of non-overlapping subdomains, called elements, which can be of various shapes – triangles, quadrilaterals, tetrahedra, or hexahedra. The dependent variables (velocity, pressure, or temperature) are approximated within each element using interpolation functions based on nodal values. These approximations are substituted into a variational formulation of the governing equations, often using weighted residual or Galerkin methods.

FEM is particularly advantageous in handling complex geometries, irregular boundaries, and multiphysics problems such as fluid–structure interaction. It allows for local mesh refinement and offers high accuracy, especially in structural mechanics and heat-transfer simulations. However, FEM tends to be computationally more expensive and complex to implement for fluid dynamics problems. Ensuring global conservation properties – especially for mass and energy – requires special care, and commercial CFD solvers using FEM are fewer than those based on other methods.

8.3.4.3 Finite volume method

The finite volume method (FVM) is the most widely used discretisation technique in commercial and academic CFD codes (Mazumdar, 2015; Lomax *et al.*, 2002). Unlike FDM or FEM, FVM directly enforces conservation laws over discrete control volumes. The computational domain is divided into small, finite volumes (cells), and the integral form of the governing equations is applied to each volume (Figure 8.4). Fluxes of mass, momentum, and energy across the surfaces of each control volume are computed, ensuring strict conservation within each cell.

FVM can be used with structured and unstructured meshes, making it highly versatile and suitable for complex industrial geometries. It also

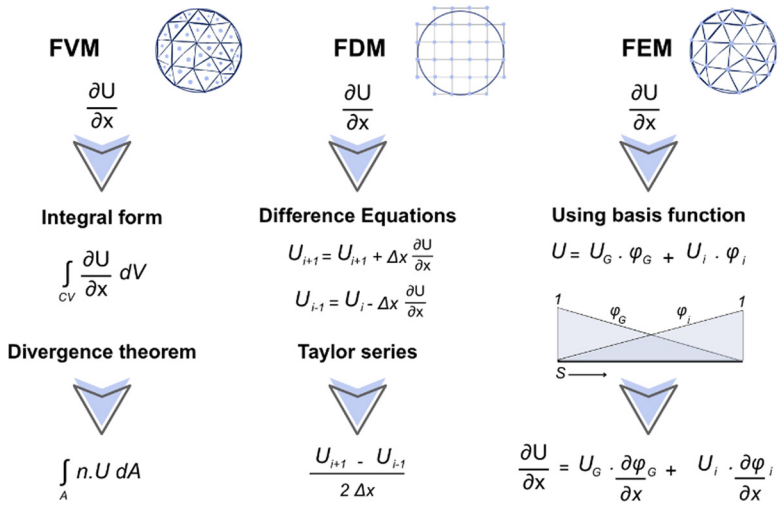


Figure 8.4 Discretisation methods in computational fluid dynamics.

handles non-uniform grids and discontinuities more effectively. The method is relatively straightforward and provides good accuracy while preserving physical conservation properties, which are critical for fluid flow and transport simulations. These advantages have made FVM the preferred method in leading CFD software packages such as ANSYS Fluent, Open FOAM, and STAR-CCM+.

8.3.5 Meshing

Meshing is critical in any CFD simulation. It involves dividing the computational domain into discrete elements or cells over which the governing equations of fluid flow, mass transfer, and energy transport are numerically solved. A CFD simulation's accuracy, stability, and computational efficiency highly depend on the mesh quality and appropriateness.

The mesh converts a complex geometry – such as an adsorption column, packed bed, or porous medium – into a finite set of control volumes or elements where equations are approximated. Each control volume must adequately capture the physical velocity, pressure, concentration, and temperature gradients. In adsorption modelling, where mass transfer at the fluid–solid interface or within porous domains is critical, careful meshing is especially important to resolve boundary layers, interstitial flow paths, and sharp concentration fronts.

Meshes can be broadly classified into structured, unstructured, and hybrid types (Mahmoud *et al.*, 2024) (Figure 8.5).

Structured mesh consists of a regular grid pattern with a logically rectangular or curvilinear arrangement. It is easy to generate in simple geometries and provides faster convergence due to lower numerical diffusion. However, applying in complex geometries such as packed beds or irregular porous domains becomes difficult.

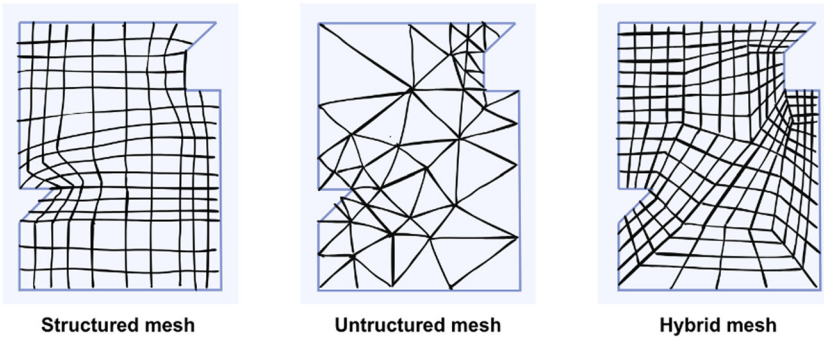


Figure 8.5 Meshes can be classified into structured, unstructured, and hybrid types.

The unstructured mesh allows for arbitrary connectivity between elements and is well-suited for complex or irregular geometries. It typically consists of triangles (in 2D) or tetrahedra (in 3D) but may include other shapes like polygons and polyhedra. Although more flexible in geometry handling, unstructured meshes may require finer resolution and increased computational effort to achieve similar accuracy.

A hybrid mesh combines structured and unstructured mesh regions within the same domain. This approach allows high accuracy and reduced computational cost by applying structured grids in simple areas and unstructured elements in complex regions. It is useful in systems like packed beds with a central symmetry axis and irregular wall regions.

Regarding element types, CFD software typically supports hexahedral, tetrahedral, prismatic (wedge), and polyhedral elements (Figure 8.6). Hexahedral elements are preferred in regions with well-aligned flow because they offer better numerical accuracy. Tetrahedral elements are easier to generate automatically and are suitable for complex 3D geometries, although they may require mesh refinement. Prismatic or wedge elements often resolve boundary layers near walls, capturing steep gradients in concentration or velocity. Polyhedral elements, available in some advanced solvers, offer a good balance between accuracy and computational cost due to their flexibility and better control of volume shapes.

An important aspect of meshing is the boundary layer mesh, which consists of multiple thin layers of cells adjacent to solid walls. This mesh refinement is necessary to resolve sharp gradients in velocity, concentration, or temperature near the wall, particularly in adsorption systems where wall interactions (e.g., surface diffusion or heat transfer) are significant.

Mesh quality must also be evaluated in terms of skewness, aspect ratio, and orthogonality metrics. Poor mesh quality can lead to convergence issues and inaccurate results. In practice, mesh independence studies are conducted to ensure that further refinement does not significantly alter the results, thereby confirming the numerical robustness of the simulation.

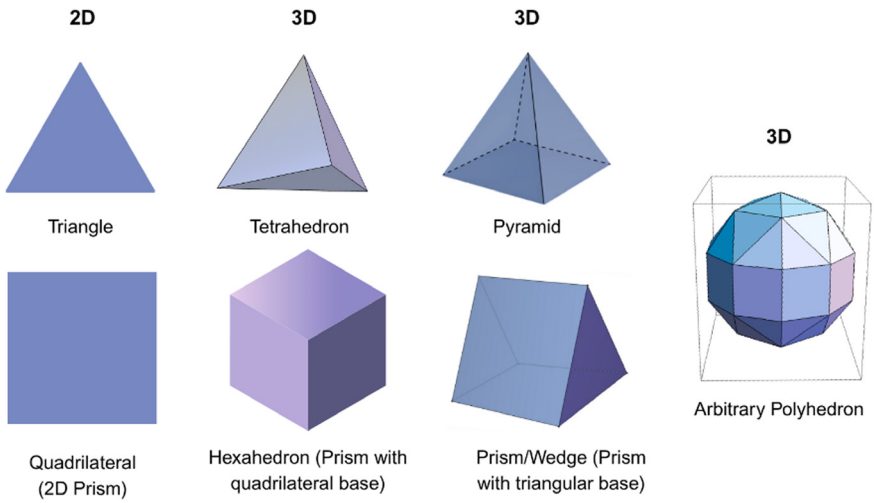


Figure 8.6 Hexahedral, tetrahedral, prismatic (wedge), and polyhedral elements.

For adsorption systems involving porous domains or packed beds, mesh generation may require advanced techniques such as porous media modelling (using a homogenised approach) or geometry-based meshing (resolving each pellet or pore). The selection depends on the scale of modelling – macroscale column design versus microscale pore-level transport.

8.4 GOVERNING EQUATIONS

Detailed computational modelling of adsorption systems requires solving strongly coupled PDEs that describe the conservation of mass, momentum, species, and energy. These equations are supplemented by constitutive relations for fluxes, adsorption kinetics, equilibrium isotherms, and auxiliary relations for calculating dependent variables. The complete modelling framework is outlined in Figure 8.7.

When applied to a fluid continuum, these governing laws relate the rate of change of fluid properties (such as velocity, temperature, or concentration) to physical driving forces, enabling systematic analysis of transport phenomena.

Several strongly coupled equations must be solved for detailed modelling of the adsorption process, which can be classified into five types: mass, momentum, species, and energy conservation equations; constitutive equations; reaction kinetic relations; equilibrium equations; and auxiliary relations for variable calculation.

These conservation laws connect the rate of change of a desired fluid attribute to outside influences when applied to a fluid continuum and can be thought of as follows (Tey *et al.*, 2017).

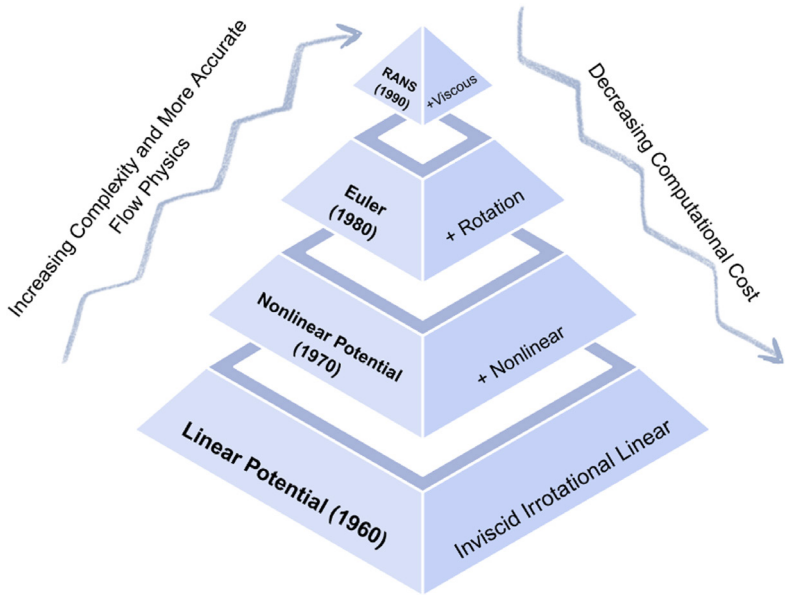


Figure 8.7 Hierarchy of governing equations for computational fluid dynamics-based adsorption modelling.

8.4.1 Continuity equation (mass conservation)

The continuity equation ensures the conservation of mass in a fluid system. For a general, compressible flow:

$$\frac{\partial \rho}{\partial t} + \frac{\partial}{\partial x_i}(\rho \boldsymbol{u_i}) = 0 \tag{8.1}$$

where $\boldsymbol{u}$ is the velocity vector, and ρ is the density.

In incompressible flow, the density ρ is constant, and the equation simplifies to

$$\frac{\partial \boldsymbol{u_i}}{\partial x_i} = 0 \tag{8.2}$$

8.4.1.1 Momentum equation (Newton's second law)

The momentum equation governs the motion of fluid under the influence of pressure gradients, viscous stresses, and body forces such as gravity:

$$\frac{\partial (\rho u_i)}{\partial t} + \frac{\partial}{\partial x_i}(\rho u_i u_j) = \frac{\partial}{\partial x_j}\left[-p\delta_{ij} + \mu\left(\frac{\partial u_i}{\partial x_j} + \frac{\partial u_j}{\partial x_i}\right)\right] + \rho g_i \tag{8.3}$$

where p is the pressure, μ is the dynamic viscosity, and g_i is the gravitational acceleration component.

8.4.1.2 Energy equation (first law of thermodynamics)

For thermally coupled systems, the conservation of energy is expressed as

$$\frac{\partial}{\partial t}\left(\rho C_P T\right)+\frac{\partial}{\partial x_j}\left(\rho u_j C_P T\right)-\frac{\partial}{\partial x_j}\left(k\frac{\partial T}{\partial x_j}\right)=q \tag{8.4}$$

where C_p is the specific heat at constant pressure, T is the temperature, k is the thermal conductivity, q is the volumetric heat generation term.

8.4.1.2.1 Buoyancy effects and density models

Buoyancy-induced flows are common in adsorption columns with thermal or compositional gradients. Two common models for handling density variations are:

Boussinesq approximation (for small temperature differences):

$$\rho=\rho_{\text{ref}}\left[1-\beta\left(T-T_{\text{ref}}\right)\right] \tag{8.5}$$

Ideal gas law (for compressible flows):

$$\rho=\frac{p_{\text{ref}}W_a}{RT} \tag{8.6}$$

where β is the thermal expansion coefficient, W_a is the molecular weight, and R is the universal gas constant.

8.4.1.3 Turbulence modelling

Turbulence is critical in adsorption processes with high flow rates or complex geometries (Hami, 2021). Direct numerical simulation (DNS) of turbulence remains computationally infeasible for most engineering applications, prompting the use of turbulence models. The Reynolds-averaged Navier–Stokes (RANS) approach introduces time-averaged variables, generating additional Reynolds stress terms that require closure models (e.g., k-ε, k-ω).

Advanced turbulence models include:

- LES (large eddy simulation) – resolves large scales and models small scales.
- DES (detached eddy simulation) – a hybrid of RANS and LES.
- DNS (direct numerical simulation) resolves all scales and is used only for small domains and benchmark studies.

8.4.1.4 Porous media and two-phase modelling

Modifying each particle or pore individually in adsorption systems involving packed beds or porous structures is computationally prohibitive. Instead, the porous media approximation is widely employed, treating the domain as a homogenised medium.

The extended Darcy–Forchheimer equation captures both viscous and inertial resistance:

$$\frac{\partial p}{\partial x} = -\frac{\mu}{K}\vartheta + \rho C_F u^2 \tag{8.7}$$

where K is the permeability, and C_F is the inertial loss coefficient (Forchheimer term).

These terms are added as momentum sinks in the CFD formulation and can be derived from empirical relations such as the Ergun equation.

8.4.1.5 Non-Newtonian fluid modelling

Many fluids exhibit non-Newtonian behaviour, where viscosity depends on shear rate. This is particularly relevant for sludge-like wastewaters, polymer solutions, or suspensions in adsorption applications.

The generalised power-law model for shear-thinning or thickening fluids is

$$\mu = m\left(\dot{\gamma}\right)^{n-1} \tag{8.8}$$

where μ is the apparent viscosity, $\dot{\gamma}$ is the shear rate, m is the consistency index, and n is the flow behaviour index. While non-Newtonian effects add complexity, they are crucial for accurately predicting flow profiles, pressure drop, and mixing behaviour in relevant systems.

8.4.2 Initial and boundary conditions

In CFD, solving the governing equations – typically PDEs for fluid flow, mass transfer, and sometimes energy transport – requires the appropriate ICs/BCs specification. These conditions serve as essential constraints that define the system's physical behaviour and ensure the problem's mathematical well-posedness (Nadamani *et al.*, 2025) (Table 8.1).

ICs are required for all time-dependent (transient) simulations. They specify the system's state at the beginning of the simulation (i.e., at time $t = 0$). Typical ICs include the fluid's velocity field, pressure distribution, concentration of the adsorbate in the fluid and porous media, and temperature, particularly in thermally coupled adsorption processes. Accurately defined ICs help reduce numerical instabilities, allow for faster convergence, and better reflect physical startup scenarios, such as the initial filling or breakthrough in an adsorption column.

On the other hand, BCs are applied at the spatial boundaries of the computational domain and govern the behaviour of fluids and species as they enter, exit, or interact with the physical surroundings. These conditions are classified into physical and numerical types.

Physical BCs are based on known or measurable variables at the domain's boundary surfaces. These are further categorised into three fundamental mathematical forms:

Dirichlet BCs specify the value of the dependent variable (e.g., velocity, pressure, concentration, temperature) directly at the boundary. For example,

Table 8.1 Typical initial and boundary conditions in computational fluid dynamics for adsorption modelling.

BC/IC	Description	CFD Application	Mathematical Type
Initial velocity field	Fluid velocity throughout the domain at time $t = 0$.	Startup of flow in a packed bed or channel.	IC
Initial pressure	Starting pressure distribution across the domain.	Required for compressible/ transient flows.	IC
Initial concentration	Solute or adsorbate concentration in fluid and porous zones.	Used in breakthrough simulations.	IC
Initial temperature	Starting temperature field.	Thermally coupled adsorption systems.	IC
Velocity inlet	Specifies the velocity vector and species concentration at the inlet.	Flow injection at reactor entry.	Dirichlet (Physical)
Pressure outlet	Static pressure and backflow conditions at the exit.	Fixed-pressure column outlet.	Dirichlet (Physical)
Mass flow inlet	Sets total mass flow and composition at entry.	Controlled flow dosing.	Dirichlet (Physical)
No-slip wall	Fluid adheres to a solid surface; velocity = 0.	Packed-bed wall or reactor wall.	Dirichlet (Physical)
Symmetry/ Axisymmetric wall	Zero normal gradients and velocity components.	2D axisymmetric geometry for columns.	Neumann (Physical)
Zero flux	No diffusion or flow across the boundary.	Impermeable walls or symmetry planes.	Neumann (Physical)
Constant heat flux	Prescribed heat addition or loss at the boundary.	Heated adsorber or jacketed column.	Neumann (Physical)
Convective transfer	Heat/mass transfer to surroundings (e.g., air).	Surface convection in cooling columns.	Robin (Physical)
Periodic	Solution at one boundary is repeated at another.	Packed-bed unit cell or repeating adsorbent structure.	Numerical (Computational)
Outflow	Assumes a fully developed flow and zero gradients at the exit.	Long columns where the outlet profile is unknown.	Numerical (Computational)
Interface	Internal boundary between different zones (e.g., fluid-solid).	Fluid-porous coupling in adsorption zones.	Coupled / Hybrid

a fixed velocity and concentration at the inlet of an adsorption column or the no-slip condition (zero velocity) at a solid wall are Dirichlet conditions.

Neumann BCs, where a variable's derivative (typically the normal gradient) is prescribed. An example is the imposition of a constant heat flux or a zero-concentration gradient across an impermeable wall.

Robin BCs are a weighted combination of Dirichlet and Neumann types. These often appear in cases involving convective transfer of heat or mass, such as heat loss from the surface of a reactor to the ambient air.

Numerical BCs are introduced for computational or geometric simplifications when physical measurements are unavailable or not directly applicable. A typical example is the periodic BCs, where the values of the dependent variables at one boundary are repeated at another. This condition is often used in simulations involving repeating geometries or fully developed flow, such as modelling a unit cell of a packed bed instead of the entire column. Another common numerical boundary is the outflow condition, which assumes a fully developed flow and applies a zero-gradient approximation at the outlet.

In adsorption modelling, the correct definition of ICs and BCs is critical to accurately simulate breakthrough curves, pressure drops, temperature profiles, and the dynamic behaviour of solute transport. For example, the inlet of an adsorption column may require the specification of a known fluid velocity and adsorbate concentration (Dirichlet), while the wall may use a no-slip velocity condition and possibly a convective heat flux (Robin). Depending on the setup, the outlet may be modelled as a pressure outlet or with a zero-gradient Neumann condition.

8.5 OPTIMISATION OF THE ADSORPTION PROCESS

Optimisation is vital in enhancing adsorption processes performance, selectivity, and cost-effectiveness. Key operating parameters must be tuned to achieve optimal adsorption capacity and efficiency, such as pH, initial solute concentration, adsorbent dosage, contact time, and temperature. Selecting appropriate optimisation techniques is essential to identify these optimal conditions accurately and efficiently.

Traditionally, the classical OVAT method has been employed to investigate the effect of each parameter individually. While this approach helps understand the basic influence of individual variables, it is time-consuming, cannot detect interaction effects, and requires many experiments.

Advanced multivariate optimisation tools have gained prominence in adsorption research to overcome these limitations. RSM and ANN are two widely adopted approaches. These data-driven techniques allow for modelling complex systems where nonlinear interactions among variables play a crucial role.

RSM is a statistical and mathematical technique that uses designed experiments to model and analyse problems influenced by multiple variables. It enables the development of empirical models (typically quadratic or higher-order polynomials) that can predict system responses and identify optimal operating conditions with significantly fewer experiments than classical methods.

On the other hand, ANN is a machine learning-based method inspired by the structure of the human brain. It excels at modelling nonlinear, complex, and multi-variable systems, even when the underlying physical relationships are poorly defined. ANN has shown great promise in adsorption studies for accurately predicting process outcomes and performing optimisation through training on experimental data.

8.5.1 Classical method

The classical optimisation method, known as the one-factor-at-a-time (OFAT) approach, involves systematically varying one parameter while keeping others constant. Although intuitive and straightforward, this method is time-consuming, ignores interaction effects, and often leads to suboptimal conclusions. Nonetheless, it remains foundational for understanding basic adsorption mechanisms.

8.5.1.1 Adsorbent dosage

Adsorbent dosage directly influences the number of available active sites and total surface area for adsorption. Generally, increasing the dose improves pollutant removal, but beyond an optimal point, the benefit plateaus or even declines due to particle agglomeration and reduced surface accessibility. Identifying this optimum is critical for cost-effective system design.

8.5.1.2 pH

Solution pH profoundly affects adsorption by altering the adsorbent's surface charge and the adsorbate's ionisation state. This governs electrostatic interactions at the adsorbent–adsorbate interface. The point of zero charge (pH_{PZC}) is often used to determine the net surface charge of the adsorbent. For instance, anionic pollutants are more favourably adsorbed at $pH > pH_{PZC}$ (positive surface charge), while cationic species prefer $pH < pH_{PZC}$. Thus, pH optimisation is essential for tailoring selectivity and efficiency.

8.5.1.3 Initial concentration and contact time

The influence of initial adsorbate concentration is associated with the driving force for mass transfer. The adsorption rate increases at higher concentrations due to a stronger concentration gradient, which may lead to quicker site saturation. Similarly, contact time affects equilibrium attainment. Rapid uptake occurs initially, followed by a plateau as the adsorbent approaches saturation. These parameters are central to developing adsorption kinetics and isotherm models.

8.5.1.4 Temperature

Temperature affects both the thermodynamics and kinetics of adsorption. Higher temperatures may reduce capacity in physical adsorption due to weaker Van der Waals forces, whereas in chemisorption, elevated temperatures can enhance bonding. Thermodynamic parameters such as ΔH (enthalpy), ΔG (Gibbs free energy), and ΔS (entropy) provide insight into the adsorption mechanism.

8.5.2 Response surface methodology

Box and Wilson (Box & Wilson, 1951) developed RSM to improve production processes in the chemical industry. RSM is a collection of mathematical and statistical techniques for determining how variables relate and how the operating system under investigation should be run. An adequate experimental design (Figure 8.8) that informs the specifics of the experiments to be conducted in the study region must be prepared before employing this technique.

Optimisation entails calculating the coefficients, projecting the response, and assessing the model's fit. The following is an example of the response model:

$$Y = f(X_1) + f(X_2) + f(X_3) + \cdots\cdots f(X_n) + e \tag{8.9}$$

where f is the response function, e is the experimental error, and X_1 and X_2 are the independent variables dependent on Y.

This model requires a suitable polynomial to approximate the f in some regions of independent process variables. The following illustrates the quadratic polynomial model:

$$Y = \beta_0 + \sum_{i=1}^{k} \beta_i x_i + \sum_{i=1}^{k} \beta_{ii} x_i^2 + \sum_{i=1}^{k-1} \sum_{j=2}^{k} \beta_{ij} x_j x_i + \varepsilon \tag{8.10}$$

where Y is the anticipated response, x_i and x_j are the input variables, k is the number of variables, β_0 is the constant term, β_i is the linear coefficient, β_{ij} is the interaction coefficient, ii is the quadratic term coefficient, and ε is the experiment-related residual.

8.5.2.1 Design strategies for response surface methodology

Several design methods for multivariate optimisation (Figure 8.8) have been used to optimise adsorption process parameters, the most popular of which are as follows:

Full factorial design

All possible combinations of input factors at specific levels are evaluated in a full factorial design. A two-level FFD explores each factor at high and low settings, generating 2^k experiments for k variables (Reji *et al.*, 2022; Bezerra *et al.*, 2008). For three-level designs, the total number becomes 3^k, which can quickly become impractical for large k. Although FFD is effective for identifying main and interaction effects, it is inefficient for fitting second-order models, especially with more than three factors. Consequently, FFD is best used when the number of variables is small and high-order precision is not required.

Central composite design

CCD is one of RSM's most widely used designs for fitting second-order models (Reji *et al.*, 2022; Bezerra *et al.*, 2008). It includes three types of points: 2^k factorial points, $2k$ axial (star) points, and centre points, with the total number of experiments given by

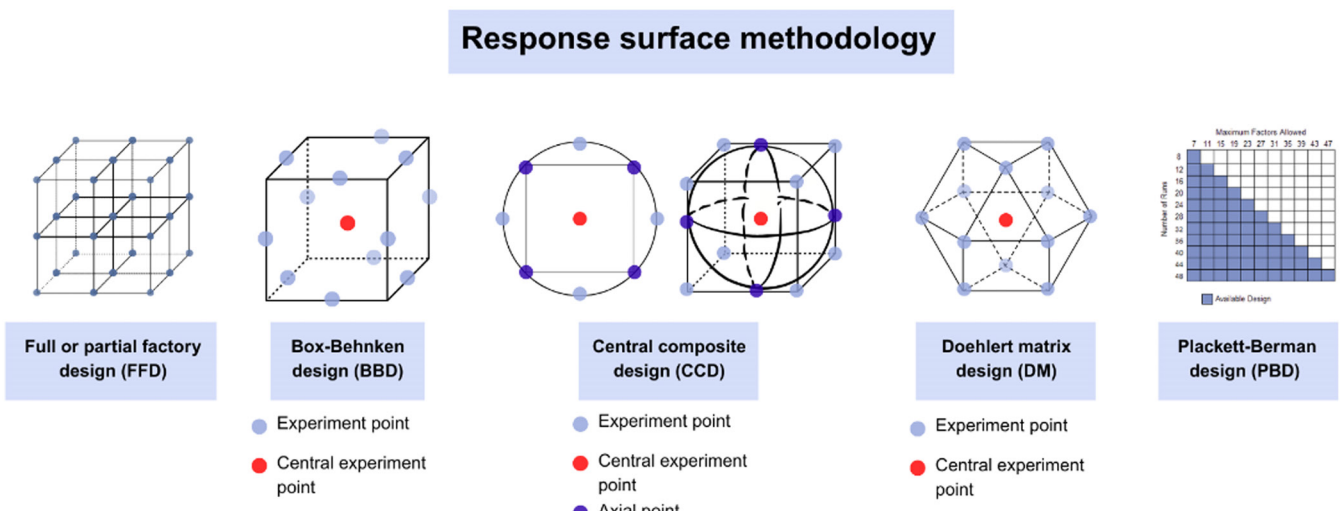


Figure 8.8 Basic model designs used in response surface methodology.

$$N = 2^k + 2k + C_0 \tag{8.11}$$

where k is the number of factors, and C_0 is the number of centre runs. CCD offers the flexibility to explore linear and quadratic effects with fewer experiments than a full factorial design. Depending on the placement of axial points, CCDs are categorised as circumscribed (CCC), inscribed (CCI), or face-centred (CCF). CCD is particularly suited for modelling curvature and is often used in environmental and adsorption system optimisation.

Box–Behnken design

The BBD is an efficient three-level design developed to fit second-order models without including combinations where all factors are at extreme values (Reji *et al.*, 2022; Bezerra *et al.*, 2008). The number of experiments required is calculated by

$$N = 2k\ (k-1) + C_0 \tag{8.12}$$

BBD is advantageous in minimising experimental effort and avoiding extreme conditions that could result in unphysical or unsafe operating conditions. However, it requires at least three variables and cannot handle modelling of higher-order interactions beyond second-order terms. Its efficiency and balanced distribution make it a strong alternative to CCD when fewer experiments are desired.

Doehlert design

The Doehlert matrix is a highly flexible and sequential design developed based on the geometry of a k-dimensional simplex. It distributes experimental points unevenly across the design space, allowing denser sampling for more critical variables (Reji *et al.*, 2022; Bezerra *et al.*, 2008). The number of experiments is given by

$$N = k^2 + k + C_0 \tag{8.13}$$

This design is beneficial when additional variables must be introduced incrementally, making it ideal for sequential optimisation. Its ability to adapt to multi-level testing with fewer experiments makes Doehlert Design a good option when experimental resources are limited.

Plackett–Burman design

The Plackett-Burman–Burman design is a first-order screening design that identifies the most influential variables from a large set. It requires only $N = k + 1$ experiments. Due to its 'saturated' structure (no degrees of freedom for error), it cannot estimate interaction or quadratic effects, making it unsuitable for complete optimisation (Reji *et al.*, 2022; Bezerra *et al.*, 2008). However, it is ideal as a preliminary step to eliminate insignificant variables before applying CCD or BBD. PBD designs typically require the number of runs to be a multiple of four, which can be accommodated using dummy variables.

Running response surface methodology simulations

RSM is a powerful statistical tool to model and optimise multivariate systems in adsorption processes. Effective implementation requires careful selection of process parameters (independent variables), responses (dependent variables), and an appropriate experimental design strategy. The two most common responses in adsorption studies are removal efficiency (%) and adsorbed amount (mg g^{-1}), reflecting system performance under varying operational conditions.

The first step in an RSM simulation is identifying critical factors through preliminary screening experiments or literature reviews. Parameters such as pH, initial dye concentration, adsorbent dose, and contact time are commonly explored. The selected variable ranges should be broad enough to capture meaningful system behaviour but realistic within experimental constraints.

Once relevant variables and ranges are selected, an experimental design – such as CCD, BBD, or FFD – is applied to generate a matrix of runs. Each experiment is executed according to the matrix, and the response values are recorded. These results are then used to construct a regression-based model, typically a quadratic polynomial, that captures the relationship between input factors and system response (Figures 8.9 and 8.10).

Screening independent variables and selecting responses

Selecting relevant and independent variables is crucial for robust modelling. This involves identifying process parameters that significantly influence adsorption – such as pH, contact time, and initial concentration – while ensuring they are not highly correlated. Defining proper ranges for each parameter ensures the model's predictive power. Poor factor selection leads to poor model fit, non-informative outcomes, and potentially misleading optimisation.

Choosing a design strategy and executing experiments After screening, the next step is choosing the DOE. Common strategies include CCD, BBD, and Doehlert design (DD). Each design balances the number of runs with the level of model detail (linear, interaction, or quadratic terms). Software tools like Design-Expert®, Minitab®, or JMP® are used to generate experimental runs and analyse results. Once experiments are completed, data are entered into the software for model fitting. The resulting mathematical model predicts the response as a function of selected variables.

Model fitting and evaluation Model fitting typically uses least-squares regression on coded variables (e.g., −1, 0, +1). To evaluate the model, several statistical metrics are considered:

- **Coefficient of determination (R^2):** Indicates the proportion of response variance explained by the model.
- **Adjusted R^2:** Accounts for the number of terms in the model; increases only if new terms improve the model significantly.
- **Predicted R^2:** Measures how well the model predicts new observations; useful for detecting overfitting.

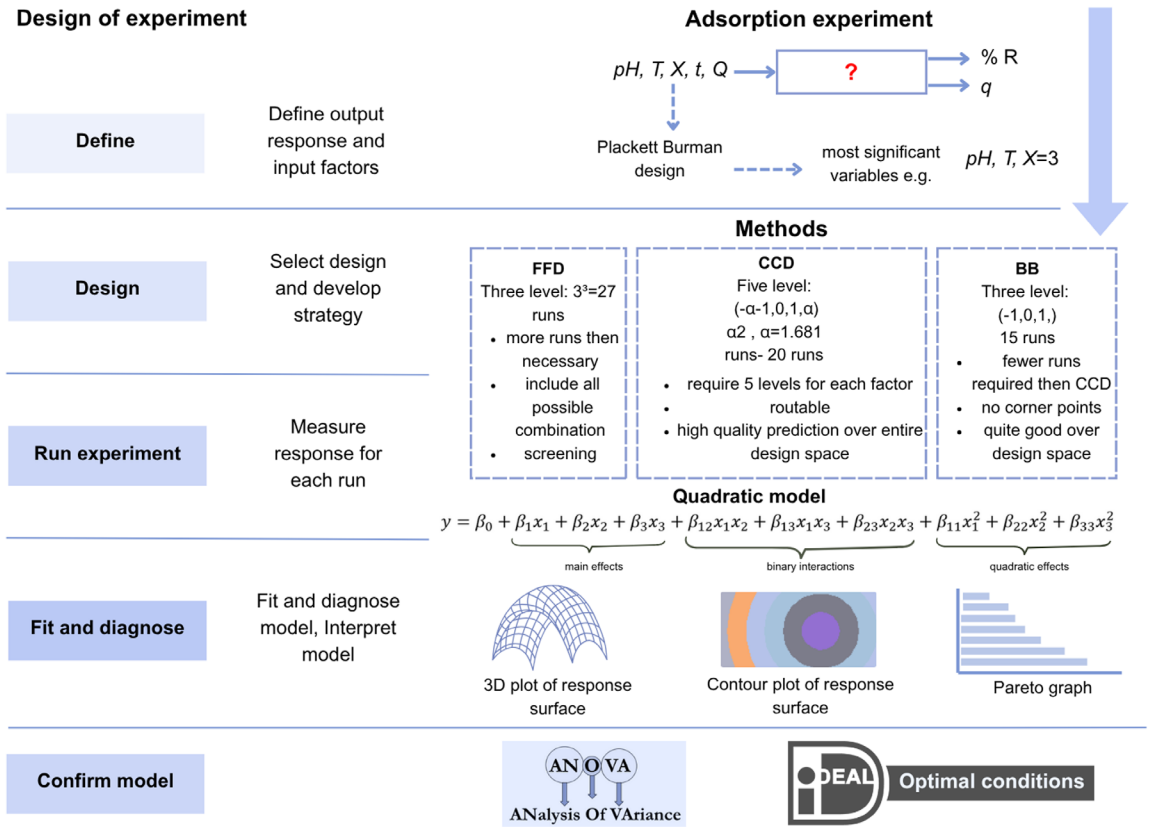


Figure 8.9 Design of experiments in response surface methodology.

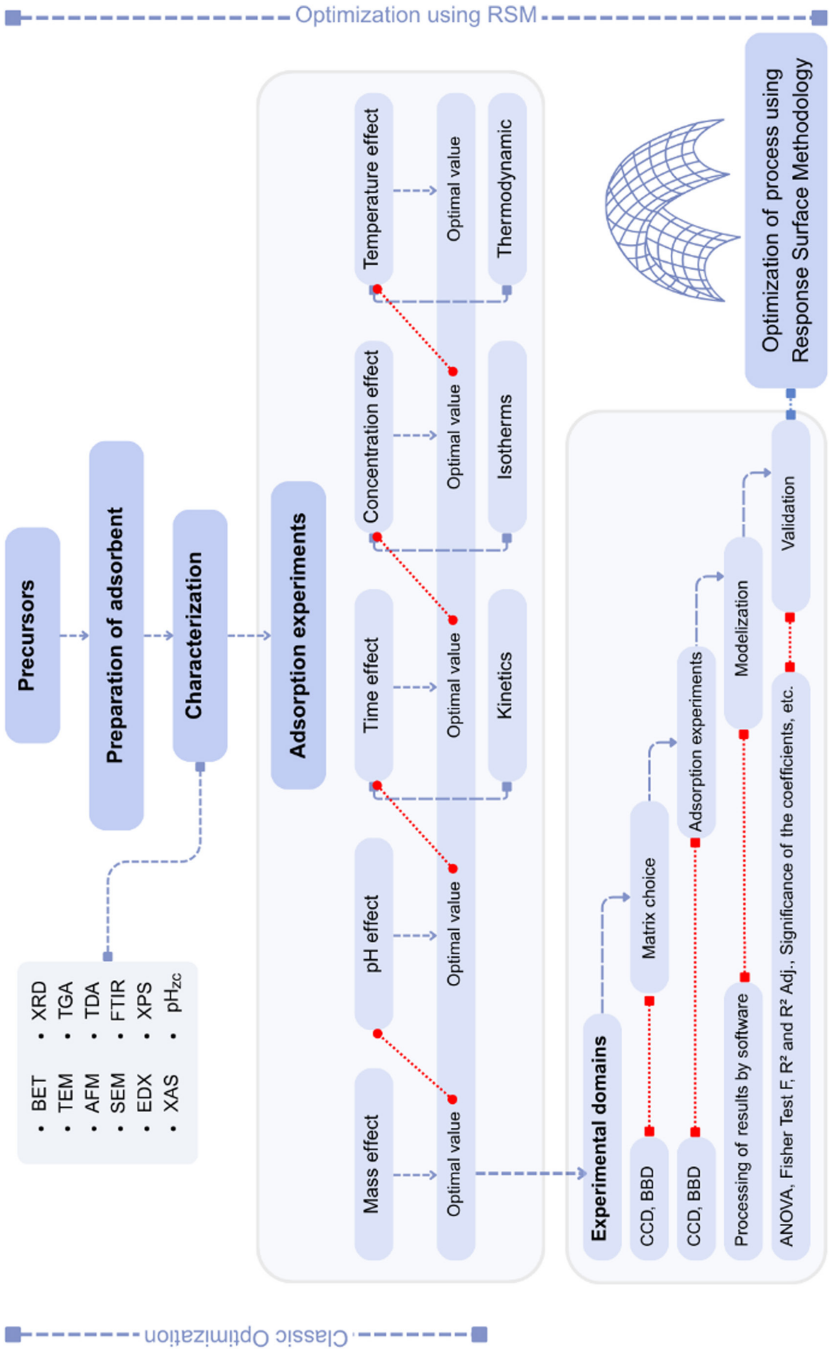


Figure 8.10 Adsorption procedure of response surface methodology.

A good model should show high and relatively close values of R^2, adjusted R^2, and predicted R^2. Discrepancies may indicate noise overfitting or irrelevant variables.

In addition, residual plots (residuals vs. run number, normal probability plots) are used to validate model assumptions such as normality and homoscedasticity. These plots help confirm that residuals are randomly distributed and no systematic patterns are present.

Graphical analysis and ANOVA test Graphical representations – such as 3D response surfaces and 2D contour plots – illustrate how variable interactions affect the response. These visuals provide intuitive insights and help in locating optimal conditions.

Statistical validation of the model is performed using analysis of variance (ANOVA). ANOVA tests whether model terms are statistically significant, using:

- **F-value:** The ratio of variance explained by the model to the unexplained variance.
- **P-value:** The probability that the observed F-value occurred by chance. A P-value <0.05 typically indicates statistical significance.

Further statistical tools such as t-tests, chi-square (χ^2), degrees of freedom (df), and confidence intervals are used to assess the significance and precision of regression coefficients.

Determination of optimal conditions and model verification The final goal of RSM is to determine the combination of factor levels that yields the most desirable outcome. This is often a single-objective optimisation (e.g., maximising dye removal) but may also involve multi-objective optimisation (e.g., balancing efficiency and cost).

Confirmatory experiments must be performed once optimal conditions are identified from the regression model and graphical analysis. If the experimental results closely match the model predictions, it confirms the robustness and predictive accuracy of the RSM model. A valid model under slight deviations in input variables is considered reliable for practical application.

8.5.3 Artificial neural network for process optimisation

ANNs are powerful computational models inspired by the functioning of the human brain (Abiodun *et al.*, 2018). Initially developed as linear modelling tools, ANNs have evolved to tackle complex, nonlinear systems where traditional mathematical formulations are insufficient or unavailable. Their strength lies in their ability to learn from data, recognise patterns, and predict outcomes without explicit prior knowledge of underlying physical laws. ANN was introduced in Chapter 7.

ANNs comprise interconnected layers of artificial neurons (nodes), typically organised into an input layer, one or more hidden layers, and an output layer. Through supervised or unsupervised learning, these networks adjust internal parameters (weights and biases) to minimise prediction error. In adsorption

research, ANNs have been successfully employed to model isotherms, kinetics, and dynamic breakthrough curves, offering robust alternatives to mechanistic and statistical models.

8.5.3.1 Artificial neural network architectures in adsorption studies

Feedforward neural networks (FNN) are the most widely used ANN structure (Figure 8.11). Data flows unidirectionally from input to output through hidden layers, making FNNs suitable for static system modelling, including equilibrium isotherms and batch adsorption processes.

Feed-backward or recurrent neural networks (RNN) incorporate feedback loops, enabling memory within the network. This architecture is particularly suitable for modelling dynamic adsorption systems and time-dependent behaviours.

Single layer perceptron (SLP) is the simplest ANN form. While it can model linearly separable problems, it lacks the capability to capture the nonlinear relationships typical in adsorption.

Multilayer perceptrons (MLPs), comprising one or more hidden layers with nonlinear activation functions, can approximate complex nonlinear relationships. MLPs are extensively used for modelling multi-variable adsorption systems where temperature, pressure, and concentration interact nonlinearly.

Radial basis function (RBF) networks use radial basis activation functions and are effective for fast training and accurate function approximation, making them suitable for interpolating experimental adsorption data.

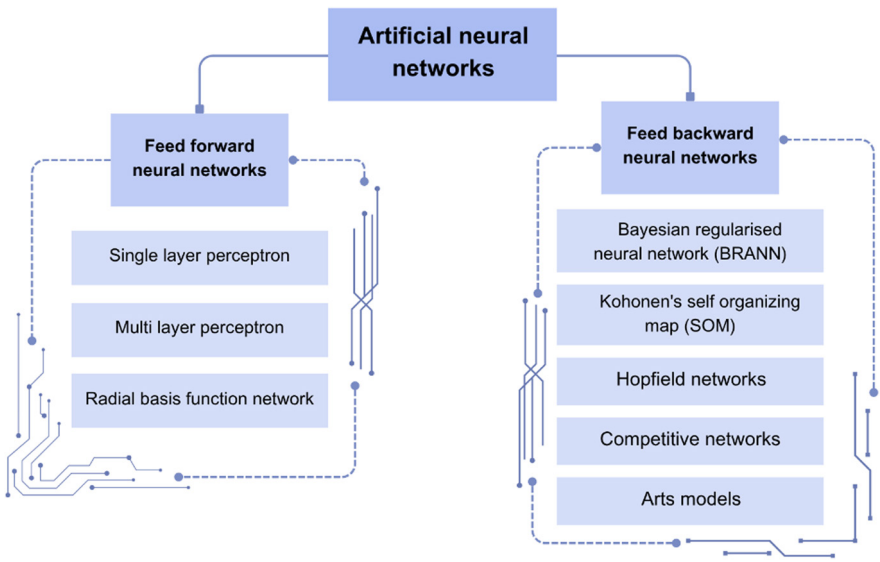


Figure 8.11 Artificial neural networks classification.

Bayesian regularised neural networks (BRANNs) incorporate Bayesian inference during training to improve generalisation, especially when datasets are small or noisy. This architecture reduces overfitting by automatically adjusting network complexity.

Based on unsupervised learning, self-organising maps (SOMs) project high-dimensional input data onto a low-dimensional grid. These maps help visualise clustering and similarities in adsorption data across different adsorbents or pollutants.

Competitive networks, which include SOMs, operate via neuron competition and are helpful for pattern recognition, clustering, and classification of multi-variable adsorption datasets.

Hopfield Networks are recurrent models with symmetric weights and binary threshold nodes. They serve as content-addressable memory systems and apply to optimisation problems involving constraint satisfaction.

Adaptive resonance theory (ART) networks maintain a balance between plasticity (learning new patterns) and stability (retaining prior knowledge), making them ideal for real-time adaptive modelling of adsorption systems under varying feed conditions.

8.5.3.2 Running artificial neural network simulations

Developing an ANN model for adsorption system prediction follows a structured workflow involving several key steps. First, appropriate input variables (e.g., pH, concentration, contact time) and output responses (e.g., removal efficiency, adsorption capacity) are selected based on experimental relevance. These inputs are preprocessed, normalised, and, if necessary, reduced using techniques like principal component analysis (PCA) or sensitivity analysis (SA).

Next, an appropriate network architecture is chosen, typically MLP, along with the number of hidden layers and neurons, which is often determined through empirical tuning. The network is then trained using algorithms such as backpropagation or Levenberg–Marquardt (LM) to minimise prediction error.

After training, model verification and validation are performed using error metrics like MAE, MSE, and RMSE on training and test datasets. A well-validated ANN can be used for accurate prediction of adsorption performance and can be coupled with optimisation algorithms for process improvement and scale-up. The development and implementation of ANN models in adsorption involves several sequential steps illustrated in Figure 8.12.

Choosing inputs and outputs

The first step is selecting relevant input and output variables. In adsorption, typical outputs include removal efficiency (%) and adsorption capacity (mg/g). Input variables may include pH, contact time, IC, temperature, and adsorbent dose.

The precise number of inputs required is problem-specific and typically determined through expert judgment or SA. SA helps identify the most influential variables, while PCA is often used to reduce dimensionality by eliminating redundant variables.

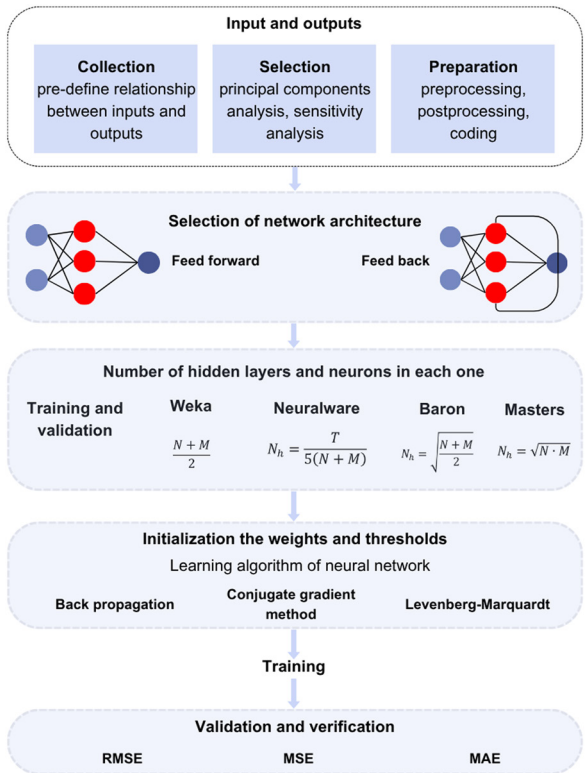


Figure 8.12 Scheme of artificial neural networks procedure.

To ensure proper ANN function, all input and output data must be numerical and normalised to a specific range (usually between 0 and 1 or −1 and +1). This preprocessing step is essential for network stability and convergence.

Selection of network architecture

Once inputs and outputs are defined, the next task is selecting the appropriate ANN architecture. The feedforward structure is most commonly used for adsorption modelling due to its simplicity and effectiveness in function approximation. For time-dependent systems, recurrent architectures may be more suitable.

A typical network includes:

- An input layer with one neuron per independent variable.
- One or more hidden layers process data using activation functions (e.g., sigmoid, tanh, ReLU).
- An output layer that delivers the predicted response.
- Three-layer networks (input–hidden–output) are often sufficient for most adsorption applications.

Number of hidden layers and neurons

Determining the number of hidden layers and neurons is critical to model performance. While a single hidden layer can approximate most continuous functions, the number of neurons in this layer significantly affects accuracy and training time.

Several heuristic methods exist for estimating the number of hidden neurons, including Weka, NeuralWare, Barron's, and Masters' rules. However, most ANN models in adsorption research rely on empirical tuning, trial and error guided by performance metrics. Too few neurons may lead to underfitting, while too many may cause overfitting and increased computational cost.

Determining weights and thresholds

Weights and biases (thresholds) are adjusted during training to minimise prediction error. The most widely used learning algorithm is backpropagation (BP), which updates weights based on the gradient of the error function with respect to each parameter.

Advanced optimisation techniques like the LM and conjugate gradient (CG) methods are also used:

- LM is efficient for small- to medium-sized datasets and achieves faster convergence.
- CG is more suitable for large-scale problems with high-dimensional input spaces.
- The choice of learning algorithm affects the speed and accuracy of training. An effective algorithm continuously reduces prediction error until convergence is achieved.

Verification and validation

Verification and validation are critical final steps in developing reliable ANN models for adsorption system analysis. These stages ensure the trained model fits the training data and generalises well to new, unseen data, making it robust for prediction and optimisation tasks.

Error metrics for model evaluation Several statistical metrics are used to quantify the accuracy and performance of ANN models:

- **Mean absolute error (MAE):** Measures the average magnitude of absolute errors between predicted and experimental values, indicating prediction deviation.

$$\mathrm{MAE} = \frac{1}{n}\sum_{i=1}^{n}\left|y_i - \widehat{y_i}\right| \tag{8.14}$$

- **Mean squared error (MSE):** Penalises larger errors more heavily by squaring the differences, emphasising the importance of reducing large prediction deviations.

$$\mathrm{MSE} = \frac{1}{n}\sum_{i=1}^{n}\left(y_i - \widehat{y_i}\right)^2 \tag{8.15}$$

- **Root mean squared error (RMSE):** It provides an error in the same units as the output variable and is often more practically interpretable.

$$\mathrm{MSE} = \sqrt{\frac{1}{n}\sum_{i=1}^{n}\left(y_i - \widehat{y_i}\right)^2} \tag{8.16}$$

  Lower values of these metrics indicate better predictive accuracy. A combination of these is often preferred for a comprehensive assessment.

Training vs. testing validation To prevent overfitting – where a model performs well on training data but poorly on new data – it is essential to split the dataset into:

- **Training set:** Used to adjust network weights during learning.
- **Testing (or validation) set:** Used to evaluate the model's predictive capability on unseen data.

Sometimes, a third set called the validation set is used during training to fine-tune hyperparameters and prevent overfitting before final testing.

Best practices and common pitfalls

While validation is vital, approaches vary widely in the literature. Some studies rely on a single error metric (e.g., only MSE or R^2), which may offer a narrow view of model performance. Others use multiple metrics and visual tools such as:

- **Parity plots** (predicted vs. experimental values)
- **Residual plots** (error distribution across cases)
- **Cumulative distribution curves** of absolute or relative error

These tools help assess accuracy, error bias, and variance distribution.

Furthermore, cross-validation techniques – like k-fold cross-validation – can enhance model generalisability by averaging performance over multiple training–testing splits.

Benchmarking against other models

Robust ANN models should ideally be compared against simpler alternatives such as RSM, polynomial regression, or empirical isotherm/kinetic models. This helps justify the complexity of ANN, mainly when only marginal improvements are observed. Metrics like Adjusted R^2, Prediction Error Sum of Squares (PRESS), and Akaike Information Criterion (AIC) can also be employed for model comparison.

Table 8.2 provides a comparative overview of CFD, RSM, and ANN with respect to their modelling capabilities, data requirements, and application scope in adsorption studies. This comparison highlights the complementary

Table 8.2 Comparison of computational fluid dynamics, response surface methodology, and artificial neural networks for adsorption process analysis.

Aspect	CFD	RSM	ANN
Primary use	Simulation of transport phenomena (flow, heat, mass)	Statistical modelling and optimisation of process variables	Data-driven modelling and prediction of complex systems
Type of model	Physics-based (first-principles)	Empirical (typically polynomial regression)	Data-driven (nonlinear black-box model)
Input requirements	Governing equations, geometry, BC/IC	Experimental design matrix with selected factors	Experimental data for training (input–output pairs)
Output	Spatially resolved fields (velocity, pressure, temperature, concentration)	Response surface, optimal settings	Predicted system response (e.g., adsorption capacity)
Handles nonlinearity	Limited, via turbulence or multiphase models	Moderate (via quadratic models)	Excellent; captures strong and complex nonlinearities
Inter-variable Interactions	Modelled via equations and mesh	Explicitly modelled via interaction terms	Implicitly captured during training
Optimisation capability	Indirect: via post-processing or integration with solvers	Direct generates response surfaces for optimisation	Direct can be combined with optimisation algorithms
Ease of interpretation	High (based on physical laws)	High (equation-based; coefficients interpretable)	Low (black box; limited interpretability)
Data requirement	Moderate to high (physical properties, geometry)	Moderate (requires structured experimental design)	High (requires a large and diverse dataset)
Computational cost	High (especially for 3D, transient simulations)	Low to moderate	Moderate to high (especially during training)
Software examples	ANSYS Fluent, OpenFOAM, COMSOL Multiphysics	Design-Expert, Minitab, JMP	MATLAB, TensorFlow, Scikit-learn, Neural Designer
Best suited for	Understanding the spatial behaviour of flow and transport	Finding optimal conditions with limited experiments	Predictive modelling of complex, nonlinear relationships
Scalability to large systems	Moderate to high (parallel computing available)	Moderate	High (especially with deep learning frameworks)

strengths of each method – CFD for mechanistic simulation, RSM for structured experimental optimisation, and ANN for complex nonlinear prediction – reinforcing their integrated use in modern adsorption process analysis.

8.6 SOFTWARE PACKAGES FOR PROCESS SIMULATION AND OPTIMISATION

Simulation and optimisation of adsorption processes are crucial for designing efficient water and wastewater treatment systems. Among the most widely used computational approaches are RSM and ANN. RSM allows for the development of statistically robust empirical models to analyse and optimise process variables, while ANN enables the creation of predictive, nonlinear models trained on experimental or simulation data. Various software packages – Figure 8.13, ranging from statistical tools and machine learning frameworks to process simulators and Multiphysics platforms, are available to facilitate simulation and optimisation tasks at various levels of complexity.

Design-Expert, Minitab, JMP, and Statistica are powerful statistical platforms tailored for RSM-based analysis. They support DoE, model fitting, response surface generation, and identification of optimum conditions in adsorption processes. These tools are widely used in laboratory-scale studies and pilot-scale optimisation of adsorbents and operating parameters.

MATLAB offers extensive toolboxes for neural networks, curve fitting, and global optimisation, making it highly suitable for RSM and ANN modelling. It



Figure 8.13 Software packages for adsorption process simulation and optimisation.

allows custom algorithm development and integration with numerical solvers, making it a flexible choice for adsorption modelling across various research domains.

Python, through its libraries such as Scikit-learn, TensorFlow, and PyTorch, provides a free and open-source environment for building sophisticated machine learning models. It supports linear and nonlinear regression, deep learning, feature selection, and hyperparameter tuning and is increasingly used in adsorption process modelling due to its adaptability and community support.

RapidMiner, Orange Data Mining, and KNIME are visual programming tools that support the drag-and-drop construction of machine learning workflows. These platforms are ideal for researchers and practitioners seeking quick deployment of classification, regression, and optimisation models without extensive coding.

Process simulation tools such as Aspen Plus, DWSIM, CHEMCAD, VMGSim, and ProSimPlus are essential for modelling adsorption as part of integrated process flowsheets. These simulators can represent physical and chemical transformations, perform sensitivity analysis, and evaluate performance under varied conditions. Many allow customisation through user-defined functions or integration with Python/MATLAB for hybrid modelling.

COMSOL Multiphysics provides detailed simulation capabilities using finite-element analysis. It enables the modelling of mass transport, adsorption kinetics, and heat transfer in porous media, making it ideal for visualising and analysing spatial variations within adsorption columns or membranes.

GAMS and gPROMS are mathematical modelling platforms for process optimisation and dynamic simulation. They are suited for solving large-scale nonlinear programming problems and simulating complex adsorption cycles such as PSA (pressure swing adsorption) or TSA (temperature swing adsorption), especially when integrated with other process units.

R is a powerful statistical environment offering various packages for regression analysis, experimental design, and machine learning. Its statistical rigour and strong visualisation tools are particularly useful for RSM and exploratory data analysis in adsorption studies.

ANSYS is a comprehensive Multiphysics simulation platform that supports fluid flow, heat transfer, and chemical reaction modelling using finite element and finite volume methods. In adsorption, ANSYS Fluent and ANSYS CFX can simulate packed-bed dynamics, adsorption kinetics, and transport phenomena in detailed reactor geometries. ANSYS is especially valuable for high-fidelity simulations where coupling between fluid dynamics and surface adsorption needs to be captured with spatial and temporal precision.

8.7 CASE STUDIES

8.7.1 Case study I: Computational fluid dynamics

This case study explores the application of CFD modelling to simulate the removal of acetaminophen (ACT) in fixed-bed adsorption columns packed with sugarcane bagasse, a sustainable biosorbent, as documented in the work by Vera *et al.* (2021). The study emphasises the value of CFD in elucidating the

internal mass transfer mechanisms, spatial concentration distributions, and fluid flow behaviours within adsorption columns. Such insights are crucial for designing and optimising adsorption systems that treat pharmaceutical-laden wastewater.

The CFD model was constructed using COMSOL Multiphysics, employing the Brinkman–Forchheimer equations to simulate fluid flow alongside mass transfer equations incorporating axial dispersion. Adsorption kinetics were described through a linear driving force (LDF) model, which accounted for macropore diffusion effects. The model operated under isothermal conditions, assumed Langmuir adsorption equilibrium, and considered external film resistance and internal pore diffusion.

The simulations focused on three different bed heights of 23, 33, and 43 cm, operated at a flow rate of 2.5 mL/min with an initial ACT concentration of 57 mg/L. Figure 8.14 illustrates the reduction of the adsorption column's geometry from a 3D representation to a 2D axisymmetric domain. This simplification, combined with the implementation of wall mesh refinement,

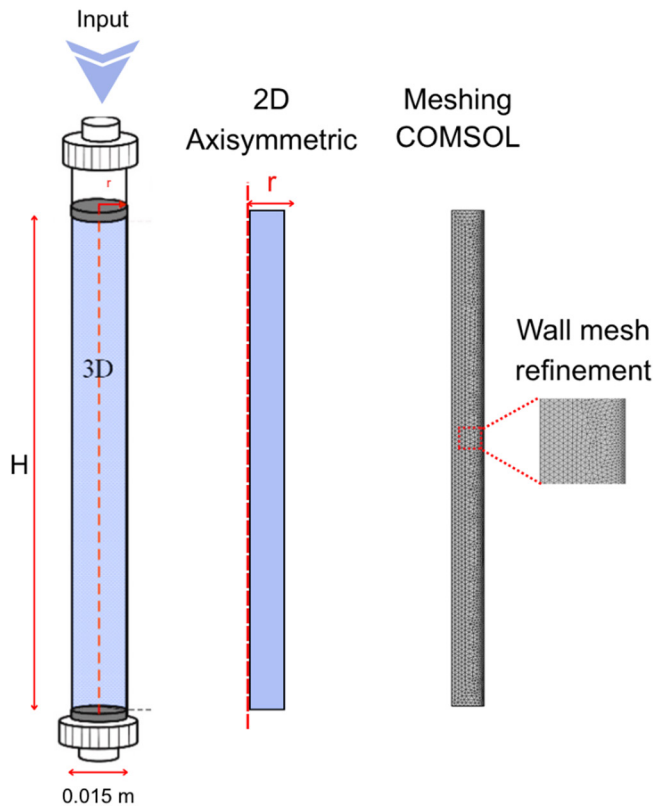


Figure 8.14 Reduction of 3D to 2D geometry of the adsorption column.

ensured accurate resolution of velocity and concentration gradients near the column boundaries, thereby enhancing the fidelity of the numerical results.

8.7.1.1 Breakthrough curves and model validation

The predictive capability of the CFD model was evaluated by comparing simulated breakthrough curves with experimental data at the three bed heights. Figures 8.15–8.17 present these comparisons, showing the normalised concentration (C/C_0) plotted over time for bed heights of 23, 33 and 43 cm, respectively. The simulations closely matched the experimentally observed S-shaped breakthrough profiles, validating the robustness of the model.

An increase in bed height from 23 to 43 cm resulted in substantial delays in breakthrough and complete saturation times. At the shortest bed height, breakthrough occurred around 6 min and saturation near 42 min, while at the tallest bed, these times extended to approximately 17 min and 66 min, respectively. This shift reflects the increased mass of adsorbent available in taller columns, providing more active sites and extending fluid residence times, thereby enhancing adsorption capacity. Additionally, the curves became less steep with increasing bed height, indicating a more gradual approach to equilibrium, characteristic of systems where internal diffusion is dominant.

8.7.1.2 Internal concentration profiles and mass transfer zone behaviour

Figures 8.15–8.17 display 2D concentration profiles that reveal the internal progression of adsorption within the columns over time. These visualisations highlight how the mass transfer zone (MTZ) – the region where adsorption

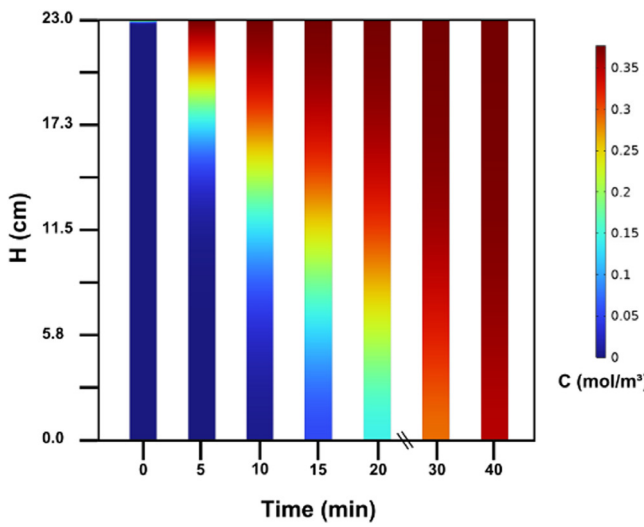


Figure 8.15 Simulated 2D concentration profiles for acetaminophen adsorption at a bed height of 23 cm.

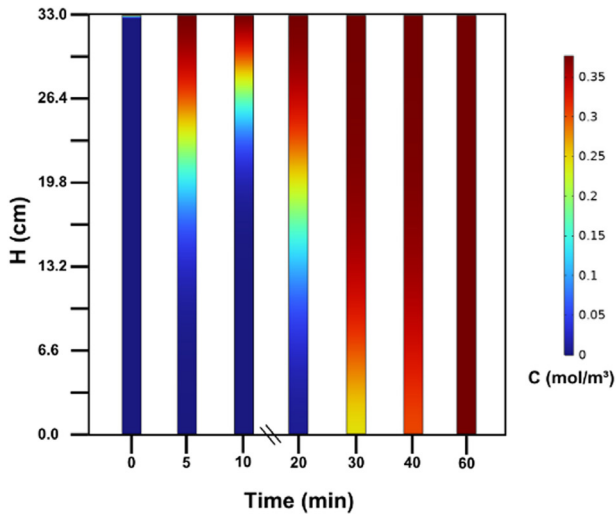


Figure 8.16 Simulated 2D concentration profiles for acetaminophen adsorption at a bed height of 33 cm.

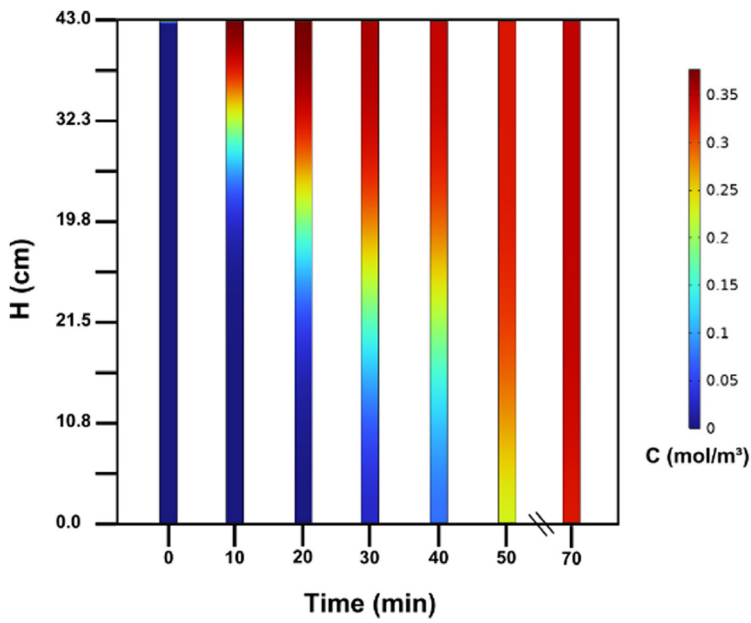


Figure 8.17 Simulated 2D concentration profiles for acetaminophen adsorption at a bed height of 43 cm.

actively occurs – propagates upward through the packed bed as the process advances. At each bed height, the lower regions of the column were observed to saturate first, while the upper sections remained relatively fresh until reached by the advancing MTZ.

The CFD simulations indicated that the MTZ expanded with increasing bed height, measuring approximately 13 cm in the 23 cm bed, 16.5 cm in the 33 cm bed, and 23 cm in the 43 cm bed. The broader MTZ in taller columns underscores the combined influence of longer residence times and greater diffusion resistances, both interparticle and intraparticle, which moderate the rate at which saturation progresses through the bed. The concentration profiles clearly illustrated axial gradients, showing a distinct transition from zones of low ACT concentration, representing fresh adsorbent, to zones of high concentration indicative of saturation.

8.7.1.3 Conclusion

Through this detailed CFD study, the complex interplay of hydrodynamics, mass transfer, and adsorption kinetics in fixed-bed columns has been effectively captured. The model's accurate prediction of breakthrough behaviour across varying bed heights and the internal concentration profiles visually demonstrating the mass transfer zone's growth and migration highlight CFD's significant utility as a design and optimisation tool. Such simulations provide insights that are difficult to obtain experimentally, offering engineers a powerful means to refine parameters like bed height, flow rate, and particle size for enhanced performance in pharmaceutical wastewater treatment applications.

8.7.2 Case study II: Artificial neural networks for optimisation

In this case study, a comprehensive investigation is carried out into removing crystal violet dye from aqueous solutions using magnetic activated carbon (MAC) (Salehi *et al.*, 2016). The study is an exemplary model for integrating experimental optimisation with advanced data-driven modelling in environmental engineering. By systematically exploring the effects of key process variables – such as pH, temperature, contact time, initial dye concentration, and adsorbent dosage – this work demonstrates the practical application of traditional statistical methods and modern machine learning techniques in adsorption process analysis.

The input variables of the trained ANN are pH, temperature, time, initial dye concentration, and amount of MAC, and the output is the adsorption efficiency of crystal violet, which are indicated in Table 8.3, along with the predicted values of adsorption efficiency by the ANN model.

8.7.2.1 Data analysis and exploration

Several data exploration techniques were employed to gain insights into the relationships between input variables and the target response. A key visualisation is the heatmap of Pearson correlation coefficients, which quantifies the linear associations between the main process parameters and the observed adsorption efficiency for crystal violet removal.

Table 8.3 Experimental conditions and corresponding adsorption efficiencies: comparison of observed and artificial neural networks-predicted adsorption (%) for crystal violet removal under various process parameter settings.

pH	Temperature (°C)	Time (min)	Concentration (mg/L)	Mass of Adsorbent (mg)	Experiments	Predicted from ANN
6	55	35	35	30	77.6	77.66
9	55	15	35	30	68.43	68.41
6	35	35	15	30	98.33	98.32
9	35	35	15	60	100.31	100.32
7.5	45	25	25	45	98.72	99.47
7.5	45	25	25	45	99.71	99.47
7.5	65	25	25	45	99.75	99.55
7.5	45	25	45	45	84.6	84.63
6	35	15	15	60	100.29	105.96
9	35	35	35	30	77.65	82.54
6	35	15	35	30	67.72	67.91
7.5	45	25	25	45	99.72	99.47
9	55	35	35	60	95.46	95.51
7.5	45	25	25	45	99.64	99.47
7.5	45	25	5	45	105.8	105.80
6	55	15	15	30	98.16	97.45
9	35	15	35	60	97.5	97.52
7.5	45	5	25	45	94.78	98.61
9	35	15	15	30	95.65	95.64
9	55	35	15	30	96.55	96.57
7.5	45	25	25	45	99.48	99.47
7.5	45	45	25	45	99.69	99.66
6	35	35	35	60	98.76	98.82
7.5	45	25	25	15	69.4	69.41
10.5	45	25	25	45	87.01	93.87
7.5	25	25	25	45	99.37	99.22
9	55	15	15	60	100.33	100.36
4.5	45	25	25	45	91.8	91.89
7.5	45	25	25	45	98.99	99.47
6	55	35	15	60	100.24	105.38
6	55	15	35	60	100.1	100.11
7.5	45	25	25	75	100.09	100.12

The heatmap in Figure 8.18 reveals a strong positive correlation (0.61) between MAC amount and adsorption efficiency, underscoring that increasing the adsorbent dosage substantially enhances dye removal. Conversely, initial dye concentration exhibits a moderate negative correlation (−0.53) with adsorption efficiency, indicating that higher dye concentrations reduce

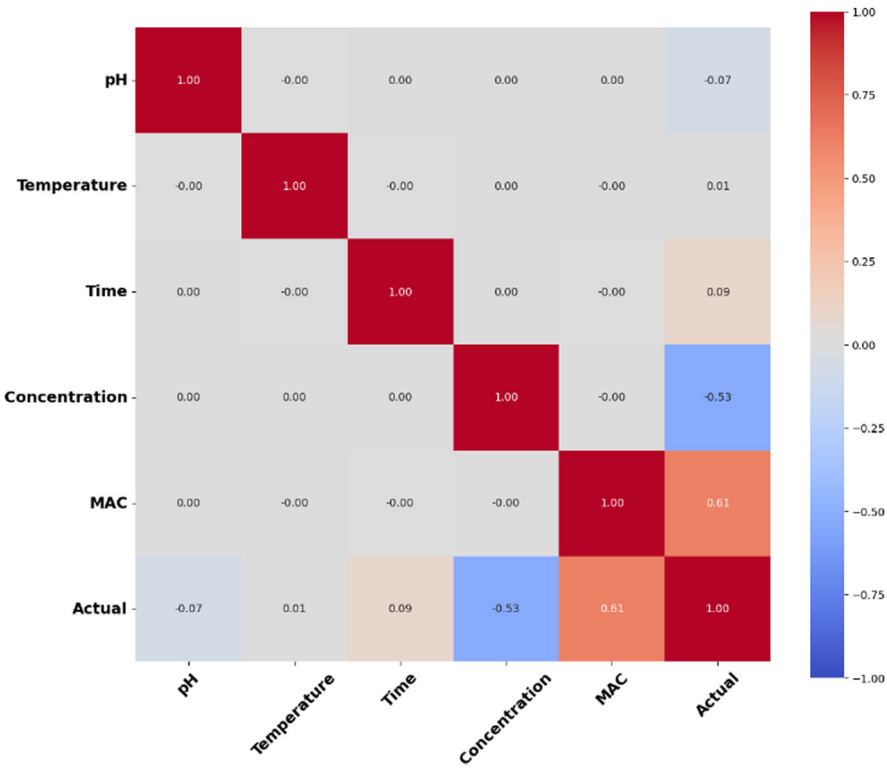


Figure 8.18 Pearson correlation heatmap showing the relationships between process parameters and adsorption efficiency.

removal performance, likely due to the saturation of available adsorption sites at elevated dye loads.

Other parameters, including pH, temperature, and contact time, display weak correlations with adsorption efficiency (correlation coefficients near zero), suggesting that their direct linear impact on the outcome is limited within the experimental range. These findings are consistent with the experimental results and discussions in the reference paper, highlighting that pH and contact time should be optimised, their influence is less significant than the dominant effects of MAC dosage and initial dye concentration.

Another valuable data exploration technique is 3D surface plots, which differ from heatmaps by visually representing how two process variables interactively influence the target response, while keeping other variables constant at their optimal values. Unlike heatmaps, which only capture pairwise linear relationships, 3D surface plots are invaluable for uncovering nonlinear and synergistic effects between variables, making them indispensable for process optimisation and interpretation in complex systems.

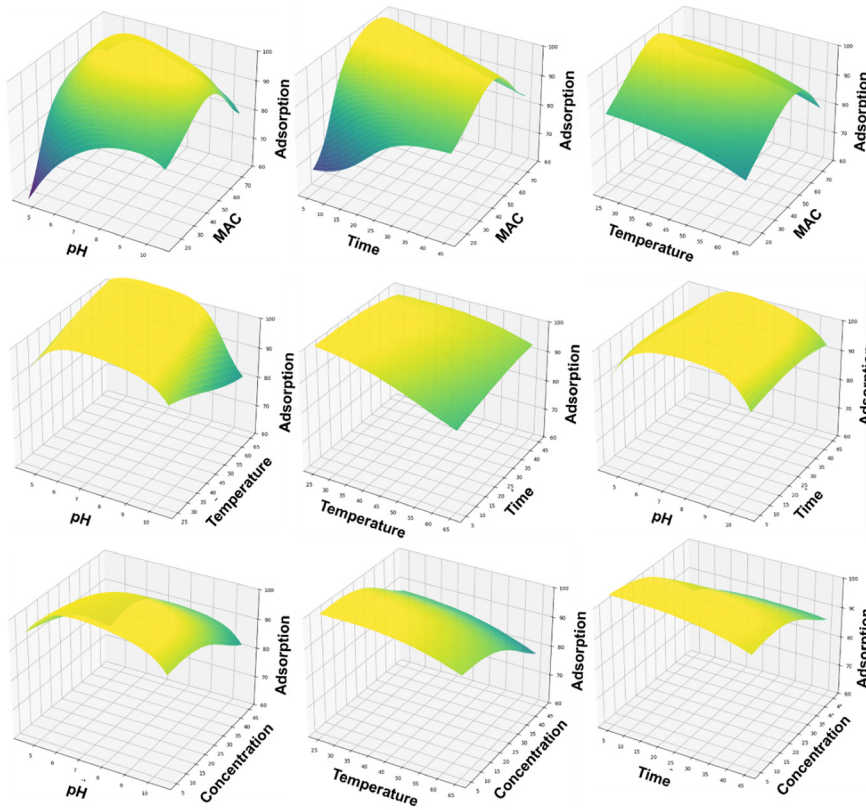


Figure 8.19 The surface plots show the effect of different parameters on the percent of crystal violet adsorption.

Figure 8.19 presents a matrix of 3D surface plots, each illustrating the combined effect of two key process variables on the crystal violet dye's adsorption efficiency (%) onto the adsorbent. These visualisations offer a comprehensive understanding of how these variables interact to affect dye removal, as established in the referenced research.

Analysis of the surface plots reveals that increasing the amount of MAC consistently enhances adsorption efficiency, especially when paired with an optimal pH of around 9.5. This improvement is attributed to the greater availability of active adsorption sites and the increased negative charge on the MAC surface at higher pH, promoting stronger cationic dye electrostatic attraction. Contact time also plays a significant role: adsorption efficiency rises rapidly with time and plateaus after approximately 36 min, indicating that equilibrium is reached quickly and that extending the process beyond this point yields minimal additional benefit.

Initial dye concentration, in contrast, demonstrates an inverse relationship with removal efficiency at higher values, likely due to the saturation of available adsorption sites. Therefore, maintaining the dye concentration within the optimal range (10–19.8 mg/L) is essential for maximising removal. Temperature exhibits only a minor effect within the studied range (25–65°C), suggesting that efficient adsorption can be achieved at room temperature, which is advantageous for practical applications.

In summary, these 3D surface plots confirm that optimising MAC dosage and maintaining pH near 9.5 are the most critical factors for high dye removal, while temperature and prolonged contact time offer limited additional improvements. The visual insights from these plots reinforce both the experimental results and the outcomes of statistical and machine learning modelling, highlighting the robustness and efficiency of MAC for crystal violet removal under optimised conditions.

8.7.2.2 Model training and evaluation

The ANN used in this study was carefully designed to achieve the best possible predictions for adsorption efficiency. As shown in Figure 8.20, the network's structure includes an input layer (which takes in all the process variables), one or more hidden layers (with a specific number of neurons), and an output layer (which gives the predicted adsorption percentage). Each neuron in a layer is connected to neurons in the next layer, and these connections have weights that the network adjusts during training. The hidden layers use special mathematical functions, called activation functions (like the tangent sigmoid or logarithmic sigmoid), which help the network learn complex and nonlinear patterns in the data.

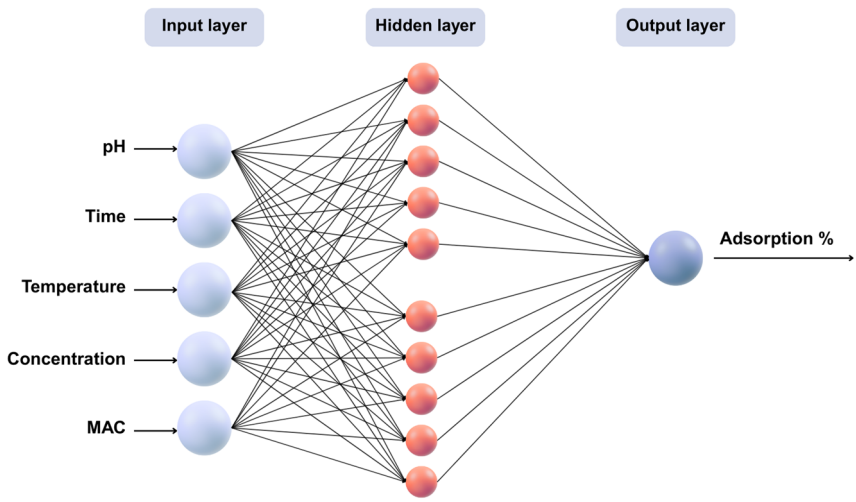


Figure 8.20 Schematic representation of the optimised artificial neural networks architecture.

During training, the ANN updates its weights to reduce the difference between its predictions and experimental results. This difference is measured using MSE. The network learns to make more accurate predictions by continuously adjusting the weights. The final ANN structure, with its optimised number of layers, neurons, and activation functions, enables the model to capture the complicated relationships in the adsorption process and deliver highly accurate results, as shown by the high R^2 and low error values reported in the study.

Figure 8.21 shows how the MSE changes during training over 1000 epochs (training cycles). The plot reveals that the MSE drops sharply within the first 100 epochs, which means the network is quickly learning and improving its predictions. After this rapid decrease, the MSE levels off and stays close to zero, showing that the model has learned from the data and is no longer making significant errors.

Another important evaluation is shown in the scatter plot in Figure 8.22, where the predicted adsorption percentages are compared to the actual experimental values. Most data points cluster tightly along the red dashed line, representing perfect agreement between experimental and predicted results, indicating a strong correlation and high predictive accuracy of the ANN model. While a few points show minor deviations from this line, the overall alignment demonstrates that the ANN effectively captures the complex, nonlinear relationships governing the adsorption process. This strong agreement is consistent with the research paper's findings, which report a high coefficient of determination ($R^2 = 0.9980$) and a very low mean absolute percentage error (MAPE = 0.38%).

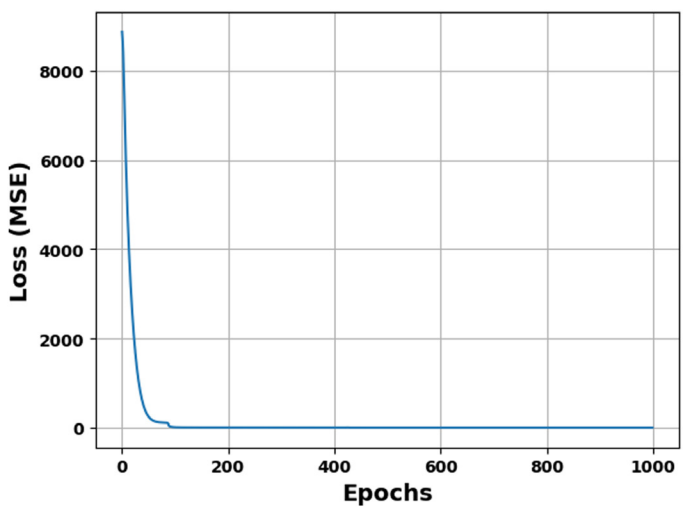


Figure 8.21 Training loss curve (MSE) vs epochs for the artificial neural networks model.

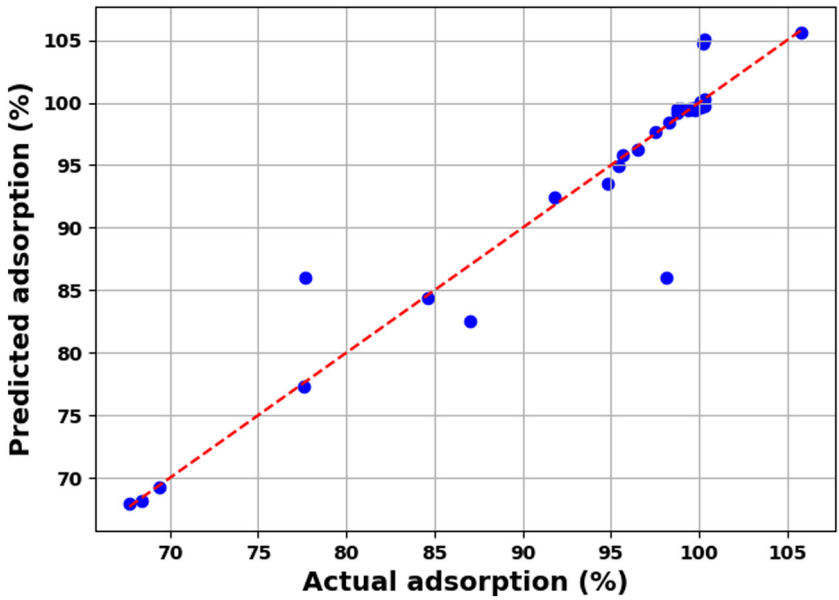


Figure 8.22 Comparison between the experimental and predicted values of adsorption (%).

8.7.2.3 Conclusion

This case study comprehensively demonstrates the successful application of MAC to remove crystal violet dye, supported by an advanced modelling approach. The 3D surface plots reveal that adsorption efficiency is most strongly influenced by the amount of MAC and solution pH, with optimal removal achieved at pH 9.5 and higher adsorbent dosages. Contact time up to 36 min is sufficient to reach equilibrium, while temperature and initial dye concentration play secondary roles, with efficient adsorption occurring even at room temperature and lower dye loads.

The Pearson correlation heatmap further confirms the dominant positive effect of MAC amount and the negative impact of higher dye concentrations on adsorption performance. These findings are reinforced by the ANN modelling results, where the loss curve shows rapid convergence and the parity plot demonstrates excellent agreement between predicted and experimental adsorption values ($R^2 = 0.9980$, MAPE = 0.38%). This highlights the ANN's superior predictive accuracy and robustness compared to traditional statistical methods.

Overall, integrating experimental data, statistical analysis, and machine learning modelling provides a clear understanding of the key factors governing crystal violet adsorption onto MAC. The study establishes that optimising adsorbent dosage and pH is critical for maximising dye removal, while temperature and prolonged contact time offer limited additional benefit. These insights validate the effectiveness of MAC as an adsorbent and underscore the value of ANN modelling for process prediction and optimisation in wastewater treatment applications.

8.7.3 Case study III: Response surface methodology

This case study investigates the adsorption performance of activated carbon for removing salicylic acid from synthetic aqueous solutions, based on the study by Taoufik *et al.* (2021). A predictive model was developed using RSM to explore the influence of key process parameters and minimise the number of experimental trials. A CCD was employed to evaluate the interactive and individual effects of four independent variables – pH (A), initial salicylic acid concentration (B), mass of adsorbent (C), and contact time (D) – on adsorption performance. The levels of each variable were chosen based on preliminary studies and are listed in Table 8.4, using both coded and natural values. This model aims to identify optimal operating conditions for maximum removal efficiency and adsorbed quantity while providing insight into each parameter's statistical significance and sensitivity in adsorption.

Table 8.5 shows the four-factor CCD in coded and uncoded values and observed and predicted responses.

The estimated regression models developed for predicting the adsorbed quantity and removal efficiency are presented as Eqs (8.17) and (8.18), respectively. These models were derived using RSM based on the experimental design matrix. The fit quality for both models was assessed using the coefficient of determination (R^2), which reflects the proportion of variance in the response explained by the model. The R^2 values for both models were reasonably high, indicating that the models accurately capture the influence of input parameters on the respective responses and can be reliably used for prediction and optimisation within the studied domain.

$$\begin{aligned}\text{Adsorbed quantity} = {} & 3.05957 + 0.170625 \times A + 1.05371 \times B - 1.22138 \times C \\ & + 0.175875 \times D + 0.203063 \times AB - 0.238937 \times AC \\ & - 0.184937 \times AD - 0.229812 \times BC + 0.212188 \times BD \\ & - 0.195812 \times CD - 0.0536741 \times A^2 + -0.101174 \times B^2 \\ & + 0.514701 \times C^2 + -0.0961741 \times D^2\end{aligned} \tag{8.17}$$

Figure 8.23a shows the normal probability plot of residuals, which demonstrates that the residuals closely follow a straight line, indicating that the errors are normally distributed and validating the assumptions of

Table 8.4 Levels of independent variables used for central composite design.

Natural Variables (x_j)	Coded Variables					ΔX
	−2	−1	0	1	2	
A = pH	3	4	5	6	7	1
B = initial concentration (mg/dm³)	5	10	15	20	25	5
C = mass of adsorbent (mg)	15	20	25	30	35	5
D = Contact time (min)	30	50	70	90	110	20

Table 8.5 Four-factor CCD in coded and uncoded values and observed and predicted responses.

Run order	A	B	C	D	Response		Response	
	pH	Initial Concentration (mg/dm^3)	Mass of Adsorbent (mg)	Contact Time (min)	Adsorbed Quantity (mg/g)		Removal Efficiency (%)	
					Experimental	Predicted	Experimental	Predicted
1	6	20	20	50	2.95	3.05	88.50	89.82
2	6	20	20	50	6.29	6.84	94.40	95.77
3	3	15	20	50	3.07	2.50	92.03	90.62
4	5	15	20	50	3.07	3.06	92.16	91.81
5	5	15	30	50	3.08	3.06	92.40	91.81
6	5	5	30	50	0.89	0.55	80.64	78.18
7	4	10	30	50	2.69	2.71	80.69	83.20
8	6	20	30	50	3.26	3.07	97.95	95.34
9	4	20	20	90	3.05	2.41	91.54	91.32
10	6	10	20	90	2.83	3.49	85.00	86.05
11	6	20	20	90	6.30	6.04	91.65	90.71
12	5	15	20	90	8.99	7.56	89.88	88.38
13	5	15	30	90	1.80	2.68	90.01	90.00
14	5	15	30	90	3.07	3.06	92.25	91.81
15	4	10	30	90	2.78	3.40	83.30	83.58
16	6	10	30	90	2.98	3.44	89.44	89.56
17	4	10	25	70	1.42	1.50	85.25	86.09
18	4	10	25	70	1.42	1.60	85.03	85.26
19	4	20	25	70	2.87	4.45	86.00	87.08
20	6	10	25	70	1.37	1.42	82.11	82.99
21	5	15	15	70	3.02	3.06	90.51	91.81
22	5	15	35	70	3.00	3.06	90.00	91.81
23	5	15	25	30	3.11	3.06	93.18	91.81
24	5	25	25	110	4.97	4.76	89.50	90.46
25	5	15	25	70	3.00	3.03	90.00	90.70
26	6	10	25	70	1.44	0.59	86.42	86.94
27	5	15	25	70	2.9	2.32	87.00	84.80
28	5	15	25	70	3.07	3.06	92.18	91.81
29	4	20	25	70	6.22	5.98	90.00	89.03
30	4	20	25	70	3.11	3.17	93.17	93.72
31	7	15	25	70	3.17	3.19	95.19	95.09

the ANOVA model. Figure 8.23b presents the predicted vs. actual values of adsorbed quantity, where the data points are tightly clustered along the diagonal line. This alignment confirms a strong agreement between experimental and model-predicted values, reflecting good predictive performance of the model.

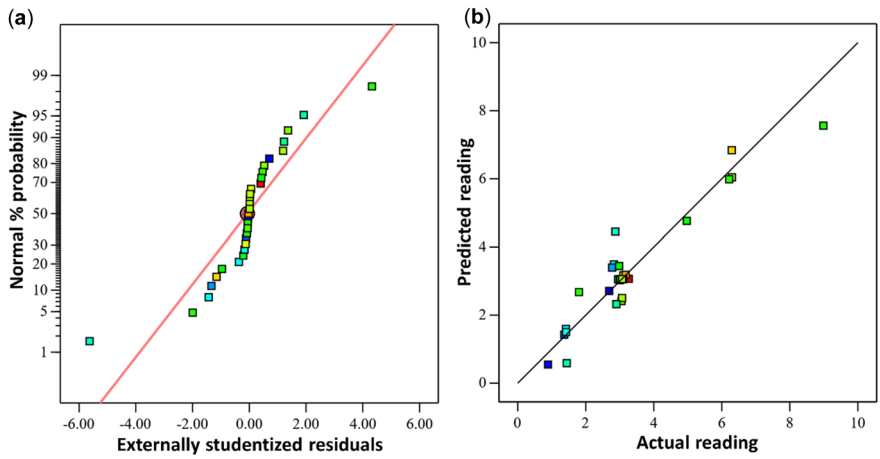


Figure 8.23 (a) Normal plot of residuals, (b) predicted vs actual.

$$\begin{aligned}\text{Removal efficiency} = {} & 91.8106 + 1.11733 \times A + 3.06958 \times B \\ & + 0.406333 \times C + 1.47475 \times D + 0.193125 \times AB \\ & - 1.281 \times AC + 0.78125 \times AD + 0.5455 \times BC \\ & + 0.391 \times BD + 0.113625 \times CD + 0.262045 \times A^2 \\ & - 1.87258 \times B^2 - 0.65508 \times C^2 + - 1.01571 \times D^2\end{aligned} \tag{8.18}$$

Figure 8.24a depicts the normal probability plot of residuals for removal efficiency, showing a reasonably linear distribution of points, supporting the

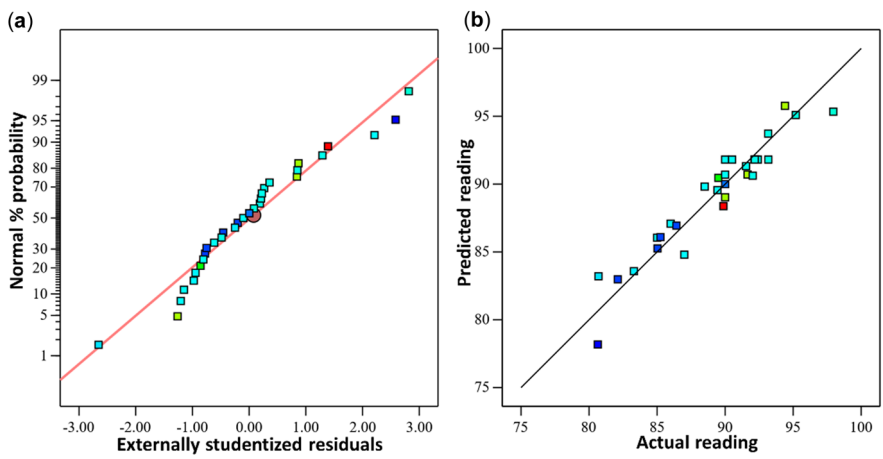


Figure 8.24 (a) Normal plot of residuals, (b) predicted vs actual.

normality of residuals and the adequacy of the model. Figure 8.24b illustrates the predicted vs. actual values, where the data points lie close to the ideal 1:1 line, suggesting that the model can reliably estimate removal efficiency across the tested range. This further validates the robustness of the regression model developed using RSM.

ANOVA was conducted to evaluate the significance and adequacy of the developed models for both the adsorbed quantity and removal efficiency responses. For adsorbed quantity, the model F-value of 10.04 indicates the model is statistically significant, with only a 0.01% probability that this result could occur due to noise. Among the model terms, variables B (e.g., adsorbent dosage), C (e.g., pH), and the quadratic term C^2 were found to be significant ($p < 0.05$), suggesting that these factors have a strong influence on adsorption behaviour. However, the model shows a significant lack of fit (F-value = 635.66, $p < 0.01$), indicating that the model may not adequately capture the variability in the experimental data and may require refinement or transformation.

For the removal efficiency, the model also proved to be statistically significant with an F-value of 11.83 and a similarly low chance (0.01%) of this occurring due to random error. The significant terms identified were A, B, D, AC, B^2, and D^2, highlighting both linear and interaction effects as important contributors to removal performance. The lack of fit F-value of 3.12 corresponds to an 8.83% probability, which, while not below the standard 5% threshold, is still relatively low and may indicate moderate model inadequacy. This suggests the need for cautious interpretation, though the model remains generally acceptable for predictive use.

These results, supported by the ANOVA Table 8.6, emphasise the critical role of selecting appropriate model terms and evaluating lack-of-fit to ensure statistical robustness and predictive accuracy in adsorption modelling.

8.7.3.1 Effect of varying input process variables on adsorbed quantity and removal efficiency

Variations significantly influenced the adsorbed quantity in key process variables. An increase in initial concentration generally led to higher adsorption, as more pollutant molecules were available to occupy active sites on the adsorbent surface. Adsorbent mass positively affected adsorption up to a certain point by increasing the number of available binding sites; however, beyond a threshold, the effect plateaued due to site saturation or particle aggregation. Contact time initially showed a strong positive effect, allowing sufficient interaction between solute and adsorbent, but reached equilibrium, after which no further significant increase in adsorption was observed. The effect of pH was more system-specific, but adsorption typically increased or decreased depending on the adsorbate's ionisation state and the adsorbent's surface charge, highlighting the importance of electrostatic interactions in the adsorption mechanism. This trend is further illustrated in the perturbation plot for adsorbed quantity (Figure 8.25), where the curves' steepness highlights each variable's relative sensitivity to the system's performance.

Table 8.6 ANOVA of responses for the adsorption process.

	Source	Sum of Squares	DF	Mean Square	F-value	p-value	
Adsorbed quantity	Model	77.2	14	5.51	10.04	<0.0001	Significant
	A-pH	0.6987	1	0.6987	1.27	0.2761	
	B-IC	26.65	1	26.65	48.5	<0.0001	
	C-M	35.8	1	35.8	65.16	<0.0001	
	D-T	0.7424	1	0.7424	1.35	0.2621	
	AB	0.6598	1	0.6598	1.2	0.2894	
	AC	0.9135	1	0.9135	1.66	0.2156	
	AD	0.5472	1	0.5472	0.996	0.3331	
	BC	0.845	1	0.845	1.54	0.2328	
	BD	0.7204	1	0.7204	1.31	0.269	
	CD	0.6135	1	0.6135	1.12	0.3063	
	A^2	0.0824	1	0.0824	0.1499	0.7037	
	B^2	0.2927	1	0.2927	0.5328	0.476	
	C^2	7.58	1	7.58	13.79	0.0019	
	D^2	0.2645	1	0.2645	0.4814	0.4977	
	Lack of Fit	8.78	10	0.8782	635.66	<0.0001	
	Pure Error	0.0083	6	0.0014			
	Total	85.99	30				
Removal efficiency	Model	489.66	14	34.98	11.83	<0.0001	Significant
	A-pH	29.96	1	29.96	10.13	0.0058	
	B-IC	226.14	1	226.14	76.46	<0.0001	
	C-M	3.96	1	3.96	1.34	0.2641	
	D-T	52.2	1	52.2	17.65	0.0007	
	AB	0.5968	1	0.5968	0.2018	0.6593	
	AC	26.26	1	26.26	8.88	0.0089	
	AD	9.77	1	9.77	3.3	0.088	
	BC	4.76	1	4.76	1.61	0.2227	
	BD	2.45	1	2.45	0.827	0.3766	
	CD	0.2066	1	0.2066	0.0698	0.7949	
	A^2	1.96	1	1.96	0.6639	0.4271	
	B^2	100.27	1	100.27	33.9	<0.0001	
	C^2	12.27	1	12.27	4.15	0.0586	
	D^2	29.5	1	29.5	9.97	0.0061	
	Residual	47.32	16	2.96			
	Lack of Fit	39.69	10	3.97	3.12	0.0883	
	Pure Error	7.63	6	1.27			
	Total	536.98	30				

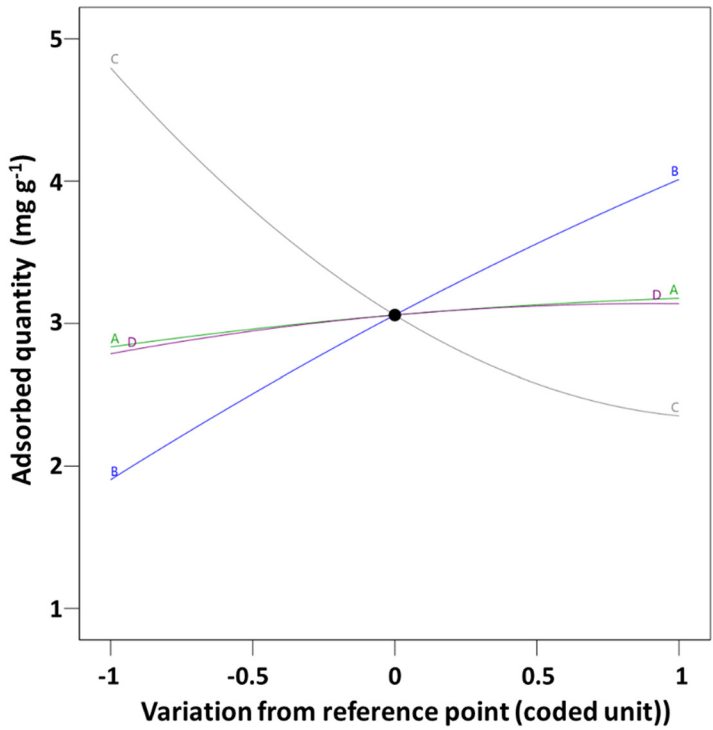


Figure 8.25 Perturbation plot for adsorbed quantity.

Changes strongly influenced the removal efficiency of the adsorption process in process variables. Adsorbent mass played a critical role, with increased mass enhancing removal efficiency due to more active adsorption sites. However, the improvement tapered beyond an optimal point as the system approached equilibrium. Initial concentration had an inverse relationship with removal efficiency at higher levels, as excessive pollutant load could exceed the adsorption capacity, leading to reduced efficiency. Contact time positively affected removal efficiency up to the equilibrium point, beyond which no significant improvement was observed. pH had a notable effect depending on the charge characteristics of both adsorbent and adsorbate; optimal pH levels enhanced adsorption by improving electrostatic interactions, while unfavourable pH values reduced efficiency due to repulsion or loss of active functional groups. This trend is further illustrated in the perturbation plot for removal efficiency (Figure 8.26), where the curves' steepness highlights each variable's relative sensitivity to the system's performance.

8.7.3.2 Interaction effect of varying input process variables on adsorbed quantity and removal efficiency

The interaction between key process variables significantly influenced the adsorbed quantity, highlighting the importance of studying combined effects

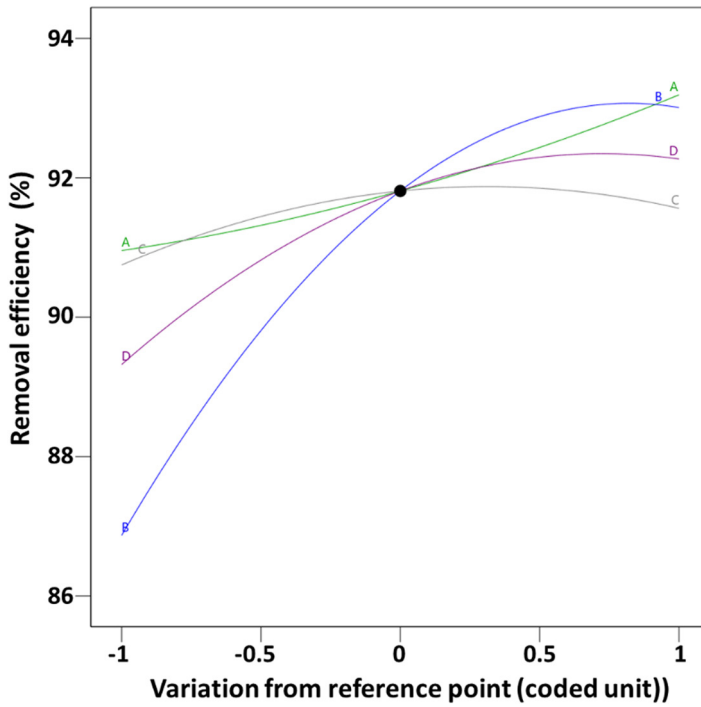


Figure 8.26 Perturbation plot for removal efficiency.

rather than individual parameters in isolation. Interaction plots revealed that the combined influence of variables such as pH and initial concentration, adsorbent mass and contact time, and pH and adsorbent mass resulted in nonlinear adsorption behaviour. For example, a higher initial concentration enhanced adsorption at moderate pH levels but showed diminished effect under extreme pH conditions, likely due to changes in surface charge and ionisation behaviour. Similarly, increasing adsorbent mass improved adsorption only when sufficient contact time was allowed, indicating that equilibrium dynamics are crucial. These synergistic and antagonistic interactions underscore the complexity of the adsorption mechanism. The detailed interaction effects are visualised in Figure 8.27, which presents the response surface and contour plots for key variable pairs, providing insight into optimal regions for maximising adsorbed quantity.

The interaction between input process variables had a pronounced effect on removal efficiency, revealing complex relationships that influence the system's overall performance. Interaction plots demonstrated that combinations such as pH and initial concentration, adsorbent mass and contact time, and pH and adsorbent dosage significantly impacted the removal efficiency nonlinearly. For instance, the removal efficiency increased with adsorbent mass at low initial concentrations but plateaued at higher concentrations, suggesting

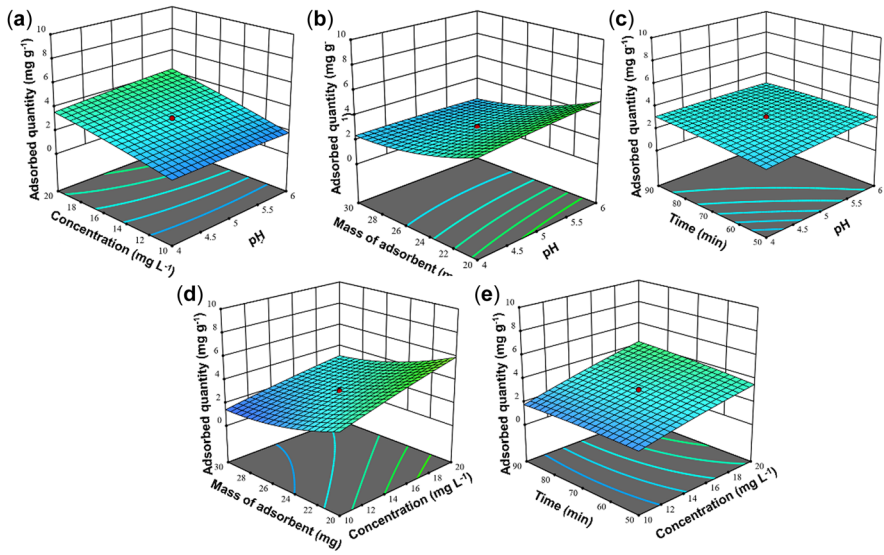


Figure 8.27 Interaction effect of input process variables on adsorption quantity.

limited active site availability under heavy pollutant loads. Additionally, the effect of pH was more pronounced at longer contact times, likely due to enhanced ionisation of functional groups and greater accessibility to adsorption sites. These findings emphasise the importance of multi-variable optimisation to capture the system dynamics fully. The response surface and contour plots shown in Figure 8.28 illustrate these interactions, identifying the most favourable combinations of process variables for achieving maximum removal efficiency.

8.7.3.3 Conclusion

This case study demonstrated the effective use of RSM for optimising the adsorption of salicylic acid onto activated carbon from synthetic aqueous solutions. The individual and interactive effects of pH, initial concentration, adsorbent mass, and contact time were systematically analysed through a CCD. The developed regression models for adsorbed quantity and removal efficiency exhibited strong predictive accuracy, as confirmed by high R^2 values and statistically significant ANOVA results. Perturbation and interaction plots provided insight into parameter sensitivity and their combined influence on system performance. Optimal process conditions were identified with minimal experimentation, reinforcing the value of RSM in guiding experimental planning, reducing cost, and enhancing process efficiency. This case study affirms that RSM is a robust and reliable tool for optimising adsorption processes in water treatment applications.

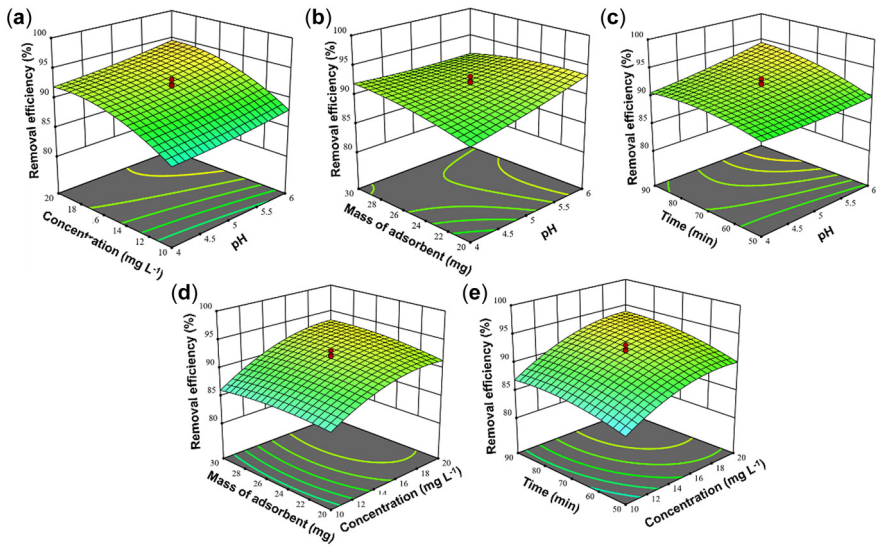


Figure 8.28 Interaction effect of input process variables on removal efficiency.

8.8 SUMMARY

With computing power and user-friendly software advancements, CFD has become a critical tool for simulating complex transport phenomena in porous adsorbent systems, reducing experimental dependency and enabling virtual prototyping. Parallel to this, the increasing availability of statistical computing tools has expanded the adoption of RSM and ANN for process modelling and optimisation. These methods enable efficient experimental design, accurate prediction of system responses, and identification of optimal operating conditions with fewer trials. RSM is particularly effective in modelling quadratic interactions, while ANN excels in capturing complex nonlinear relationships without needing an explicit functional form.

The integration of CFD for simulation and RSM/ANN for optimisation provides a comprehensive framework for understanding, designing, and scaling up adsorption systems. These tools offer significant advantages in reducing experimentation time, identifying critical factors, and improving system performance under realistic operating conditions. As computational tools continue to advance, their combined use is expected to become even more integral to research and industrial applications in adsorption and environmental engineering.

This chapter explored the simulation and optimisation of adsorption processes through computational and data-driven approaches. It began with an overview of the historical development of CFD, followed by a detailed explanation of its governing equations, numerical solution methods, meshing techniques, and

application-specific considerations such as turbulence modelling, porous media flow, and non-Newtonian fluid dynamics. The chapter then transitioned to process optimisation using statistical and machine learning methods, focusing on RSM and ANN. Each technique was explained with respect to experimental design, model building, and optimisation strategy, followed by a comparison of their capabilities for complex multi-variable systems.

References

Abd-elaziem, A. H. and Soliman, T. H. (2023). A multi-layer perceptron (MLP) neural networks for stellar classification: A review of methods and results. *International Journal of Advances in Applied Computational Intelligence*, **3**(10.54216). https://doi.org/10.54216/IJAACI.030203

Abiodun, O. I., Jantan, A., Omolara, A. E., Dada, K. V., Mohamed, N. A. and Arshad, H. (2018). State-of-the-art in artificial neural network applications: A survey. *Heliyon*, **4**(11). https://doi.org/10.1016/j.heliyon.2018.e00938

Aguayo-Villarreal, I. A., Cortes-Arriagada, D., Rojas-Mayorga, C. K., Pineda-Urbina, K., Muñiz-Valencia, R. and González, J. (2020). Importance of the interaction adsorbent–adsorbate in the dyes adsorption process and DFT modeling. *Journal of Molecular Structure*, **1203**, 127398. https://doi.org/10.1016/j.molstruc.2019.127398

Ahamad, A., Madhav, S., Singh, A.K., Kumar, A., Singh, P. (2020). Types of Water Pollutants: Conventional and Emerging. In: Pooja, D., Kumar, P., Singh, P., Patil, S. (eds) Sensors in Water Pollutants Monitoring: Role of Material. Advanced Functional Materials and Sensors. Springer, Singapore. https://doi.org/10.1007/978-981-15-0671-0_3

Akhtar N., Ishak M. I. S., Bhawani S. A. and Umar K. (2021). Various natural and anthropogenic factors responsible for water quality degradation: a review. *Water*, **13**(19), 2660. https://doi.org/10.3390/w13192660

Alaqarbeh, M. (2021). Adsorption phenomena: definition, mechanisms, and adsorption types: short review. *RHAZES: Green and Applied Chemistry*, **13**, 43–51. https://doi.org/10.48419/IMIST.PRSM/rhazes-v13.28283

Alavi, S. (2020). Molecular simulations: fundamentals and practice. John Wiley and Sons, United States. https://doi.org/10.1002/9783527699452

Alder B. J. and Wainwright T. E. (1957). Phase transition for a hard sphere system. *The Journal of Chemical Physics*, **27**(5), 1208–1209. https://doi.org/10.1063/1.1743957

Alex K., Ilya S., Geoffrey E. H., 2012. ImageNet classification with deep convolutional neural networks. In: Proceedings of the 25th International Conference on Neural Information Processing Systems - (NIPS'12), **1**, 1097–1105. https://doi.org/10.1145/3065386.

Alfaifi H. J., Kahal A. Y., Abdelrahman K., Zaidi F. K., Albassam A. and Lashin A. (2020). Assessment of groundwater quality in Southern Saudi Arabia: case study of Najran area. *Arabian Journal of Geosciences*, **13**(3), 101. https://doi.org/10.1007/s12517-020-5109-2

Al-Ghouti M. A. and Da'ana D. A. (2020). Guidelines for the use and interpretation of adsorption isotherm models: a review. *Journal of Hazardous Materials*, **393**, 122383. https://doi.org/10.1016/j.jhazmat.2020.122383

Ali I. and Gupta V. K. (2006). Advances in water treatment by adsorption technology. *Nature Protocols*, **1**(6), 2661–2667. https://doi.org/10.1038/nprot.2006.370

Al Mahmoud, Z., Safaei, B., Sahmani, S., Asmael, M., Shahzad, M. A., Zeeshan, Q. and Qin, Z. (2024). Implementation of different types of meshfree technique in computational solid mechanics: a comprehensive review across nano, micro, and macro scales. *Archives of Computational Methods in Engineering*, **31**(2), 725–838. https://doi.org/10.1007/s11831-023-09999-6

Al-Tohamy, R., Ali, S. S., Li, F., Okasha, K. M., Mahmoud, Y. A. G., Elsamahy, T., Jiao H., Fu Y. and Sun, J. (2022). A critical review on the treatment of dye-containing wastewater: Ecotoxicological and health concerns of textile dyes and possible remediation approaches for environmental safety. *Ecotoxicology and environmental safety*, **231**, 113160. https://doi.org/10.1016/j.ecoenv.2021.113160

Anfar, Z., Ait Ahsaine, H., Zbair, M., Amedlous, A., Ait El Fakir, A., Jada, A. and El Alem, N. (2020). Recent trends on numerical investigations of response surface methodology for pollutants adsorption onto activated carbon materials: A review. *Critical Reviews in Environmental Science and Technology*, **50**(10), 1043–1084. https://doi.org/10.1080/10643389.2019.1642835

Arrhenius, S. (1889). Über die Dissociationswärme und den Einfluss der Temperatur auf den Dissociationsgrad der Elektrolyte. *Zeitschrift für physikalische Chemie*, **4**(1), 96–116. https://doi.org/10.1515/zpch-1889-0408

Awfa, D., Ateia, M., Mendoza, D. and Yoshimura, C. (2021). Application of quantitative structure–property relationship predictive models to water treatment: a critical review. *ACS ESandT Water*, **1**(3), 498–517. https://doi.org/10.1021/acsestwater.0c00206

Bachmann S. J. and van Gunsteren W. F. (2014). An improved simple polarisable water model for use in biomolecular simulation. *The Journal of Chemical Physics*, **141**(22). https://doi.org/10.1063/1.4897976

Bahuguna, A., Singh, S. K., Bahuguna, A., Sharma, S. and Dadarwal, B. K. (2021). Physical method of Wastewater treatment - A review. *J. Res. Environ. Earth Sci*, **7**, 2348–2532.

Basconi J. E. and Shirts M. R. (2013). Effects of temperature control algorithms on transport properties and kinetics in molecular dynamics simulations. *Journal of Chemical Theory and Computation*, **9**(7), 2887–2899. https://doi.org/10.1021/ct400109a

Bezerra, M. A., Santelli, R. E., Oliveira, E. P., Villar, L. S. and Escaleira, L. A. (2008). Response surface methodology (RSM) as a tool for optimization in analytical chemistry. *Talanta*, **76**(5), 965–977. https://doi.org/10.1016/j.talanta.2008.05.019

Bolboaca, S. D., Jantschi, L. and Diudea, M. V. (2013). Molecular design and QSARs/QSPRs with molecular descriptors family. *Current computer-aided drug design*, **9**(2), 195–205. https://doi.org/10.2174/1573409911309020005

Box G. E. P. and Wilson K. B. (1951). On the experimental attainment of optimum conditions. *Journal of the Royal Statistical Society: Series B (Methodological)*, **13**(1), 1–38. https://doi.org/10.1111/j.2517-6161.1951.tb00067.x

Boyd G. E., Adamson A. W. and Myers L. S. (1947). The exchange adsorption of ions from aqueous solutions by organic zeolites. II. Kinetics. *Journal of the American Chemical Society*, **69**(11), 2836–2848. https://doi.org/10.1021/ja01203a066

Brereton, R. G. (2012). Self organising maps for visualising and modelling. *Chemistry Central Journal*, **6** (Suppl 2), S1. https://doi.org/10.1186/1752-153X-6-S2-S1

Briffa J., Sinagra E. and Blundell R. (2020). Heavy metal pollution in the environment and their toxicological effects on humans. *Heliyon*, **6**(9), e04691. https://doi.org/10.1016/j.heliyon.2020.e04691

Brunauer S., Emmett P. H. and Teller E. (1938). Adsorption of gases in multimolecular layers. *Journal of the American Chemical Society*, **60**(2), 309–319. https://doi.org/10.1021/ja01269a023

Brusseau M. L., Pepper I. and Gerba C. (2019). Environmental and pollution science. Academic Press. https:doi//.org/10.1016/C2017-0-00480-9

Bučko T., Hafner J. and Ángyán J. G. (2005). Geometry optimization of periodic systems using internal coordinates. *The Journal of Chemical Physics*, **122**(12), 124508. https://doi.org/10.1063/1.1864932

Bureau of Indian Standards (2012). IS 10500: Drinking Water Specification. BIS, New Delhi, India.

Cao, A. and Nørskov, J. K. (2023). Spin effects in chemisorption and catalysis. *ACS Catalysis*, **13**(6), 3456–3462. https://doi.org/10.1021/acscatal.2c06319

Carpenter S. R., Caraco N. F., Correll D. L., Howarth R. W., Sharpley A. N. and Smith V. H. (1998). Non-point pollution of surface waters with phosphorus and nitrogen. *Ecological Applications*, **8**(3), 559–568. https://doi.org/10.1890/1051-0761(1998)008[0559:NPOSWW]2.0.CO;2

Carrard N., Foster T. and Willetts J. (2019). Groundwater as a source of drinking water in Southeast Asia and the Pacific: a multi-country review of current reliance and resource concerns. *Water*, **11**(8), 1605. https://doi.org/10.3390/w11081605

CGWB (2014). Concept Note on Geogenic Contamination of Ground Water in India. Central Ground Water Board, Ministry of Water Resources, Government of India, India.

Chakraborty, A., Adhikary, S., Bhattacharya, S., Dutta, S., Chatterjee, S., Banerjee, D., Ganguly A. and Rajak, P. (2023). Pharmaceuticals and personal care products as emerging environmental contaminants: prevalence, toxicity, and remedial approaches. *ACS Chemical Health and Safety*, **30**(6), 362–388. https://doi.org/10.1021/acs.chas.3c00071

Charbuty, B. and Abdulazeez, A. (2021). Classification based on decision tree algorithm for machine learning. *Journal of applied science and technology trends*, **2**(01), 20–28. https://doi.org/10.38094/jastt20165

Chaudhry, F. N. and Malik, M. F. (2017). Factors affecting water pollution: a review. *J. Ecosyst. Ecography*, **7**(1), 225–231. https://doi.org/10.4172/2157-7625.1000225

Choudri, B. S., Charabi, Y., Al-Nasiri, N., and Al-Awadhi, T. (2020). Pesticides and herbicides. *Water environment research*, **92**(10), 1425–1432. https://doi.org/10.1002/wer.1380

Clifton, J. and Laber, E. (2020). Q-learning: Theory and applications. *Annual Review of Statistics and Its Application*, **7**(1), 279–301. https://doi.org/10.1146/annurev-statistics-031219-041220

Coasne, B. (2016). Multiscale adsorption and transport in hierarchical porous materials. *New Journal of Chemistry*, **40**(5), 4078–4094. https://doi.org/10.1039/C5NJ03194J

Coasne, B., Galarneau, A., Gerardin, C., Fajula, F. and Villemot, F. (2013). Molecular simulation of adsorption and transport in hierarchical porous materials. *Langmuir*, **29**(25), 7864–7875. https://doi.org/10.1021/la401228k

Committee on the Implications of Dioxin in the Food Supply (2003). Dioxins and dioxin-like compounds in the food supply: Strategies to decrease exposure. National Academies Press, United States.

Courant R., Friedrichs K. and Lewy H. (1928). Über die partiellen differenzengleichungen der mathematischen physik. *Mathematische Annalen*, **100**(1), 32–74. https://doi.org/10.1007/BF01448839

Crini G. and Lichtfouse E. (2019). Advantages and disadvantages of techniques used for wastewater treatment. *Environmental Chemistry Letters*, **17**(1), 145–155. https://doi.org/10.1007/s10311-018-0785-9

De Jong, K. (1988). Learning with genetic algorithms: An overview. *Machine learning*, **3**(2), 121–138. https://doi.org/10.1007/BF00113894

De Souza, O. N. and Ornstein, R. L. (1997). Effect of periodic box size on aqueous molecular dynamics simulation of a DNA dodecamer with particle-mesh Ewald method. *Biophysical journal*, **72**(6), 2395–2397. https://doi.org/10.1016/S0006-3495(97)78884-2

Dhanabal, S. and Chandramathi, S. J. I. J. C. A. (2011). A review of various k-nearest neighbor query processing techniques. *International Journal of Computer Applications*, **31**(7), 14–22.

Dickenson, E. R., Drewes, J. E., Stevens-Garmon, J., Khan, S. and McDonald, J. (2010). Evaluation of QSPR techniques for wastewater treatment processes. *WEFTEC* **2010**, 4084–4096. https://doi.org/10.2175/193864710798181629

Dindorkar, S. S., Patel, R. V. and Yadav, A. (2023). Adsorption behaviour of graphene, boron nitride and boron carbon nitride nanosheets towards pharmaceutical and personal care products. *Computational and Theoretical Chemistry*, **1220**, 113995. https://doi.org/10.1016/j.comptc.2022.113995

Dindorkar, S. S., Patel, R. V. and Yadav, A. (2022). Unravelling the interaction between boron nitride nanosheets and organic pesticides through density functional theory studies. *Colloids and Surfaces A: Physicochemical and Engineering Aspects*, **649**, 129550. https://doi.org/10.1016/j.colsurfa.2022.129550

Do, D. D. and Do, H. D. (2006). Modeling of adsorption on nongraphitized carbon surface: GCMC simulation studies and comparison with experimental data. *The Journal of Physical Chemistry B*, **110**(35), 17531–17538. https://doi.org/10.1021/jp062386r

Doney S. C., Busch D. S., Cooley S. R. and Kroeker K. J. (2020). The impacts of ocean acidification on marine ecosystems and dependent human communities. *Annual Review of Environment and Resources*, **45**, 83–112. https://doi.org/10.1146/annurev-environ-012320-083019

Dotto, G. L. and McKay, G. (2020). Current scenario and challenges in adsorption for water treatment. *Journal of environmental chemical engineering*, **8**(4), 103988. https://doi.org/10.1016/j.jece.2020.103988

Dubinin M. M. and Radushkevich L. V. (1973). Kinetics and Dynamics of Physical Adsorption. *Nauka*, Moscow.

Ekberg, V., Samways, M. L., Misini Ignjatović, M., Essex, J. W. and Ryde, U. (2022). Comparison of grand canonical and conventional molecular dynamics simulation methods for protein-bound water networks. *ACS Physical Chemistry Au*, **2**(3), 247–259. https://doi.org/10.1021/acsphyschemau.1c00052

Elfghi, F. M. (2016). A hybrid statistical approach for modeling and optimization of RON: A comparative study and combined application of response surface methodology (RSM) and artificial neural network (ANN) based on design of experiment (DOE). *Chemical Engineering Research and Design*, **113**, 264–272. https://doi.org/10.1016/j.cherd.2016.05.023

Elovich S. Y. and Larionov O. G. (1962). Theory of adsorption from nonelectrolyte solutions on solid adsorbents. *Bulletin of the Academy of Sciences of the USSR Division of Chemical Science*, **11**(2), 198–203. https://doi.org/10.1007/bf00908017

Fallahzadeh R. A., Almodaresi S. A., Ghadirian D., Fattahi A. and Homayoni Bezi N. (2019). Spatial analysis and probabilistic risk assessment of exposure to nitrate in drinking water of Abarkouh, Iran. *Journal of Environmental Health and Sustainable Development*, **4**(4), 1054–1064. https://jehsd.ssu.ac.ir/article-1-194-en.html

Farmahini, A. H., Krishnamurthy, S., Friedrich, D., Brandani, S. and Sarkisov, L. (2018). From crystal to adsorption column: challenges in multiscale computational screening of materials for adsorption separation processes. *Industrial and Engineering Chemistry Research*, **57**(45), 15491–15511. https://doi.org/10.1021/acs.iecr.8b03065

Faust, S. D. and Aly, O. M. (2013). Adsorption processes for water treatment. Elsevier, Netherlands. https://doi.org/10.1016/C2013-0-04267-3

Fischer J. and Wendland M. (2023). On the history of key empirical intermolecular potentials. *Fluid Phase Equilibria*, **573**, 113876. https://doi.org/10.1016/j.fluid.2023.113876

Flory P. J. (1942). Thermodynamics of high polymer solutions. *The Journal of Chemical Physics*, **10**(1), 51–61. https://doi.org/10.1063/1.1723621

Freundlich V. H. (1909). Die Bedeutung der Kapillarchemie für technische und physiologische Fragen. *Zeitschrift für Angewandte Chemie*, **1766**(1904), 1905–1907.

Fritz W. and Schluender E. U. (1974). Simultaneous adsorption equilibria of organic solutes in dilute aqueous solutions on activated carbon. *Chemical Engineering Science*, **29**(5), 1279–1282. https://doi.org/10.1016/0009-2509(74)80128-4

Gad, A. G. (2022). Particle swarm optimization algorithm and its applications: A systematic review. *Archives of computational methods in engineering*, **29**(5). https://doi.org/10.1007/s11831-021-09694-4

Geerlings, P., De Proft, F. and Langenaeker, W. (2003). Conceptual density functional theory. *Chemical reviews*, **103**(5), 1793–1874. https://doi.org/10.3390/i3040276

Geerlings, P. and De Proft, F. (2002). Chemical reactivity as described by quantum chemical methods. *International Journal of Molecular Sciences*, **3**(4), 276–309.

Gelpi J., Hospital A., Goñi R. and Orozco M. (2015). Molecular dynamics simulations: advances and applications. *Advances and Applications in Bioinformatics and Chemistry*, **10**(1), 37. https://doi.org/10.2147/AABC.S70333

Gleick P. H. and Iceland C. (2018). Water, Security, and Conflict. World Resources Institute, United States. https://www.wri.org/publication/water-security-and-conflict

Glueckauf E. and Coates J. I. (1947). 241. Theory of chromatography. Part IV. The influence of incomplete equilibrium on the front boundary of chromatograms and on the effectiveness of separation. Journal of the Chemical Society (Resumed), 1947; 1315–1321. https://doi.org/10.1039/jr9470001315

Goodman, D. and Keene, R. (1997). Man versus machine: Kasparov versus deep blue. *ICGA Journal*, **20**(3), 186–187. https://doi.org/10.3233/ICG-1997-20308

Greenacre, M., Groenen, P. J., Hastie, T., d'Enza, A. I., Markos, A. and Tuzhilina, E. (2022). Principal component analysis. *Nature Reviews Methods Primers*, **2**(1), 100. https://doi.org/10.1038/s43586-022-00184-w

Guo X. and Wang J. (2019). A general kinetic model for adsorption: theoretical analysis and modeling. *Journal of Molecular Liquids*, **288**, 111100. https://doi.org/10.1016/j.molliq.2019.111100

Gupta, V. K., Ali, I., Saleh, T. A., Nayak, A. and Agarwal, S. (2012). Chemical treatment technologies for waste-water recycling–an overview. *RSC advances*, **2**(16), 6380–6388. https://doi.org/10.1039/C2RA20340E

Haenlein, M. and Kaplan, A. (2019). A brief history of artificial intelligence: On the past, present, and future of artificial intelligence. *California management review*, **61**(4), 5–14. https://doi.org/10.1177/0008125619864925

Halsey G. (1948). Physical adsorption on non-uniform surfaces. *The Journal of Chemical Physics*, **16**(10), 931–937. https://doi.org/10.1063/1.1746689

Hami, K. (2021). Turbulence Modeling a Review for Different Used Methods. *International Journal of Heat and Technology*, **39**(1). https://doi.org/10.18280/ijht.390125

Harlow F. H. (2004). Fluid dynamics in group T-3 Los Alamos National Laboratory. *Journal of Computational Physics*, **195**(2), 414–433. https://doi.org/10.1016/j.jcp.2003.09.031

Harrison J. A., Schall J. D., Maskey S., Mikulski P. T., Knippenberg M. T. and Morrow B. H. (2018). Review of force fields and intermolecular potentials used in atomistic computational materials research. *Applied Physics Reviews*, **5**(3). https://doi.org/10.1063/1.5020808

Hastings W. K. (1970). Monte Carlo sampling methods using Markov chains and their applications. *Biometrika*, **57**(1), 97. https://doi.org/10.2307/2334940

Heidari, Z., Pelalak, R., Malekshah, R. E., Pishnamazi, M., Marjani, A., Sarkar, S. M. and Shirazian, S. (2021). Molecular modeling investigation on mechanism of cationic dyes removal from aqueous solutions by mesoporous materials. *Journal of Molecular Liquids*, **329**, 115485. https://doi.org/10.1016/j.molliq.2021.115485

Hess J. L. and Smith A. M. O. (1967). Calculation of potential flow about arbitrary bodies. *Progress in Aerospace Sciences*, **8**, 1–138. https://doi.org/10.1016/0376-0421(67)90003-6

Hill T. L. (1952). Theory of physical adsorption, pp. 211–258. https://doi.org/10.1016/S0360-0564(08)60615-X

Hines A. L. and Maddox R. N. (1985). Mass Transfer: Fundamentals and Applications. Prentice-Hall, United States, Vol. **434**.

Hira, N. E., Lock, S. S. M., Shoparwe, N. F., Lock, I. S. M., Lim, L. G., Yiin, C. L. and Hassam, M. (2023). Review of adsorption studies for contaminant removal from wastewater using molecular simulation. *Sustainability*, **15**(2), 1510. https://doi.org/10.3390/su15021510

Ho Y. S., Wase D. A. J. and Forster C. F. (1996). Removal of lead ions from aqueous solution using sphagnum moss peat as absorbent. *Water SA*, **22**(3), 219–224.

Huang, J., Chen, M., Xue, J., Li, M., Cheng, Y., Lai, Z., Hu J., Zhou F., Qu N., Liu Y. and Zhu, J. (2024). A Study of the adsorption properties of individual atoms on the graphene surface: Density functional theory calculations assisted by machine learning techniques. *Materials*, **17**(6), 1428. https://doi.org/10.3390/ma17061428

Huggins M. L. (1941). Solutions of long chain compounds. *The Journal of Chemical Physics*, **9**(5), 440–440. https://doi.org/10.1063/1.1750930

Ibrahim, Q., Creedon, L. and Gharbia, S. (2022). A literature review of modelling and experimental studies of water treatment by adsorption processes on nanomaterials. *Membranes*, **12**(4), 360. https://doi.org/10.3390/membranes12040360

International Organization for Standardization (1984). ISO 6777: Water Quality — Determination of Nitrite — Molecular Absorption Spectrometric Method. ISO, Geneva, Switzerland.

International Organization for Standardization (1986). ISO 7890-1: Water Quality — Determination of Nitrate — Part 1: 2,6-Dimethylphenol Spectrometric Method. ISO, Geneva, Switzerland.

International Organization for Standardization (1988). ISO 7890-3: Water Quality — Determination of Nitrate — Part 3: Spectrometric Method After Cadmium Reduction. ISO, Geneva, Switzerland.

International Organization for Standardization (1992). ISO 10304-1: Water Quality — Determination of Dissolved Anions by Liquid Chromatography of Ions — Part 1: Determination of Bromide, Chloride, Fluoride, Nitrate, Nitrite, Phosphate and Sulfate. ISO, Geneva, Switzerland.

International Organization for Standardization (1996). ISO 13395: Water Quality — Determination of Nitrite and Nitrate by Flow Analysis (CFA and FIA) and Spectrometric Detection. ISO, Geneva, Switzerland.

Ioannidou K., Labbez C. and Masoero E. (2022). A review of coarse grained and mesoscale simulations of C–S–H. *Cement and Concrete Research*, **159**, 106857. https://doi.org/10.1016/j.cemconres.2022.106857

Irons, T. J., David, G. and Teale, A. M. (2021). Optimizing molecular geometries in strong magnetic fields. *Journal of Chemical Theory and Computation*, **17**(4), 2166–2185. https://doi.org/10.1021/acs.jctc.0c01297

Isaacs, E. B. and Wolverton, C. (2018). Performance of the strongly constrained and appropriately normed density functional for solid-state materials. *Physical Review Materials*, **2**(6), 063801. https://doi.org/10.1103/PhysRevMaterials.2.063801

Janesko, B. G., Proynov, E., Scalmani, G. and Frisch, M. J. (2018). Long-range-corrected Rung 3.5 density functional approximations. *The Journal of Chemical Physics*, **148**(10). https://doi.org/10.1063/1.5017981

Johnson N. L. (1996). CFD.pdf. The Legacy and Future of CFD at Los Alamos.

Jovanović D. S. (1969). Physical adsorption of gases. *Kolloid-Zeitschrift & Zeitschrift Für Polymere*, **235**(1), 1203–1213. https://doi.org/10.1007/BF01542530

Kaelbling, L. P., Littman, M. L. and Moore, A. W. (1996). Reinforcement learning: A survey. *Journal of artificial intelligence research*, **4**, 237–285. https://doi.org/10.1613/jair.301

Karpatne, A., Atluri, G., Faghmous, J. H., Steinbach, M., Banerjee, A., Ganguly, A., Shekhar S., Samatova N. and Kumar, V. (2017). Theory-guided data science: A new paradigm for scientific discovery from data. *IEEE Transactions on knowledge and data engineering*, **29**(10), 2318–2331. https://doi.org/10.1109/TKDE.2017.2720168

Kelvin (1903). The scientific work of Sir George Stokes. *Nature*, **67**(1737), 337–338. https://doi.org/10.1038/067337a0

Kohn, W. and Sham, L. J. (1965). Self-consistent equations including exchange and correlation effects. *Physical review*, **140**(4A), A1133. https://doi.org/10.1103/PhysRev.140.A11334

Koopmans, T. (1934). Über die Zuordnung von Wellenfunktionen und Eigenwerten zu den einzelnen Elektronen eines Atoms. *physica*, **1**(1-6), 104–113. https://doi.org/10.1016/S0031-8914(34)90011-2

Kristanti, R. A., Hadibarata, T., Syafrudin, M., Yılmaz, M. and Abdullah, S. (2022). Microbiological contaminants in drinking water: Current status and challenges. *Water, Air, and Soil Pollution*, **233**(8), 299. https://doi.org/10.1007/s11270-022-05698-3

Kulkarni, A. S., Kasabe, A. J., Bhatia, M. S., Bhatia, N. M. and Gaikwad, V. L. (2019). Quantitative structure–property relationship approach in formulation development: an overview. *AAPS PharmSciTech*, **20**(7), 268. https://doi.org/10.1208/s12249-019-1480-2

Kumar, B., Vyas, O. P. and Vyas, R. (2019). A comprehensive review on the variants of support vector machines. *Modern Physics Letters B*, **33**(25), 1950303. https://doi.org/10.1142/S0217984919503032

Lagergren S. (1898). About the theory of so-called adsorption of solution substances.

Lagergreen S. (1907). Zur theorie der sogenannten Adsorption gelöster Stoffe. *Zeitschrift Für Chemie Und Industrie Der Kolloide*, **2**(1), 15–15. https://doi.org/10.1007/BF01501332

Langmuir I. (1918). The adsorption of gases on plane surfaces of glass, mica and platinum. *Journal of the American Chemical Society*, **40**(9), 1361–1403. https://doi.org/10.1021/ja02242a004

Le, T., Epa, V. C., Burden, F. R. and Winkler, D. A. (2012). Quantitative structure–property relationship modeling of diverse materials properties. *Chemical reviews*, **112**(5), 2889–2919. https://doi.org/10.1021/cr200066h

Lenhard, J., Stephan, S. and Hasse, H. (2024). On the History of the Lennard-Jones Potential. *Annalen der Physik*, **536**(6), 2400115. https://doi.org/10.1002/andp.202400115

Li, M., Yu, H., Wang, Y., Li, J., Ma, G. and Wei, X. (2020). QSPR models for predicting the adsorption capacity for microplastics of polyethylene, polypropylene and polystyrene. *Scientific reports*, **10**(1), 14597. https://doi.org/10.1038/s41598-020-71390-3

Lieb, E. H. and Simon, B. (1977). The Thomas-Fermi theory of atoms, molecules and solids. *Advances in mathematics*, **23**(1), 22–116. https://doi.org/10.1016/0001-8708(77)90108-6

Lim, J. S. (2022). Dynamics of surfaces and interfaces: From first-principles modeling to machine-learning molecular dynamics (Doctoral dissertation, Harvard University).

Linse J.-B. and Hub J. S. (2021). Three- and four-site models for heavy water: SPC/E-HW, TIP3P–HW, and TIP4P/2005-HW. *The Journal of Chemical Physics*, **154**(19). https://doi.org/10.1063/5.0050841

Liu, D., Wang, Z., Cai, Y., Chen, J., Jin, J. and Zhao, B. (2024). Computational fluid dynamics based modeling of gas absorption process: a state-of-the-art review. *Industrial and Engineering Chemistry Research*, **63**(18), 7959–8002. https://doi.org/10.1021/acs.iecr.3c02941

Lomax, H., Pulliam, T. H., Zingg, D. W. and Kowalewski, T. A. (2002). Fundamentals of computational fluid dynamics. *Appl. Mech. Rev.*, **55**(4), B61–B61. https://doi.org/10.1115/1.1483340

Lowe, M., Qin, R. and Mao, X. (2022). A review on machine learning, artificial intelligence, and smart technology in water treatment and monitoring. *Water*, **14**(9), 1384. https://doi.org/10.3390/w14091384

Lu, J., Ma, G. and Zhang, G. (2024). Fuzzy machine learning: A comprehensive framework and systematic review. *IEEE Transactions on Fuzzy Systems*, **32**(7), 3861–3878. https://doi.org/10.1109/TFUZZ.2024.3387429

Lustig R. (1994). Statistical thermodynamics in the classical molecular dynamics ensemble. I. Fundamentals. *The Journal of Chemical Physics*, **100**(4), 3048–3059. https://doi.org/10.1063/1.466446

Madhav S. and Singh P. (eds.). (2021). Groundwater Geochemistry: Pollution and Remediation Methods. Wiley, United States.

Malloum, A., Adegoke, K. A., Ighalo, J. O., Conradie, J., Ohoro, C. R., Amaku, J. F., Oyedotun K. O., Maxakato N. W., Akpomie G., Okeke E. S. and Olisah, C. (2023). Computational methods for adsorption study in wastewater treatment. *Journal of Molecular Liquids*, **390**, 123008. https://doi.org/10.1016/j.molliq.2023.123008

Marczewski A. W. and Jaroniec M. (1983). A new isotherm equation for single-solute adsorption from dilute solutions on energetically heterogeneous solids. *Monatshefte Für Chemie – Chemical Monthly*, **114**(6–7), 711–715. https://doi.org/10.1007/BF01134184

Mazumder, S. (2015). Numerical methods for partial differential equations: finite difference and finite volume methods. Academic Press, United States.

McCready, C., Sladekova, K., Conroy, S., Gomes, J. R., Fletcher, A. J. and Jorge, M. (2024). Quantifying the uncertainty of force field selection on adsorption predictions in MOFs. *Journal of Chemical Theory and Computation*, **20**(11), 4869–4884. https://doi.org/10.1021/acs.jctc.4c00287

McCulloch, W. S. and Pitts, W. (1943). A logical calculus of the ideas immanent in nervous activity. *The bulletin of mathematical biophysics*, **5**(4), 115–133. https://doi.org/10.1007/BF02478259

Metcalf & Eddy (2014). Wastewater Engineering: Treatment and Resource Recovery, 5th ed., McGraw-Hill Education, United States.

Metropolis N., Rosenbluth A. W., Rosenbluth M. N., Teller A. H. and Teller E. (1953). Equation of state calculations by fast computing machines. *The Journal of Chemical Physics*, **21**(6), 1087–1092. https://doi.org/10.1063/1.1699114

Miettinen, A. and Siikonen, T. (2015). Application of pressure-and density-based methods for different flow speeds. *International Journal for Numerical Methods in Fluids*, **79**(5), 243–267. https://doi.org/10.1002/fld.4051

Nachiyar, C. V., Rakshi, A. D., Sandhya, S., Jebasta, N. B. D. and Nellore, J. (2023). Developments in treatment technologies of dye-containing effluent: A review. *Case Studies in Chemical and Environmental Engineering*, **7**, 100339. https://doi.org/10.1016/j.cscee.2023.100339

Nadamani, M. N., Shadloo, M. S. and Dbouk, T. (2025). A Review on Theoretical and Computational Fluid Dynamics Modeling of Coupled Heat and Mass Transfer in Fixed Beds of Adsorbing Porous Media. *Energies*, **18**(24), 6418. https://doi.org/10.3390/en18246418

Nagata Y., Ohto T., Backus E. H. G. and Bonn M. (2016). Molecular modeling of water interfaces: from molecular spectroscopy to thermodynamics. *The Journal of Physical Chemistry B*, **120**(16), 3785–3796. https://doi.org/10.1021/acs.jpcb.6b01012

Naidu R., Biswas B., Willett I. R., Cribb J., Kumar Singh B., Paul Nathanail C., Coulon F., Semple K. T., Jones K. C., Barclay A. and Aitken R. J. (2021). Chemical pollution: a growing peril and potential catastrophic risk to humanity. *Environment International*, **156**, 106616. https://doi.org/10.1016/j.envint.2021.106616

Nelms S. E., Duncan E. M., Patel S., Badola R., Bhola S., Chakma S., Chowdhury G. W., Godley B. J., Haque A. B., Johnson J. A., Khatoon H., Kumar S., Napper I. E., Niloy M. N. H., Akter T., Badola S., Dev A., Rawat S., Santillo D., Sarker S., Sharma E. and Koldewey H. (2021). Riverine plastic pollution from fisheries: insights from the Ganges River system. *Science of the Total Environment*, **756**, 143305. https://doi.org/10.1016/j.scitotenv.2020.143305

Newell A. and Simon H.A. (1956) The logic theory machine - a complex information processing system. *IRE Trans Inf Theory*. (**2**) 61–79. https://doi.org/10.1109/TIT.1956.1056797

Ottewill, R. H., Rochester, C. H. and Smith, A. L. (Eds.). (2012). Adsorption from solution. Elsevier, Netherlands. https://doi.org/10.1016/B978-0-12-530980-6.X5001-3

Ozer A. (2007). Removal of Pb(II) ions from aqueous solutions by sulphuric acid-treated wheat bran. *Journal of Hazardous Materials*, **141**(3), 753–761. https://doi.org/10.1016/j.jhazmat.2006.07.040

Panagiotopoulos A. Z. (1992). Direct determination of fluid phase equilibria by simulation in the Gibbs ensemble: a review. *Molecular Simulation*, **9**(1), 1–23. https://doi.org/10.1080/08927029208048258

Park, J. S. (2021). Comparison study of exchange-correlation functionals on prediction of ground states and structural properties. *Current Applied Physics*, **22**, 61–64. https://doi.org/10.1016/j.cap.2020.12.005

Patankar, S. (2018). Numerical heat transfer and fluid flow. CRC press, United States. https://doi.org/10.1201/9781482234213

Patankar S. V. and Spalding D. B. (1972). A calculation procedure for heat, mass and momentum transfer in three-dimensional parabolic flows. *International Journal of Heat and Mass Transfer*, **15**(10), 1787–1806. https://doi.org/10.1016/0017-9310(72)90054-3

Pellenz L., de Oliveira C. R. S., da Silva Júnior A. H., da Silva L. J. S., da Silva L., Ulson de Souza A. A., de Souza S. M. D. A. G. U., Borba F. H. and da Silva A. (2023). A comprehensive guide for characterization of adsorbent materials. *Separation and Purification Technology*, **305**, 122435. https://doi.org/10.1016/j.seppur.2022.122435

Pradhan, B., Chand, S., Chand, S., Rout, P. R. and Naik, S. K. (2023). Emerging groundwater contaminants: A comprehensive review on their health hazards and

remediation technologies. *Groundwater for Sustainable Development*, **20**, 100868. https://doi.org/10.1016/j.gsd.2022.100868

Rahman A. (1964). Correlations in the motion of atoms in liquid argon. *Physical Review*, **136**(2A), A405–A411. https://doi.org/10.1103/PhysRev.136.A405

Rahman A. and Stillinger F. H. (1971). Molecular dynamics study of liquid water. *The Journal of Chemical Physics*, **55**(7), 3336–3359. https://doi.org/10.1063/1.1676585

Redlich O. and Peterson D. L. (1959). A useful adsorption isotherm. *The Journal of Physical Chemistry*, **63**(6), 1024–1024. https://doi.org/10.1021/j150576a611

Reji, M. and Kumar, R. (2022). Response surface methodology (RSM): An overview to analyze multivariate data. *Indian J. Microbiol. Res*, **9**, 241–248. https://doi.org/10.18231/j.ijmr.2022.042

Reveles, J. U. and Köster, A. M. (2004). Geometry optimization in density functional methods. *Journal of computational chemistry*, **25**(9), 1109–1116. https://doi.org/10.1002/jcc.20034

Reynel-Ávila, H. E., Aguayo-Villarreal, I. A., Diaz-Muñoz, L. L., Moreno-Pérez, J., Sánchez-Ruiz, F. J., Rojas-Mayorga, C. K., Mendoza-Castillo D. I. and Bonilla-Petriciolet, A. (2022). A review of the modeling of adsorption of organic and inorganic pollutants from water using artificial neural networks. *Adsorption Science and Technology*, **2022**, 9384871. https://doi.org/10.1155/2022/9384871

Richardson L. F. (1911). IX. The approximate arithmetical solution by finite differences of physical problems involving differential equations, with an application to the stresses in a masonry dam. *Philosophical Transactions of the Royal Society of London. Series A, Containing Papers of A Mathematical or Physical Character*, **210**(459–470), 307–357. https://doi.org/10.1098/rsta.1911.0009

Riffat, R. and Husnain, T. (2022). Fundamentals of wastewater treatment and engineering. CRC Press, United States. https://doi.org/10.1201/9781003134374

Ritchie A. G. (1977). Alternative to the Elovich equation for the kinetics of adsorption of gases on solids. *Journal of the Chemical Society, Faraday Transactions 1: Physical Chemistry in Condensed Phases*, **73**, 1650. https://doi.org/10.1039/f19777301650

Roy K. and Ambure P. (2016). The 'double cross-validation' software tool for MLR QSAR model development. *Chemometrics and Intelligent Laboratory Systems*, **159**, 108–126. https://doi.org/10.1016/j.chemolab.2016.10.009

Roy, K., Kar, S. and Das, R. N. (2015). A primer on QSAR/QSPR modeling: fundamental concepts. Springer, Netherlands. https://doi.org/10.1007/978-3-319-17281-1

Rumelhart D.E., Hinton G.E. and Williams R.J. (1986) Learning representations by back-propagating errors. *Nature*. (**323**) 533–536. https://doi.org/10.1038/323533a0

Ruthven D. M. (1984). Principles of Adsorption and Adsorption Processes. John Wiley & Sons, United States.

Safwat, S. M., Mohamed, N. Y., Meshref, M. N. and Elawwad, A. (2022). Adsorption of phenol onto aluminum oxide nanoparticles: performance evaluation, mechanism exploration, and principal component analysis (PCA) of thermodynamics. *Adsorption Science and Technology*, **2022**, 1924117. https://doi.org/10.1155/2022/1924117

Salahshoori I., Wang Q., Nobre M. A. L., Mohammadi A. H., Dawi E. A. and Khonakdar H. A. (2024). Molecular simulation-based insights into dye pollutant adsorption: a perspective review. *Advances in Colloid and Interface Science*, **333**, 103281. https://doi.org/10.1016/j.cis.2024.103281

Salehi I., Shirani M., Semnani A., Hassani M. and Habibollahi S. (2016). Comparative study between response surface methodology and artificial neural network for adsorption of crystal violet on magnetic activated carbon. *Arabian Journal for Science and Engineering*, **41**(7), 2611–2621. https://doi.org/10.1007/s13369-016-2109-3

Salman, H. A., Kalakech, A. and Steiti, A. (2024). Random forest algorithm overview. *Babylonian Journal of Machine Learning*, **2024**, 69–79. https://doi.org/10.58496/BJML/2024/007

Sathya, R., Arasu, M. V., Al-Dhabi, N. A., Vijayaraghavan, P., Ilavenil, S. and Rejiniemon, T. S. (2023). Towards sustainable wastewater treatment by biological methods–A challenges and advantages of recent technologies. *Urban Climate*, **47**, 101378. https://doi.org/10.1016/j.uclim.2022.101378

Seow, T. W., Lim, C. K., Nor, M. H. M., Mubarak, M. F. M., Lam, C. Y., Yahya, A. and Ibrahim, Z. (2016). Review on wastewater treatment technologies. *Int. J. Appl. Environ. Sci*, **11**(1), 111–126.

Shewa W. A. and Dagnew M. (2020). Revisiting chemically enhanced primary treatment of wastewater: a review. *Sustainability*, **12**(15), 5928. https://doi.org/10.3390/su12155928

Sinanoğlu, O. and Pitzer, K. S. (1960). Interactions between molecules adsorbed on a surface. *The Journal of Chemical Physics*, **32**(5), 1279–1288. https://doi.org/10.1063/1.1730910

Singh R. L. (ed.). (2017). Principles and Applications of Environmental Biotechnology for A Sustainable Future. Springer, Germany. https://doi.org/10.1007/978-981-10-1866-4

Singh N. B., Kumar A. and Rai S. (2014). Potential production of bioenergy from biomass in an Indian perspective. *Renewable and Sustainable Energy Reviews*, **39**, 65–78. https://doi.org/10.1016/j.rser.2014.07.110

Sips R. (1948). On the structure of a catalyst surface. *The Journal of Chemical Physics*, **16**(5), 490–495. https://doi.org/10.1063/1.1746922

Sips R. (1950). On the structure of a catalyst surface. II. *The Journal of Chemical Physics*, **18**(8), 1024–1026. https://doi.org/10.1063/1.1747848

Soares, A. P. D. M. R., de Oliveira Carvalho, F., de Farias Silva, C. E., da Silva Gonçalves, A. H. and de Souza Abud, A. K. (2020). Random Forest as a promising application to predict basic-dye biosorption process using orange waste. *Journal of Environmental Chemical Engineering*, **8**(4), 103952. https://doi.org/10.1016/j.jece.2020.103952

Steele, W. (1993). Molecular interactions for physical adsorption. *Chemical reviews*, **93**(7), 2355–2378. https://doi.org/10.1021/cr00023a002

Sumiea, E. H., Abdulkadir, S. J., Alhussian, H. S., Al-Selwi, S. M., Alqushaibi, A., Ragab, M. G. and Fati, S. M. (2024). Deep deterministic policy gradient algorithm: A systematic review. *Heliyon*, **10**(9). https://doi.org/10.1016/j.heliyon.2024.e30697

Taoufik N., Elmchaouri A., El Mahmoudi S., Korili S. A. and Gil A. (2021). Comparative analysis study by response surface methodology and artificial neural network on salicylic acid adsorption optimization using activated carbon. *Environmental Nanotechnology, Monitoring & Management*, **15**, 100448. https://doi.org/10.1016/j.enmm.2021.100448

Tarazona, P., Marconi, U. M. B. and Evans, R. (1987). Phase equilibria of fluid interfaces and confined fluids: non-local versus local density functionals. *Molecular Physics*, **60**(3), 573–595. https://doi.org/10.1080/00268978700100381

Tempkin M. I. and Pyzhev V. and others. (1940). Kinetics of ammonia synthesis on promoted iron catalyst. *Acta Physicochimica URSS*, **12**(1), 327.

Tey, W. Y., Asako, Y., Sidik, N. A. C. and Goh, R. Z. (2017). Governing equations in computational fluid dynamics: Derivations and a recent review. *Progress in Energy and Environment*, 1–19.

Thomas H. C. (1944). Heterogeneous ion exchange in a flowing system. *Journal of the American Chemical Society*, **66**(10), 1664–1666. https://doi.org/10.1021/ja01238a017

Toriyama, M. Y., Ganose, A. M., Dylla, M., Anand, S., Park, J., Brod, M. K., Munro J. M., Persson, K. A., Jain, A. and Snyder, G. J. (2022). How to analyse a density of states. *Materials Today Electronics*, **1**, 100002. https://doi.org/10.1016/j.mtelec.2022.100002

Tóth J. (1981). A uniform interpretation of gas/solid adsorption. *Journal of Colloid and Interface Science*, **79**(1), 85–95. https://doi.org/10.1016/0021-9797(81)90050-3

Toxvaerd, S. (1991). Algorithms for canonical molecular dynamics simulations. *Molecular Physics*, **72**(1), 159–168. https://doi.org/10.1080/00268979100100101

Tran H. N., You S.-J., Hosseini-Bandegharaei A. and Chao H.-P. (2017). Mistakes and inconsistencies regarding adsorption of contaminants from aqueous solutions: a critical review. *Water Research*, **120**, 88–116. https://doi.org/10.1016/j.watres.2017.04.014

Turing, A. M. (1950). Mind. *Mind*, **59**(236), 433–460.

Tylianakis, E. and Froudakis, G. E. (2009). Grand canonical Monte Carlo method for gas adsorption and separation. *Journal of Computational and Theoretical Nanoscience*, **6**(2), 335–348. https://doi.org/10.1166/jctn.2009.1040

United Nations Environment Programme (2021). Global Environment Outlook – GEO-6: Healthy Planet, Healthy People. UNEP, Nairobi, Kenya.

Van Mourik, T., Bühl, M. and Gaigeot, M. P. (2014). Density functional theory across chemistry, physics and biology. *Philosophical Transactions of the Royal Society A: Mathematical, Physical and Engineering Sciences*, **372**(2011), 20120488. https://doi.org/10.1098/rsta.2012.0488

van Vliet B. M., Weber Jr. W. J. and Hozumi H. (1980). Modeling and prediction of specific compound adsorption by activated carbon and synthetic adsorbents. *Water Research*, **14**(12), 1719–1728. https://doi.org/10.1016/0043-1354(80)90107-4

Vega C. and Abascal J. L. F. (2011). Simulating water with rigid non-polarizable models: a general perspective. *Physical Chemistry Chemical Physics*, **13**(44), 19663. https://doi.org/10.1039/c1cp22168j

Vera M., Juela D. M., Cruzat C. and Vanegas E. (2021). Modeling and computational fluid dynamic simulation of Acetaminophen adsorption using sugarcane bagasse. *Journal of Environmental Chemical Engineering*, **9**(2), 105056. https://doi.org/10.1016/j.jece.2021.105056

Wang J. and Guo X. (2020). Adsorption kinetic models: physical meanings, applications, and solving methods. *Journal of Hazardous Materials*, **390**, 122156. https://doi.org/10.1016/j.jhazmat.2020.122156

Wang, Y., Li, J., Ma, T., Xie, X., Deng, Y. and Gan, Y. (2021). Genesis of geogenic contaminated groundwater: As, F and I. *Critical Reviews in Environmental Science and Technology*, **51**(24), 2895–2933. https://doi.org/10.1080/10643389.2020.1807452

Warshel A. and Karplus M. (1972). Calculation of ground and excited state potential surfaces of conjugated molecules. I. Formulation and parametrization. *Journal of the American Chemical Society*, **94**(16), 5612–5625. https://doi.org/10.1021/ja00771a014

Weber, W. J. and Smith, E. H. (1987). Simulation and design models for adsorption processes. *Environmental science and technology*, **21**(11), 1040–1050. https://doi.org/10.1021/es00164a002

World Health Organization (2022). Guidelines for Drinking-Water Quality, 4th edn., incorporating the 1st and 2nd addenda. WHO, Geneva, Switzerland.

World Health Organization (2023). Drinking-water: Key facts. WHO, Geneva, Switzerland.

Yadav A., Dindorkar S. S., Ramisetti S. B. and Sinha N. (2022). Simultaneous adsorption of methylene blue and arsenic on graphene, boron nitride and boron carbon nitride nanosheets: insights from molecular simulations. *Journal of Water Process Engineering*, **46**, 102653. https://doi.org/10.1016/j.jwpe.2022.102653

Yang R. T. (1997). Gas Separation by Adsorption Processes. Imperial College Press, United Kingdom, Vol. **1**, https://doi.org/10.1142/p037

Yuan, L., Li, S., Ma, Y., Zhang, H., Chen, C., Zhang, W., Zhang, Y., Hua, M., Lv, L. and Pan, B. (2025). Machine learning-aided design of adapted water treatment adsorbents: Advances, challenges, and opportunities. *Chemical Engineering Journal*, **171262**. https://doi.org/10.1016/j.cej.2025.171262

Zhang, Q., Barri, K., Jiao, P., Salehi, H. and Alavi, A. H. (2021). Genetic programming in civil engineering: advent, applications and future trends. *Artificial Intelligence Review*, **54**(3), 1863–1885. https://doi.org/10.1007/s10462-020-09894-7

Zhao, H., Yang, Y., Shu, X., Wang, Y. and Ran, Q. (2018). Adsorption of organic molecules on mineral surfaces studied by first-principle calculations: A review. *Advances in Colloid and Interface Science*, **256**, 230–241. https://doi.org/10.1016/j.cis.2018.04.003

Zhao, S., Guo, J., Tang, Y. and Zhou, Y. (2025). Applications of machine learning in heavy metal adsorption modeling: A review. *Separation and Purification Technology*, **134168**. https://doi.org/10.1016/j.seppur.2025.134168

Zhou, K. and Liu, B. (2022). Molecular dynamics simulation: fundamentals and applications. Academic Press, United States. https://doi.org/10.1016/C2017-0-04711-0

As global water resources face growing threats from pollution and overuse, sustainable treatment solutions are urgently needed. Among these, adsorption stands out as an effective and versatile method for removing a broad spectrum of contaminants from water and wastewater. However, optimizing adsorption for large-scale applications is a complex challenge that demands both a solid understanding of adsorption science and the use of advanced computational tools. *Computational Techniques for Modelling and Simulating Adsorption Processes for (Waste)Water Treatment* addresses this challenge by providing a comprehensive guide integrating core adsorption principles with cutting-edge computational approaches for enhancing adsorption efficiency and system design.

Structured to lead readers from fundamental concepts to advanced applications, the book includes:

- an overview of water pollution and treatment
- a detailed exploration of adsorption principles and models
- an introduction to general computational strategies for modelling and optimization, leading on to density functional theory, molecular dynamics, Monte Carlo simulations and QSAR techniques
- AI and machine learning in adsorption modelling
- computational fluid dynamics and system-level optimization.

Together, these topics provide researchers, engineers, and practitioners with the tools needed to model, simulate, and optimize adsorption processes for more efficient and sustainable water treatment.



iwaponline.com
@IWAPublishing

ISBN: 9781789063936 (paperback)
ISBN: 9781789063943 (eBook)
ISBN: 9781789063950 (ePub)

ISBN: 9781789063936
9 781789 063936